



UNIVERSIDAD
NACIONAL
DE COLOMBIA

Oil palm rachis gasification for synthesis gas production

Juan Camilo Solarte Toro

Universidad Nacional de Colombia – Sede Manizales
Facultad de Ingeniería y Arquitectura, Departamento de Ingeniería Química
Ciudad, Colombia

2017

Oil palm rachis gasification for synthesis gas production

Juan Camilo Solarte Toro

Thesis submitted in partial fulfillment of the requirements for the degree of:

Master of Science in Engineering - Chemical Engineering

Advisor:

Ph.D., M. Sc, Chemical Engineering Carlos Ariel Cardona Alzate

Research line:

Chemical and Biotechnological Process Engineering

Research group:

Chemical, Catalytic and Biotechnological Processes

Universidad Nacional de Colombia – Sede Manizales
Facultad de Ingeniería y Arquitectura, Departamento de Ingeniería Química
Ciudad, Colombia

2017

Gasificación del raquis de palma de aceite para la producción de gas de síntesis

Juan Camilo Solarte Toro

Tesis presentada como requisito parcial para optar al título de:

Magister en Ingeniería Química

Director:

Ph.D., M. Sc, Ingeniero Químico Carlos Ariel Cardona Alzate

Línea de Investigación:

Ingeniería de Procesos Químicos y Biotecnológicos

Grupo de Investigación:

Procesos Químicos, Catalíticos y Biotecnológicos

Universidad Nacional de Colombia – Sede Manizales

Facultad de Ingeniería y Arquitectura, Departamento de Ingeniería Química

Ciudad, Colombia

2017

A mis padres y hermano quienes me han apoyado incondicionalmente en el camino que he escogido

“Lo que distingue las mentes verdaderamente originales no es que sean la primeras en ver algo nuevo, sino que son capaces de ver como nuevo lo que es viejo, conocido, visto y menospreciado por todos”.

Friedrich Nietzsche

Acknowledgements.

First that all, I want to express my grateful to my parents, brother and my godmother. They have always been with me in the good and bad times of my life. To Yessica for support and help me during the last years, also, for allow me stay with her during the development of this work. In addition, I want to thank to my advisor Carlos Ariel Cardona for trust and give me different opportunities to grow up as person and professional, also for show me the way that I want to follow. Thanks Daniela, Ashley and Sebastian for the laughs and good moments that I have passed with you in the last two years. Regardless the way that you choose, I will always be for all of you in the same place where we will end this chapter of our life. There are two persons that always have been to help me in my doubts and give me ideas or advices. Thanks Carlos Andrés García and Valentina Aristizábal. Thanks, Laura Vanessa for introduce me into the laboratory and teach me the basis of the research work, I want to express my gratitude to Cesar, Christian, Daissy, Jimmy, Jhonny, Mariana, Estefanny and Paula for share with me in the PQCB group.

On the other hand, I want to acknowledge to the Universidad Nacional de Colombia at Manizales, to the Universidad de Jaén, to the Pontificia Universidad de Valparaíso, to the Dirección de Investigación (DIMA), to the Sistema de Información de la Investigación (HERMES), to the Facultad de Ingeniería y Arquitectura (FIA) an to COLCIENCIAS for the financial support to develop this thesis. In addition, I express my gratefulness to the Productive Process Laboratory, Residues Laboratory and Polymers Laboratory for support me in my work when I needed. Additionally, I want to express my recognize to Maria Fanny, Wilmar, Alneira Cuellar, Fabio Mesa, Diego Lopez and Andres Felipe Rojas for their help. Finally, I want express my gratitude with the PhD. Eulogio Castro, PhD. Germán Aroca, PhD. Julián Quintero, PhD Karlo Guerrero, PhD. Ivan Paredes, PhD. Juan Miguel Romero, PhD. Carlos Martínez Patiño and their research groups for assist and receive me in their laboratories.

Agradecimientos.

Primero que todo, deseo expresar mi gratitud hacia mis padres, hermano y mi madrina. Ellos siempre han estado conmigo en los buenos y malos momentos de mi vida. A Yessica por su apoyo e incondicional ayuda en los últimos años. También por permitirme haber compartido tantos momentos junto a ella durante el desarrollo de este trabajo. Asimismo, quisiera expresar mis más sinceros agradecimientos al profesor Carlos Ariel Cardona Alzate por su confianza así como por todas y cada una de las oportunidades que me ha dado para crecer a nivel personal y profesional. Además, le agradezco por haberme mostrado el camino que quiero seguir de aquí en adelante. Gracias, Daniela, Ashley y Sebastián por las risas y buenos momentos que compartí con ustedes en estos dos años que estuvimos juntos. Por eso, sin importar el camino que cada uno elija, yo estaré para ustedes en el mismo sitio donde terminamos esta etapa de nuestras vidas. Por otro lado, hay dos personas que siempre han estado allí para guiarme, darme ideas y solucionar mis dudas. Gracias Carlos Andrés García y Valentina Aristizábal. Igualmente, quisiera destacar a Laura Vanessa Daza ya que me introdujo al grupo de investigación y me enseñó las bases del trabajo de investigación. Finalmente, quiero agradecer a Cesar, Christian, Daissy, Jimmy, Jhonny, Mariana, Estefanny, Paula y José por compartir conmigo en el grupo de investigación PQCB.

Igualmente, gracias Universidad Nacional de Colombia – sede Manizales, Universidad de Jaén y Pontificia Universidad de Valparaíso. A la dirección de investigación (DIMA), Al Sistema de Información para la Investigación (HERMES), a la Facultad de Ingeniería y Arquitectura (FIA) y a COLCIENCIAS por el apoyo financiero en este trabajo. Además, quisiera destacar la enorme colaboración del laboratorio de procesos productivos, el laboratorio de polímeros y materiales así como el laboratorio de residuos. Gracias to María Fanny, Wilmar, Alneira Cuellar, Fabio Mesa, Diego Lopez and Andres Felipe Rojas por su ayuda. Finalmente, quiero expresar mi gratitud con el PhD. Eulogio Castro, PhD. Germán Aroca, PhD. Julián Quintero, PhD Karlo Guerrero, PhD. Ivan Paredes, PhD. Juan Miguel Romero, PhD. Carlos Martínez Patiño y sus grupos de investigación me ayudan y me reciben en sus laboratorios.

Abstract.

The use of fossil fuels and the environmental detriment caused by the greenhouse gas emissions has encouraged the search of new energy sources as well as processes for their use. On the other hand, the energy security has become an issue of international interest due to the changing oil prices. Colombia is a tropical country that has been characterized by its high production of palm oil currently. However, the processing of the oil palm (*Elaeis guineensis*) in large amounts generates a great quantity of waste biomass. The oil palm rachis is a residue that has been characterized by not receiving any use as a raw material to obtain bioenergy. This one is used as source of nutrients in the crop. Consequently, the potential of this agro-industrial residue to obtain value-added products is enormous. The present work presents an opportunity to use the oil palm rachis through its gasification to obtain synthesis gas, which is considered an energy vector and a chemical platform. In order to develop this work, the physicochemical characterization of the palm rachis, syngas production in a downstream fixed bed gasifier, the technical, economic and environmental evaluation of the gasification processes were developed. Additionally, the syngas is used as a chemical platform for the production of two value-added products and the production of bioenergy after a cogeneration cycle.

Key words: Bioenergy, Biomass gasification, syngas, energy vectors, chemical platform, Process simulation, Oil palm rachis.

Resumen.

El uso de combustibles fósiles y el deterioro ambiental provocado por las emisiones de gases de efecto invernadero ha incentivado la búsqueda de nuevas fuentes de energía así como de procesos para su aprovechamiento. Por otro lado, a causa de los constantes cambios en el precio del petróleo, la seguridad energética se ha vuelto un tema de interés internacional. Colombia es un país tropical que se ha caracterizado por su alta producción de aceite de palma a nivel mundial. No obstante, durante el procesamiento de la palma de aceite (*Elaeis guineensis*) grandes cantidades de biomasa residual son generadas. El raquis de la palma de aceite es un residuo que se ha caracterizado por no recibir ningún uso como materia prima en procesos de obtención de bioenergía. Por ende, el potencial de aprovechamiento que posee este residuo agroindustrial para la generación de productos de valor agregado es enorme. El presente trabajo plantea una oportunidad de aprovechamiento del raquis de palma a través de su gasificación para la obtención de gas de síntesis, el cual, es considerado un vector energético y una plataforma química. Con el fin de desarrollar esta propuesta se realizará la caracterización fisicoquímica del raquis de palma, la obtención de gas de síntesis en un gasificador de lecho fijo de flujo descendente, la evaluación técnica, económica y ambiental de los procesos en donde se realiza la gasificación del raquis de palma, el uso del gas de síntesis como una plataforma química para la obtención de dos productos de valor agregado y la obtención de bioenergía cuando este es sometido a un ciclo para la generación de calor y potencia.

Palabras clave: Raquis de palma de aceite, Gasificación de biomasa, Gas de síntesis, Vectores energéticos, Plataforma química, Simulación de procesos.

Content.

	Pág.
Contents	
1. Energy vectors from biomass.....	3
1.1 Energy supply overview.....	3
1.2 Paths for energy vectors production.....	9
1.3 Energy vectors obtained from biomass processing.....	17
1.3.1 Bioethanol.....	17
1.3.2 Biogas/Bio-methane.....	18
1.3.3 Biodiesel.....	19
1.3.4 Wood pellets.....	20
1.3.5 Synthesis gas (syngas) or producer gas.....	21
1.4 Final Remarks.....	22
2. The oil palm crop in Colombia.....	23
2.1 The oil palm tree.....	25
2.2 Palm oil production.....	27
2.2.1 Sterilization.....	28
2.2.2 Bunch Threshing (Stripping).....	28
2.2.3 Digestion.....	29
2.2.4 Pulp pressing.....	29
2.2.5 Clarification.....	30
2.2.6 Yields and prices.....	30
2.3 Biodiesel production from palm oil.....	32
2.3.1 Biodiesel production process.....	33
2.3.2 Biodiesel facilities in Colombia.....	34
2.4 Olein and stearin production from palm oil.....	37
2.5 Second generation oil palm biomass.....	39
2.5.1 Empty fruit bunches (EFB).....	39
2.5.2 Oil palm leaves (OPL).....	40
2.5.3 Oil palm fronds (OPF).....	40
2.6 The oil palm productive chain in Colombia.....	42
2.7 Final remarks.....	43
3. Gasification and Syngas: A technology overview.....	45
3.1 Introduction.....	45
3.2 Raw materials used in gasification process.....	49
3.3 Gasification process stages.....	50
3.3.1 Drying.....	51
3.3.2 Pyrolysis.....	51
3.3.3 Combustion.....	51

3.3.4	Reduction.....	51
3.4	Syngas.....	53
3.4.1	Syngas applications.	55
3.5	Biorefineries as join point for the energy vectors and value-added products obtainment.	56
3.5.1	The biorefinery concept.	56
3.5.2	Biorefineries classification.	57
3.5.3	Biorefineries design.	59
3.6	Final remarks.	60
4.	Oil palm rachis characterization.	61
4.1	Chemical composition.	61
4.1.1	Extractives content determination.	62
4.1.2	Holocellulose content determination.	63
4.1.3	Cellulose content determination.	64
4.1.4	Hemicellulose content determination.	65
4.1.5	Lignin content determination.	66
4.1.6	Ash content determination.	67
4.2	Proximate and ultimate analysis.	68
4.2.1	Proximate analysis.	69
4.2.2	Ultimate analysis.	71
4.3	Thermogravimetric analysis.	72
4.4	Atomic absorption analysis.	73
4.5	Final remarks.	73
5.	Pilot – scale air downdraft gasification.	75
5.1	Equipment description and recognizing.....	75
5.2	Operation run.....	79
5.2.1	Feedstock requirements.	80
5.2.2	Start – up and shut – down.....	82
5.2.3	Temperature profile estimation.	83
5.2.4	Synthesis gas determination.....	83
5.3	Parameters to evaluate the performance of the gasification process.....	84
5.4	Final Remarks.....	87
6.	Analysis of characterization results and synthesis gas production from oil palm rachis.....	89
6.1	Chemical characterization.....	89
6.2	Proximate and ultimate analysis.....	92
6.3	TG, DTG curves and kinetic parameter estimation for the oil palm rachis pyrolysis.	95
6.3.1	Thermogravimetric curves analysis.	95
6.3.2	Pyrolysis kinetics of oil palm rachis.....	98
6.3.3	Experimental data from pilot scale air-downdraft gasification.....	103
6.3.4	Economic value of syngas and biochar.	113
6.3.5	Environmental aspects of the oil palm rachis gasification process.	115
6.3.6	Energy balance of the pilot-scale downdraft gasification process.	117
6.4	Final remarks.	120
7.	Modeling and simulation of oil palm rachis gasification.....	121
7.1	Consecutive blocks simulation.	121
7.2	Aspen plus simulation of the gasification process.	130

7.3	Final remarks.	138
8.	Oil palm rachis and syngas based simulations.	139
8.1	Oil palm rachis simulations with and without heterogeneous catalysis.....	139
8.1.1	Biorefinery without catalysis.....	139
8.1.2	Biorefinery with catalysis.....	142
8.1.3	Simulation procedure and economic assessment.	144
8.1.4	Results and discussion.	149
8.2	Heat and power generation.	157
8.2.1	Simulation procedure.	157
8.2.2	Simulation results.	160
8.3	Final remarks.	165

List of Figures.

	Pág.
Figure 1-1. World energy consumption 2000 – 2040 [3]	4
Figure 1-2. Worldwide oil production and consumption [6].	5
Figure 1-3. Energy security concept.	6
Figure 1-4. World net electricity generation by energy source [15].	7
Figure 1-5. Biomass transformation pathways, key products and main uses.	11
Figure 1-6. Biomass combustion diagram and carbon cycle closed loop.	13
Figure 2-1. Geographical location of the growing areas of oil palm in Colombia.	24
Figure 2-2. Oil production yields of different crops [80].	24
Figure 2-3. Area Harvested and Vegetable oil production in 2012, data source: [86].	26
Figure 2-4. The oil palm tree.	26
Figure 2-5. Fresh Fruit Bunches from Oil Palm crop in Puerto Salgar	28
Figure 2-6. Sterilization equipment used to cook the fresh fruit bunches.	29
Figure 2-7. Palm pressed fiber after kernel separation.	30
Figure 2-8. Price of palm oil in Colombia in the period 2004 – 2014 [78]	32
Figure 2-9. Biodiesel process flow diagram	36
Figure 2-10. Crude palm oil production in Colombia since 2008.	36
Figure 2-11. Simplified palm olein and stearin process flow diagram.	38
Figure 2-12. Oil palm fronds location and its main parts.	42
Figure 2-13. Stages and products in the palm oil production chain including the integration of lignocellulosic residues.	43
Figure 3-1. Gasification facilities around the world.	47
Figure 3-2. Cumulative gasification plants capacity and growth.	48
Figure 3-3. Capacity of produced syngas according the type of feedstock.	49
Figure 3-4. Types of gasifiers.	53
Figure 5-1. Photos of the downdraft gasifier used to produce syngas.	76
Figure 5-2. Gasifier cross section, zones, inlet and outlet streams.	78
Figure 5-3. Process flow diagram of the pilot-scale GEK TOTTI system.	81
Figure 6-1. Pyrolysis curves of the oil palm rachis samples.	95
Figure 6-2. Thermogravimetric analysis at different heating rates.	97
Figure 6-3. Arrhenius plot at 10 K/min for hemicellulose decomposition of oil palm rachis samples.	100
Figure 6-4. Arrhenius plot at 10 K/min for cellulose decomposition of oil palm rachis samples.	100
Figure 6-5. Variation of the volumetric syngas composition with the operation time	104

Figure 6-6. Temperature profile in the gasifier vs time.	106
Figure 6-7. Syngas components change with the reduction temperature.	108
Figure 6-8. Temperature profile along the gasifier	109
Figure 6-9. GEK TOTTI system mass balance for the oil palm rachis gasification experience.....	110
Figure 6-10. Environmental indicators of the biodiesel production process and gasification process using palm oil raw materials.	116
Figure 6-11. Sankey diagram of the oil palm rachis gasification process.	118
Figure 6-12. Sankey diagram of the oil palm rachis gasification process coupled with an gas engine.....	119
Figure 7-1. Block simulated to perform the oil palm rachis gasification simulation	121
Figure 7-2. Molar density of pyrolysis gases as a function of the temperature and pressure.	124
Figure 7-3. Molar composition change of the pyrolysis gas at different temperatures at 1.m.c.a of pressure.....	125
Figure 7-4. Molar composition change of the pyrolysis gas at different temperatures at 15.m.c.a of pressure.....	125
Figure 7-5. Comparison of the pyrolysis constant calculated for the oil palm rachis and wood with the temperature.	126
Figure 7-6. Mass composition of the pyrolysis gases.	126
Figure 7-7. Change of the molar composition in the oxidation zone with the equivalence ratio.	128
Figure 7-8. CO, CO ₂ and H ₂ compositional change with oxidation zone temperature....	128
Figure 7-9. Oil palm rachis gasification process flow diagram.....	131
Figure 7-10. Deviation of the simulated data with the experimental data obtained.	132
Figure 7-11. Effect of the equivalence ratio and feedstock moisture content in the H ₂ /CO ratio at a relative air humidity of 91%.....	134
Figure 7-12. Effect of the equivalence ratio and feedstock moisture content in the H ₂ /CO ratio at a relative air humidity of A) 66% and B) 81%.....	134
Figure 7-13. Effect of the equivalence ratio and feedstock moisture content in the syngas LHV at a relative humidity of 66%.....	136
Figure 7-14. Effect of the equivalence ratio and feedstock moisture content in the syngas LHV at a relative air humidity of A) 81% and B) 90%.....	136
Figure 8-1. Simplified block diagram for the ethanol, lactic acid, xylitol and biogas production using oil palm rachis as feedstock into a biorefinery without heterogeneous catalysis.	140
Figure 8-2. Simplified block diagram for the n-pentane, methanol, ethyl levulinate, ethanol, and lactic acid using oil palm rachis as feedstock into a biorefinery with heterogeneous catalysis.	142
Figure 8-3. Share of the feedstock employed to produce the value-added products proposed in both scenarios.....	149
Figure 8-4. Share of energy consumed by the proposed products in each biorefinery. .	153
Figure 8-5. Plant capacity of scenarios 1 and 2 vs total operating cost.	155

Figure 8-6. Net Present Value of oil palm rachis biorefinery without (scenario 1) and with (scenario 2) heterogeneous catalysis.....	156
Figure 8-7. Biomethane production process with a liquid hot water pretreatment stage.	158
Figure 8-8. Cogeneration system plant.....	160
Figure 8-9. Economic analysis of each scenario according to the OPEX (gray bars) and CAPEX (black line).	164

List of Tables.

	Pág.
Table 1-1. Advantages and disadvantages of bioethanol [66].	18
Table 2-1. Fruit yields and palm oil production in Colombia.	31
Table 2-2. Biodiesel facilities located in Colombia [92]	35
Table 3-1. Main reactions given in the gasification process.	52
Table 3-2. Syngas composition obtained from the gasification of different raw materials.	54
Table 4-1. Standard methods used to perform the chemical characterization of the oil palm rachis.	68
Table 4-2. Standard methods used to perform the proximate analysis of the oil palm rachis.	70
Table 4-3. Standard methods employed to find the ultimate analysis of the oil palm rachis	72
Table 5-1. Main parts of the GEK TOTTI system (10 kW Power Pallet v1.08).	77
Table 5-2. High and Low heating value of main combustible gases into syngas.	85
Table 6-1. Chemical composition of the oil palm rachis.	90
Table 6-2. Chemical composition of solid waste from the oil palm crop in Colombia.	91
Table 6-3. Proximate analysis of the oil palm rachis.	92
Table 6-4. Proximate analysis of different raw materials used in the GEK TOTTI system.	93
Table 6-5. Comparison of the ultimate analysis results for the oil palm rachis samples.	94
Table 6-6. Oil palm rachis pyrolysis data from DTG curve at different heating rates.	98
Table 6-7. Kinetic parameters of hemicellulose and cellulose decomposition at 10 K/min.	101
Table 6-8. Kinetic parameters of hemicellulose and cellulose decomposition at different heating rates	102
Table 6-9. Overall kinetic parameters for the pyrolysis of oil palm rachis at different heating rates.	103
Table 6-10. Operation parameters and results of the oil palm rachis gasification.	111
Table 6-11. Oxides composition of the gasified oil palm rachis.	112
Table 7-1. Reactions and kinetic expressions of the combustion zone	127
Table 7-2. Kinetic model employed to simulate the reduction zone of a downdraft gasifier.	129
Table 7-3. Comparison of experimental data, simulation results and reported data for oil palm rachis gasification.	132
Table 7-4. Points evaluated in the parametric analysis (Box-Behnken based analysis).	133

Table 8-1. Raw material and utilities costs used in the economic assessment.....	148
Table 8-2. Calculated mass yields for each product obtained from both biorefineries. ..	150
Table 8-3. Annualized costs and economic metrics for each biorefinery scenario	153
Table 8-4. Capital investments of both biorefineries to obtain the desired products.	154
Table 8-5. Main characteristics of the simulated gas turbine.....	159
Table 8-6. Mass balances of the cogeneration plant.....	161
Table 8-7. Syngas process mass balances.....	161

List of Symbols.

Symbols with Latin letters

Symbol	Term	Unit SI
\dot{Q}	Heat flow	W/m ²
T	Temperature	K
P	Pressure	Pa
W	Weight	g or kg
ΔH_f°	Enthalpy of formation	kJ/mol
ΔH_r°	Enthalpy of reaction	kJ/mol

Symbols with Greek letters

Symbol	Term	Unit SI
β	Heating rate	K/s

Subscripts

Subscripts	Term
i	Specie i
db	Dry basis

Abbreviations

Abbreviation	Term
M	Moisture
TG	Thermogravimetric curve
TS	Total solids
VS	Volatile solids
VM	Volatile matter
FC	Fixed carbon
DTG	Differential thermogravimetric curve
ODW	Oven Dry Weight
HHV	High heating value
LHV	Low heating value

List of Publications.

Research Papers.

L. V. Daza Serna, **J. C. Solarte Toro**, S. Serna Loaiza, Y. Chacón Perez, and C. A. Cardona Alzate, "Agricultural Waste Management Through Energy Producing Biorefineries: The Colombian Case" *Waste and Biomass Valorization*, pp. 1–10, 2016.

DOI: 10.1007/s1264.

J. C. Solarte Toro, J. P. Mariscal Moreno. B. H. Aristizábal Zuluaga "Evaluation of anaerobic digestion and co-digestion of food waste and grass cuttings in laboratory scale bioreactors". *ION*, 30(1), pp. 105 – 116. 2017.

DOI: 10.18273/revion.v30n1-2017008.

C. A. Cardona Alzate, **J. C. Solarte Toro** and Á. Gómez P., "Fermentation, thermochemical and catalytic processes in the transformation of biomass through efficient biorefineries," *Catalysis Today*, pp. 61 – 72(302), 2017.

DOI: 10.1016/j.cattod.2017.09.034.

J. C. Solarte Toro, Y. Chacón Perez and C. A. Cardona Alzate, "Evaluation of biogas and syngas as energy vectors for heat and power generation using lignocellulosic biomass as raw material". *Electronic Journal of Biotechnology*, 2018. In Press.

Papers under review.

C. A. García-Velásquez, J. A. Martínez-Ruano, **J. C. Solarte-Toro**, A. S. Caballero, E. Carmona, C. A. Cardona, "Effect of the alkaline pretreatment of *Pinus Patula* in the production and economic profitability to biomethane through anaerobic digestion". *Renwable Energy*. 2018. Submitted.

J. C. Solarte Toro, C. A. Cardona Alzate, “Analysis of syngas production using oil palm waste to provide heat and power in non-interconnected zones: The Colombian case”. *Energy*, 2018. Under Review.

J. C. Solarte Toro, C. A. Cardona Alzate, “Pyrolysis kinetic study of Colombian oil palm fronds using thermogravimetric analysis”. *BioResources*, 2018. Under Review

J. C. Solarte Toro, C. A. Cardona Alzate, “Comparison thermochemical conversion pathways for lignocellulosic biomass conversion focused in heat and power generation. *Bioresources Technology*, 2018. Under Review.

J. C. Solarte Toro, C. A. Cardona Alzate, “Techno-economic and environmental assessment of the syngas biomass derived use as chemical platform”. *Energy and Fuels*, 2018. Under Review.

J. C. Solarte Toro, J. M. Romero García, E. Ruiz, E. Castro, C. A. Cardona, “Influence of the dilute acid pretreatment stage optimization in the techno-economic feasibility of bioethanol production”, *Advances in biorefineries*. 2018. Under Review.

J. C. Solarte Toro, J. M. Romero García, J. C. Lopez-Linares, E. Ruiz, E. Castro, C. A. Cardona, “Evaluation of different schemes for antioxidants, lignin and ethanol production using organosolv pretreatment and simultaneous saccharification processes”, *Biomass conversion in biorefineries*. 2018. Under Review.

Book Chapters.

C. A. Cardona, V. Aristizábal, and **J. C. Solarte Toro**, “Improvement of Palm Oil Production for Food Industry through Biorefinery Concept,” *Advances in Chemistry Research*. Volume 32, J. C. Taylor, Ed. Nova Science Publishers, 2016.

C. A. Cardona Alzate, **J. C. Solarte Toro**, J. A. Tamayo, A. Castro Montoya, and B. A. García, “Palm oil for food or biodiesel, A disjunction in tropical countries,” *Advances in Chemistry Research*, J. C. Taylor, Ed. Nova Science Publishers, 2016, pp. 1–36.

J. C. Solarte Toro and C. A. Cardona Alzate, "The environmental Aspects of Bioenergy Production in Peru," in *Paraguay and Peru: Political, Social and Environmental Issues*, Karla Santiago, Nova Science Publishers, 2017, pp: 61 – 97.

J. M. Romero García, C. D. Botero Gutiérrez. **J. C. Solarte Toro**, C. A. Cardona Alzate and E. Castro Galeano. "Environmental Assessment of Biorefineries", in: *Biosynthetic Technology and Environmental Challenges*, Varjani S., Parameswaran B., Kumar S., Khare S. Energy, Environment, and Sustainability. Springer, Singapore, 2018, pp: 377-401.

International conferences participation.

J. C. Solarte Toro, J. M. Romero García, J.C Martínez-Patiño, E. Ruiz Ramos, E. Castro Galeano, C. A. Cardona Alzate, " Techno-economic evaluation of bioethanol production using optimized conditions for the sulfuric acid pretreatment of extracted olive tree biomass". 6th International Conference on Sustainable Solid Waste Management, Naxos, Greece. 13 – 16 June, 2018. (*Submitted*).

J. C. Solarte Toro, J. M. Romero García, J.C López Linares, E. Ruiz Ramos, E. Castro Galeano, C. A. Cardona Alzate, " Prefeasibility assessment of the lignin, antioxidants and bioethanol production using a two-stage organosolv pretreatment and simultaneous saccharification and fermentation process". 6th International Conference on Sustainable Solid Waste Management, Naxos, Greece. 13 – 16 June, 2018. (*Submitted*).

J. C. Solarte Toro, J. M. Romero García, E. Ruiz Ramos, E. Castro Galeano, C. A. Cardona Alzate, "Simulation approach through the biorefinery concept of the antioxidants, lignin and ethanol production using olive leaves as raw material". 21st Conference on Process Integration, Modeling and Optimization for Energy Saving and Pollution Reduction (PRES), Prague, Czech Republic. 2018. (*Accepted*).

D. L. Restrepo Serna, **J. C. Solarte Toro**, J. M. Romero García, E. Ruiz Ramos, E. Castro Galeano, C. A. Cardona Alzate, "Exergy analysis of different bioethanol production

schemes using olive tree pruning as raw material". International Conference on Materials and Energy (ICOME), San Sebastian, Spain. 2018 (*Accepted*).

J. A. Martínez Ruano, **J. C. Solarte Toro**, C. A. Cardona Alzate, "Análisis de pre-factibilidad de la digestión anaerobia y co-digestión de residuos de palma de aceite usando un modelo cinético experimental", 9° Encuentro RedBioLAC, Buenos Aires, Argentina. 2017.

D. Parra, **J. C. Solarte Toro**, Y. Chacón, C. A. Cardona Alzate, "Influence of the pretreatment stage in the biomethane production from different lignocellulosic residues: A techno-economic and environmental assessment", 10th World Congress of Chemical Engineering, Barcelona, Spain. 2017

V. Aristizábal, C. D. Botero Gutiérrez, **J. C. Solarte Toro**, C. A. Cardona Alzate. "Comparison between sugars and syngas for the production of ethanol from lignocellulosic biomass under biorefinery concept", 10th World Congress of Chemical Engineering, Barcelona, Spain. 2017

J. C. Solarte Toro, Y. Chacón Pérez, C. A. Cardona Alzate. "Comparison of biomethane and syngas production as energy vectors for heat and power generation from palm residues: A techno-economic, energy and environmental assessment". 5th International Conference on Sustainable Solid Waste Management. Athens. Greece. 21 – 24 June 2017.

R. A. Tolosa, **J. C. Solarte Toro**, D. L. Restrepo, V. Ramírez, D. Rojas, N. Arias, O. H. Giraldo, C. A. Cardona. "Innovative use of residual biomass from agricultural processes. Case study: Use of Oil Palm and Sugar Cane Bagasse fibers for the improvement of construction materials". 5th International Conference on Sustainable Solid Waste Management. Athens. Greece. 21 – 24 June 2017.

V. Aristizábal, C. D. Botero Gutiérrez, **J. C. Solarte Toro**, C. A. Taimbú, C. A. Cardona Alzate. "Analysis of the improvement of a biorefineries based on sugarcane through the sugarcane bagasse inclusion as raw material". 5th International Conference on Sustainable Solid Waste Management. Athens. Greece. 21 – 24 June 2017.

J. C. Solarte Toro, C. A. Cardona Alzate. "Bioethanol production using synthesis gas from the oil palm rachis gasification". World Sustainable Energy Days. Young Researches Conference. Wels, Austria. 2017

C. A. Cardona Alzate, **J. C. Solarte Toro**, S. Serna Loaiza, G. Aroca Arcaya. "Analysis of the influence of microorganisms recirculation on biorefineries sustainability". XXVIII Congreso Interamericano de Ingeniería Química, Cusco, Perú. 2016.

National conferences participation

J. C. Solarte Toro, C. D. Botero Gutiérrez, C. A. Cardona Alzate, "Comparación técnica y ambiental de la producción de biodiesel a partir de aceite de soja, colza, palma y *Jatropha* en el contexto latinoamericano", 29° Congreso Colombiano de Ingeniería Química y Profesiones Afines, Manizales, Colombia. 2017

Y. Chacón, **J. C. Solarte Toro**, D. Parra, C. A. Cardona Alzate, "Comparación tecnoc-económica de la producción de energía o etanol celulósico a partir de Zoca de café en el contexto colombiano", 29° Congreso Colombiano de Ingeniería Química y Profesiones Afines, Manizales, Colombia. 2017

J. C. Solarte Toro, Y. Chacón, D. Parra. "Diseño conceptual y simulación de Biorefinerías". XXVII ENEIQ: Encuentro Nacional de Estudiantes de Ingeniería Química. Manizales, Colombia. 2017.

Participation of this Thesis in research projects.

Análisis Tecno-económico y Ambiental de Biorefinerías a partir de Residuos Lignocelulósicos con Esquemas de Recirculación de Microorganismos. COLCIENCIAS – CONICYT PCCI140052, HERMES code 23567 (23876).

Evaluación de la producción de gas de síntesis a partir del raquis de palma aceitera para la generación de energía en zonas no interconectadas en el contexto colombiano. COLCIENCIAS Jóvenes Investigadores e Innovadores program, Convocatoria 761 de 2016, HERMES code 35218.

Internships experiences.

Eulogio Castro Galeano. Department of Chemical, Environmental and Materials Engineering; Agrifood Campus of International Excellence. Universidad de Jaén. Campus Las Lagunillas s/n | 23071 - Jaén (España).

German Aroca Arcaya. Pontificia Universidad Católica de Valparaíso, Brasil 2950, Valparaíso, Región de Valparaíso (Chile)

Introduction.

The technological and energy development acquired in recent years has been achieved given the use and application of non-renewable energy sources such as coal, oil and natural gas [1]. In fact, the use of fossil fuels in 2013 represented about 80% of the total energy consumed globally, which is expected to increase by approximately 56% in 2040 due to the accelerated increase in population [2], [3], [4]. However, recent fluctuations in oil prices and environmental damage caused by greenhouse gases (GHG) emissions have stimulated the search for new renewable and sustainable energy sources [5], [6], [7].

Biomass is the most abundant renewable resource in the world. For this reason, it has been used as raw material in different processes related to the production of energy for different sectors (e.g. industrial, transport) and its management has been considered as a fundamental step in the development of sustainable communities [8], [9]. Thus, the importance given to this renewable resource has been able to contribute 9% of the total energy consumed in 2013 [2]. However, biomass has been used in the same way for the production of a wide variety of compounds with high added value (e.g. PHB, lactic acid, citric acid, antioxidants) [10]. Accordingly, the transition from the use of fossil fuels to the use of biomass as the main energy source and value-added products is expected to grow steadily over time [11].

The transformation and exploitation of biomass for the generation of energy and the elaboration of value-added products can be carried out through physical-chemical, biochemical and thermochemical processes [11], [12]. According to the type of processing used to transform the biomass, it can be converted into three main products (i.e. heat and / or electricity, biofuels and chemicals), which could be generated simultaneously from the same material using concepts of sustainable integration framed in the design, development and implementation of biorefineries [13], [14], [15]. A common aspect in the

execution of any technology of exploitation is the inclusion of a pre-treatment stage, which aims to adapt the raw material to improve its performance during the transformation process (e.g. pelletizing, hydrolysis).

Physical-chemical processes are those that do not modify the chemical composition of the raw material, however, make significant changes in its structure in order to improve its properties for the use. On the other hand, biochemical conversion methods employ the fraction of sugars contained in biomass in fermentation processes for the production of biofuels (e.g. bioethanol, bio-butanol, and biogas) [17]. Finally, thermochemical conversion methods consist of the thermal decomposition of the biomass under certain conditions in which the production of solid, liquid and gaseous compounds is encouraged. These are characterized by having an energy content that can be directly exploited [18]. Due to current problems, energy consumption and the techno-economic difficulty of the immediate installation of biochemical processes (e.g. sustainable production of bioethanol and biodiesel) in developing countries, the implementation of thermochemical processes for Energy generation as an effective and efficient solution for mitigating the environmental damage generated by the use of fossil fuels [11], [19].

Biomass gasification is one of the thermo-chemical processes that has taken a big rise in recent years due to its ease of scaling and the ability to generate energy in a decentralized way with high economic yields [9]. This process consists of the partial oxidation of biomass in the presence of a gasifying agent (i.e. oxygen, air and water vapor) in a temperature range between 700°C and 1300°C. The most important product obtained from the gasification process is a mixture of combustible gases called synthesis gas, which can be applied directly in internal combustion engines for power generation or used as a chemical platform for the production of ethanol, diesel, Fuels for airplanes, methanol and different additives [20], [21].

According to the above, the main objective of this work is based on the technical, economic and environmental evaluation of the production of syngas in a downstream fixed lab bed gasifier from the oil palm rachis and, in its use as a chemical platform for obtaining value-added products as well as heat and power.

Thesis Hypothesis.

The oil palm rachis allows obtaining economically syngas with low environmental impact in order to use it as an energy platform in the industry

Thesis Objectives.

General Objective.

To evaluate, from the technical, economic and environmental point of view, the production of synthesis gas from the gasification of the oil palm rachis.

Specific Objectives.

- To perform the physical-chemical characterization of the oil palm rachis.
- To evaluate experimentally the production of synthesis gas from the gasification of the oil palm rachis
- To model and simulate the gasification process of the oil palm rachis to obtain synthesis gas.
- To simulate the production of value-added products from the synthesis gas.
- To compare the synthesis gas with natural gas as a bioenergy platform in the Colombian context.

1. Energy vectors from biomass.

The production of energy from renewable resources has increased in the last years as consequence of the excessive fossil fuels use. Biomass is the most abundant renewable resource that can be used directly to produce energy. Thus, this one is considered as a primary energy source. However, high quality products obtained by applying processes such as refining, fermentation, thermo-processing and mechanical treatment are called secondary energy sources or energy vectors, which are considered as the new base to produce chemicals, heat and power without affect the environment.

1.1 Energy supply overview.

Nowadays, fossil fuels have been the main energy sources used to supply a great quantity of needs in the daily life. These ones are burned to generate electricity, used to produce energy to internal combustion engines and, employed for heating and cooling. On the other hand, mostly of chemicals, medications, fertilizers, cosmetics, polymers and so forth are produced from fossil fuel derivatives [1]. Therefore, it is easy to conclude that fossil fuels are one of the most important pillars in our day-to-day functions and development.

In 2015, an estimated 78.4% of global energy consumption was provided by fossil fuels [2]. This value demonstrates that our society has an economy based on non-renewable resources that can at any moment be exhausted causing a great variety of problems from economic, political and environmental point of view. Besides, the use of this type of resources provides an apparent energy security because we have these resources today, but we do not know if tomorrow will be like this [1]. Therefore, it has been necessary to search other energy sources to avoid or prevent any problem in a near future due to the progressive increase of the energy consumption in the world [3].

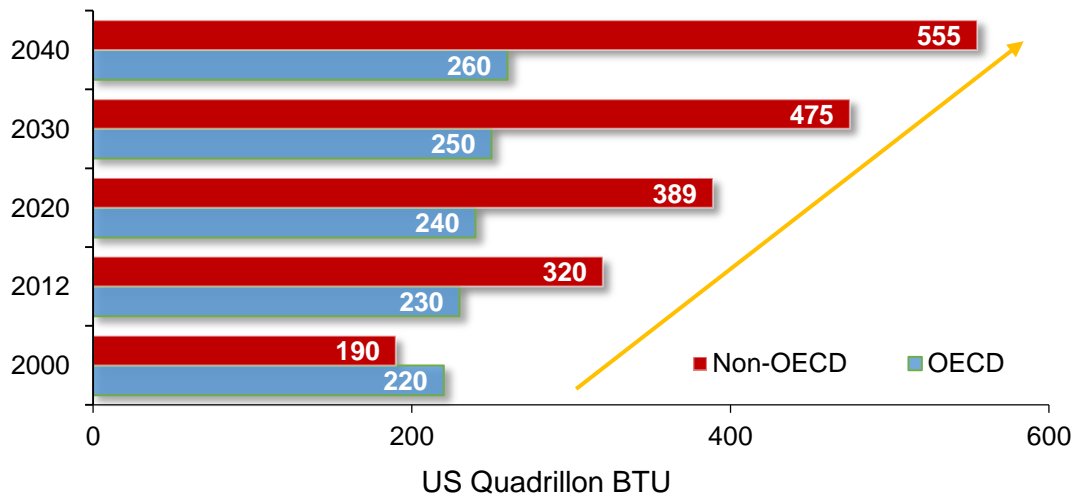


Figure 1-1. World energy consumption 2000 – 2040 [3]

As can be seen in **Figure 1-1**, the total energy consumption in the world will increase 30% from 2020 to 2040 where non-OECD countries such as Argentina, Brazil, Chile and Colombia will consume more than a half of the total energy in the world. This increase in the energy consumption is attributed to the accelerated population in the last years [4], [5].

The share of crude oil, natural gas and coal, the main energy sources produced in the world, has been stable lately. Nevertheless, some changes in the net production and consumption of these ones have been registered in their statistics. In the crude oil case, its global consumption growth 1.6% in 2016 (i.e. 1.6 million barrels per day) while the production only increased 0.4%. On the other hand, a 0.5% growth in worldwide natural gas production was recorded last year, while a consumption of this energy source increased 1.5% (i.e. 63 billion cubic meters) the same year. At last, coal statistics related on consumption and production decreased in 2016 because its direct combustion generates a great amount of carbon dioxide (CO₂), carbon monoxide (CO) and particle matter, which are considered air pollutants and greenhouse gases. As a result, the coal consumption fell 1.7% as well as its production in 6.2% (i.e. 231 million tonnes of oil equivalent). The production and consumption of crude oil in the last years are presented in **Figure 1-2**.

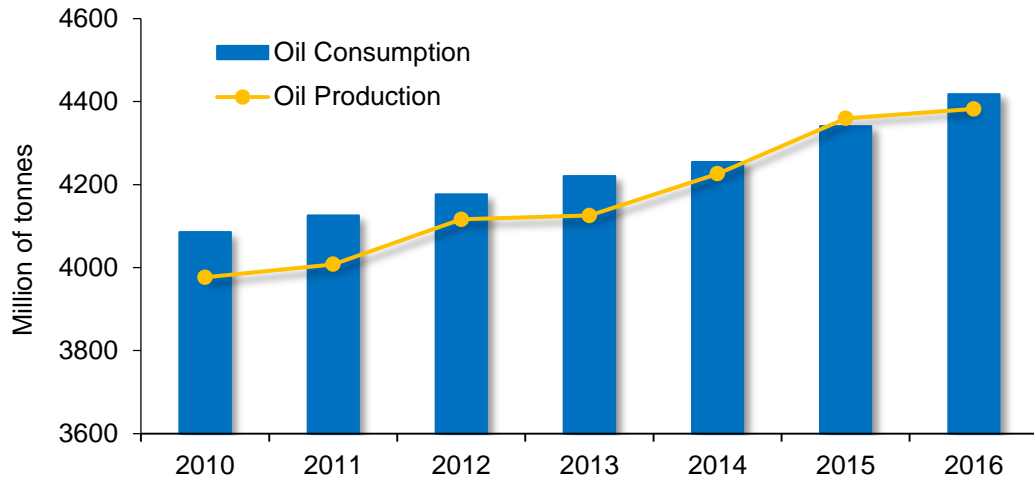


Figure 1-2. Worldwide oil production and consumption [6].

The growth in the oil production and consumption showed in **Figure 1-2** has contributed to most of the world progress in industry, transport and urban development [7]. Nevertheless, some issues identified by international organizations such as global warming, environmental detriment and energy security have been related with this actual oil-based economy [8].

The main environmental problems caused by the use of fossil fuels are the natural resources pollution (i.e. air and water), land desertification and greenhouse gases emissions (GHG) [9], [10]. The last one can be evidenced in the net carbon dioxide emissions increase in the last years. In 2015, the net emissions were 31,760 million metric tonnes (MtCO₂), which were 13.54% higher than its historical average from 2000 [11]. The main regions that contribute to carbon dioxide emissions are Asia, North America and Europe with the following shares: 46.59%, 17.96% and 11.52% [12]. The above has had different consequences that are mentioned below:

- ✓ Ice is melting all over the world
- ✓ The rise of sea level during the last century has been faster.
- ✓ The average rainfall (rain and snow) has increased across the globe.

Another issue associated with the continuously fossil fuels use is the energy security. This term can be defined as the continuous and enough energy supply to the population

through an efficient, safe and quality system avoiding any risk that can affect the development of daily activities. [1], [13]. Thus, energy security can be achieved if the statements listed in **Figure 1-3** are accomplished.

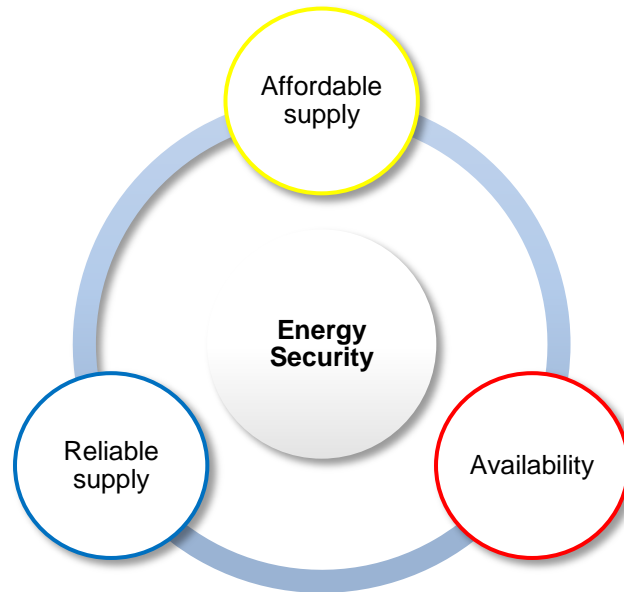


Figure 1-3. Energy security concept.

The main three components to ensure energy security showed in **Figure 1-3** are: affordable supply, reliable supply and availability. To accomplish these items, it is necessary to change international and national policies related with technical, logistical and social subjects. Therefore, guarantee an uninterrupted energy supply using self-contained and self-supporting energy systems is practical impossible for any country in the world. Even, if this were possible, it would involve a complete isolation from the outside world, which is not convenient. [1], [14].

Energy security has been considered as one of the main issues associated to our dependence of fossil fuels as energy source due to great part of the world economy depends on the crude oil prices. Then, the instability of their price have been considered as a risk factor in many countries [6]. Therefore, new energy sources that can be used without affect the environment are the most suitable option to reduce our oil dependence and diversify the energy market.

In accordance with the above problems associated to the continuous use of fossil fuels, the energy production from renewable sources such as wind, water, sunlight, biomass and solid waste have been studied. For this reason, the implementation of alternative technologies to use these resources has been considered as an opportunity to strengthen the energy basket of any region in the world. However, factors such as location, availability and economy could influence the use of these renewable resources. In this way, renewable energy production boom began given the consequences of fossil fuel use and it has increased over the years. Hence, a 224% growth of the electricity from renewables since 2012 to 2040 is expected as can be seen in **Figure 1-4**.

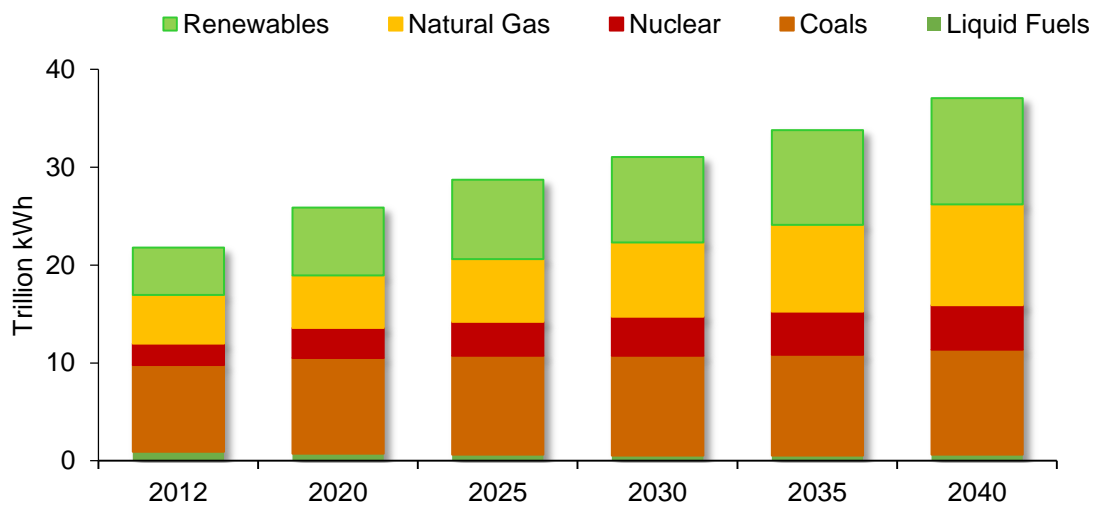
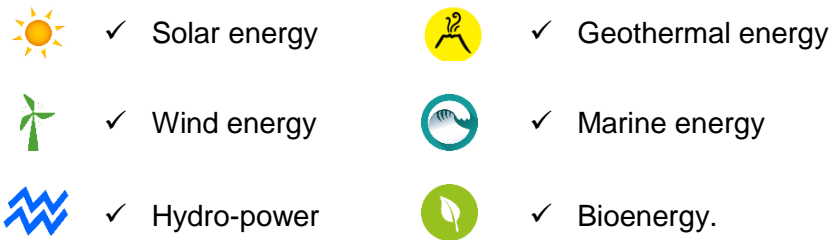


Figure 1-4. World net electricity generation by energy source [15].

The energy produced from renewable resources is called renewable energy and it has many definitions. However, the International Energy Agency (IEA) provides the following explanation “*Renewable energy is energy that is derived from natural processes (e.g. sunlight and wind) that are replenished at a higher rate than they are consumed. Solar, wind, geothermal, hydropower, bioenergy and ocean power are sources of renewable energy. The role of renewables continues to increase in the electricity, heating and cooling and transport sectors*” [16], [17]. Thus, renewable energy can be divided according to the source used to produce it as is observed below:



The above mentioned renewable energy forms supplied 19.25% of the worldwide energy demand in 2015. Besides, 8.9%, 4.2%, 3.9% and 1.4% were related to biomass use, geothermal energy, hydropower and wind energy, respectively. According with this information, it is possible to observe that the highest share of energy produced comes from bioenergy. Hence, this result indicates that bioenergy is the most accessible type of renewable energy in the world [18].

Bioenergy is a concept that has many definitions given by different authors [19], [20]. However, an inclusive definition is given in this work taking into account an exhaustive revision of this term: “*Bioenergy is the renewable energy generated from any type of biomass. This one can be generated from chemical, biochemical and thermochemical pathways as long as its production and application are feasible from technical, economic and environmental point of view*” [20]–[22]. Thus, the bioenergy concept is supported in the biomass use with energy purposes. However, it is necessary to establish the type of energy vector that is more convenient to produce according to the main biomass features as well as its main trade and logistical characteristics.

As was mentioned above, bioenergy comes from the use of biomass as renewable resource that can be used to produce energy vectors (i.e. bioethanol, biogas). Though, this one also is used to produce chemical platforms (i.e. syngas, bio-butanol) and chemical products directly (i.e. antioxidants, PHB). Biomass is generally classified taking into account different approaches. Nevertheless, the most recognized classification divides biomass in three categories: First, Second and Third Generation [23].

First generation biomass comes from edible crops such as corn, sugarcane, cassava and oil palm [24], [25]. Second generation biomass derives from agro-waste, non-edible crops, forestry residues and the organic fraction of municipal solid waste (OFMSW) [23], [24]. To close, third generation biomass is all organic matter derived from the use of algae. From

the above mentioned categories, the most employed type of biomass is the second generation biomass because of the use of first generation raw impact, at all levels, the food security of a country due to the competition on the natural resources that are available in a region (i.e. land and water) [26], [27].

Second generation biomass has had great application in the last years in many productive sectors such as heating, cooling and transport [28]. For this reason, its use, as raw material to obtain energy directly or indirectly, has been the most representative option of developing countries to increase their independency of fossil fuel at least in some productive sectors. Therefore, it is important to establish its chemical composition and energy content with the aim to define the most suitable application for it. Next, a brief review of the processes implied in the transformation of biomass into energy vectors as well as value-added products is performed.

1.2 Paths for energy vectors production.

There are different methods to convert biomass into useful products such as chemicals and energy vectors. Nowadays, great quantities of wastes and energy crops have been used for power, heating and cooling production. Even, these feedstocks can be transformed into gaseous and liquids fuels to be employed in different productive sectors [29]. Nevertheless, biomass conversion technologies have not been well-established and they are considered as bioenergy production focus that later can achieve a fully commercial scale [30], [31]. Therefore, a set of conversion processes are maturing rapidly as is the case of the production of synthetic natural gas (SNG) from syngas via heterogeneous catalysis [32].

Biomass can be transformed through different pathways that include the implementation of biochemical, thermochemical and chemical processes [33], [21]. Each one represents, globally, a technologies group to convert, extract or upgrade the main biomass components (i.e. cellulose, hemicellulose, lignin and antioxidants) [34]. Additionally, it must be taken into account that the biomass productive chain not only includes its transformation in a chemical facility, this one also includes the feedstock producers and all the logistic necessary for its transportation and storage [2], [35]. Thus, the biomass

productive chain could be established in developed and developing countries in a near future because of the entire infrastructure has been growing and consolidating over the years.

In 2016, other type of biofuels (e.g. biogas & biomethane) have been researched and implemented in some regions of the world to demonstrate that it is possible to produce different energy vectors [36]. The goal of producing and commercializing other biofuels different to bioethanol and biodiesel has been supported in the three following reasons. The first one is to find new secondary energy sources that can provide higher carbon savings in its life-cycle [37]. The second one is to produce biofuels from other sources (e.g. lignocellulosic residues and organic waste) different of energy crops to decrease the land use, reduce the competition for food or productive agricultural land [5]. Finally, The third one is to decrease the fossil fuels use through the production of biofuels that can be blended in high proportions with fossil fuels, even, used directly to avoid a technical change in most of the energy systems employed in the industrial and transport sectors [2], [6], [15].

A wide variety of pathways are being researched produce advanced biofuels such as methanol, ethanol, butanol, jet fuel and fuel additives (e.g. ethyl levulinate) integrating different branches of knowledge from an array of feedstocks. An example of the above mentioned is the inclusion of heterogeneous catalysis in the light and heavy hydrocarbons production using the main biomass components via dehydration and deoxygenation of them.

The main paths used to convert biomass into chemicals, biofuels, heat and power is presented in **Figure 1-5**, which shows three levels. The first level surrounded by a green dashed line shows the different biomass processing lines derived from the main knowledge branches which are chemical, thermochemical and biochemical processes. The second level delimited by a yellow dashed line shows the main products that can be obtained from the processes named in the above level. Finally, the third level that is enclosed by a red dashed line shows the main applications in which the above products can be used. Following, a brief description of each one of the biomass processing lines is done.

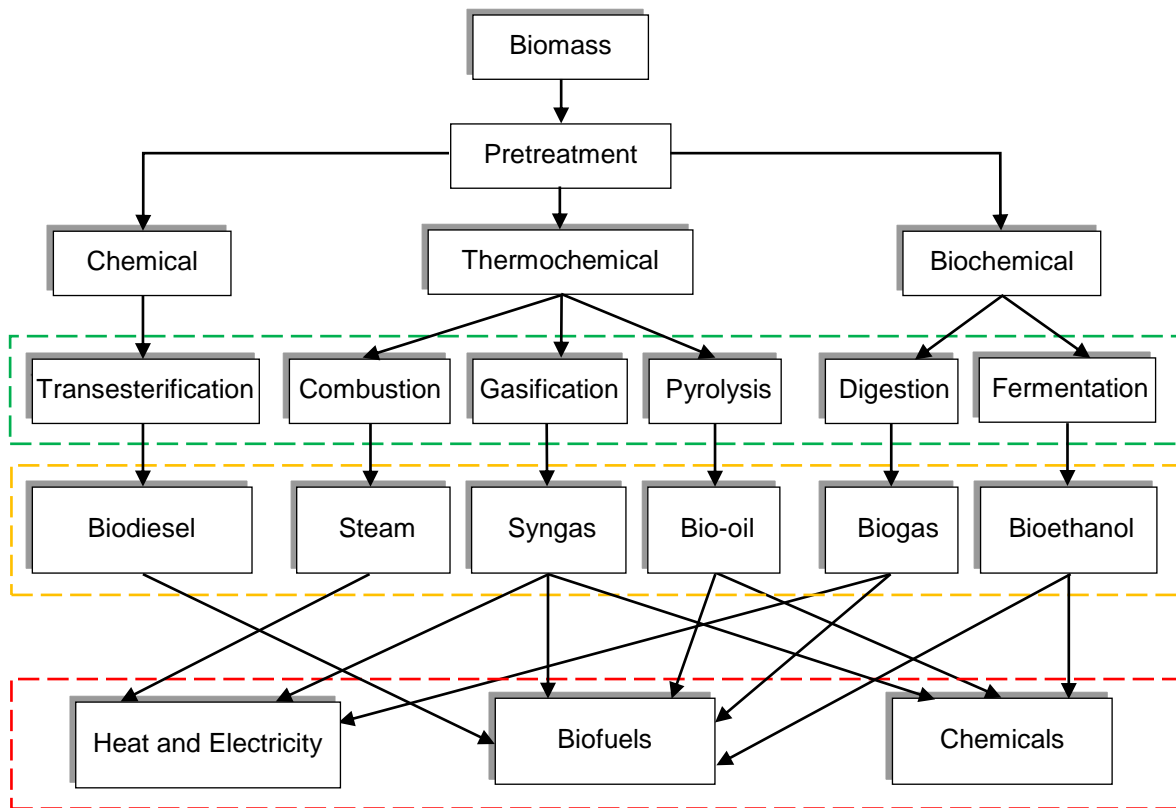


Figure 1-5. Biomass transformation pathways, key products and main uses.

The ***transesterification*** process comes from the chemical route. In this process, a hydroxyl group of an ester is substituted by another alcohol in presence of an acid or alkali ion. Indeed, this reaction can be considered as the simplest example of a nucleophilic substitution [38]. Thus, biodiesel is produced through this process using as raw material edible and non-edible oils as well as alcohols like methanol, ethanol, propanol, butanol and amyl alcohol. However, methanol and ethanol are most used due to their low cost and physicochemical advantages [39], [40]. Transesterification can be classified as a reversible reaction. Consequently, this process requires the presence of a catalyst (i.e. strong acid or base) that accelerates the reaction rate to achieve more quickly the highest conversion as be possible. In addition, an excess of alcohol is necessary to shift the equilibrium towards to the desired ester formation [41].

As was mentioned above, edible oils can be used to perform the transesterification reaction due to these ones represent a sustainable and cheap raw material that can be available in all countries, specially, tropical countries. Nevertheless, their use has been

criticized due to the disjunctive between food security and the biodiesel production. Therefore, the use of fats and other oil sources (e.g. algae) has been growing [42].

Combustion is a thermochemical process applied widely at industrial level that is carried out in a temperature range between 600°C – 1000°C. This option is employed to provide heat, power or both, using a cogeneration system, for small scale or large scale applications. Then, biomass combustion can be considered as a link between a renewable resource and sustainable utilities such as heat, refrigeration, shaft power and electricity [18]. Thus, the combustion process consists on the burn of a fuel (i.e. biomass, natural gas, oil, coal, anthracite, and kerosene) with an excess of air to release the stored chemical energy in heat form using different equipment such as burners, boilers, internal combustion engines (ICE) and gas turbines [43]. In steady and normal conditions ($T=25^{\circ}\text{C}$ and $P=101.325\text{ kPa}$), biomass combustion only releases carbon dioxide (CO_2) and water vapor. However, various problems in biomass combustion must be improved. These problems include the impacts in the human health and the environmental impact due to the damage in productive ecosystems of the earth [44].

To understand the biomass combustion is necessary take into account that this process only generates two product streams. The first one is a mixture of hot gases composed by carbon dioxide (CO_2), carbon monoxide (CO), nitrogen oxides (NO_x) and sulfur compounds (H_2S) and the second one is a solid residue called ash that is composed by mineralogical compounds (e.g. SiO_2 , Al_2O_3 , K_2O) and unburned material. This process is considered as a neutral source of carbon because the carbon monoxide released to the atmosphere is captured by new biomass through the photosynthesis process. **Figure 1-6** shows the biomass combustion diagram and the carbon cycle closed loop.

The biomass combustion process starts with a temperature increase of solid fuel through direct heat to produce a mixture of gases (i.e. carbon monoxide and hydrogen), volatile liquids and char (i.e. coal burned). In this stage, the volatiles rate production is a function of the process temperature (T) and heat flux (\dot{Q}) supplied. Also, a liquid and solid phase appears, however their relative quantities decrease. At the final of the process, only compounds that have volatilization points higher than the process temperature remain as unburned solids and ashes [30].

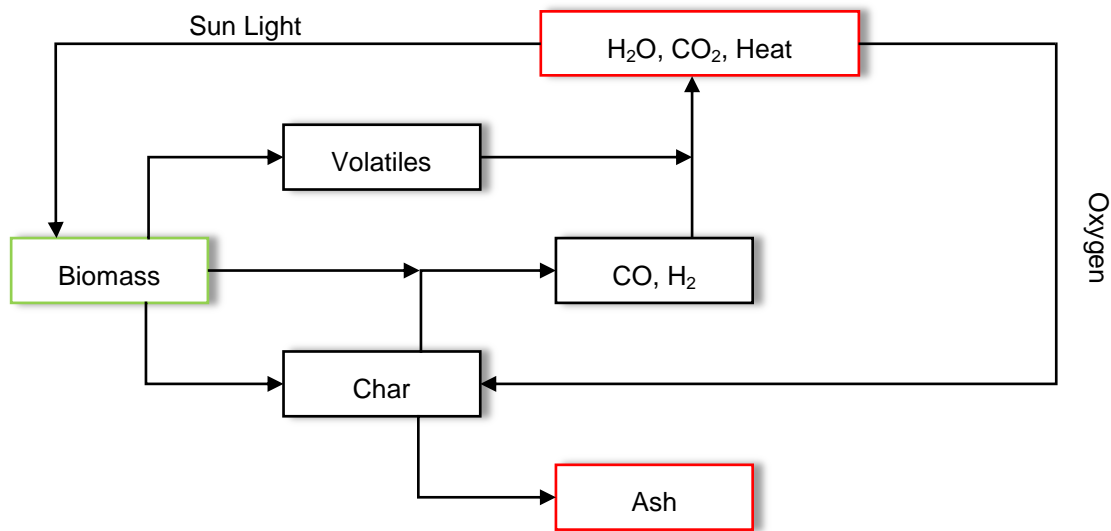


Figure 1-6. Biomass combustion diagram and carbon cycle closed loop.

Gasification can be defined as a process that converts carbonaceous materials from a wide variety of sectors (e.g. petrochemical and forestry) into a mixture of gases commonly called as product gas or synthesis gas (syngas), a mixture of heavy hydrocarbons called tars and a solid fraction known as char, which includes the non-converted fraction and feedstock minerals. Therefore, the gasification process generates three products in different phases. However, their mass distribution depends on the operational conditions. Common temperatures reached in biomass gasification facilities vary from 700°C to 900°C [45].

The conversion process is carried out with a gasifying agent or carrier. The commonly gasifying agents are: air, steam and oxygen. In the last years, the gasification process has been considered as a way to extend and speed up the use of agro-waste, forestry residues and municipal solid waste to produce energy and to decrease problems related with their disposal and use. On the other hand, the biomass gasification process has been encouraged by the same reasons that boost the liquid biofuels production (i.e. continuous increase in oil prices and environmental issues) [46].

As was mentioned above, other products formed in the gasification process are char and ash. The first product consists of a mixture of unconverted organic fraction and its

composition depends of the quantity of organic carbon present in the feedstock or lignocellulosic material. Its low heating value (LHV) varies from 25 to 30 MJ/kg according to the mass fraction of unconverted material. The second product is the ash, which is composed by oxides such as SiO_2 , Al_2O_3 , FeO , MnO_2 . The quantity and quality of ash depends on the treatment that the biomass has had and the operating conditions of the process. [47].

The gasification process has been considered as a technology that can replace the combustion process in thermochemical facilities due to this process also can be used to provide energy directly applicable (i.e. electricity). Even so, aspects related with its economy have generated various opinions in the energy sector [48]. Gasification reactions take place in a reactor, so-called gasifier. Inside of it, without matter its design, several reactions occur simultaneously, which have not been fully established by the scientific community due to the process complexity. Nevertheless, the main reactions that have been identified in this process are those between the gas phase and solid fuel [49].

The above was a brief overview about biomass gasification, but in following chapters will be possible to find more information related with this process.

Pyrolysis is the third option for biomass conversion via thermochemical processing. This process is carried out under anoxic conditions in a temperature range that varies from 300°C to 600°C. The main products that can be obtained from this thermochemical process are char and bio-oil. Nevertheless, the heating rate determines which of the above mentioned products will be obtained in high proportion. When the pyrolysis process is carried out to produce char, this process is known as slow pyrolysis (i.e. low heating rate). On the contrary, if bio-oil is the objective, the pyrolysis process is called fast pyrolysis (i.e. high heating rate) [46].

Bio-oil production from fast pyrolysis process has been researched due to this mixture of hydrocarbons can be used to produce liquid fuels and minerals using catalysis and process intensification technologies. In addition, this product offers some advantages respect to the biomass such as lower transport costs, reduced storage costs and easy conveying into reactors. Its high heating value (HHV) varies from 16 to 19 MJ/kg and can be processed to obtain n-hexane soluble compounds, dichloromethane (DCM) soluble

compounds and water soluble compounds [46]. Finally, this process increases the calorific values of its products via deoxygenation and re-condensation reactions [10].

Fermentation can be defined as a set of chemical reactions carried out by living or non-living elements (isolated enzymes). In this process, an organic compound is partially oxidized in absence or presence of oxygen. The biological function of the fermentation process is to obtain energy to satisfy all the cell needs. Moreover, this process can be classified according to the final products obtained. Some types of fermentations are alcoholic, lactic, mixed acid, butyric, propionic and ABE.

The fermentation process is widely applied in biotechnology to obtain a great variety of products at industrial level. The most common is the bioethanol that is produced as alternative fuel. However, other products that are obtained via fermentation are butanol, lactic acid and malic acid [50]. In normal conditions, the fermentations process is carried out at mesophilic temperatures (i.e. 30°C – 40°C) at pH conditions close to neutrality. This process has been developed at industrial level in different configurations such as air-lift, continuous, batch and, even, it has been integrated through process intensification in the so-called simultaneous saccharification and fermentation (SSF) process [51], [52].

There are many feedstocks that can be submitted to the fermentation process to obtain the above mentioned products. Starch materials and feedstocks with high sugars content are preferred to ease the process. Nevertheless, materials such as lignocellulosic biomass have been used in this process if a pretreatment stage is included in the process line [36]. Finally, in the open literature is possible to find a lot of information related with this topic [53], [54]

Anaerobic digestion is a process that can be defined as a complex sequence of chemical reactions where organic matter is degraded and stabilized through different metabolic routes carried out by a microorganism consortium in a free-oxygen environment [55], [56]. Four stages have been identified in the anaerobic digestion process: hydrolysis, acidification, production of acetate and production of methane. These steps are interrelated and depending on the substrate employed for biogas production anyone can be considered as a limiting step in this process [57].

The main product of the digestion process is a gas mixture composed mainly by methane (CH_4), carbon dioxide (CO_2) and nitrogen (N_2). Nevertheless, hydrogen sulfide (H_2S), ammonia (NH_3), hydrogen (H_2) and carbon monoxide (CO) are other trace gases that are present [58]. Furthermore, the so-called raw biogas is saturated with water and it has other impurities like dust particles and siloxanes [55]. Other product from the anaerobic digestion process is a wet solid or liquid that has the potential to be used as fertilizer called digestate. However, a conditioning process must be done to avoid any risk in its use [59].

The anaerobic digestion process must meet some basic conditions to ensure efficient substrate degradation. The conditions are related with typical operating parameters considered in biotechnological processes such as temperature, pH, nutrients supply (C/N/P ratio) and redox potential [55]. Moreover, important features related with the substrate employed as feedstock also must be known. These features are the total solids (TS) and volatile solids (VS) content, carbon to nitrogen ratio (C/N), theoretical methane yield, biochemical methane potential (BMP) and surface area [60], [61]. Commonly, this process is carried out at mesophilic conditions ($32^\circ\text{C} - 42^\circ\text{C}$), pH values between 5.2 and 6.3, C/N ratio between 10 – 45 and redox potential between +400 mV and -300 mV. These variables and values allow designing a well-supported digestion process without drawbacks in biogas production [55]. However, the anaerobic digestion process can be performed at low and high temperatures which are called psychrophile and thermophile digestion respectively.

This process at industrial level can be carried out using one-step or two-step reactors with one-phase or two-phases in batch or continuous mode with and without liquid phase recirculation [62]. However, the reactor type and design must take into account the above mentioned feedstock characteristics. Once biogas has been produced, it can be cleaned to increase its heating value and applications range. Current biogas upgrading technologies employed are absorption, adsorption, membrane separation and cryogenic separation. Each one has different advantages and disadvantages related with its energy requirements, solvents employed, fixed and variable costs [58], [63]. In addition, these technologies are considered relatively mature.

1.3 Energy vectors obtained from biomass processing.

In the previous section was possible to observe that there are a lot of processes to convert biomass in different energy vectors (e.g. gasification, anaerobic digestion and fermentation). Furthermore, it is possible to perceive that the above mentioned processes excluding the transesterification are applied to second generation biomass. This is important because demonstrates that the use of first or third generation biomass has been encouraged in the last years. The following energy vectors are derived from this type of biomass, which normally, it is possible find in the three states of matter: Solid, Liquid and Gaseous.

1.3.1 Bioethanol.

Bioethanol is an energy vector obtained through the fermentation of sugars using several microorganisms (e.g. *Saccharomyces cerevisiae*, *Zymomonas Mobilis*, *Escherichia Coli*) and it is considered as one of the most important liquid biofuel produced at industrial level. This one has a well-established market in transport sector and its implementation to be blended with gasoline, as oxygenating agent, has been successful [64]. Its production together the biodiesel production generate around of 1.7 million of jobs. Then, the liquid biofuels production has the second place in terms of employment generation being the solar photovoltaic the first place [65].

When gasoline is compared with this biofuel some differences can be analyzed. First, the low heating values (LHV) of gasoline and bioethanol are 41.3 and 21.2 MJ/kg, respectively [66]. Thus, gasoline provides more energy than bioethanol. Second, the octane number of the bioethanol (109) is higher than the octane number of the gasoline (91), which indicates that the bioethanol has better antiknock characteristics than the gasoline. Therefore, the use of bioethanol in internal combustion engines improve its efficiency [66] and third the Reid vapor pressure of the gasoline is higher than the bioethanol. However, the above implies that the gasoline has more evaporative emissions, which increases the risk of explosions. Finally, the use of bioethanol in place of gasoline reduces the carbon monoxide emissions and it does not pollute water sources [67].

On the other hand, bioethanol has several applications in the chemical industry. This one can be used as additive in paints, to produce perfumes and deodorants. Even, bioethanol could be used as antiseptic agent. However, its main use has been concentrated as biofuel due to the current environmental problems mentioned by the use of fossil fuels. The use of bioethanol as renewable biofuel has many advantages and disadvantages, which have been discussed by many authors [66], [68]. **Table 1-1** resumes the main positive and negative aspects of this liquid biofuel.

Table 1-1. Advantages and disadvantages of bioethanol [66].

Advantage	Disadvantage
- Ethanol is a renewable biofuel that can be used in internal combustion engines without major modifications	- Ethanol has a lower calorific value than the gasoline. Therefore, it offers less power.
- Diversification of the energy basket and increase of the energy security in those countries that produce it.	- Ethanol is produced using starch based material and energy crops. Therefore, large amounts of land are required.
- No toxic, low emissions and high biodegradability.	- The start of vehicles at low temperatures is difficult when ethanol is used as fuel.
- Ethanol combustion close the carbon cycle of the biomass employed to produce it.	- Engine modification could be necessary, if high ethanol concentrations are employed in current engines.

1.3.2 Biogas/Bio-methane.

Biogas is a mixture of gases. However, the main gases that compose the biogas obtained by the anaerobic digestion of lignocellulosic biomass are methane (CH₄) and carbon dioxide (CO₂). The methane concentration depends on the amount of fats, proteins and carbohydrates added in the anaerobic digester. Generally, raw biogas has a methane concentration higher than 50% and lower than 70%. On the other hand, carbon dioxide

has a concentration higher than 30% and lower than 45% [69]. The high heating value of methane is 37.78 MJ/m_n^3 . Therefore, raw biogas has an energy content between 19 MJ/m_n^3 and 26 MJ/m_n^3 or 6.0 kWh/m_n^3 and 6.5 kWh/m_n^3 , which can replace 0.65 liters of crude oil [55].

Raw biogas has a limited applications range due to the presence of trace compounds that can have a negative effect on equipment dedicated for biogas utilization. Thus, compounds such as hydrogen sulfide (H_2S), ammonia (NH_3), water vapor (H_2O), nitrogen (N_2) and siloxanes must be avoided with the goal to guarantee an appropriate biogas use [58], [70]. Some effects caused by the above mentioned impurities are the corrosion of pipelines, decrease of the biogas calorific value and the undesired products formation such as NO_x and SO_2 after a combustion process.

Biogas can be upgraded through purification technologies to biomethane. This one has similar applications than the natural gas. Thus, its main application is the energy production in cogeneration facilities. In addition, the biomethane not only is important as a renewable energy carrier but also as a renewable chemical platform due to the well-defined routes to use methane as feedstock. Therefore, it can be converted in syngas that is the basis for obtaining fuels such as methanol, dimethyl ether, and hydrogen.

1.3.3 Biodiesel.

Biodiesel is an alternative diesel fuel. It is obtained from renewable biological sources such as vegetable oils and animal fats. This biofuel is nontoxic and environmentally beneficial [71]. Some features that have made biodiesel a possible solution to environmental problems in recent decades are its ability to reduce emissions of unburned hydrocarbons, carbon monoxide (CO), and particulate matter and sulfur oxides. Moreover, the production of biodiesel stimulates planting high yield oil crops, which reduces importations of vegetable oils. Finally, this alternative offers security and energy independence in the transport sector [72].

The physicochemical properties of this biofuel are similar to those present in the diesel obtained from oil. Hence, it can be used in internal combustion systems. However, currently biodiesel is not used in pure form but in mixtures ranging from 5% to 35% [64]. The commercial used mixtures are 5% and 20% by volume (i.e. B5, B20).

The environmental benefits of the use of biodiesel have been evaluated quantitatively through a life-cycle assessment (LCA). Sheehan et al [33] established an inverse relationship between the environmental impact caused by the use of biodiesel and the percentage in this mixture with diesel oil. Therefore, in the case of using pure biodiesel (B100), the use of fossil fuels will decrease 95% and in the case of using blends of 20% biodiesel (B20) the use of fossil fuels will decrease only by 19%. Carraretto et al [73] reported that about 0.72 kilograms of carbon dioxide are released per kilogram of used biodiesel and about 0.82 kilograms of carbon dioxide are released per kilogram of burned diesel, demonstrating the positive impact on the environment provided by the use of biodiesel.

1.3.4 Wood pellets.

Wood pellets can be considered as another source of energy for heating and cooling as well as to produce power in some facilities. Therefore, these ones can be considered as an alternative product to oil. Wood pellets are characterized by have a cylindrical shape. Pellets are produced by grinding wood residues under high pressure through a hammer mill and then compressing the sawdust in a pelletizer die. Wood pellets have relatively low moisture content, 7-12%, high density, 1100-1500 kg/m³ and an energy content of 4.7-5.0 kWh/kg. Moreover, they have an ideal behavior as feedstock for thermochemical applications due to these ones are easy to store and transport [74].

The wood pellets market has grown in the last years, especially in Europe to be applied in low scale cogeneration systems [2]. The use of wood pellets has wide variety of advantages related with a wide variety of factor, which are briefly mentioned [75].

- Wood pellets are a renewable resource of energy. Therefore, it can be considered as a neutral energy source.
- The wood pellets are cheaper than oil. This difference is more significant when wood pellets are used in household applications.
- In general terms, the wood pellets market is stable in most of the countries that produce it. Therefore, this energy source can offers more long-term stability than

the use of fossil fuels (e.g. natural gas) in household applications. Nevertheless, there are some exceptions as is the case of Northern Ireland.

- Wood pellets are considered as an accessible energy source in Europe, especially in countries as Austria.

The above advantages of the wood pellets use as energy source should be compared with the following disadvantages to consider their use [75].

- Wood pellets industry is dedicated to household applications only for heating. Therefore, its use at large scale still is restricted.
- The maintenance and labor time associated with the wood pellets use is one the major drawbacks of this energy source.
- Wood pellets production could represent an environmental problems due to the wood extraction from forest. Thus, the unsustainable use of wood could cause degradation of watershed and catchment areas as well as a loss of biodiversity and habitat.
- The total capital investment associated with the wood pellets use is high due to the current technologies to provide heat are designed to use fossil fuels as natural gas or gasoline. Therefore, the wood pellets use requires a technological change.

Finally, it is possible to conclude that wood pellets are a renewable energy source that needs to overcome the above mentioned disadvantages. In addition, it is possible to observe that the main market associated with this energy source is the heat generation.

1.3.5 Synthesis gas (syngas) or producer gas

Producer gas, product gas or synthesis gas (syngas) are common names to describe the mixture of gases obtained from the biomass gasification. This product gas is composed by hydrogen (H₂), carbon monoxide (CO), methane (CH₄) and traces of carbon dioxide (CO₂). This gas can be used to produce heat and power in thermochemical facilities through its implementation in cogeneration plants. In addition, syngas is susceptible to be subjected in catalytic processes to obtain liquid biofuels. However, the quality of the gas is a key factor that determines the syngas use. Thus, impurities such as nitrogen (N₂), hydrogen sulfide (H₂S) and hydrochloric acid (HCl) must be avoided. Different

experiences on gasification have demonstrated that the heating value of the syngas can range between 4 MJ/ m_n³ to 28 MJ/ m_n³ [76], [77].

1.4 Final Remarks.

The use of fossil fuels has caused many environmental damages and its use has produced an oil-based economy that needs to be reduced. For this reason, the use of renewable resources will be important in a near future due to these ones give more energy security. Thus, the bioenergy is and will be the most important energy form that can be produced by any country. Therefore, the use of biomass to produce it and its administration is a fundamental factor that allows the consolidation of second generation biomass as raw material to supply our energy needs without affect aspects like energy security.

On the other hand, there are many energy vectors that can be produced from lignocellulosic biomass. However, its production depends on the real needs that must be satisfied. Thus, bioethanol and biodiesel are the best option, until now, to be used in the transport sector. Biogas, syngas and wood pellets are the best option for cooling and heating as well as power generation. Therefore, a direct comparison of these energy carries could result in an error due to these ones have different fields of application and specifications that make them useful under specific conditions

2. The oil palm crop in Colombia.

Colombia is a tropical country located in the northwestern region of South America with latitudinal coordinates 17° north and 4° south. It has a large crop biodiversity due to its great variety of zones with different weathers. Moreover, Colombia is characterized for producing large amounts of sugarcane, bananas, palm fruits, tomatoes, coffee and rice [78]. However, the Food and Agriculture Organization of the United Nations (FAO) postulates Colombia as the fifth largest producer of palm oil in the world [78]. Therefore, this crop is one of the most important in the country.

Oil palm is grown in Colombia in four different zones, which are southwestern, northern, central and eastern [79]. The departments of Casanare, Meta, Caquetá and some municipalities of Cundinamarca compose the eastern zone. On the other hand, La Guajira, Magdalena, Atlántico, Sucre and Cordoba compose the northern region. These ones also include some municipalities of Antioquia such as Necoclí. To close, the Central and Western areas are composed by Norte de Santander and Santander as well as Nariño and Cauca, respectively.

In 2013, Colombia was considered as the first producer in America due to it reached a palm oil production of 1 million of tonnes, increasing 5.44% its production respect 2012. **Figure 2-1** shows the geographic location of the main growing areas of oil palm (*Elaeis guineensis*) in Colombia according to reports provided by the Statistical Information System of Palm Sector (SISPA).

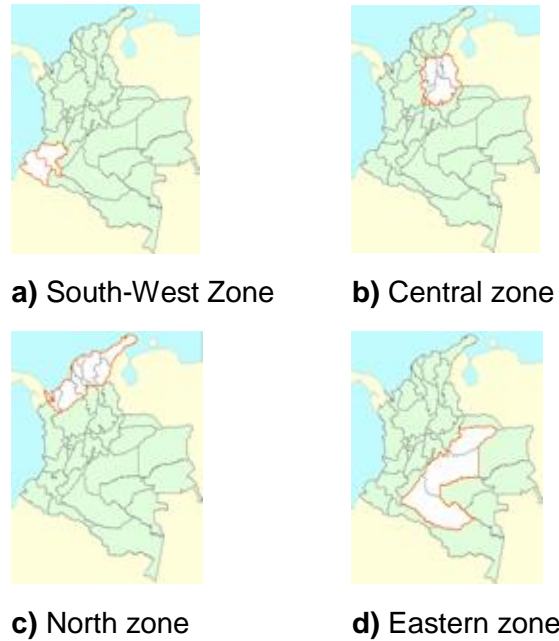


Figure 2-1. Geographical location of the growing areas of oil palm in Colombia.

The oil palm crop became one of the most important oil crops in the world due to the following features: steady and continuous oil production [80], absorbance of large amounts of CO₂, low biodiversity compared to the crops that it replaces. In addition, its production yields are higher than those achieved by other oil crops such as soybean, rapeseed and sunflower [81]. **Figure 2-2** shows the yields of oil production from different oil crops (tonne/ha).

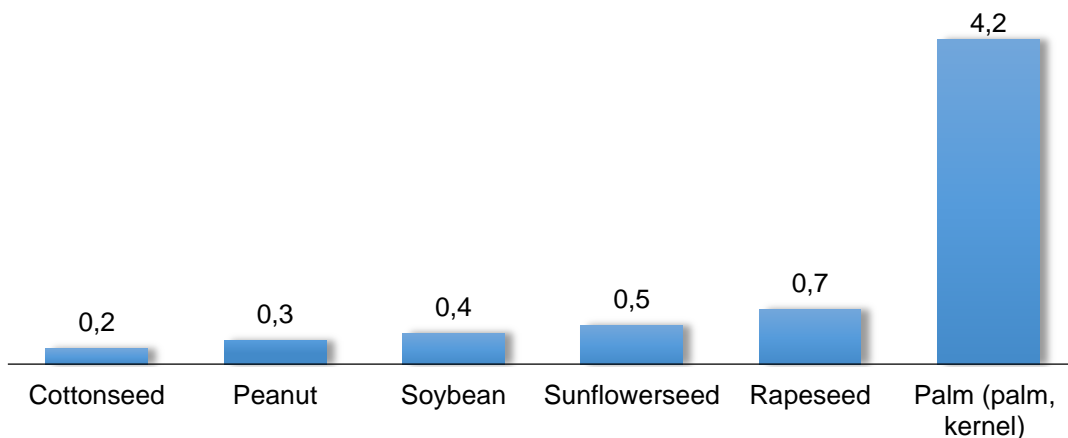


Figure 2-2. Oil production yields of different crops [80].

The oil palm crop has great potential due to the commercial products that can be obtained from it. Even so, by-products from the oil palm crop and its processing also shows a great potential to be used as alternatives to accomplish a sustainable development. Therefore, it is necessary to understand all the productive chain that the oil palm generates with the goal to identify critical points where could be interesting to propose new products and strengthen the palm oil sector in Colombia.

2.1 The oil palm tree.

Oil palm (*Elaeis guineensis*) is a native crop with origin in tropical west Africa, which has been characterized as a source of oil and other value-added products during several decades [82]. The cultivation of this oleaginous plant has spread from Africa to tropical regions in South America and Southeast Asia. The oil palm harvesting has been become in a profitable activity for a huge quantity of persons due to the high oil production that it exhibits [83]. The high productivity of oil palm crop can be observed in the amount of oil produced per unit of cultivated area.

Palm trees may grow up to sixty feet and more in height. The trunks of young and mature trees are wrapped in fronds which give them a rather rough appearance. The older trees have smoother trunks apart from the scars left by the fronds which have withered and fallen off. Oil palm tree will start bearing fruits after 30 months of field planting and will continue to be productive for the next 20 to 30 years. Thus, the above is to ensure a consistent supply of oils. Each ripe bunch is commonly known as fresh fruit bunch (FFB) and they are considered as one of the most important part of the oil palm tree because from this one, the palm oil is obtained [84].

In 2012, about 258.9 million hectares were sown in the world with oil seeds of which oil palm seeds accounted only for 5.5% of the total cultivated land compared to the area dedicated to soy plantations, which occupied almost 40%. However, 32% of the oil generated from these crops proceeded from oil palm trees, while only 22.4% was extracted from soy [85]. **Figure 2-3** shows the percentage of soil dedicated to the cultivation of different oil seeds, as well as the oil production of these crops in the year 2012. From this, it can be observed that the oil palm crop has the highest oil production to harvested area.

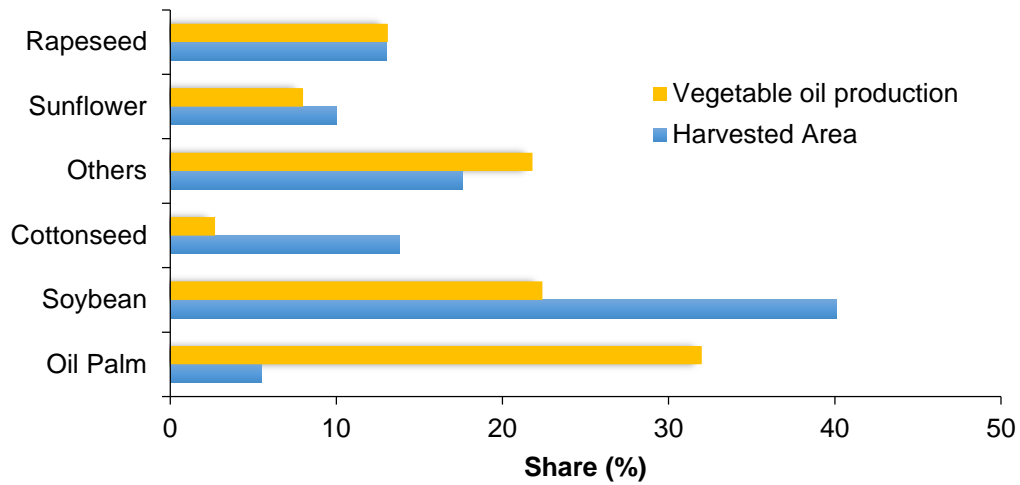


Figure 2-3. Area Harvested and Vegetable oil production in 2012, data source: [86]

A photo of the oil palm tree cultivated in Colombia is presented in **Figure 2-4**. The main parts of this one are indicated with the aim to avoid any confusion related with the literature. This picture was taken in the central zone, more accurately in Puerto Salgar, Cundinamarca, Colombia.



Figure 2-4. The oil palm tree.

From **Figure 2-4** it is possible to identify the following parts:

1. Oil palm trunk. 2. Oil palm frond, 3. Fresh fruit bunch,
4. Oil palm leaves, 5. Empty fruit bunch, 6. Oil palm rachis.

The above listed parts of the oil palm tree have many applications. The palm oil comes from the fresh fruit bunches. Therefore, these ones are the most important part of the plant. On the other hand, the empty fruit bunches are used to produce energy and provide nutrients to soil in the oil palm plantation. However, other parts like the trunk and the oil palm rachis do not have any specific application. Here, it is the main point of this work. ***To give value-added to the oil palm rachis for syngas generation through its gasification.***

As was mentioned, it is important to know all the productive chain that involves the cultivation of the oil palm to identify possible points of improvement through the integral use of the waste generated in harvesting as well as the waste generated in the oil palm mills. Therefore, in the following sections some aspects related with the productive chain of the oil palm crop are reviewed.

2.2 Palm oil production.

The palm oil extraction process is carried out in oil palm mills. In these places the fresh fruit bunches are processed and the palm oil is produced. In addition some lignocellulosic residues such as the empty fruit bunches (EFB) and palm pressed fiber (PPF) are generated in this process. Therefore, a knowledge related with the palm oil obtainment is necessary to understand one of the main constituents of the palm oil productive chain. The fresh fruit bunches are subjected to the following unit operations:

Sterilization → Bunch Threshing → Digestion → Pulp pressing → Clarification

The following is a brief description of the main steps carried out for the palm oil extraction process used in the Colombian oil palm mills. The following explanations are based on an industrial visit performed in the oil palm mill “Morrocolorado” and literature.

2.2.1 Sterilization.

The fresh fruit bunches from the oil palm crop are carried to an industrial pot with the goal to soft them. The steam used to accomplish this process has a pressure of 2 bars and temperature of 120°C. This process is performed to avoid the production of free fatty acids (FFA) due to the lipases action into the oil palm fruit. In addition, the sterilization process has as objective to ease the fruit and bunch separation in the following steps of the palm oil extraction. The fresh fruit bunches ready to start the process are presented in **Figure 2-5** and The sterilization process is carried out in two or more parallel industrial pots to cook the fresh fruit bunches as is shown in **Figure 2-6** [95], [103], [104].



Figure 2-5. Fresh Fruit Bunches from Oil Palm crop in Puerto Salgar

2.2.2 Bunch Threshing (Stripping).

In this process the cooked fresh fruit bunches are carried to a rotary drum where the oil palm fruits are separated from the palm bunches. The rotatory drum has an inclination angle with the goal to get out the fruits and bunches of the drum. The oil palm fruits are separated through the metal bars of the equipment. This process is carried out at atmospheric conditions [87].



Figure 2-6. Sterilization equipment used to cook the fresh fruit bunches.

2.2.3 Digestion.

The digestion process has as objective to separate the pulp from the oil palm kernel. This process is performed in steam presence. Besides, a maceration process is accomplished to homogenize the pulp and to ease the pressing process. Here, the oil palm fruits have been separated from the oil palm kernels. However, a low quantity of palm oil is produced. The condensates from the digestion process are recovered and taken to the wastewater treatment process (i.e. anaerobic lagoon and facultative lagoon). Thorough digestion is critical for efficient pressing [87].

2.2.4 Pulp pressing.

The pressing process is the crucial stage of the palm oil obtainment. This process can be used as a measuring parameter to determine at a glance the plant mill capacity. In the pulp pressing stage, the palm oil is extracted from the pulp, which is called as Crude Palm Oil (CPO) [88]. Crude palm oil has approximately 50% of saturated fatty acids and the other 50% is a liquid fraction rich in unsaturated fatty acids. In addition, it has tocopherols and tocotrienols that are a very interesting components with antioxidant capacity that can be postulated as a high value-added product in biorefineries [89]. However, the purity of CPO is very low due to water and another impurities presence. Thus, the main product of this stage is a liquid called as “*press liquor*”, which must be carried to the clarification stage to increase the CPO purity. After the liquor production, a cake is obtained and it is called palm pressed fiber (PPF). Finally, it is necessary to remember that the PPF is

mixed with the kernel. **Figure 2-7** shows the palm pressed fiber produced after the pulp pressing process and kernel separation.



Figure 2-7. Palm pressed fiber after kernel separation.

2.2.5 Clarification.

In the clarification process, the press liquor is mixed with water to dilute and to facilitate the crude palm oil separation and purification. This stage also is very important in the palm oil extraction process due to the purity and quality of the end product are given here [88]. The clarification process uses the immiscibility characteristics of the water – oil mixture to remove light and heavy sludges and other impurities. The clarification process can be divided in two steps: the static and dynamic clarification. The first one can remove about 90% of the CPO through decantation at moderate temperature and pressure. The second stage is performed using a centrifuge that operates at high velocities. This step achieve a 10% recover of CPO from the effluent of the previous stage [87]. Finally, after the CPO obtainment, the palm oil is carried to a dryer tank to remove any trace of water. Then, the crude palm oil is stored in cylindrical tanks.

2.2.6 Yields and prices.

Production yields of palm fruit and extracted oil have remained constant in recent years for oil palm cultivation in Colombia. However, the palm fruits and extracted palm oil production decreased in 2016. On the other hand, the area that most has contributed to the growth of the oil palm production in the current year has been the eastern region with

a 46.2%, followed by the central and north zones with a production shares of 27.9% and 23.8%, respectively. Southwestern region has contributed only 2.1% [90]. The above mentioned results, related with the participation of each zone in the oil palm production, can be considered as a constant over time. Since 2013, the eastern region has produced higher quantities of palm oil than the other three regions due to there are a high density of oil palm crops as well as oil palm mills. Finally, the total amount of palm oil produced in Colombia this year has been 1'486,034 of tonnes until October. **Table 2-1** summarizes the crop yields of palm fruit and palm oil production yields per harvested area unit.

Table 2-1. Fruit yields and palm oil production in Colombia.

Year	Yield [Tonne/Ha]	
	Palm fruit	Extracted oil
2012	15.46	3.22
2013	14.92	3.07
2014	15.43	3.14
2015	16.56	3.38
2016	14.14	2.87

Based on the oil palm yields, which are close to those reported in **Table 2-1**, it has occurred a change in the historical evolution of the prices of this product. However, Colombia does not have sufficient capacity to affect international market prices [72]. For this reason, the reference prices for the palm oil and palm kernel oil marketing in the domestic sector are based on international prices. **Figure 2-8** shows the change in prices of palm oil in Colombia according to FAO [78].

The palm oil price has increased gradually in recent years. Even so, the palm oil price remained stable in the 2016 - 2017 period. The palm oil price in Colombia is 660 USD/tonne according to the resolution No. 000181, 2017. This price is lower than the price reported in Malaysia (the first producer in the world), which is 718 USD/tonne. This situation can be attributed to the use of this product in the generation of biofuels [90]. In 2017, the palm oil price fell 23.53% compared with the previous year. However, it is higher than the average price in the period 2008 – 2017, which is 631 USD/tonne (see **Figure 2-8**).

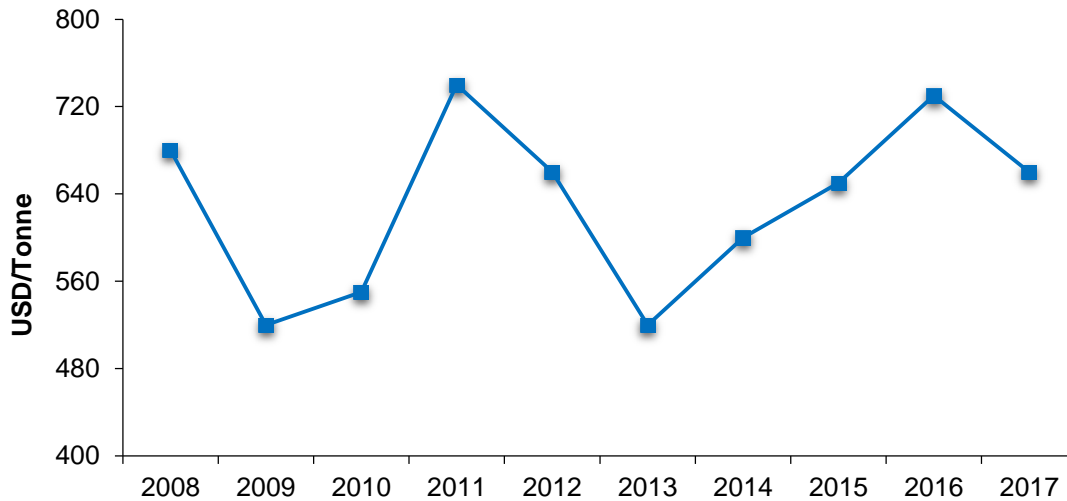


Figure 2-8. Price of palm oil in Colombia in the period 2004 – 2014 [78]

2.3 Biodiesel production from palm oil.

Colombia is a developing country that seeks to increase its production of clean energy from renewable sources by promoting their inclusion in the national energy system and its application in non-interconnected areas (NIA). This inclusion was performed by means of the law 1715 of May 13, 2014, which aims to reduce the energy dependence on fossil fuels [91].

The biodiesel industry started in 2008 and it is composed by three levels: agricultural, industrial and services [92]. The first level consists of oil palm farmers (large, medium and small producers). The collection, in which the extraction of palm oil is carried out, is part of this level. The industrial level is constituted by plants where the transesterification processes for obtaining biodiesel and glycerin are performed. Currently there are only ten (10) plants working and other five (5) are in planning [92]. Finally, the services level consists mainly of companies that handle the distribution and marketing of palm oil until they reach the final consumer.

In Colombia, there are plenty oilseed crops that can be used as raw materials for the biodiesel industry (e.g. coconut, peanuts, cotton, sesame, soy and sunflower). However, the raw material used is palm oil given its high yields. According to the above, the main suppliers to the biodiesel industry are companies engaged in the planting, harvesting and

extraction of palm oil. Currently, the palm oil market is divided into three sectors. The first is the traditional market, which includes all sales to the production of foodstuffs intended for human consumption (e.g. candies, margarines), manufacture of concentrated products, soaps and paints. The second is dedicated to the biodiesel industry and the third one to international trade.

2.3.1 Biodiesel production process.

Biodiesel production can be performed through different technologies, which are classified in conventional and unconventional. However, all of them contemplate the transformation of triglyceride esters through a transesterification process. Conventional technologies include the reaction using basic catalysis, acid catalysis, heterogeneous catalysis and enzymatic catalysis while non-conventional processes contemplate binding transesterification process with the separation of products obtained in the reaction. Therefore, alternatives such as the implementation of reactive distillation and reactive extraction have been employed [93]. Nevertheless, conventional technologies have been used in the Colombian context.

In general terms, the biodiesel production process is composed by the following stages: Pretreatment, free fatty acids esterification, triglycerides transesterification, alcohol recuperation, glycerol washing, neutralization, glycerol purification and biodiesel purification [94].

The pretreatment stage consists on conditioning the raw materials temperature before to be carried to any reaction stage. Then, the preheated palm oil is subjected to an esterification reactor to decrease the free fatty acids (FFA) content below 1% [95], [96]. The esterification reaction is accomplished using any alcohol and a homogeneous or heterogeneous catalyst. After the esterification reaction, the palm oil with low content in FFA is carried to the transesterification reactor. The typical conditions of this stage are: temperature 60°C, pressure 1 bar, residence time 60 min, molar ratio 6:1, agitation 400 rpm and catalyst loading of 0.8g NaOH/100g oil. The product streams from transesterification reactor are composed by not converted triglycerides, intermediates products and esters [94].

The outlet stream from the reaction stage is introduced in a distillation tower to separate the methanol and water from the organic mixture. The alcohol recovery is a very important stage to decrease the raw materials cost in the overall process due to that the recovered alcohol is recirculated. Then, two streams are generated. The distillate that is composed by alcohol, and the bottoms, which have a complex triglycerides and esters mixture at high temperatures [97].

The organic mixture from alcohol recovery column is cooled using a heat exchanger [98], [99]. Afterward, this stream is treated with water to separate the glycerol from the other organic compounds in an extractive column [100]. Then, two streams are produced. One stream is composed by triglycerides and esters and it is send to purification process. The other stream is composed by a glycerol – water mixture that is subjected to a treatment stage to separate the glycerol with the purpose of decreasing the environmental impact. The outlet stream from the extractive column composed mainly by glycerol is neutralized with phosphoric acid to produce sodium phosphate and water. The formed solid is separated in a filter and the liquid phase is distilled in a column to recovery the glycerol produced.

Biodiesel is obtained in a purification stage, where methyl-esters (primary components of the biodiesel) are separated from the non-converted oil fraction (i.e. triglycerides) into a distillation column. On the other hand, the bottoms streams is recycled and mixed with new oil. **Figure 2-9** shows the process flow diagram for the biodiesel production from vegetable oils.

2.3.2 Biodiesel facilities in Colombia.

There are ten (10) biodiesel operating plants and five (5) plants under construction in Colombia with different capacities [92]. These are distributed around the four main zones designated to be used as oil palm crops. The future biodiesel plants that are being built will generate around of 13,800 jobs, which will improve the quality of life of many people in Colombia. **Table 2-2** resumes the main characteristics of these plants.

Table 2-2. Biodiesel facilities located in Colombia [92]

Region	Company	Capacity (tonne/year)	Planted area (Ha)	Total jobs
	Biocombustibles			
North, Santa Marta	Sostenibles del Caribe	170,000	29,240	12,531
North, Codazzi	Oleoflores	60,000	17,544	7,519
North, Barranquilla	Romil de la Costa	10,000	2,924	1,253
North, Galapa	Biodiesel de la Costa	10,000	2,924	1,253
North, Santa Marta	Odin Energy	36,000	10,526	4,512
Eastern, Facatativa	BioD	200,000	36,810	15,776
Central, Barrancabermeja	Ecodiesel de Colombia	120,000	38,585	16,536
Eastern, San Carlos de Guaroa	Aceites Manuelita	120,000	38,585	16,536
Eastern, Castilla la Grande	Biocastilla	15,000	4,823	2,067
Eastern, San Carlos de Guaroa	La Paz	70,000	21,472	9,202

The Colombian companies dedicated to the production of biodiesel have been created in order to mitigate the impact that the use of fossil fuels such as gasoline and diesel in the transport sector have caused in the last years. Therefore, the national government has encouraged the use of biofuels. Biodiesel is used in our country in four different blends. The first one (B0) is applied in la Guajira department. The second one (B2) is applied in Norte de Santander, Vichada, Arauca y Guainía departments. The third one (B9) is applied in Vaupés, Guaviare, Meta, Casanare, Boyacá and Cundinamarca. Finally, the fourth one (B10) is used in the rest of the country. This distribution was actualized in May 2017.

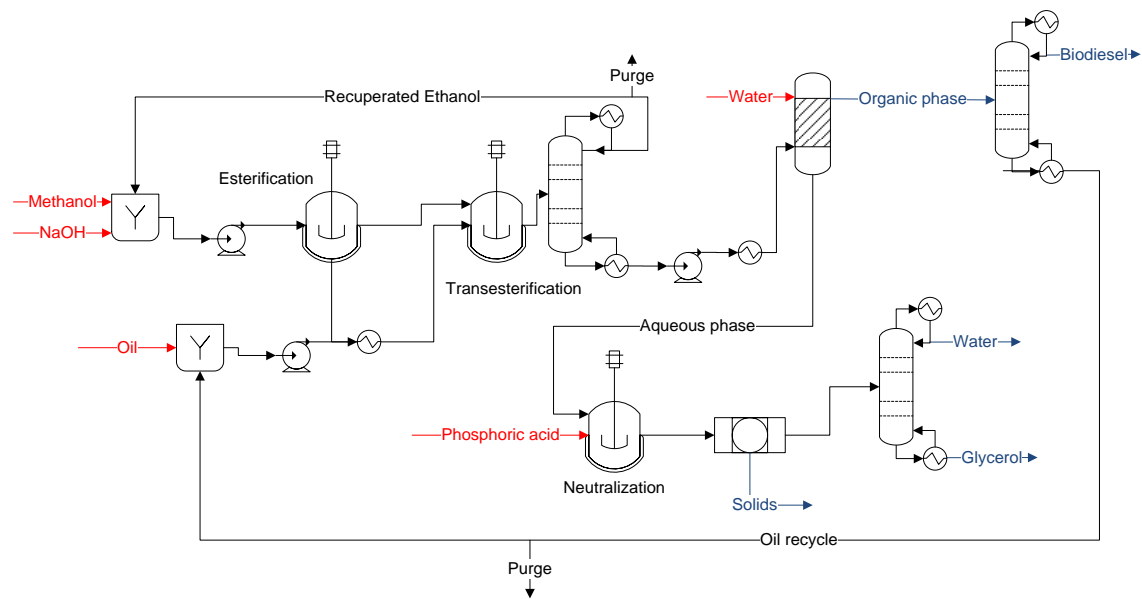


Figure 2-9. Biodiesel process flow diagram

In 2017, the biodiesel production in Colombia decreased as a result of the difficult weather conditions that affected the oil palm crops in each zone. In addition, an indecision related with the increase of the biodiesel blend has caused that its production have resulted in little incentive to increase production [101]. In the last year (2016) Colombia produced around of 530 million of liters, which represents a decrease in biodiesel production of 9%. In **Figure 2-10** is possible to observe the historical production of crude palm oil.

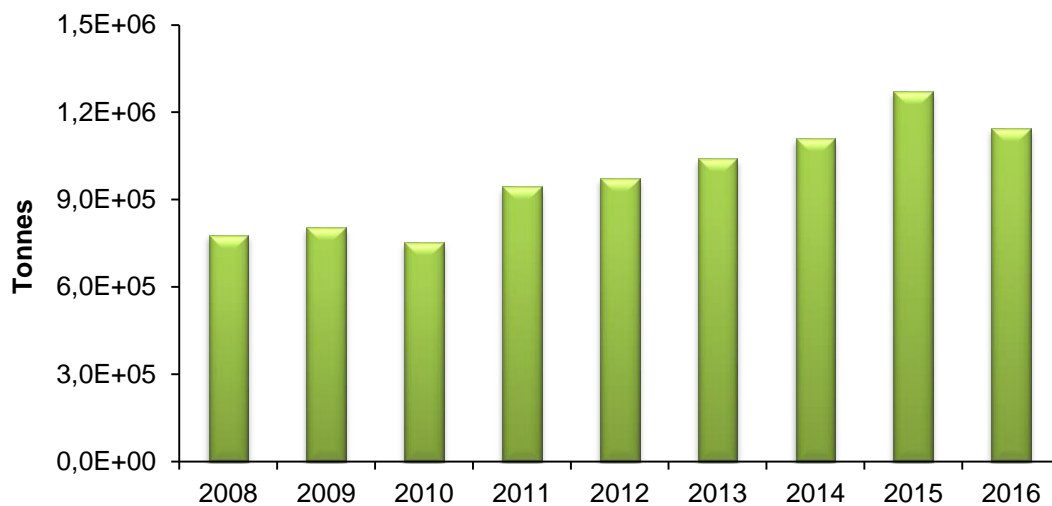


Figure 2-10. Crude palm oil production in Colombia since 2008

Currently, the biofuels production such as bioethanol and biodiesel has been subsidized by the national government to soften the economic conditions for the biofuels access into the market. Likewise, the government has stipulated the mixture of gasoline and diesel with their respective biofuels. Finally, the framework of the production of biofuels in Colombia has been focused on the use of the oil from the oil palm as the main raw material. In accordance with the above, the socio-economic and technical conditions in our country are predisposed to increase the oil palm industry to another level

2.4 Olein and stearin production from palm oil.

Palm olein and stearin are two products that are obtained from refined palm oil (RBD PO). The first one can be defined as a liquid fraction rich in oleic acid and it is considered as stable and neutral taste oil. On the other hand, palm stearin is the solid fraction of the refined palm oil obtained when it is crystallized. The ratio of palm olein and stearin obtained after the fractionation process of refined palm oil is 80/20. Moreover, these fractions can be obtained from the refined palm kernel oil (RBD PK). However, the ratio of these products in this case is 60/40. Finally, the olein and stearin obtained from both, palm oil and palm kernel oil are used to produce detergents, cosmetics, oleo-chemicals and food additives.

The crude palm oil (CPO) obtained from the oil palm mills can be processed to obtain three important products. The first one is a refined, bleached and deodorized palm oil (RBD PO), which is used as raw material to produce margarines, shortenings, frying fats and ice cream. The second one is the palm olein, which is produced in the same process that the palm stearin. Both can be subjected in a refinement, bleaching and deodorization processes to produce RBD palm olein (RBD POL) and RBD palm stearin (RBD PS). The palm olein is used for frying and cooking, while the other one is used to produce shortenings and margarines with high cholesterol levels. The RBD POL and RBD PS are commonly subjected to an inter-esterification, hydrogenation and glycerolysis processes with the aim to increase the amount of products that are derived from the oil palm crop. The degumming, bleaching and deodorization processes that are employed to produce palm olein and stearin are briefly explained below:

The degumming process consists on the removal of phospholipids, mineral compounds, gums and impurities present in the crude palm oil. This process is performed using a solution of phosphoric acid. On the other hand, bleaching earth (bentonite earth) is added as absorbent material during the bleaching process in order to remove those compounds which give the reddish color to crude palm oil such as alpha and beta carotene [102].

Therefore, these stages can be considered as purification processes. Finally, the deodorization stage removes free fatty acids (FFA) using high pressure steam at low pressures. Then, this stage can be considered as a stripping stage that produces as by-product fatty acids distilled that can be used as feedstock to produce animal feed and detergents. However, the degummed and bleached palm oil must be deaerated and heated before the deodorization process. . The process flow diagram of the olein and stearin production process is showed in

Figure 2-11

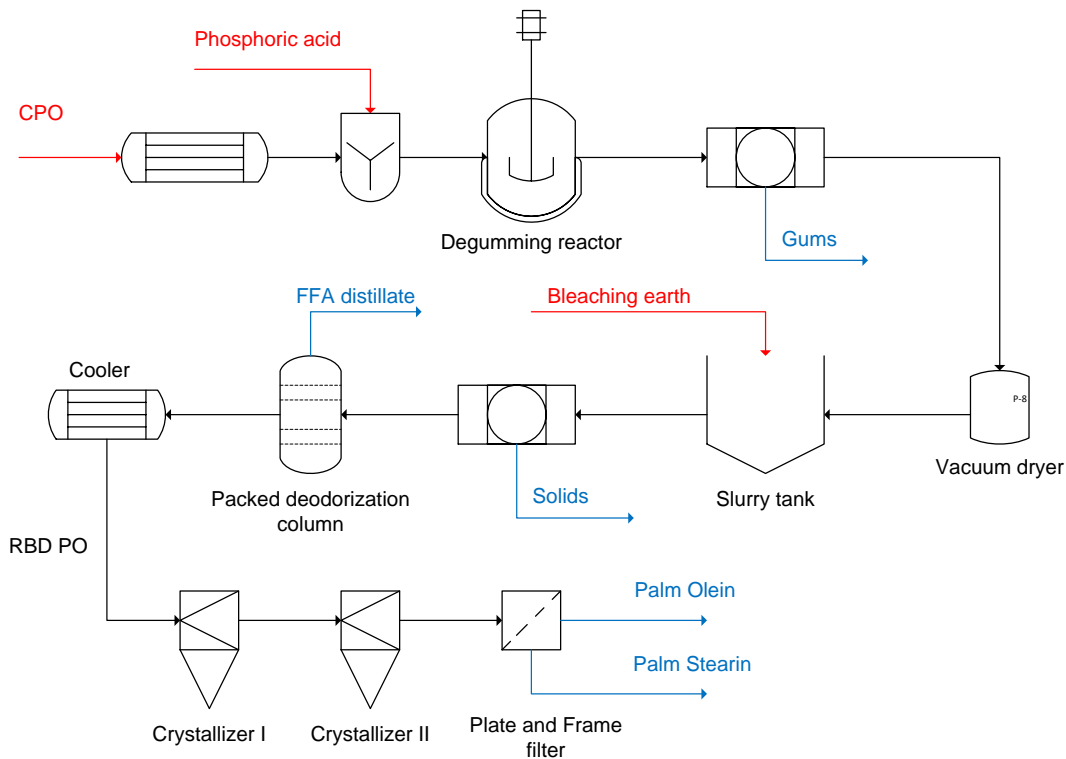


Figure 2-11. Simplified palm olein and stearin process flow diagram.

The RBD palm oil is subjected in a dry fractionation process, where the main unit operation involved are crystallization and filtration. In Colombia, the crude palm oil

production is performed in the oil palm mills, while the RBD palm oil, palm olein and stearin are produced in a refining plant.

2.5 Second generation oil palm biomass.

A wide variety of lignocellulosic residues are generated during the oil palm harvesting. This biomass can become in potential sources of value-added products and energy vectors. Thus, it is necessary to identify and classify the lignocellulosic residues generated in this crop with the aim to propose different ways to treated them. Following, only a few residues that are generated during the cultivation and processing of the oil palm fruits to obtain palm oil are mentioned.

2.5.1 Empty fruit bunches (EFB).

Empty fruit bunches are a lignocellulosic residue that is obtained from the bunch threshing stage during the crude palm oil production [103]. This solid residue has the highest rate of production in the oil palm mills due to 1.3 tonnes of EFB are generated in the production of one tonne of CPO. The EFB management can be complicated because of its handling is a difficult task. The above is related with its physical appearance because of this one has a main stalk, spikelets and sharp spines that can produce hurts and injuries. In general, the stalk represents a 25% wt. while the spikelets and spines represent a 75% and its moisture content ranges from 55% to 58% [104].

In Colombia, empty fruit bunches (EFB) are used to produce compost, animal food and it is used as nutrients source. These applications are the most common in the oil palm mills. On the other hand, the moisture content of the EFB difficult their use in thermochemical processes such as combustion or gasification. However, the associated costs in its removing and disposal were considered as a drawback of the process. Therefore, the EFB use in boilers to produce utilities such as steam is beginning to be considered in the oil palm mills [105].

The above mentioned option is based in the EFB properties as fuel. Its calorific value, volatile matter, fixed carbon content and ash content are around of 18 MJ/kg, 82.58%, 8.97% and 3.45% in dry basis [106], [107]. These values are in agreement with other type

of biomass used as fuels in this type of processes such as *pinus patula* and coffee cut stems [108], [109]. Moreover, the cellulose content of the empty fruit bunches ranges from 41.3% to 46.5%. This amount of cellulose suggests that this lignocellulosic material can be used to produce a wide variety of products via fermentation processes to produce fuel ethanol and butanol [110]. Afterward, its hemicellulose content is around of 32.5%, which increase the option to obtain other products such as furfural [111].

2.5.2 Oil palm leaves (OPL).

Oil palm leaves are other lignocellulosic residue produced during the oil palm harvesting. This residue has a generation rate of 25 kg/year/palm tree and it is used as animal food or as source of nutrients. However, the oil palm leaves do not have any other application at industrial level. Therefore, this residue does not generate any value to the oil palm productive chain [112]. In addition, the nutritive value and potential to contribute nutrients of the oil palm leaves change over time. Nevertheless, oil palm leaves have a considerable quantity of phenolic compounds that can be extracted and commercialized [113].

In the same way that the empty fruit bunches, the oil palm leaves can be considered as a source of sugars to be used in fermentation processes. Both, cellulose and hemicellulose fraction represent more than a half of the entire residue (i.e. 68%) [112]. Therefore, these can be used to produce energy vectors and chemicals through chemical and biochemical processes. Other important compounds that can be obtained from the oil palm leaves are vitamins A and E, which are about of 1900 ppm and 14805 ppm, respectively. As a result, oil palm leaves could be used as a feedstock to produce phytochemicals [114].

2.5.3 Oil palm fronds (OPF)

Oil palm fronds are the largest lignocellulosic biomass that is produced during the oil palm tree harvesting activities. This one can has a length from 7 m to 8 m [104], [112]. Also, oil palm fronds can constitute a 70% of the total amount of lignocellulosic residues generated in the oil palm industry. The worldwide production of this residue has been estimated in 250 million of metric tonnes in wet basis (92.4 million of metric tonnes in dry weight) [115].

This residue is produced and left to rot in the soil to promote the nutrients recycle (see **Figure 2-4**). However, other type of applications has been proposed by different researchers. In first place, oil palm fronds can be used as a sustainable carbon source to produce succinic acid, ethanol, PHB and low molecular alcohols due to its cellulose, hemicellulose and lignin content is 16.96%, 46.19% and 34.26%, respectively [115]. Moreover, this lignocellulosic biomass can be used in thermochemical applications due to this one has good fuel properties [116], [117]. Alternatively, interest compounds such as glutamic acid, serine and proline can be extracted as well as carotenoids and tocopherols too [112].

The properties of the oil palm fronds change over the time. In fact, the use of fresh or ancient fronds will change the result of any experiment due to the natural material degradation process. Therefore, properties such as the moisture content, aminoacid content, acid detergent fiber and neutral detergent fiber change. Then, depending on the application of the fronds could be more convenient use a fresh or ancient material [112].

In literature, it can be found different papers that are researched the use of the oil palm fronds in different applications as was mentioned above. Nevertheless, there is not done a difference between oil palm rachis (OPR) and oil palm fronds, even, it has been confused the oil palm petiole with the oil palm rachis (see **Figure 2-12**). Therefore, it is important to clarify each part of the oil palm fronds to give clarity.

The oil palm frond is the set composed of the rachis, petiole and leaves. The petiole is the transition between the stem (rachis) and the leaves. The rachis is the stem that supports all the leaves of the oil palm tree. In this thesis work, the oil palm rachis was used as raw material. Thus, the leaves and petiole were cut from the oil palm frond.

The oil palm fronds production in Colombia depends of each productive zone and crop. In general, this residue is generated during the oil palm fruit harvesting only removing the dry fronds. This activity also is known as oil palm frond pruning. In a productive year, oil palm fronds pruning are performed minimum twice a year. Moreover, always this activity must be performed once a year in the months of least rainfall.

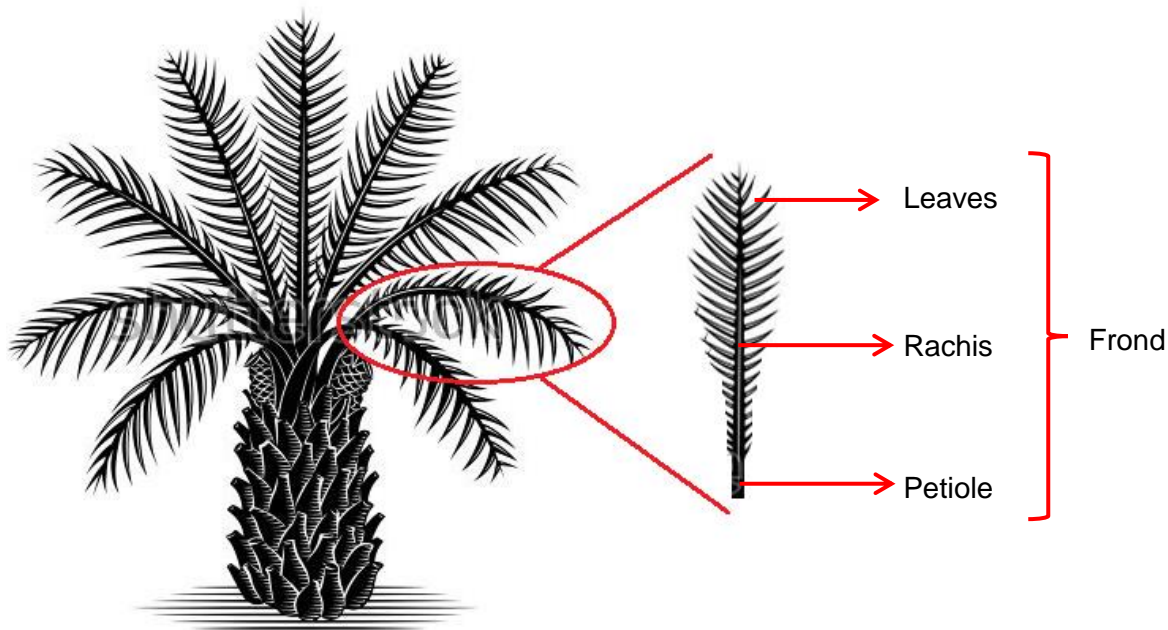


Figure 2-12. Oil palm fronds location and its main parts.

2.6 The oil palm productive chain in Colombia

In the above sections, it was mentioned that the inclusion of lignocellulosic biomass into the oil palm productive chain with the goal to increase the amount of value-added products that can be obtained from it. This idea is presented in **Figure 2-13**.

In this figure it is possible to observe the main stages that conforms the oil palm productive chain (i.e. crop, oil palm mill, intermediate products obtainment, basic goods and services; and industrial transformation) and the main products in each one of them. Thus, the blue blocks represent the current elements that are considered in the oil palm sector in Colombia and the green blocks shows the new elements that can be included if the lignocellulosic biomass from the oil palm crop is included. In addition, it is possible to observe that some of the products proposed in this figure (e.g. heat and power) can be used to supply the energy demand in the oil palm mills or, even, the energy demand at industrial level. Moreover, the inclusion of value-added products like PHB, succinic acid and lactic acid can diversify the oil palm market. Finally, the above mentioned is totally in agree with the biorefinery concept and sustainable development ideas.

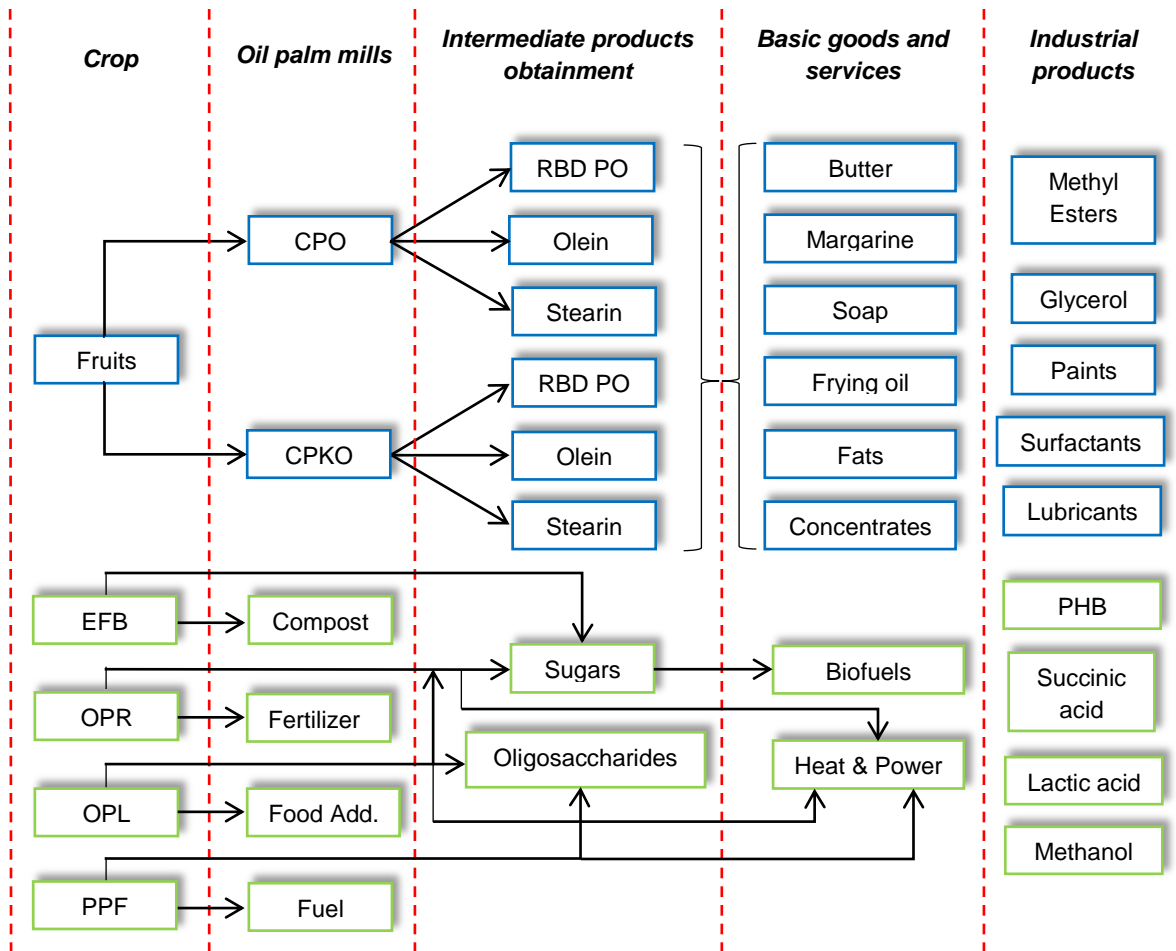


Figure 2-13. Stages and products in the palm oil production chain including the integration of lignocellulosic residues.

2.7 Final remarks.

The oil palm crop in Colombia is one of the most important in the world due to the amount of crude palm oil produced. However, the large generation of solid waste to obtain this product has caused some environmental problems. Therefore, it is necessary to propose alternative uses to most of these residues with the aim of strengthening even more the oil palm productive chain. Biodiesel is not the only value-added product that can be obtained from the oil palm crop. Heat and power from oil palm rachis gasification, bioethanol from empty fruit bunches fermentation, antioxidants from oil palm leaves extraction are other alternatives that can be used and industrialized in the future. Thus, the inclusion of biomass processing technologies could build up the oil palm productive chain and encourage the sustainable use of residues in other productive chains.

3. Gasification and Syngas: A technology overview.

Biomass gasification has been widely researched since the Second World War to use hardwood as fuel for vehicles. This technology provides a relative low-cost energy production due to the amount of fuel gas that can be obtained from it. On the other hand, many types of gasifiers and designs have been proposed to increase the energy efficiency of the process, solids flow, gases flow as well as the heat and mass transfer issues that are typical in during the biomass gasification due to the feedstock properties. The main product that is obtained from the biomass gasification process is a gas mixture called syngas, which can be used as chemical platform and energy source.

Biomass gasification has not been implemented at industrial level widely. Only coal gasification has been applied to produce syngas as chemical platform. Nevertheless, co-gasification has been emerged as alternative for use lignocellulosic feedstocks at industrial level in this process. For the moment, low-scale applications related with the heat and power production has been implemented in the world. In this chapter a short review related with the gasification technology is done.

3.1 Introduction.

Gasification is defined as thermal conversion of organic material to combustible gases under reducing conditions with oxygen added in sub-stoichiometric amounts compared with the amount needed for complete combustion to carbon dioxide and water. Gasification may be accomplished through the direct addition of oxygen, using exothermic oxidation reactions to provide the energy necessary for gasification, or by pyrolysis through the addition of sensible heat in the absence of added oxygen. In both cases,

water, in the form of steam, may be added to promote additional production of hydrogen via the water-gas shift reaction. Through gasification of biomass, a heterogeneous solid material is converted into a gaseous fuel intermediate of consistent quality that can be used reliably for heating, industrial process applications, electricity generation, and liquid fuels production [46].

In the gasification process by-products such as tars and char as well as ashes are produced. These ones are produced in low quantities when the gasification technology is used. However, there are other thermochemical processes such as pyrolysis and torrefaction that produce syngas, bio-oil and char. The differences between these processes, as thermochemical ways for biomass processing, are the operating conditions and the amounts of syngas, bi-oil and char that are obtained. Thus, gasification is employed to produce syngas in large amounts, while torrefaction process produces low quantities of gases because this process is mostly used to increase the energy content of lignocellulosic feedstocks removing its oxygen content. Finally, pyrolysis is a process that is used for both bio-oil and char production. These products are obtained under different process conditions. Bio-oil (i.e. a mixture light and heavy hydrocarbon, similar to crude oil) is obtained in a fast pyrolysis process, which is characterized to use high heating rates (higher than 1000 °C/min). Meanwhile, char is produced in a slow pyrolysis process, which use slow heating rates (lower than 100 °C/min) to avoid the volatiles production [118]–[120].

The gasification technology has already been studied and implemented in the last years to produce energy [121]. However, a renovated interest for this technology has been aroused due to the use of lignocellulosic biomass (e.g. forestry and wood residues) as raw material, which combined with pretreatment technologies (e.g. densification) can be able to produce energy at low scale as well as value-added products [122]. The above can be reflected in the statistics provided by the Gasification and Syngas Technologies Council (GSTC), who reports that there are more than 250 gasification facilities operating and more than 680 gasifiers around the world. From this, 10 % of these plants operate using lignocellulosic biomass as main feedstock. Currently, gasification facilities are distributed in North America, Europe and Asia. Nevertheless, Asia, specifically China, will become in a worldwide potency, as far as gasification plants are concerned, due to a planned increase of 190,000 MW in its installed capacity from 2013 to 2020, which

exceeds the rest of regions in the world. This behavior is supported in the market growth of chemical, fertilizer and coal-to-liquids industries located in Asia [123].

According to Gasification and Syngas Technologies Council (GSTC), there are more than 272 operating gasification plants worldwide with 686 gasifiers. The worldwide distribution of gasification facilities has changed significantly in the last four years. Gasification plants had been fairly evenly distributed between Asia, Australia, Africa, Middle East and North America. The gasification capacity including both operational and under construction in the Asia and Australia exceeds the rest of the world put together. The main fields of application of gasification plants in Asia are the chemical, fertilizer, and coal-to-liquids industries, which has the highest demand of syngas from coal and petcoke. **Figure 3-1** shows the distribution of the gasification facilities operating currently around the world.



Figure 3-1. Gasification facilities around the world.

As can be seen in **Figure 3-1**, the highest density of gasification plants is given in Europe and Asia region as was mentioned above. In this map gasification facilities related with the use of lignocellulosic biomass is lower. However, different policies proposed in the EU countries have encouraged the use of gasification plants to produce heat and power. Austria is a country that expects rise its biomass use in thermal application through the use of wood pellets as main energy source to be employed in thermal applications like cogeneration and trigeneration, which can be obtained not from a combustion process of the wood pellets but with the gasification technology.

On the other hand, the number of gasification facilities will grow in the next years. Since 1970 the number of gasification plants has grown progressively. The sharpest increase can be perceived in the last years (more exactly from 2010). There is approximately a 25% of the actual syngas plant capacity projected to be constructed in 2019. **Figure 3-2** shows the cumulative worldwide gasification capacity and growth.

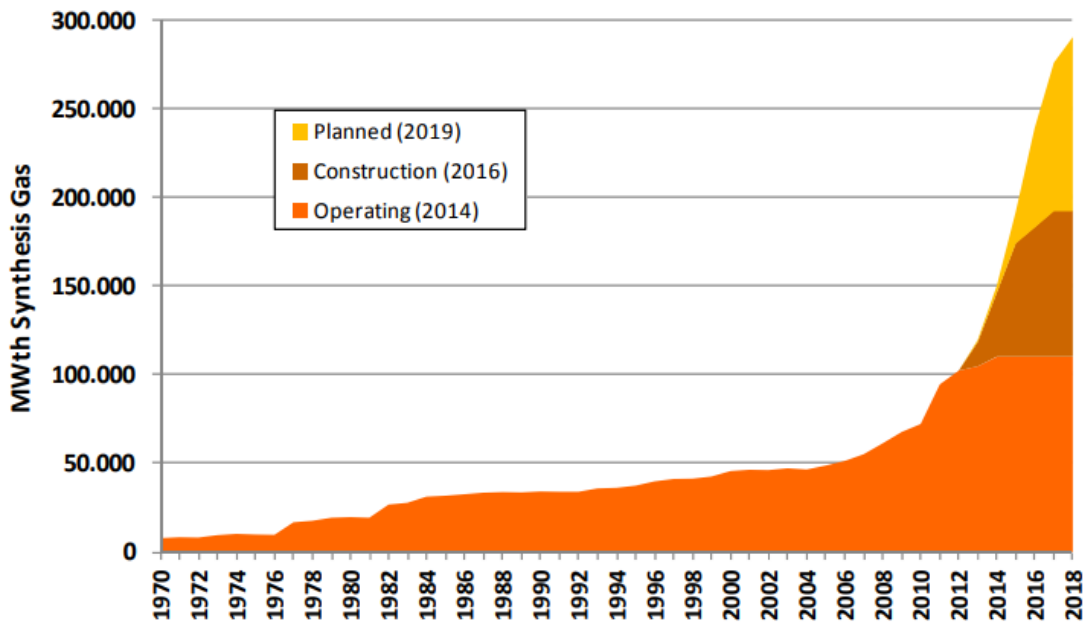


Figure 3-2. Cumulative gasification plants capacity and growth.

From a technical point of view, the gasification process involves a series of complex gas – solid and gas phase reactions carried out in a temperature range between 800 °C and 1000 °C. These reactions have been studied by different authors using software tools such as MatLab, Aspen Plus and CFD programs [124]–[126] . However, a complete modeling with kinetics and reaction mechanisms is still researched. On the other hand, this process has a well-established four steps in which raw materials are converted into syngas. These are: Drying, Pyrolysis, Combustion/Oxidation and Reduction [31], [127]. These steps involve the water removing, raw materials devolatilization, thermal energy production and gaseous species formation, respectively. Finally, this process can be classified taking into account different criteria such as heating method and feedstock disposition into the gasifier [48], [127].

3.2 Raw materials used in gasification process.

Coal, petcoke, biomass and waste are feedstocks employed to produce syngas through the gasification. The first one is the most used raw material due to its conversion and its treatment is considered as a mature technology. In addition, coal is the cheapest non-renewable energy source, which makes it an ideal feedstock. Besides, the gasification of biomass and waste has grown as a response to the search of new alternatives to dispose them. However, there are few gasification plants in the world operating with biomass as their main feedstock. For this reason, the implementation of biomass gasification into the renewable energy sector has been at low scale to provide energy in non-interconnected zones. Shows the main feedstocks employed currently in biomass gasification facilities.

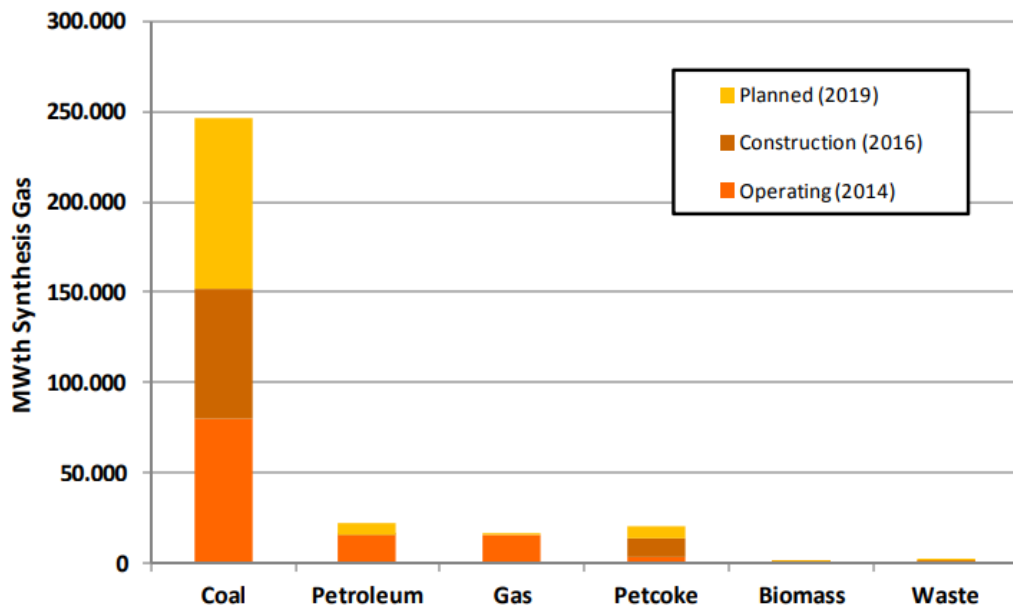


Figure 3-3. Capacity of produced syngas according the type of feedstock.

As can be seen in **Figure 3-3**, coal is and will be the dominant feedstock employed at industrial level for syngas production. This is because of coal is the most cheap raw material that has a great calorific value and syngas conversion efficiencies. Moreover, biomass and waste use for syngas production still is studied by different researchers [125], [128], [129].

The gasification process must meet some features, which are related with the moisture content and the particle size. These characteristics can affect the performance of the gasification processes in terms of efficiency and gas product conversion. Then, moisture content below 30 % and a particle size lower than 38.10 mm and higher than 25.40 mm in are common feedstock characteristics, even if the raw material has been pelletized [130]. On the other hand, the syngas composition is affected by the elemental composition of the raw material employed in this process. Therefore, different analysis such as the proximate and ultimate analysis should be performed [118]. From these analyses, it is possible to calculate the HHV of the raw material and to determine if this is suitable for syngas production. The HHV of coal is about 34 MJ/kg, while the high heating value of lignocellulosic biomass is between 17 – 20 MJ/kg. In addition, an advantage of coal over lignocellulosic biomass is the few tars production as well as its high content of silicon dioxide in its ash fraction [131].

Finally, new alternatives to increase the energy density of lignocellulosic biomass to be used in thermochemical processes, not only in gasification, have been developed. As example, torrefaction is a pretreatment that is carried out in a temperature range between 200 °C and 300 °C in absence of oxygen to remove the most volatile fraction of the raw material (i.e. hemicellulose), which increasing the energy content between 20 % - 60 % [132].

3.3 Gasification process stages.

The gasification process consists of four well-distinguished stages, these are: drying, pyrolysis, combustion and reduction. However, to carry out this process requires a medium such as air, steam or oxygen. These media are referred to as gasifying agents and in general their main objective is to react with the fuel to generate low molecular weight gases such as carbon monoxide (CO) and hydrogen (H₂). According to the choice of the gasifying agent, the calorific value of the gas produced by gasification will have different properties, which largely determine the energy content of the synthesis gas. In general, when air is used, the calorific value of the synthesis gas is from 4 MJ / Nm³ to 7 MJ / Nm³. In the case of water vapor 10 MJ / Nm³ at 18 MJ / Nm³ and in the case of pure oxygen 12 MJ / Nm³ at 28 MJ / Nm³ [26].

In each of the stages of the gasification process different types of reactions are carried out which result in the final composition of the synthesis gas. A description of each stage is done below:

3.3.1 Drying

In this stage of the process, the removal of unbound moisture from the raw material is done to increase the energy efficiency of the process. This stage is considered endothermic [20].

3.3.2 Pyrolysis

During this stage of the process, the decomposition of the lignocellulosic matrix of the biomass is carried out to produce components of lower molecular weight. In this stage of the process generates a waste called tar, which can generate problems within the process of gasification since it is a very viscous and dense liquid that generates technical problems within the gasification equipment. The pyrolysis process is considered as an endothermic stage and occurs in a temperature range between 250 ° C and 700 ° C [20].

3.3.3 Combustion.

This stage is also called oxidation and in it the partial oxidation of the biomass is carried out. This partial oxidation refers to the amount of oxygen available in this stage will always be below the stoichiometric amount to achieve complete combustion, therefore, the main products of this stage are carbon monoxide, carbon dioxide and water vapor , however, according to the type of gasifying agent used other gases could be present (eg nitrogen). On the other hand, given that this is a partial combustion process, all the reactions that arise there are exothermic, therefore, this stage is the one that supplies the energy requirements of the other stages [20].

3.3.4 Reduction.

Finally, in this stage the final formation of the synthesis gas takes place from the gases resulting from the oxidation and pyrolysis steps. This stage has endothermic and

exothermic reactions. However, from a global point of view this stage is considered endothermic [20].

All the stages described above are governed by the effects of mass and heat transfer; therefore, their analysis must be carried out carefully. The reactions that take place in each of the stages of the gasification process are showed in **Table 3-1**.

Table 3-1. Main reactions given in the gasification process.

ID	Reaction	ΔH_r° (kJ/mol)
1	$C + CO_2 \leftrightarrow 2CO$	+172
2	$C + H_2O \leftrightarrow CO + H_2$	+131
3	$C + 2H_2 \leftrightarrow CH_4$	-74.8
4	$C + 1/2 O_2 \rightarrow CO$	-111
5	$C + O_2 \leftrightarrow CO_2$	-394
6	$CO + 1/2 O_2 \rightarrow CO_2$	-284
7	$CH_4 + 2O_2 \leftrightarrow CO_2 + 2H_2O$	-803
8	$H_2 + 1/2 O_2 \rightarrow H_2O$	-242
9	$CO + H_2O \leftrightarrow CO_2 + H_2$	-41.2
10	$2CO + 2H_2 \rightarrow CH_4 + CO_2$	-247
11	$CO + 3H_2 \leftrightarrow CH_4 + H_2O$	-206
12	$CO_2 + 4H_2 \rightarrow CH_4 + 2H_2O$	-165
13	$CH_4 + H_2O \leftrightarrow CO + 3H_2$	+206
14	$CH_4 + 1/2 O_2 \rightarrow CO + 2H_2$	-36

There are different types of gasifiers, which have been designed to improve different issues of the gasification process. **Figure 3-4** shows the types of gasifiers reported in the literature.

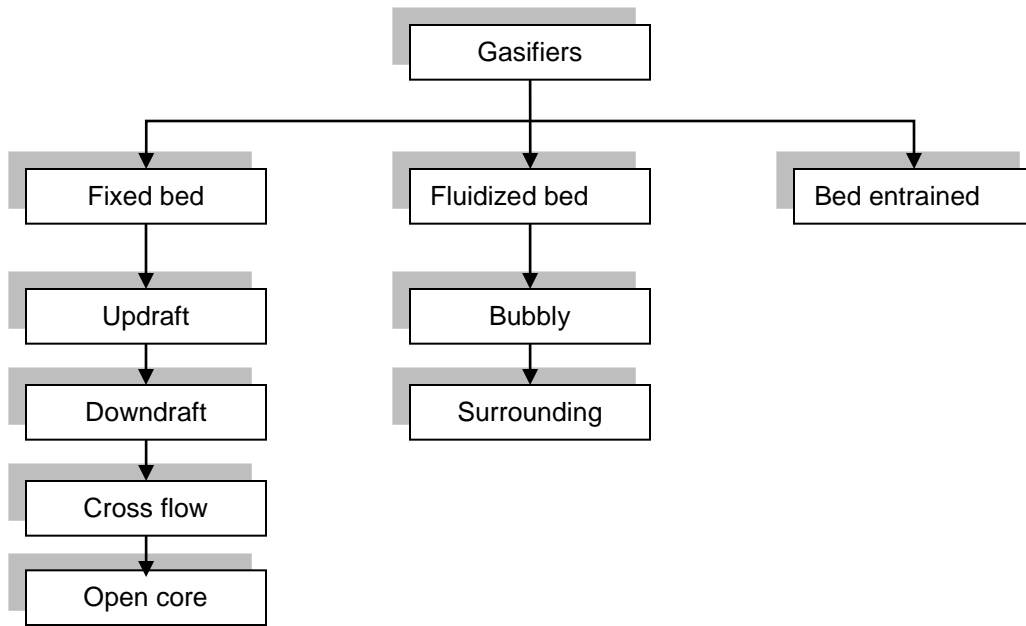


Figure 3-4. Types of gasifiers.

3.4 Syngas.

The syngas composition obtained from coal, petcoke, lignocellulosic biomass and municipal solid waste gasification as well as its quality and energy content is a function of a wide variety of variables such as the gasifier design, gasifying medium employed, raw material elemental composition and operating pressure. These variables have been studied by different authors with the goal to find better operation conditions to carry out an optimal gasification process [116], [117], [133], [134]. However, different experiences on gasification have demonstrated that the heating value of the syngas can vary between 4 MJ/ m_n³ to 28 MJ/ m_n³. The compositional range of the syngas obtained from coal, petcoke, lignocellulosic biomass and municipal solid waste as well as their heating value is reported in the open literature and they are showed in **Table 3-2**.

Table 3-2. Syngas composition obtained from the gasification of different raw materials.

Feedstock	H ₂ (% mol)	CO (% mol)	CH ₄ (% mol)	CO ₂ (% mol)	Ref.
Coal	25 – 30	30 – 60	0 – 5	5 – 15	[135]
Petcoke	22 – 30	39 – 48	0 – 1	18 – 34	[136], [137]
Biomass	5 – 16	10 – 22	1 – 6	8 – 20	[49]
MSW	8 – 23	22 – 24	0 – 3	6 – 15	[138]

As can be seen in **Table 3-2**, the syngas obtained from coal and petcoke has a higher HHV than the HHV obtained from lignocellulosic biomass and municipal solid waste gasification. For this reason, the use of these raw materials, at industrial level, has been preferred. However, the compositions showed in the previous table can vary significantly if the operating conditions mentioned above are optimized. Therefore, the use of lignocellulosic biomass has a great opportunity to become in the main raw material employed for this process to decrease the coal exploitation in different regions around the world. On the other hand, it was mentioned that air, oxygen and steam are the main gasifying mediums employed to perform the gasification process. The use of each one of these mediums provides different heating values to the syngas due to the increase of components such as H₂ and CO. Next a brief description of the syngas properties obtained with these agents is done.

Air, is one of the most employed gasifying mediums due to this one does not have costs associated with its acquisition and use. However, the syngas produced from air-blown gasification has the lowest heating value that can be obtained through this technology. The above is because the presence of N₂ and another impurities into the syngas composition. Thus, the syngas obtained using these oxidizing agent has a HHV between 4 MJ/m_n³ - 7 MJ/m_n³ with a H₂ content of 16 %, CO content of 22 % and CH₄ content of 6 %. However, some benefits related with the use of air are the low tar formation and higher syngas yield [49]. On the other hand, the amount of air needed to perform the gasification process is evaluated using the equivalence ratio (ER) concept. This concept is used to describe the ratio between the air–fuel of the gasification and the air–fuel ratio for complete combustion [139]. A higher ER, the amount of O₂ in the gasifier increase reducing the calorific value of the syngas. Moreover, a lower ER results in higher calorific syngas [109]. In the biomass case, the ER employed to carry out the gasification process is 0.25 approximately [46].

Oxygen and steam are preferred oxidizing agents to perform the gasification of different raw materials due to the use of these ones can increase the energy content of the syngas [118]. However, there are some economic issues related with its production that have restricted their use. When biomass is used as raw material to be gasified, the heating value of the produced syngas is $10 \text{ MJ/m}_n^3 - 18 \text{ MJ/m}_n^3$ and $12 \text{ MJ/m}_n^3 - 28 \text{ MJ/m}_n^3$ for steam and oxygen, respectively [118]. This increase in the heating value of the syngas is due to the absence of inert gases such as N_2 and the high content of H_2 and CO in the mixture.

3.4.1 Syngas applications.

Syngas can be used for heat and power generation as well as used to obtain value-added products such as biofuels (i.e. methanol, ethanol), ammonia, hydrogen, synthetic natural gas and dimethyl ether [11]. However, the production of the above-mentioned compounds is related with the syngas composition. Some applications are mentioned below:

- **Heat and power generation.**

The generation of heat and power from syngas in combined heat and power systems commonly known cogeneration systems are not considered as a transformation technology. In contrast, this is considered as a process that allows obtaining useful energy from the syngas through thermodynamic cycles. These cogeneration processes normally employ equipment such as turbines, compressors, generators, boilers and heat exchangers, which are strategically arranged to obtain high energy efficiencies [33], [34].

- **Fischer-Tropsch process.**

This process consists on the chemical transformation of syngas to produce hydrocarbons in the liquid phase through highly exothermic reactions. The Fischer-Tropsch process can be described as the catalytic conversion of H_2 and CO to hydrocarbon compounds such as diesel. This process has been implemented in different plants at industrial level for the production of different types of olefins and paraffins [26], [35].

- **Syngas fermentation.**

Syngas fermentation consists on the employment of the CO and CO₂ present in the syngas to produce ethanol using the following microorganisms: *Clostridium Ljungdahlii* and *Clostridium autoethanogenum* [36], [37]. An advantage of this process is its low energy requirements that are necessary to carry out the fermentation and the application of the already recognized techniques of ethanol separation and dehydration [38]. However, major challenges from an engineering point of view have been required to improve production yields and to improve aspects related with the mass and energy transfer.

3.5 Biorefineries as join point for the energy vectors and value-added products obtainment.

All the above mentioned energy carries can be produced under the biorefinery concept with the aim to increase their feasibility from technical and economic point of view. The application of thermochemical and biochemical processes together can increase the revenues expected from any type of biomass increasing the possibilities to improve the use of the different lignocellulosic resources.

3.5.1 The biorefinery concept.

The biorefinery idea contemplates the possibility to obtain many types of products from lipids, starches and biopolymers (i.e. cellulose, hemicellulose) derived from biomass. Therefore, its conception and basic definition arises from the concept that defines a crude oil refinery in which a great number of compounds are obtained from a single feedstock (i.e. oil) [24], [140], [141]. The above has been the basic principle used by different authors to express their definitions and explanations associated with the biorefinery concept. The following are some notions related to this idea.

Hines [142] presented the biochemical refinery concept as a group of biotechnological transformations where microorganisms produce more than one value-added product. Nevertheless, the biomass concept is not introduced directly in this perception. After, Huang et al [143] describes a biorefinery as a process that uses bio-based resources as crops or agro-industrial waste to produce energy and wide variety of chemicals. Alternatively, Demirbas [29] defines biorefinery as a facility that integrates biomass

conversion processes and equipment to produce fuels, power and value-added chemicals from biomass. Among the above explanations, the International Energy Agency (IEA) Bioenergy Task 42 gave the most exhaustive biorefinery definition as follows: “Biorefining is the sustainable processing of biomass into spectrum of marketable products and energy” [144].

In accordance with the above mentioned definitions, Moncada, Aristizábal and Cardona [145] define biorefinery as a complex system where biomass is integrally processed or fractionated to obtain more than one product including bioenergy, biofuels, chemicals and high added-value compounds that only can be extracted from bio-based sources. The last after a comprehensive study of the raw materials to be used and a sustainable design based on the latest state of the art technologies and approaches which include aspects of the three pillars of sustainability.

3.5.2 Biorefineries classification.

As was mentioned previously, biorefineries can include the use of many types of feedstocks, transformation processes, separation technologies and products. Thus, these can be classified taking into account different guidelines according to the analysis approach [23], [146]. Some of these classifications involve the raw material, conversion routes, products type and complexity level.

Attending the biorefinery definition is possible to establish that these can be classified considering the conversion routes employed to obtain different products. In this sense, bio-syngas, pyrolysis and hydrothermal based biorefineries are the three main types of facilities from thermochemical conversion pathway. Similarly, fermentation and oil plant based biorefineries are conceived from biochemical and chemical conversion pathways, respectively. Nevertheless, the difference between the thermochemical and biochemical biomass biorefining consists on the building blocks production that allow the chemicals, fuels and additives obtainment through catalytic reactions [29].

Depending on the raw material type, biorefineries can be classified into first, second and third generation. First generation biorefineries uses starch, sugars and vegetable oils derived from edible crops such as corn, sugarcane, cassava and oil palm [24], [25]. Second generation biorefineries uses lignocellulosic biomass from agro-waste, non-edible

crops, forestry residues and the organic fraction of municipal solid waste (OFMSW) as feedstocks [23], [24]. Third generation biorefineries considers the use of algae as feedstock. The above classification is performed according to the raw material type [147], [148]. However, Demirbas classifies biorefineries based on the physicochemical composition and nature of the raw material in green, cereal, oilseed, forest and lignocellulosic biorefineries [29].

Other way to classify the biorefineries is according to the product type obtained. In consequence, these can be classified into energy-driven and product-driven biorefineries [141], [146]. In energy-driven biorefineries, the system outputs are used as energy vectors or secondary energy sources to produce heat and power in combined systems [149]. The main energy-driven products are biofuels (i.e. biodiesel and bioethanol), biogas/biomethane and syngas [150], [151]. On the other hand, product-driven biorefineries are focused to produce biomaterials, bulk chemicals (e.g. acetone, ammonia), specialty chemicals (e.g. surfactants) and fine chemicals (e.g. lactic acid, *n*-butyric acid) [152].

A most comprehensive classification is related to the complexity level. This consider the quantity of generated products and its type. Accordingly, a biorefinery can be classified in first, second and third level. First level biorefineries produces only one product from a specified raw material (e.g. biodiesel from jatropha). Second level biorefineries produces two or more products that have chemical applications (e.g. xylitol, *n*-butanol from lignocellulosic material). Third level biorefineries are characterized by produce two or more products and generate electricity or directly usable energy [140], [153]. The mentioned classifications are interrelated. This means that a biorefinery can be cataloged in two or more items due that the criteria employed to classify these are independent.

The use of first generation raw materials for energy or industrial purposes impacts, at all levels, the food security of a country because their production generates competition on the natural resources that are available in a region (i.e. land and water) [26], [27]. For this reason, the lignocellulosic materials have been researched in the last years as main feedstock to be processed into a biorefinery. However, if only biochemical and thermochemical conversion pathways are applied, the variety of products would be limited only to fermentation metabolites and energy carriers. Therefore, catalytic processes can

contribute to increase the number of products of a common biorefinery. Additionally, the inclusion of these processes, which have a high maturity, could boost the biorefineries implementation in a future.

3.5.3 Biorefineries design.

The biorefinery design is an important issue that has been studied by many researchers through different methodologies [25], [153]. There are three major approaches to design biorefineries which can be summarized in superstructure and conceptual design, optimization and the combination of these two. The first one is a holistic methodology that considers a wide range of feedstocks and processes. However, restrictions related to the applications and uses of the final products are the main requirements of the biorefinery. Therefore, the high value-added products obtainment such as fine chemicals must have priority over bulk chemicals and services [145]. Instead, the optimization approach seeks to find the best design of a biorefinery based on special features such as maximum production yield and minimum production cost using a group of well-known technologies and a great number of conversion routs.

Finally, other methodological approach employed to design biorefineries is established on the so-called knowledge based approach for the synthesis of chemical processes. However, the hierarchy, sequencing and integration concepts are included to cover complex biorefinery systems. The hierarchy concept comprises the identification and classification of the main elements that conforms a biorefinery such as feedstock, technologies and products. The sequencing concept involves the logical and systematic design of each transformation stage, and the integration concept, implies the application mass and energy balances to increase the biorefineries productivity [23], [152]. This methodological approach can be used to evaluate the application of different processes for biomass-derived compounds valorization using catalytic routes to increase the biorefineries feasibility.

In accordance with the above definitions and explanations related with the biorefineries design, it is possible to observe that energy vectors and value-added products can be produced in the same facility. In addition, it was observed that the value-added products obtainment must be favored in order to increase the revenues. However, the energy vector production is important because of these ones provide more energy security and

less environmental issues. Therefore, the energy vectors and value-added products obtainment in future biorefineries must be discretized according to the real needs of the society and not only thinking in economic aspects.

3.6 Final remarks.

The gasification technology can be used to produce syngas, which has been considered as an energy vector and a chemical platform. The gasification industry has grown in the last years. However, coal is the most important feedstock employed in to produce syngas currently at high scale applications. Nevertheless, biomass is a promising raw material that can be used to produce heat and power through its use in a cogeneration cycle. On the other hand, gasification and syngas are promising players into future biorefineries due to its great applicability. Therefore, the gasification technology research based on the biomass use to produce energy vectors and chemical is well supported.

4.Oil palm rachis characterization.

Oil palm rachis samples were collected from an oil palm crop located in Puerto Salgar municipality, Cundinamarca, Colombia, localized at latitude 5°42'46.2" north and longitude 74°34'56.4" West. The raw material was dried at 50°C inside a convective furnace up to reach its equilibrium moisture to avoid the fungus formation. In addition, it was subject to a grinding process using a knives mill with the aim to decrease the samples particle size until ASTM 40 sieve. The samples were stored until its physicochemical characterization at room temperature.

The physicochemical characterization of the oil palm rachis involves the chemical composition, proximate, ultimate, thermogravimetric and atomic absorption analysis. The scope and main purpose of these analyses are described in the following sub-sections.

4.1 Chemical composition.

The chemical characterization of the oil palm rachis was done to determine its extractives, cellulose, hemicellulose, lignin and ash content. All the experimental procedures described in the following sections were performed by triplicate to ensure the reproducibility of the obtained data for the samples analyzed. The chemical characterization procedures were carried out in the Institute of Biotechnology and Agroindustry (IBA), Block T, Campus la Nubia, Universidad Nacional de Colombia – Manizales.

4.1.1 Extractives content determination.

There are a group of components that are present in biomass samples that must be removed prior to continue with the other steps of characterization. Moreover, it is necessary to remove these materials to avoid interference in experimental assays related with microorganisms such as fermentation and anaerobic digestion. These components are called **extractives** and they are composed by non-structural materials, inorganic compounds, sugars, nitrogenous compounds, chlorophyll, phenolic compounds (e.g. chlorogenic acid, tyrosol) and waxes [154]. The above mentioned components can be removed using several types of solvents. However, water and ethanol were the solvents used to carry out the extractives content determination of the oil palm rachis. The followed methodology to find both water and ethanol extractives was based on the National Renewable Energy Laboratories (NREL/TP-510-42619) [154], and it is described below:

The necessary materials to carry out the water and ethanol extractions are a group of thimbles, an analytical balance, a glass soxhlet extraction tubes (soxhlet syphon), condensers (NS 45/40), heating plates, flat-bottom flasks (500 ml) and hoses. In first place, the soluble water extractives content was determined weighting 10 grams of dry and milled oil palm rachis. Then, the sample was added into a pre-weighted extraction thimble. At the same time, the flat-bottom flasks were filled with 250 ml of distillated water and placed on the turn off heating plates. To avoid abrupt boiling, several boiling chips were put inside too. Afterward, the soxhlet extraction assembly was done. The thimble was placed inside the soxhlet syphon considering that the thimble must not exceed its height. Later, this one was placed over the flat-bottom flask and the condenser was used to close the extraction system. Once, the cooling water flow was started and stabilized, the heating plates were adjusted to ensure a minimum of 4-5 syphon cycles per hour. The water extractives determination assay lasted 24 hours.

After 24 hours of water extraction, the heating plates were turned off and the cooling water flow was stopped. Then, the thimble was removed from the soxhlet syphon and placed in a convective oven at 50°C. The dried thimble was transferred to a desiccator for one hour and weighted. After, this one was placed again inside the oven; and the above described procedure was performed until reach a thimble constant weight. On the other hand, the soluble ethanol extractives content was determined following the same procedure explained in the above paragraph.

The NREL method suggest to calculate either water or ethanol extractives content in dry basis. Thus, it is necessary use the following equations:

$$\text{Oven dry weight (ODW)} = \frac{(W_{\text{Sample}}) * \% \text{Total solids}}{100} \quad (4.1)$$

$$\text{Extractives (\%, db)} = \frac{(W_{\text{Sample before extraction}} - W_{\text{Sample after extraction}})}{\text{ODW}_{\text{Sample}}} * 100 \quad (4.2)$$

4.1.2 Holocellulose content determination.

Oil palm rachis can be considered as a lignocellulosic material. Therefore, it is mainly composed by a mixture of carbohydrate polymers such as cellulose, hemicellulose and lignin. The holocellulose content makes reference to the total polysaccharide fraction of lignocellulosic biomass contributed by cellulose and hemicellulose. Despite the raw material, the amount of both cellulose and hemicellulose in second generation feedstocks ranges from 50% to 75%. [155]. The holocellulose determination was performed as a method to calculate indirectly the hemicellulose content of the samples.

Holocellulose content was determined following the methodology described in the ASTM standard method entitled "*Method of Test for Holocellulose in Wood*", which could be found as ASTM D1104-56(1978) and described in more detail in the book entitled "*Paper and Composites from Agro-Based Resources*" [156]. This method must be carried out carefully to avoid any health and physical problem. Therefore, it is necessary follow all established safety protocols in chemical laboratories (i.e. masks, gloves, glasses, lab coat and so forth). The reagents used in this experimental method are sodium chlorite industrial grade, distilled water and acetic acid. On the other hand, the employed materials are a thermostatic bath, 1 mL pipette, analytical balance, Erlenmeyer flask (100 and 200 mL) and qualitative filter paper.

The process starts weighting 2.5 grams of dry and free-extractives oil palm rachis sample and introducing it inside of the 200 mL Erlenmeyer flasks. Then, 80 mL of distilled water, 500 μ L of acetic acid and 1 gram of sodium chlorite are added. The chlorination reaction produces toxic gases after a short time. Therefore, 100 ml Erlenmeyer flasks are

put over the reaction flask with the goal to avoid release and breathing such gases. In addition, the entire process must be done with the extraction cabin on. Simultaneously, the thermostatic bath must be set to 70°C. Afterward, the reaction mixture must be placed inside the bath and mixed manually. Each hour must be added 500 µL of acetic acid and 1 gram of sodium chlorite until reach six (6) reaction hours. Afterward, the samples were left 24 hours without further addition of sodium chlorite and acetic acid. Once the process has been completed, the holocellulose samples are filtered using a vacuum system and washed with 20 ml of acetone and sufficient distilled water to remove the yellow color and the chlorine odor. Finally, the filtered samples were placed inside the oven at 40°C to remove the moisture excess. The samples were weighted until reach constant weight.

The holocellulose content was calculated according to following equation (4.3).

$$\text{Holocellulose (\%, db)} = \frac{(W_{\text{Holocellulose}})}{\text{ODW}_{\text{Sample free of extractives}}} * 100 \quad (4.3)$$

4.1.3 Cellulose content determination.

Cellulose is an un-branched linear polymer of glucose [157]. This natural polymer is the most used fraction in biochemical processes to produce monomeric glucose to be converted in value-added products such as ethanol, lactic acid, succinic acid and so forth. In addition, this material has been considered as the greatest renewable resources in the world.

Cellulose content was determined following the methodology proposed in the test method T222 os-74 proposed by Kurschner & Hoffer, which is described detail in the book entitled “*Paper and Composites from Agro-Based Resources*” [156]. The reagents used in this experimental method are sodium hydroxide, distilled water and acetic acid. Alternatively, the employed materials are a 250 ml beaker, watch glass, qualitative filter paper and a vacuum filtration system. This process is less toxic than the holocellulose procedure. However, it is necessary to follow with the same safety rules until finish all the experimental characterization.

To perform the cellulose content determination 2 grams of dry holocellulose are necessary. This sample must be put inside of the 250 mL beaker. Simultaneously, prepare two NaOH solutions one at 17.5% w/v and the other one 8.3% w/v. Then, 10 mL of first NaOH solution must be added and well mixed maintaining a temperature of 20°C. Afterwards, each five (5) minutes, it is necessary to add 5 mL of a NaOH solution (17.5% w/v) until consume all this solution. Allow the mixture to stand at 20°C for 30 min, making the total time for NaOH treatment 45 min. Later, add 33 mL of distilled water at 20°C to the reactive mixture and let repose for one hour (1h) before filtering. Once the time has run out, transfer the holocellulose to the vacuum filter system and wash it with 100 mL of the second NaOH solution. After this, add 10 mL of acetic acid solution (10% v/v) to the Buchner funnel and turn off the vacuum system to increase the contact time between the holocellulose and the acetic acid. Three (3) minutes are sufficient contact time. The remaining solid was washed with distilled water until remove most of the acetic acid added previously. Finally, the solid cellulose is removed from the vacuum system and placed inside of the oven at 35°C is removed the moisture excess. The samples are weighted until reach constant weight.

The cellulose content was calculated according to following equation (4.4).

$$\text{Cellulose (\%, db)} = \left[\frac{(W_{\text{Cellulose}})}{(W_{\text{Holocellulose}})} \right] * \left[\frac{(W_{\text{Holocellulose}})}{[\text{ODW}_{\text{Sample free of extractives}}]} \right] * 100 \quad (4.4)$$

4.1.4 Hemicellulose content determination.

Hemicellulose is a natural polymer that is constituted by different monomeric sugars. Therefore, hemicellulose is considered as a hetero-polymer that contains C5 and C6 sugars [157]. For this reason, most research articles do not report the hemicellulose fraction as a unique compound. In general, hemicellulose can be divided in xylan, mannan, arabinan and galactan which can be determined using a HPLC column following the NREL standard method entitled “*Determination of sugars, by-products, and degradation products in liquid fraction process samples*” [158]. However, xylan content is higher in comparison with the other components. Therefore, it is possible to assume that the hemicellulose can be found by difference, which has been comparable with the xylan content reported by other authors.

The cellulose content was calculated according to following equation (4.5).

$$\text{Hemicellulose (\%, db)} = (W_{\text{Holocellulose}}) - (W_{\text{Cellulose}}) \quad (4.5)$$

4.1.5 Lignin content determination.

Unlike cellulose and hemicellulose, lignin is a macro-molecule that has not been well defined due to its difficult isolation and structural characterization. Nevertheless, this hetero-polymer has some characteristics that can be highlighted. This one is an amorphous polymer composed by three main compounds (i.e. p-cumarilic alcohol, coniferyl alcohol and sinapyl alcohol) partially resistant to acid hydrolysis and soluble in alkaline solutions [159]. Two types of lignin can be experimentally found. The first one is the most common and it is the determined here. This is called as “acid insoluble lignin”. The second one is called “acid soluble lignin” and requires other methodology that can not be applied. However, the acid insoluble lignin is a good estimate of the total lignin present in the lignocellulosic biomass due to the ratio between the insoluble and soluble acid lignin is 20/1 approximately [160].

Acid insoluble lignin was determined using the methodology described on a modified version of the test method TAPPI T222 om-02. The reagents used in this experimental method are sulfuric acid and distilled water. Otherwise, the employed materials are test tubes, test tube rack, thermostatic bath, analytical balance, 100 mL Erlenmeyer flasks, qualitative filter paper, vacuum filtration system and an autoclave.

The acid insoluble lignin determination requires a free extractive and dry sample of oil palm rachis. The amount to perform the characterization is 200 mg, which must be added into the test tubes. Then, a sulfuric acid solution (72% w/w) is added and mixed in a water bath at 30°C during one hour. The ratio between the volume of acid added and the mass of sample is 1 ml of 72% (w/w) H₂SO₄ per each 100 mg of sample. Afterward, it is necessary to add 56 mL of distilled water with the aim to reduce the acid concentration. However, this process must be performed carefully. The diluted solution is transferred into a 100 mL Erlenmeyer flask and covered with aluminum foil. This mixture is autoclaved for one hour at 121°C and 2 bars. After this process, it is possible to identify a solid residue (that is the acid insoluble lignin). Therefore, this mixture must be filtered. Finally, the solid lignin is removed from the vacuum system and placed inside of the oven at 30°C to

remove the moisture excess. The samples are weighted until reach constant weight. This temperature is recommended to avoid that the filter paper burns due to this one is impregnated of acid.

The acid insoluble lignin content was calculated according to following equation (4.6).

$$\text{Acid insoluble lignin (\%, db)} = \frac{(W_{\text{Acid insoluble lignin}})}{\text{ODW}_{\text{Sample free of extractives}}} * 100 \quad (4.6)$$

4.1.6 Ash content determination.

Ashes are considered as all inorganic fractions that the lignocellulosic biomass have. It is possible to identify some minerals such as Aluminum (Al), silicon (Si), potassium (K), magnesium (Mg), manganese (Mn) and iron (Fe) through atomic absorption equipment. However, the ash content generally is reported as the solid residue after a combustion process at controlled temperatures. The mineralogical composition is important to analyze if the raw material will be subjected in a thermochemical process. Therefore, both ash and mineralogical composition were found for the oil palm rachis in this work.

The followed methodology to find the ash content was based on the National Renewable Energy Laboratories (NREL/TP-510-42622) [161]. The materials that are required are a muffle and a crucible. The process starts with 500 mg of free extractives and dry sample. The crucible is weighted to avoid any confusion in the future. After this, the samples are put inside of the muffle and a series of heating ramps are programmed. First, the heating ramp goes from room temperature to 105°C and this temperature is maintained during 12 minutes. Then, the second ramp goes until 250°C at 10 °C/min. This ramp is retained for 30 minutes. The next ramp has a heating rate of 20 K/min and it is programed to reach a temperature of 575°C for 180 minutes. Finally, the temperature is decreased until reach a temperature of 105°C. In this moment, the crucibles are removed from the muffle and placed directly into a desiccator. Once, the ashes have reached room temperature these ones are weighted.

The ash content was calculated according to following equation (4.7).

$$\text{Ash (\%, db)} = \frac{(W_{\text{Crucible + ash}} - W_{\text{Crucible}})}{\text{ODW}_{\text{Sample}}} * 100 \quad (4.7)$$

Finally, a summary of the standard methods employed to find the chemical composition of the oil palm rachis can be found below:

Table 4-1. Standard methods used to perform the chemical characterization of the oil palm rachis

Analysis	Method	Reference
Total solids and moisture	ASTM E1756– 08 (2015)	[162],
	NREL/TP-510-42621	[163]
Extractives	ASTM E1690-08 (2016)	[154],
	NREL/TP-510-42619	[164]
Holocellulose	ASTM D1104-56(1978)	[165]
Cellulose	(T 203 os-74)	[166]
Acid insoluble lignin	(T 222 om-02)	[167]
Ash	ASTM E1755 - 01(2015)	[166]

4.2 Proximate and ultimate analysis.

Second generation raw materials are composed by different organic compounds as well as small amounts of inorganic impurities which can affect its properties as fuel. These organic compounds are formed by carbon (C), hydrogen, (H), oxygen (O), nitrogen (N) and sulfur (S), which can be used to predict possible products formation and chemical species produced. On the other hand, important aspects related with the volatile matter content and solid residue after a thermochemical process are an important way to characterize the lignocellulosic biomass that will be used as raw material in this type of processes. In addition, the above mentioned information can be used to estimate other relevant properties in the energy system analysis such as the high heating value (HHV), heat of formation (ΔH_f) and empirical formula.

Thus, ultimate and proximate analysis are used to determine the elemental composition in terms of C, H, O, N, S as well as the volatile matter, fixed carbon and ash content of the raw material, respectively. These methods are employed as a basis to build-up the theory related with biomass gasification systems. A description and explanation of these methods are done below:

4.2.1 Proximate analysis.

This analysis classifies the lignocellulosic biomass in terms of gross components such as volatile matter (VM), fixed carbon (FC), moisture (M) and ash content. This process is easy to carry out and it is simple in comparison with the information that can be obtained from it [118], [168]. Each one of the above mentioned gross components are described below:

- **Volatile matter (VM) determination.**

Volatile matter can be defined as a group of gaseous products, excluding moisture vapor, which are released when a sample of biomass is subjected at $950 \pm 20^\circ\text{C}$. The volatile matter determination was carried out following the procedure explained in the standard test method ASTM E872 – 82 [169]. The necessary materials are a platinum crucible, a muffle, analytical balance, heat resistant gloves and a heat resistant mask.

Firstly, the platinum crucible weight must be recorded using an analytical balance. Then, 1000 mg of dry sample are added into the crucible and both are weighted. Afterward, insert the crucible into the muffle previously heated at $950 \pm 20^\circ\text{C}$. The sample must remain inside the muffle for 7 minutes. It is necessary to mention that the crucible must be covered before to be introduced in the muffle with a platinum cap in order to avoid that the carbon deposit burn away. The volatile matter content was determined using the following equations (8) and (9)

$$\text{Weight loss (\%)} = \frac{(W_{\text{Crucible + sample}}) - (W_{\text{Crucible + solid residue}})}{(W_{\text{Crucible + sample}}) - (W_{\text{Crucible}})} * 100 \quad (4.8)$$

$$\text{Volatile matter (\%)} = \text{Weight loss (\%)} - \text{Moisture content (\%)} \quad (4.9)$$

- **Fixed carbon (FC) determination.**

Fixed carbon is a poly-nuclear aromatic residue that is combustible. This one is the solid residue produced after the volatile matter determination minus the mineralogical content of the samples (i.e. ash content). The fixed carbon content can be calculated using the following balance equation (10):

$$\text{Fixed carbon (\%)} = 1 - \text{VM (\%)} - \text{M (\%)} - \text{Ash content (\%)} \quad (4.10)$$

The above equation reports the fixed carbon content in an air dry basis. However, it is more useful report all the parameters found in the proximate analysis in a totally dry basis. For this, the equation (10) can be modified as follows:

$$\text{Fixed carbon (\%, db)} = 1 - \text{VM (\%, db)} - \text{Ash content (\%)} \quad (4.11)$$

In general terms, lignocellulosic materials have a high volatile matter content. Therefore, this type of feedstocks can be used in thermochemical process due to these ones generate low amounts of solid residues. On the other hand, the ash content of biomass materials is considerably lower than for coals [168]. A summary of the standard methods taken into account to perform the proximate analysis is presented in **Table 4-2**.

Table 4-2. Standard methods used to perform the proximate analysis of the oil palm rachis.

Analysis	Method	Reference
Total Moisture	ASTM E871 – 82 (2013)	[170]
Volatile Matter	ASTM E872 – 82 (2013)	[169]
Ash	ASTM E1755 - 01(2015)	[166]
Fixed Carbon	ASTM E870 – 82 (2013)	[167]

4.2.2 Ultimate analysis.

The elemental raw material composition is important information that can be used to calculate material balances in thermochemical processes. Ultimate analysis reports the carbon (C), hydrogen (H), nitrogen (N), sulfur (S) and oxygen (O) content of any type of biomass or solid fuel. Previously to perform this analysis the moisture content of the sample must be removed with the aim to avoid over-estimate the amount of hydrogen and oxygen [168].

The content of atomic carbon in biomass is lower than the carbon content in other solid fuels such as coals. On the other hand, the oxygen content in lignocellulosic biomass is higher than the oxygen content in coals. Therefore, the high heating value of coals is higher than the biomass. For this reason, many researchers have focused in deoxygenation processes to increase the energy density of second generation materials to become more competitive in the energy market. Finally, any solid fuel can be characterized comparing its H/C ratio and O/C ratio [118].

From dried biomass and C, H, O and N content is possible write the empirical chemical formula of the solid fuel as follows:

- Express the dry biomass $\text{CH}_x\text{O}_y\text{N}_z$
- Calculate each variable

$$x = \frac{H M_C}{C M_H}; \quad y = \frac{O M_C}{C M_O}; \quad z = \frac{N M_C}{C M_N} \quad (4.12)$$

Where M_C , M_H , M_O , M_N are the molecular weights of carbon, hydrogen, oxygen and nitrogen respectively and C, H, O and N are mass fractions of those elements.

The elemental composition analysis was carried out in the University of Jaen (Spain) following the standard methods presented in **Table 4-3**

Table 4-3. Standard methods employed to find the ultimate analysis of the oil palm rachis

Analysis	Method	Reference
Carbon	ASTM E777-17 (2017)	[171]
Hydrogen	ASTM E777-17 (2017)	[171]
Nitrogen	ASTM E778-15 (2015)	[172]
Sulfur	ASTM E775-15 (2015)	[173]
Oxygen	ASTM E870 -82 (2013)	[167]

4.3 Thermogravimetric analysis.

Thermogravimetric analysis can be described as a technique in which the weight loss of a sample is measured as a function of the temperature and time. This method is based in the volatile matter formation at controlled heating rates with the aim to characterize the thermal properties of different materials through the pre-exponential and activation energy calculation [174]. There are two types of atmospheres to carry out the analysis. The first one is an oxidative environment (i.e. air, oxygen) and the second one is an inert atmosphere (i.e. nitrogen, argon, helium). Generally, if pyrolysis kinetics parameters are necessary an inert atmosphere is employed. In contrast, if combustion kinetic parameters are necessary an oxidative atmosphere must be used.

Thermogravimetric analysis is a useful method to know the decomposition behavior of any lignocellulosic biomass under different atmospheres. In this work, this analysis was used to identify the volatilization of the oil palm rachis under anoxic conditions with the aim to calculate the kinetic parameters of the pyrolysis process of the oil palm rachis.

The thermogravimetric (TG) and differential thermogravimetric curve (DTG) were performed in the Laboratorio de Polímeros y Materiales Estructurados located at National University in Manizales. To provide inert atmosphere nitrogen was used as carrier gas with a volumetric flow of 60 mL/min. The initial temperature of the entire process was 18°C and its final temperature was 930°C. The used heating rates were: 10, 20, 30, 40 and 50 °C/min [106], [175].

4.4 Atomic absorption analysis.

Atomic absorption spectroscopy analysis (AAS) is an analytical method based on the absorption of ultraviolet or visible radiation by free atoms in the gaseous state [176]. AAS was performed to find the composition of the ashes produced after the gasification process. This process was carried to know the mineralogical composition of the ashes generated by the conversion process. In addition, to confirm if the oil palm rachis employed in the gasification process can produce clinker and slagging. Finally, the alkali index is calculated using the information from the atomic absorption analysis with the goal to determine the possible fouling of the equipment. The alkali index can be calculated using the following balance equation (13)

$$\text{Alkali index (kg/MJ)} = \frac{1000}{(\text{HHV})} * \frac{\text{Ash (\%, db)}}{(100)} * \frac{\text{K}_2\text{O (\%, ash)} + \text{Na}_2\text{O (\%, ash)}}{(100)} \quad (4.13)$$

4.5 Final remarks.

The methods of physicochemical characterization described above are in accordance with international standards, so that the results that are derived when applying these methods will be comparable with the literature. However, aspects directly related to the raw material such as crop age, soil type and other aspects could be differentiating factors between the raw material studied in this thesis work and other works reported in other bibliographic sources such as articles, book chapters, thesis and others.

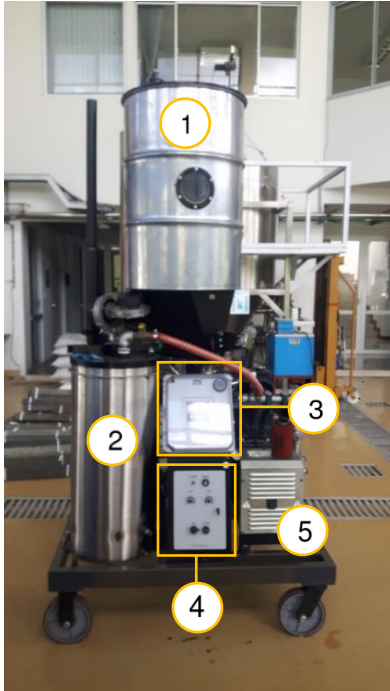
5. Pilot – scale air downdraft gasification.

The oil palm rachis gasification process was performed in the Institute of Biotechnology and Agroindustry, located at Universidad Nacional de Colombia Manizales campus. This chapter gives a brief description of the employed equipment, its operation and items used to evaluate the process performance. However, other aspects related with the equipment maintenance as well as recommendations for its future use can be found in the operation manual of the equipment.

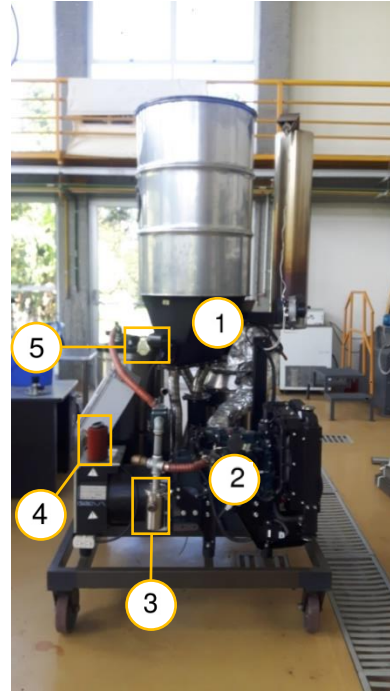
5.1 Equipment description and recognizing.

The pilot-scale equipment used is a downdraft gasifier without external heat source (i.e. auto-thermal gasifier), which uses air as gasifying agent. This equipment is commonly known as an Imbert style gasifier due to the constricted hearth that characterizes it (**Figure 5-2**) [177]. In addition, this type of gasifier is considered as a prototype. However, it has a number of disadvantages that has been mentioned in chapter 3. The gasification system was built by the All Power Labs industry in California, USA and it can be identified as a 10 kW Power Pallet model GEK gasifier version 1.08.

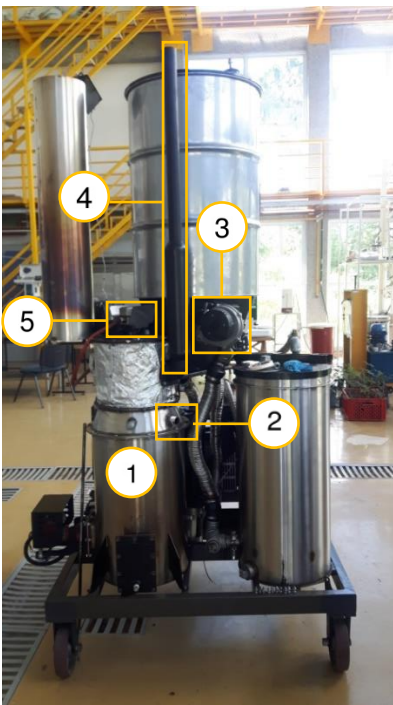
The GEK TOTTI (i.e. Gasifier Experimenter's Kit, Tower of Total Thermal Integration) system is comprised of a gasifier, an engine and a generator. Moreover, this system is supplemented with electronic controls and pre-heating process adaptations with the aim to be a small scale off-grid electricity generator [130]. Thus, this equipment was designed to carry out drying, pyrolysis, combustion and reduction of high grade biomass fuels such as hardwood with low moisture contents as well as specific shape and size. **Figure 5-1** shows a picture of the employed gasification system from different perspectives.



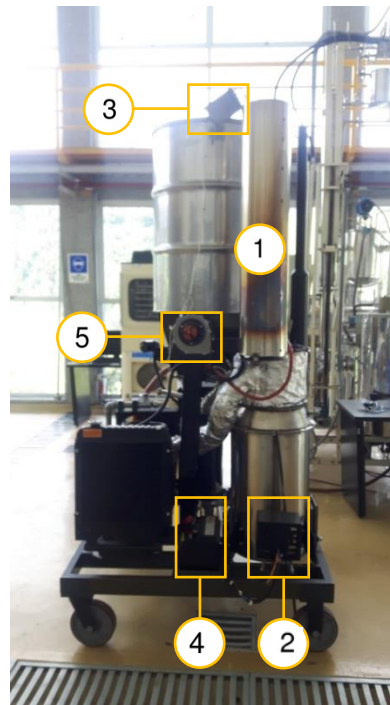
a) Front side.



b) Right side.



c) Left side



d) Back side.

Figure 5-1. Photos of the downdraft gasifier used to produce syngas.

The main parts that can be identified in the above figure are mentioned in **Table 5-1**. It is important to mention that all the gasifier system parts mentioned here must be checked before and after each run to avoid any type of problem.

Table 5-1. Main parts of the GEK TOTTI system (10 kW Power Pallet v1.08).

No.	Front side (5.a)	Right side (5.b)	Left side (5.c)	Back side (5.d)
1	Hopper	Drying bucket	Gasifier	Flare
2	Gas filter	Engine	Air inlet check valve	Grater
3	PCU panel	Condensate vessel	Gas blower	Flare igniter
4	Operation panel	Air filter	Exhaust stack	12V DC battery
5	Generator	Auger	Fuel switch	Air blower

Additional parts that are not mentioned have an important role in the equipment operation. Thus, these parts are described concisely with the aim to complete the GEK TOTTI system knowledge. The gasifier has two main valves that regulate the gas flow into the equipment. The first valve regulates the syngas flow between the flare and gas filter. In open position, this valve allows the syngas flow to the flare to be tested and burned. In contrast, when the valve is closed, the syngas flow is re-directed to the gas filter to be upgraded and used in the engine. This valve is located behind the gas blowers. In addition, it should not be confused with the air inlet check valve. The other valve regulates the syngas flow that can be supplied to the engine. This valve is located at the top of the gas filter and it can be seen in **Figure 5-1a**. At the beginning of the operation, the first valve must be open while the other one must be closed. Only when the engine is going to be used, the second valve can be open and the other must be close softly.

In addition, the air servo and the oxygen sensor are parts that play an important role in the equipment operation. The air servo regulates the air intake in the engine with the aim to reach a good syngas combustion. This element is controlled by a PID loop, which uses the oxygen concentration in the exhaust given by the oxygen sensor. This controller has been tuned to maintain the quotient of the detected air/syngas ratio and the stoichiometric air/syngas ratio in 1.05. Other important part that must be taken into account is the fly-ash cyclone. This one is used to separate ashes from the produced syngas. However, this element could be obstructed due to the tar condensation.

A general description of the GEK TOTTI system was performed above. However, a more detailed description of the gasifier must be done to understand how it works. The gasifier was presented in **Figure 5-1a**. However, its outside corresponds to a jacket that prevents excessive heat losses.

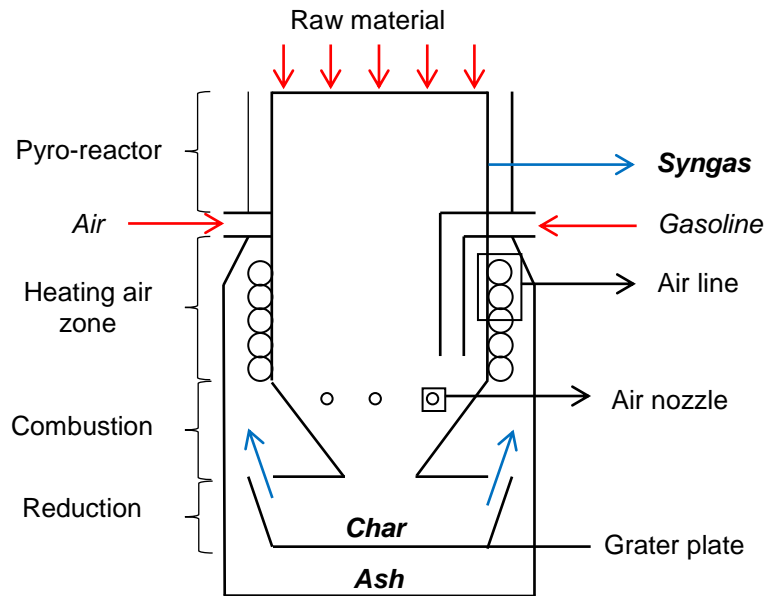


Figure 5-2. Gasifier cross section, zones, inlet and outlet streams.

A cross section of the gasifier is shown in **Figure 5-2**. This system can be divided in four zones according to their distribution. The first zone is the pyro-reactor. Here the feedstock is fed to the gasifier and it is heated using the exhaust gases from the engine. This zone can be identified due to it is covered by an aluminum jacket (see **Figure 5-1c**). The internal diameter of the pyro-reactor is 210 mm and its height is 200 mm. After this zone, the air and gasoline intake points can be found. The air intake point is open during all the operation while the gasoline intake point only is used at the beginning. In this section the air employed in the combustion zone is heated through a coil heat exchanger, which surrounds the gasification reactor. The internal diameter of this section is the same that the pyro-reactor and its height is 260 mm. The third zone can be denominated as projected hearth or combustion zone. At this point, pre-heated air is injected in the raw material bed using air nozzles. Thus, this zone is the hottest zone of the gasifier due to the combustion reaction is exothermic. This section is conical with the aim to increase the residence time of the feedstock in this zone. Its dimensions are: largest base 210 mm, smallest base 73.62 mm and height of 170 mm. Finally, the reduction zone is located at

630 mm from the top of the gasifier and it is composed by the char and ash sub-zones, which are separated by the grater plate. The total height of the gasifier is 1000 mm and the height from the grater plate to the gasifier bottom is about 80 mm. Using the above dimensions, it is possible to calculate an approximate value of the gasifier capacity, which is 0.022158 m³ excluding the ash sub-section. Therefore, the range of feedstock that can fill the gasifier varies from 2 kg (e.g. shavings) to 13 kg (e.g. wood pellets) [178].

According to the above, the calculated volume can be used to find the minimal amount of feedstock that is required to fill the gasifier and also calculate the amount of fuel that is present in each zone of the reactor. On the other hand, it is important to note that this part of the GEK TOTTI system is the heart of the equipment due to the solids flow in the system ends there as well as the producer gas flow starts.

5.2 Operation run.

Once the entire system has been prepared to be used, the gasifier is started and the operation of the equipment begins. In the process to obtain syngas and electricity, there is a sequence of flows from the hopper to the exhaust pipe. The identification of these flows allows explaining the operation run of the entire system. Therefore, these ones are explained below:

The **solids flow** in the GEK TOTTI system starts introducing the raw material into the hopper. Then the feedstock is transported from the hopper to the gasifier through an auger (i.e. endless screw). This one is controlled by a level switch located on the top of the gasifier. Thus, this system works as a level controller and it allows keep the reactor full. Afterward, the raw material is subjected in each one of the gasification sub-processes (i.e. drying, pyrolysis, combustion and reduction) to produce syngas, char and ash. Nevertheless, the char and ashes are separated using a grate basket shaker, which has been programmed to shake three seconds once every five minutes. Moreover, fly-ashes dragged by the syngas can be collected in the bottom of the cyclone. Summarizing, the solids flow in the system has the following order: Hopper → Drying bucket → Pyro-reactor → Heating air zone → Projected hearth → Reduction zone → ash collection sub-zone.

Finally, the solids flows is related with the gases flow and exhaust flow in heat transfer processes to pre-heat the inlet air and heat up the feedstock into the pyro-reactor.

The **gases flow** starts with the air entrance to the system in the combustion zone and the syngas production after gas – solid reactions in the reduction zone. Hot syngas passes through the cyclone to remove particulate matter. Then, this one goes to the drying bucket to perform the feedstock drying process through heat exchange. Subsequently, it is sent to the gas filter with the aim to remove tars, water and remaining char particles. The gas filter is composed by a four-level bed of wood. The first level is composed by big wood pieces (i.e. 0-5" – 1"), the second level has middle wood pieces with a particle size between 1/8" to 1/2" and the third level contains shavings from the furniture industry with a particle size of 16 mesh. Finally, two foam disks and a steel screen are placed on the top of the packed bed. In this point, the syngas has been cooled and upgraded to be used in the gas engine. Thus, the gases flow into the equipment can be summarized as follows: Gasifier → Cyclone → Drying bucket → Gas filter → Engine.

To conclude, the **exhaust flow** starts in the engine after the syngas combustion with air. The exhaust gases are addressed from the engine to the pyro-reactor to heat up the feedstock there. Then, these gases are released to the atmosphere. In this point the raw material has been converted into syngas and burned to produce electricity. The generator installed in the GEK TOTTI system has an electrical capacity between 2 – 10 kW. In general terms, gasifying 1.2 kg of biomass produces 3 m³ of syngas approximately, which produce about 1 kWh. A detailed scheme of the GEK TOTTI system employed and each one of the above mentioned flows are shown in **Figure 5-3**.

5.2.1 Feedstock requirements.

The raw material to be employed into the gasifier must have a particle size between 0.5" to 1.5" as well as to have moisture content higher than 10% and lower than 20%. For this reason, the oil palm rachis samples were prepared to accomplish the above mentioned requirements. Each step to condition the raw material is described as follows:

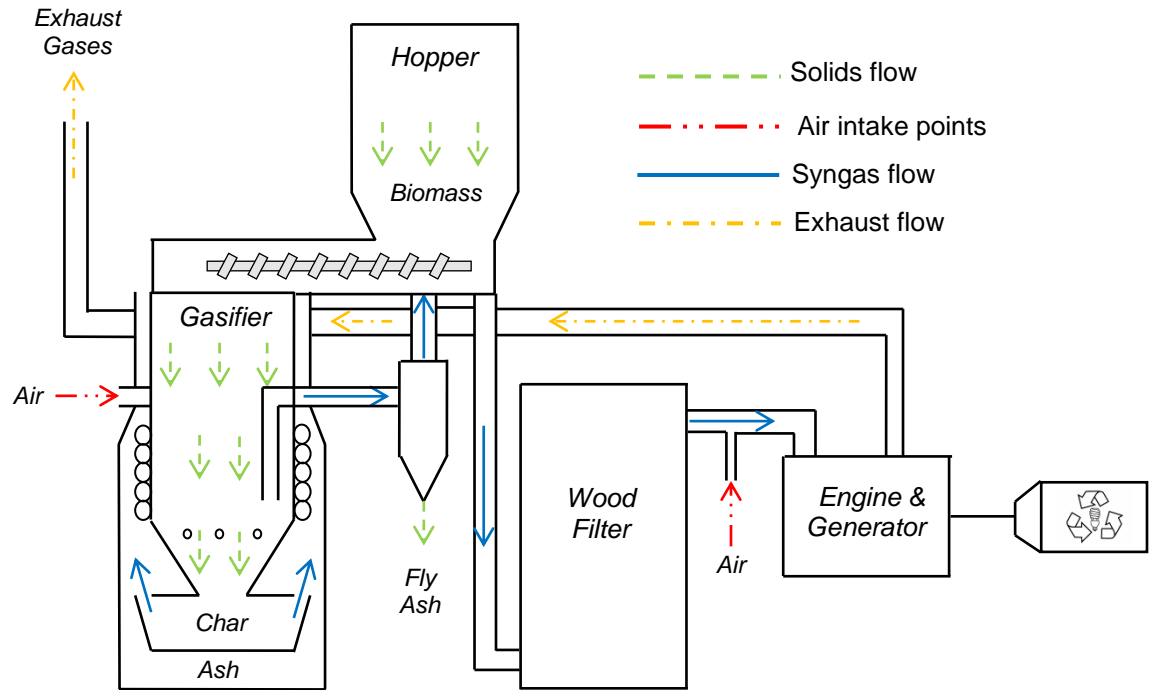


Figure 5-3. Process flow diagram of the pilot-scale GEK TOTTI system.

The oil palm rachis samples were dried at room temperature with the aim to remove by natural convection un-bound moisture. The first drying process was carried out during 4 weeks due to their high moisture content and their dimensions (i.e. longitude of 80 cm and diameter of 7"). After this first drying stage, the oil palm rachis samples (i.e. 80 kg) were cut using two steps. The first one was to reduce the samples longitude from 80 cm to pieces of 5 cm making cross section cuts. This cutting step was performed using a band saw Dewalt Dw739. As a result, 40 kg of oil palm rachis samples were cut and only 38 kg were recovered due to the sawdust production (i.e. 2 kg). Then, the size of these pieces was reduced manually using a knife producing 1 kg of sawdust. Therefore, a total of 23,125 pieces of oil palm samples were made. Afterward, the correct sized samples were subjected to the second drying stage using a convective furnace during 24 h to remove any trace of moisture. The final amount of oil palm rachis samples ready to be used in the GEK TOTTI systems was 34 kg. According to the above, 3 months were necessary to prepare the raw material.

5.2.2 Start – up and shut – down.

First that all, the GEK TOTTI system must be operated out of enclosed areas to avoid gases inhalation. It is necessary to make sure that the 12VC DC battery is charged and all the equipment parts are in good conditions. To check this, a test of the blowers, flare, grater and engine can be performed from the control panel.

Thus, the **start – up** of the gasification process begins introducing the oil palm rachis into the hopper and sealing it hermetically. Then, char is added into the gasifier, avoiding add more than 10% of the total feedstock amount, with the aim to reach rapidly the gasification temperatures (650°C - 900°C). After this, the auger system is turned on to feed the raw material until fill the gasifier. Then, gasoline, used as lighter, was added through the ignition port and the valve that regulates the syngas flow between the flare and gas filter must be open. After this, the gas blowers are turned on to produce a suction of 2 WC (i.e. inch of water) and direct fire must be provided using a gas pipe and a blowtorch until reach a temperature of 70°C. Subsequently, it is necessary to close the ignition port and the suction must be raised to 4 WC.

Once the system has increased its temperature, white smoke is produced. This one can not be breathed directly. Meanwhile, the air blower must be turned on and manipulated until these gases are burned. Generally, to accomplish the above, it is necessary that the flare igniter stays lighting. After that the produced gases are flammable and the equipment has stabilized its temperatures, the valve that regulates the syngas flow that will be supplied to the engine must be open and the other one closed. At the same time, the gas and air blower are turned off. The engine star up is similar to the star up of a car. Therefore, the engine starter must be powered until reach a constant operation. It is advisable do not overstress the starter to avoid its damage. Finally, the equipment operation until consume more than a 70% of the feedstock is related with observe the control panel and monitoring temperatures and pressures.

On the other hand, the **shut – down** of the gasifier is a simpler task. Firstly, the engine is turned off as well as the air and gas blowers. Then, close the valve that regulates the syngas flow to the engine and open the other one. Make sure that the system does not have any ventilation point and that the gasifier is completely closed. Finally, wait that the temperatures decrease until reach 350°C or 300°C (if it is possible).

5.2.3 Temperature profile estimation.

The temperatures profile into the gasifier was measured using five (4) K-type thermocouples located at different heights from the pyro-reactor top. Two of these four thermocouples are included in the equipment and they are monitored in the control panel, which are named as *T_tred* and *T_bred*. These ones are fixed and located at 540 mm and 630 mm from the top of the gasifier and shows the temperature at the restriction of the reduction zone and the temperature at the bottom of the reduction zone (above the grate basket), respectively. The other two (i.e. *T_pyro* and *T_bottom*) thermocouples were added to the gasifier. These ones were located at 400 mm and 900 mm from the top of the reactor. Moreover, these thermocouples were designed with a threaded connection to ensure air tightness in the system. The temperature profile was recorded each one or two minutes during the operation using a FLUKE 50S K/J thermometer provided by the productive processes laboratory located at the Universidad Nacional de Colombia, Manizales campus, block L. The designed thermocouples have a diameter of 1/8" and they were manufacture by *Termocuplas S.A* in Medellín, Colombia.

Other temperatures were registered in the gasification experience introducing another K-thermocouple at 300 mm approximately from the pyro reactor top and measuring the gas temperature at the entrance of the cyclone. These temperatures also were registered with the aim to complete the knowledge of the temperatures that are reached in different parts of the GEK-TOTTI system.

5.2.4 Synthesis gas determination.

As has been mentioned in the above chapters, synthesis gas, syngas or producer gas is a mixture of hydrogen (H₂), carbon monoxide (CO), carbon dioxide (CO₂) and methane (CH₄) as main components. However, other low molecular weight hydrocarbons are present [127]. The gas composition from the gasification of oil palm rachis can be used to calculate some indicators of the gas quality (i.e. high heating value) as well as process variables such as cold gas efficiency and syngas volumetric flow. For these reasons, it is important to record the gas composition during the gasifier operation.

The syngas composition was measured using a gas analyzer "Gasboard—3100P portable infrared syngas analyzer", which can record the volumetric composition of

oxygen (O₂), carbon monoxide (CO), carbon dioxide (CO₂), hydrogen (H₂), methane (CH₄) and light hydrocarbons such as ethane and propane (C_nH_m). The composition gas measurement is performed in continuously. However, only each 5 seconds the syngas composition gas saved into the gas analyzer memory. Before the syngas entrance to the analyzer, this one passes through a cleaning system composed by a water column, bed of activated carbon and coalescing filter to avoid any damage to the gases detectors inside the equipment. Finally, the data is exported from the gas analyzer to a computer. The data is discharged in a excel file that shows the following items: group, register (date), CO (%), CO₂ (%), CH₄ (%), C_nH_m (%), H₂ (%), O₂ (%) and calorific value.

5.3 Parameters to evaluate the performance of the gasification process.

The parameters used to evaluate the performance of the gasification process were the reported by Guangul et al [179]. These ones are:

- ✓ Oil palm rachis high heating value (HHV) and Low Heating Value (LHV)
- ✓ Syngas high heating value (HHV) and low heating value (LHV)
- ✓ Syngas flow rate (F_{gas})
- ✓ Gas yield (Y_G)
- ✓ Carbon conversion efficiency (η_C)
- ✓ Cold gas efficiency (η_g)
- ✓ Ash and Char yields (Y_{ash} , Y_{char})

In general terms, the high heating value (HHV), gas yield (Y_G), carbon conversion efficiency (η_C) and cold gas efficiency (η_g) values ranged from 2.80 to 5.90 MJ/Nm³, 1.67 to 2.25 Nm³/kg, 71.8 to 93.4% and 36.9 to 62.5%, respectively [125], [136].

The HHV of the oil palm rachis used in this work was calculated using the non-linear correlation proposed by Shen et al [180], which is written in the following equation.

$$\begin{aligned} \text{HHV} = & 20.7999 - 0.3214(\text{VM}/\text{FC}) + 0.0051(\text{VM}/\text{FC})^2 - \\ & 11.2277(\text{ASH}/\text{VM}) + 4.4953(\text{ASH}/\text{VM})^2 - 0.7723(\text{ASH}/\text{VM})^3 + \\ & 0.0383(\text{ASH}/\text{VM})^4 + 0.0076(\text{FC}/\text{ASH}) \end{aligned} \quad (5.1)$$

The HHV and LHV of the syngas produced by the gasifier can be calculated using the compositional or molar concentrations of each combustible compound into the gas. In addition, the ideal gas relation for their calculation can be applied due to these one is produced at low pressure and relative high temperature

$$\text{HHV} = \sum \text{HHV}_i x_i \quad (5.2)$$

$$\text{LHV} = \sum \text{LHV}_i x_i \quad (5.3)$$

These calculations can be performed using the reported values of the HHV or LHV for each gas. For this, Waldheim and Nilsson have been reported the heating value of the syngas components [181], which can be found in **Table 5-2**.

Table 5-2. High and Low heating value of main combustible gases into syngas

Item (MJ/Nm ³)	H ₂ (% mol)	CO (% mol)	CH ₄ (% mol)
LHV	10.788	12.622	35.622
HHV	12.769	12.622	39.781

The mass balance of the gasifier can be completed calculating the syngas flow rate using the equations given by the **nitrogen based method** or the **carbon based method**. The nitrogen based method was used here due to the carbon method requires the mass fraction of carbon in ash and tars, which were not determined in this work. Nevertheless, both equations are shown below:

$$F_{\text{gas}} \left[\frac{\text{Nm}^3}{\text{h}} \right] = F_{\text{Air}} \frac{\% \text{N}_2 \text{ air}}{\% \text{N}_2 \text{ gas}} \quad (5.4)$$

$$F_{OPR}CC_{fuel} + \sum F_{Air}CC_{Air} = F_{gas}(CC_{gas} + C_{Tar}CC_{Tar} + C_{Part}CC_{Part}) + F_{Ash}CC_{Ash} \quad (5.5)$$

In equation (5.3), F_{gas} has the same units of the equation (5.2). The overall units of this equation are kilograms per hour. Refer to the “List of Symbols and Abbreviations” to find each unit of the written equations. Once the syngas volumetric flow has been calculated, it is possible to determine the gas yield of the process using the following equation.

$$Y_G \text{ (Nm}^3\text{/kg)} = \frac{F_{gas}}{F_{OPR}} = \left[\frac{F_{Air}}{F_{OPR}} \right] \left[\frac{\% N_2 \text{ air}}{\% N_2 \text{ gas}} \right] \quad (5.6)$$

On the other hand, two efficiencies can be calculated. The carbon conversion efficiency can be calculated as follows:

$$\eta_C \text{ (\%)} = \frac{\text{Carbon output}}{\text{Carbon input}} * 100 = \frac{LHV_{gas}}{LHV_{feedstock}} * \frac{F_{gas}}{F_{OPR}} \quad (5.7)$$

Where x_{CO_2} , x_{CO} and x_{CH_4} are the mole fractions at normal temperature and pressure of carbon dioxide, carbon monoxide and methane into the syngas and x_C is the carbon content of the feedstock by weight.

Finally, the cold gas efficiency is calculated as follows:

$$\eta_g \text{ (\%)} = \frac{Y_G LHV_{gas}}{LHV_{feedstock}} * 100 = \frac{LHV_{gas}}{LHV_{feedstock}} * \frac{F_{gas}}{F_{OPR}} \quad (5.8)$$

These parameters can be calculated using the experimental data obtained in the oil palm rachis gasification performed in the Institute of Biotechnology and Agroindustry.

5.4 Final Remarks.

The development of gasification at the pilot plant level is a process that must be developed with sufficient care to avoid any type of injury. It is important to read the gasifier user manual to identify the control panel language and to look in more depth at each of the aspects discussed in this chapter. The temperature measurement is performed externally as described by the manual so an understanding on issues related to gas leaks and types of sensors to use must be acquired. The process of biomass gasification has been described without taking into consideration the pretreatment that the raw material must carry. Basically, the two steps to follow before performing the biomass gasification are: Drying and chipping. The first one is to reduce the humidity of the raw material below 30% and the second to adjust the particle size. However, the second stage can become very time consuming since it must be performed manually

6. Analysis of characterization results and synthesis gas production from oil palm rachis.

In this chapter the experimental results obtained from the physicochemical characterization, proximate analysis, ultimate analysis and thermogravimetric analysis as well as the data obtained from the oil palm rachis gasification using the All Power Labs equipment (i.e. GEK gasifier) are presented and discussed. In first place, the overall raw material characterization is compared with reported data in open access literature and some properties are compared with coal and other fossil fuels. On the other hand, the thermogravimetric and differential thermogravimetric curves are shown and used to calculate the pyrolysis kinetic constants, which will be used to model the pyrolysis zone in the next chapter. Finally, the temperatures and syngas composition profiles are shown as well as the compositional tendencies of each gas with the reduction temperature and the parameters presented in the above chapter to evaluate the performance of the gasification process.

6.1 Chemical characterization.

The oil palm rachis was characterized in terms of the extractives, cellulose, hemicellulose, lignin and ash content with the aim to evaluate its potential as raw material to be used in different processes such as fermentation, anaerobic digestion and so forth. For this, two comparisons are performed. The first one is done comparing the obtained results for the oil palm rachis samples with the reported data by other authors for this raw material. However, this comparison is realized taking into account that differences between the reported data and the experimental results may appear due to the possible change of properties of this raw material in different crops. Additionally, the second comparison is

performed between the chemical characterization of the oil palm rachis and other solid residues from the oil palm crop.

In general terms, the results show that the studied raw material has a great potential to be employed in both biochemical and thermochemical processes due to its relative high cellulose and lignin content as well as its low ash content. The first and second comparisons are presented in **Table 6-1** and **Table 6-2**, respectively.

Table 6-1. Chemical composition of the oil palm rachis.

Feature	Content (% w/w, db.)		
	Oil palm fronds [182]	Oil palm fronds [183]	Oil palm rachis*
Extractives	12.21	22.20	15.59 ± 0.91
Cellulose	33.65	33.47	41.98 ± 4.39
Hemicellulose	27.04	13.95	23.12 ± 3.37
Lignin	14.44	30.16	17.32 ± 0.67
Ash	12.66	0.23	1.99 ± 0.11

*Data obtained in this work.

As can be seen in **Table 6-1**, the obtained data from the characterization of the oil palm rachis is comparable with the reported data by Goh et al [182]. This similarity can be explained due to this author report that the leaflet was left in the plantation and only the petiole was used (the same process that was performed in the samples collection). However, the ash content in the OPF reported is higher than the ash content in the raw material studied in this work. This difference can be attributed to the soil properties in terms of mineralogical material. On the other hand, the cellulose, hemicellulose and lignin content reported by Goh et al [182] and Triwahyuni et al [183] are similar with the obtained for the oil palm rachis. Thus, it is possible to observe that this feedstock has high levels of cellulose, so it can be used to produce value-added products through biochemical processes. Finally, the cellulose, hemicellulose and lignin content of the oil palm rachis were compared with other literature reports in water, extractives and ash free basis. From this, it was possible to observe that the obtained data for the studied raw material is in the range of the reported data [184]. [185].

The lignocellulosic composition of the raw material suggests that the oil palm rachis must be subjected in a pretreatment stage such as acid hydrolysis, alkaline hydrolysis or organosolv process before to be used in any biotechnological process with the aim to enhance the productivity of such processes. Moreover, the ash content in the oil palm rachis shows that this raw material can be used in thermochemical transformations due to the low risk of slagging. The above is affirmed taking into account the low ash content that this raw material have in comparison with other feedstocks that have been used in gasification processes (e.g. rice husk, empty fruit bunches) [186].

Table 6-2. Chemical composition of solid waste from the oil palm crop in Colombia.

Feature	Content (%w/w)		
	Empty Fruit Bunch [103]	Palm Press Fiber [103]	Oil Palm Rachis*
Moisture	65.00	40.00	9.68 ± 0.39
Extractives	-----	2.52	14.08 ± 0.91
Cellulose	15.47	24.00	37.92 ± 4.39
Hemicellulose	11.73	14.40	20.88 ± 3.37
Lignin	7.14	12.60	15.64 ± 0.67
Ash	0.67	3.00	1.80 ± 0.11

*Data obtained in this work.

According to the information showed in **Table 6-2**, the oil palm rachis shows high levels of cellulose than the empty fruit bunch and the palm pressed fiber (approximately 5% in a extractives, ash and moisture free basis), which can be related with the ethanol, lactic acid or other products derived from this fraction. On the other hand, the hemicellulose content is similar to the palm pressed fiber, but lower than the empty fruit bunches. This also suggests that this raw material can be used to produce furfural, jet fuels and C₅ derivatives. Finally, the lignin content in this basis is 21%, which is lower than the palm pressed fiber lignin content (24.7%) and higher than the empty fruit bunch (20.5%). Thus, it is possible to conclude, from the chemical characterization point of view, that the oil palm rachis is a raw material that can be used in the same processes in which EFB and PPF have been subjected. Nevertheless, other properties such as porosity and crystallinity must be evaluated to confirm the above statement. .

6.2 Proximate and ultimate analysis.

The proximate and ultimate analysis are widely used to describe the behavior of the gaseous, liquid and solid components that are obtained through thermochemical processes. In first place, the proximate analysis shows the amount of volatile matter, fixed carbon and ash content of biomass. The volatile matter is a term to refer the hydrogen, oxygen and other elements that are produced during the pyrolysis. In the same way that the chemical composition analysis, the proximate analysis of the oil palm rachis is compared with reported data for this raw material and also, it is compared with other raw materials that have been used in the GEK TOTTI system. In second place, the ultimate analysis can be used to calculate the empirical formula and atomic ratios of the elements into the raw material with the aim to classify and compare it with other fuels. Once more, these results are compared with the reported data for this raw material and the feedstock used in the GEK TOTTI system. **Table 6-3** and **Table 6-4** show the results of the proximate analysis of the oil palm rachis and their two comparisons.

Table 6-3. Proximate analysis of the oil palm rachis.

Feature	Content (% w/w, db.)		
	Oil palm fronds [117]	Oil palm fronds [179]	Oil palm rachis
Volatile matter	85.10	83.50	83.47
Fixed carbon	11.50	15.20	14.73
Ash	3.40	1.30	1.80
HHV (MJ/kg)	15.72*	17.00	18.56

*Low heating value (LHV).

The results of the oil palm rachis proximate analysis are in agreement with the results reported by Atnaw et al [117] and Guangul et al [179]. These similarity can be justified due to the leaves in both cases were cut. The volatile to fixed carbon ratios that are recommended to gasification processes should be in the range of 3 to 4. This ratio is important because gives an idea of the temperatures that can be reached in the gasification process. Thus, raw materials with high volatile matter to fixed carbon ratio trend to have low temperatures. Meanwhile feedstocks with low ratios trend to have high

temperatures. In the oil palm rachis case, this ratio is 5.67. Therefore, this raw material has a high volatile to fixed carbon ratio according to the above range. This suggests that the raw material trend to burn too cool to support efficient tar cracking and temperatures below of 1000°C can be expected.

Additionally, the oil palm rachis proximate analysis was compared with other raw materials that have been used to produce syngas in the GEK TOTTI system. This comparison aims to shows the theoretical suitability that this raw material has to be used for syngas production. The comparison was performed with *Pinus patula* and *Coffee Cut Stems*, which are typical raw materials in our region. **Table 6-4** shows this comparison. From this, it is possible to observe that the *Pinus patula* has the highest fixed carbon content and lowest volatile matter/fixed carbon ratio (4.66) that the raw material used in this work. Therefore, *Pinus patula* can reach higher temperatures than the oil palm rachis in the gasification experience. However, the coffee cut stems also have been gasified and good results have been obtained despite its high ratio (5.7). Moreover, it is important to mention that other characteristics related with the physical properties of the raw material such as the bulk density and the angle of repose are important parameters to determine the suitability of any raw material in the gasification process.

Table 6-4. Proximate analysis of different raw materials used in the GEK TOTTI system.

Feature	Content (% w/w, db.)		
	<i>Pinus Patula</i> [109]	Coffee cut stems [187]	Oil Palm Rachis*
Fixed Carbon	17.64	14.57	14.73
Volatile Matter	82.14	83.14	83.47
Ash	0.25	2.29	1.80
HHV (MJ/kg)	19.97	17.52	18.56

*Data obtained in this work

Other important aspect that must be mentioned is the high heating value (HHV) of the oil palm rachis. Thus, it is possible to observe that this raw material has a higher HHV than the coffee cut stems and lower HHV than the *Pinus Patula*. Therefore, more energy can be obtained from oil palm rachis than the coffee cut stems. On the other hand, a

difference of 9.17% in the high heating value of the oil palm rachis is found. This situation can be attributed to the calculated value of this work comes from an empirical relation reported by Nhuchhen et al [188] and the value reported by Guangul et al [179] comes from a calorimetric assay. According to the above, it is possible to conclude that the oil palm rachis has a good potential to be used in thermochemical processes to produce energy carriers such as syngas. The ultimate analysis results of the oil palm rachis and their comparison with other results reported in literature for the same raw material are presented in **Table 6-5**.

Table 6-5. Comparison of the ultimate analysis results for the oil palm rachis samples.

Feature	Content (% w/w, db.)		
	Oil palm frond [179]	Oil palm frond [117]	Oil palm rachis*
Carbon	44.58	42.40	44.53
Hydrogen	4.53	5.80	5.75
Oxygen	48.80	48.20	49.41
Nitrogen	0.71	3.60	0.31
Sulphur	0.07	-----	0.00
Empirical formula	$C_6H_{7.26}O_5$	$C_6H_{7.05}O_5$	$C_6H_{9.23}O_5$

*Data obtained in this work

The reported data in **Table 6-5** shows that the oil palm rachis has an atomic H/C ratio of 1.54 and O/C ratio of 0.83. This information can be used to understand the behavior of the high heating value for different materials. These values of H/C and O/C ratios for the oil palm rachis are comparable with the results obtained for different raw materials such as sugarcane bagasse, rice husks, *Pinus patula*, coffee cut stems and so forth, which ranges from 0.6 to 1.2 in the O/C case and 1.4 to 1.6 in the H/C case. However, non-depreciable differences between the HHV values of these feedstocks can be observed. From these information and the specific values for the above mentioned raw materials (results are not showed in this work), it is possible to observe that the HHV decreases when the O/C atomic ratio increases as well as the HHV reduces with an increase in the H/C atomic ratio. In addition, oil palm rachis has a lower calorific value than other fuels such as anthracite, coal, lignite and peat. The above is caused by the high oxygen content of the raw material in comparison with these ones, which not makes any useful

contribution to the heating value and, therefore, it makes difficult the conversion of the oil palm rachis into liquid biofuels [45].

6.3 TG, DTG curves and kinetic parameter estimation for the oil palm rachis pyrolysis.

The results obtained from the thermogravimetric analysis of the oil palm rachis samples are divided in two groups. The first one comprises the analysis of the TG curves to determine the range of temperatures where the hemicellulose, cellulose and lignin are volatilized. The second group is the determination of the kinetic parameters of this process.

6.3.1 Thermogravimetric curves analysis.

The thermogravimetric analysis was performed with the aim to obtain the kinetic parameters of the oil palm rachis pyrolysis and to determine the behavior of this raw material under an anoxic environment at different heating rates for a slow pyrolysis process, which by definition occurs until a heating rate of 1000 K/min [189]. The thermogravimetric curves for heating rates from 10 K/min to 30 K/min are presented in **Figure 6-1**.

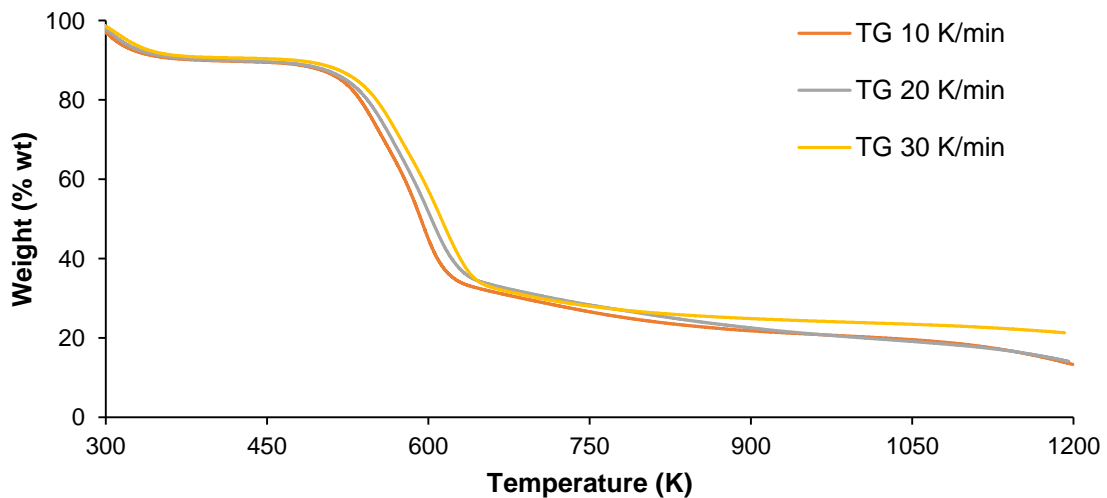


Figure 6-1. Pyrolysis curves of the oil palm rachis samples.

According to the behavior showed in **Figure 6-1**, it is possible to observe four different stages in the decomposition of the oil palm rachis samples. The first stage is composed in the range from 300 K to 423 K, where the weight loss is moderate, reaching a 10.5% of conversion (approximately). The recorded weight loss can be attributed to the moisture content reduction of the samples. This statement can be verified due to the moisture content obtained during the chemical characterization procedure is quite similar. The second stage has temperatures between 423 K and 493 K, which is characterized to have the slowest decomposition rate of the TG curve. In this stage about 2% of weight loss is registered. The above is due to the volatilization of organic compounds that can be present at the surface of the samples. The third stage can be identified from 493 K to 613 K, where the weight loss rate is the fastest, which is understood as the start of the samples thermal degradation. In fact, about 65% of the weight sample is lost, which can be associated with the hemicellulose and cellulose volatilization. This behavior is similar with the behavior reported by Yang et al [190] for other residues from the oil palm crop such as empty fruit bunches, palm pressed fiber and shell waste. According to the information published by the NREL [191], hemicellulose is the first component to be volatilized. Therefore, hemicellulose starts to be volatilized at 493 K. On the other hand, the cellulose volatilization temperature can not be calculated only with the TG curves. However, to give an estimated using the DTG curve presented in **Figure 6-2** can be done. Thus, cellulose is volatilized in the range of 560 K to 590 K, which is in agreement with Yang et al [190], who reports that cellulose starts to volatilize at 573 K. Finally, the fourth stage is composed by a weight loss of the lignin fraction. Therefore, the temperature of volatilization of the lignin fraction is about 650 K according to **Figure 6-1**. Nevertheless, other components in this temperature range can be carbonized, but, these ones do not contribute to the volatile matter formation. Attending to the above information, the volatilization temperatures of each lignocellulosic fraction from the performed thermogravimetric analysis are:

- **Moisture and organic compounds:** temperatures lower than 493K
- **Hemicellulose:** 493 K to 573 K
- **Cellulose:** 573 K to 613 K
- **Lignin and other compounds:** 613 K to 1100 K

From **Figure 6-1**, the same behavior of the weight loss is obtained at different heating rates, which allows identifying that the weight loss increase proportionally with the heating rate. Nevertheless, the solid residue at 30 K/min differs from the amount in the other two assays. Concretely, the obtained volatilized fraction at 10, 20 and 30 K/min were 86.69%, 85.92% and 78.69%, respectively. Therefore, it is possible to perceive that the volatile yield (or solid residue yield) does not change significantly with the heating rate. This trend is declared as a statement by Sharma et al [189] only for biomass pyrolysis at heating rates below of 100 K/min.

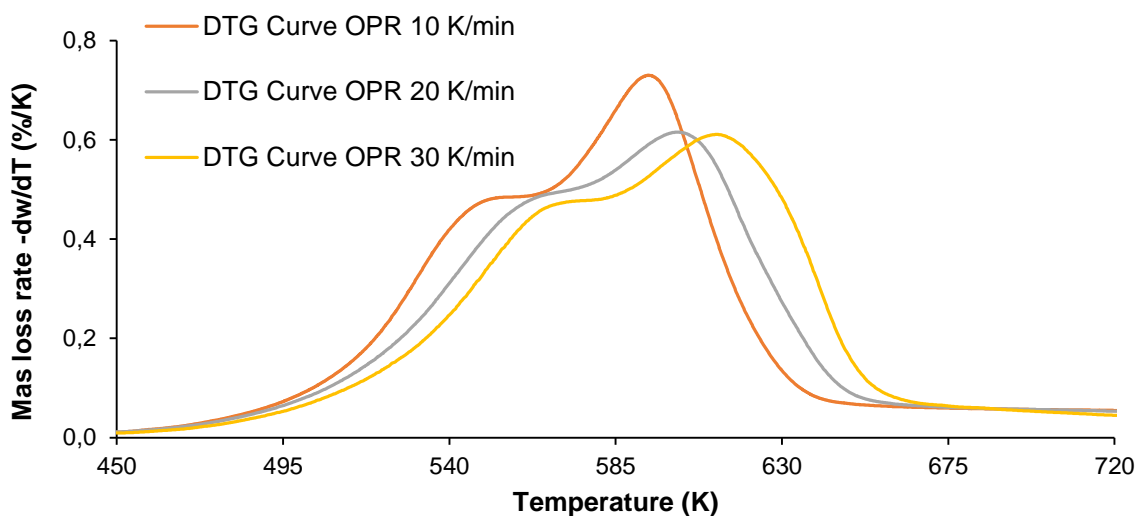


Figure 6-2. Thermogravimetric analysis at different heating rates

As was mentioned above, the maximum weight loss rate in the TG curve can be identified through the slope of the curve. In **Figure 6-1** the slope is greater in the 493 K to 650 K range. This slope can be traduced in the curves presented in **Figure 6-2**. Here, the change of the weight loss is related with the temperature of the pyrolysis process. Thus, the highest peaks are exhibited in the above range of temperatures. In DTG curve, two peaks can be observed. These peaks show two inflection points that can not be perceived in the TG curve. The first peak can be related with the hemicellulose volatilization meanwhile the second peak is related with the cellulose volatilization. A trend can be observed, at high heating rates the value of the derivative weight decrease. Therefore, it can be concluded that the mass loss rate is proportional to the heating rate attending to the mass loss rate in DTG curve was calculated as $-dw/dT$. Therefore, peaks values near to the abscissa axis are related with high decomposition rates. This conclusion can be

supported with the behavior reported by Yang et al [190]. In addition, it must be taken into account that the mass loss rate also is a function of the particle size of the sample. Therefore, bulk pyrolysis assays employing the recommended particle size for the gasification process must be performed with the aim describe, in a better way, the volatilization process into the gasifier. Other important aspects that must be analyzed are the initial and final temperatures of the main decomposition stage as well as the temperature at the maximum peak value. This information is showed in **Table 6-6**.

Table 6-6. Oil palm rachis pyrolysis data from DTG curve at different heating rates

Heating Rate (K/min)	T _o (K)	T _f (K)	T _{max} (K)	Peak value (% wt/K)
10	445	645	594	7,30E-01
20	446	655	601	6,15E-01
30	454	665	612	6,11E-01

In accordance with the above table, a trend with the initial, final and maximum temperature can be established. In all temperatures, an increase in the heating rate can be traduced as an increase in these temperatures. This increase in all temperatures apparently moves the DTG curve to the right side. Nevertheless, this fact is caused by the thermal lag, which can be defined as the difference between the temperature of the sample environment controlled by the TGA equipment and the temperature of the sample [192]. The thermal lag is caused due to the resistance to heat transfer of the oil palm rachis particles, which is related with the material conductivity.

Figure 6-1. Pyrolysis curves of the oil palm rachis samples. **Figure 6-1 and 6.2** can be used to calculate the kinetic parameters of the oil palm rachis pyrolysis. This information is useful due to these ones can help to understand the behavior of the feedstock in the gasification process. The above is taking into account that the pyrolysis process is the first step in the global gasification process and remembering that the pyrolysis process produces char and a mixture of gases rich in hydrogen, methane and carbon monoxide.

6.3.2 Pyrolysis kinetics of oil palm rachis.

The kinetic parameters determination of the oil palm rachis for a given heating rate was calculated assuming a pseudo-first order reaction kinetic model. This one considers the

transformation of the solid raw material in volatiles and char according to the following reaction.



If the reaction rate of the above reaction is assumed of first order, it is possible express the pre-exponential factor according to the Arrhenius equation.

$$k = A \exp\left(-\frac{E_a}{RT}\right) \quad (6.1)$$

Therefore, the decomposition velocity of biomass can be written as:

$$\frac{dx}{dt} = k(T) f(x) \quad (6.2)$$

Where x is the conversion ratio defined as: $x = (m_o - m) / (m_o - m_{oo})$, in which m_{oo} is the residue mass of the pyrolysis process at the end of the entire process, m_o is the initial mass weighted at the beginning of the process and m is the actual mass registered at time t . On the other hand, $f(x)$ is a normalized function defined as: $f(x) = (1 - x)^n$. Therefore, replacing these definitions in equation 6.2 gives:

$$\frac{dx}{dt} = A \exp\left(-\frac{E_a}{RT}\right) (1 - x)^n \quad (6.3)$$

However, equation 6.3 still can not be integrated because of the temperature changes with the time. Therefore, it is necessary introduce the effect of heating rate in the above equation.

$$\frac{dx}{dt} = A/\beta \exp\left(-\frac{E}{RT}\right) (1 - x)^n \quad (6.4)$$

Separating variables and integrating, it can be obtained the following expression:

$$\ln[-\ln(1-x)] = \left(-\frac{E_a}{R}\right) \frac{1}{T} + \ln\left(\frac{ART^2}{\beta E}\right) \quad (6.5)$$

If we plot $\ln[-\ln(1-x)]$ vs. $1/T$ a linear plot is obtained. The slope is $-E_a/R$ and the intercept is $\ln(ART^2/\beta E_a)$. However, as can be seen in **Figure 6-2**, there are more than one peak. Therefore, it is necessary to find an overall energy activation and pre-exponential factor as a function of the heating rate and each one of the stages presented by each heating rate (i.e. 10, 20 and 30 K/min).

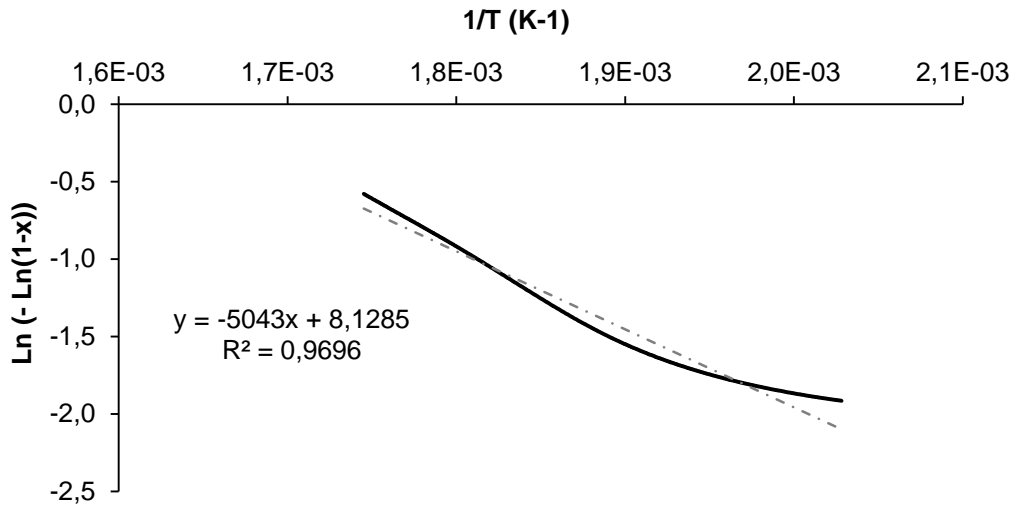


Figure 6-3. Arrhenius plot at 10 K/min for hemicellulose decomposition of oil palm rachis samples.

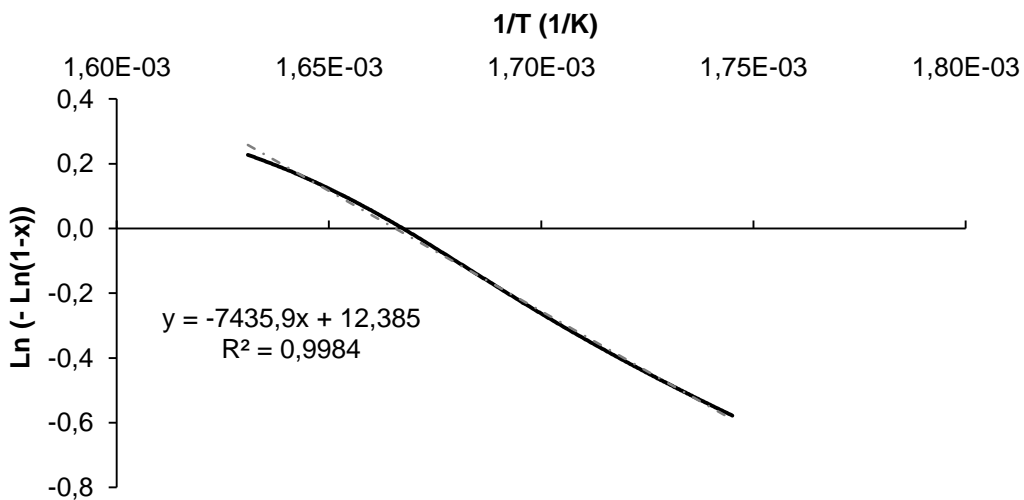


Figure 6-4. Arrhenius plot at 10 K/min for cellulose decomposition of oil palm rachis samples.

Figure 6-3 and **Figure 6-4** are the linear plots obtained from the TGA analysis and the above mentioned equations to determine the kinetic parameters of the oil palm rachis pyrolysis at 10 K/min. It can be observed that the coefficient of determination is greater than 0.97. Nevertheless, this fact does not occur always, especially in the hemicellulose decomposition plot for the heating rates at 20 K/min and 30 K/min. Therefore, the linear equation presented in both figures can be used to determine the activation energy and pre-exponential factor of this process. In addition, the weight loss recorded in each decomposition stage is showed in **Table 6-7**. This value will be used to normalize the kinetic parameters at each heating rate according to the relative weight loss achieved during the cellulose and hemicellulose stages.

Table 6-7. Kinetic parameters of hemicellulose and cellulose decomposition at 10 K/min.

Feature	Hemicellulose stage.	Cellulose stage.
Activation energy, E_a (kJ/mol)	41.93	61.82
Pre-exponential factor, A_0 (s^{-1})	10.03	842.97
Weight loss (%)	28.72	39.43

The activation energies and the pre-exponential factors calculated for the hemicellulose and cellulose decomposition of the oil palm rachis samples are similar with the reported data by Soon et al [192]. The activation energies reported by this author are 33.77 kJ/mol and 56.22 kJ/mol for hemicellulose and cellulose, respectively. However, the pre-exponential factor reported by this author are 55 min^{-1} and 8828 min^{-1} , which are very different with those, reported in **Table 6-7**. These differences in the pre-exponential factor are attributed to temperature range selected for the hemicellulose and cellulose volatilization. In fact, Soon et al [192] reports that the hemicellulose decomposition range is 468 K – 571 K and the cellulose decomposition range is 571 K – 641 K, which covers more points in the DTG curve. However, include more points into the linear plot not necessary increase the accurately of the calculation process. The above mentioned can be observed in the correlation coefficient reported by Soon et al [192] for the hemicellulose decomposition which is 0.90 while the obtained in this work is the 0.97.

The pre-exponential factors calculated for the oil palm rachis in this work are comparable with the pre-exponential factors reported by Yang et al [190] for other residues from the oil palm crop (e.g. empty fruit bunches) using the same range of hemicellulose and cellulose

decomposition. Therefore, it is possible to conclude that the obtained data in this work is comparable with the literature and it can be used to model the pyrolysis process in the following chapter. In addition, it was perceived that the pre-exponential factor calculated from TGA analysis is very sensitive to the temperature range selected for its calculation. Therefore, well defined and supported temperature range must be proposed taking into account reported data in the literature and good fitting criteria.

The data reported in **Table 6-7** can be used to calculate the overall activation energy and pre-exponential factor of the pyrolysis process at a heating rate of 10 K/min. These values are 53.44 kJ/mol and 492 s⁻¹, respectively. To complete the thermogravimetric analysis of the oil palm rachis samples at the other heating rates, the kinetic parameters (i.e. activation energy, pre-exponential factor and weight loss) calculated are presented in **Table 6-8**.

Table 6-8. Kinetic parameters of hemicellulose and cellulose decomposition at different heating rates

Heating rate (K/min)	Feature	Hemicellulose stage.	Cellulose stage.
10	E _a (kJ/mol)	41.93	61.82
	A _o (s ⁻¹)	10.03	842.97
	Weight loss (%)	28.72	39.43
	R ²	0.97	0.99
20	E _a (kJ/mol)	36.76	56.32
	A _o (s ⁻¹)	5.01	423.18
	Weight loss (%)	24.45	33.86
	R ²	0.96	0.99
30	E _a (kJ/mol)	38.37	57.26
	A _o (s ⁻¹)	10.55	747.58
	Weight loss (%)	20.80	29.97
	R ²	0.96	0.99

The thermal degradation of the oil palm rachis samples in the temperature range of 493 K – 613 K (i.e. hemicellulose and cellulose decomposition) was, in all cases, more than 50%. Therefore, the specified temperature range covers appropriately the main stage of the oil palm rachis samples degradation. In addition, the activation energies for each

heating rate for both hemicellulose and cellulose do not have a great difference, which is not higher than 14% and 9%, respectively. This behavior, also can be compared with the results reported by Yang et al [190] where a relative difference of 5% in the activation energies of cellulose can be observed. Finally, to conclude the kinetic parameter estimation of the oil palm rachis, **Table 6-9** shows the overall activation energies and pre-exponential factors at each heating rate.

Table 6-9. Overall kinetic parameters for the pyrolysis of oil palm rachis at different heating rates.

Heating rate (K/min)	Kinetic parameters		
	Ea (kJ/mol)	A (1/s)	R ²
10	53.44	492	0.9863
20	48.12	248	0.9824
30	49.52	446	0.9852

The results reported in **Table 6-9** shows that the activation energy as well as the pre-exponential factor at different heating rates are similar. Therefore, a mean value of the activation energy and pre-exponential factor will be used in the pyrolysis modeling into the gasification process. **Thus, the values are 50.36 kJ/mol and 395.33 s⁻¹, respectively.** These values are comparable with the activation energy obtained by Atnaw et al [77] of 59.2 kJ/mol using the following heating rates: 20 K/min, 50 K/min and 100 K/min. The obtained value of the activation energy, for pyrolysis of oil palm rachis could be explained attending to its high volatile matter content of 83.47%, which makes it a highly reactive fuel. This low activation energy and high reactivity of the oil palm rachis samples are a major advantage for its application as energy fuel in thermochemical conversion.

6.3.3 Experimental data from pilot scale air-downdraft gasification.

The experimental results obtained from the oil palm rachis gasification using a downdraft gasifier are showed below. As was mentioned in the above chapter, the gas composition, temperature and syngas heating value were monitored during the gasification process. On the other hand, the inlet air flow rate did not have measured during the equipment operation. However, a mean value of 110 lpm (i.e. liters per minute) was recorded. This

value was measured using a rotameter calibrated at 15°C and 101.325 kPa. The operation time of the gasification process was about of 60 minutes.

In first place, the gas composition of the produced syngas is analyzed. The hydrogen (H₂), carbon monoxide (CO), carbon dioxide (CO₂), methane (CH₄) and nitrogen (N₂) compositions are showed as a time function in **Figure 6-5**.

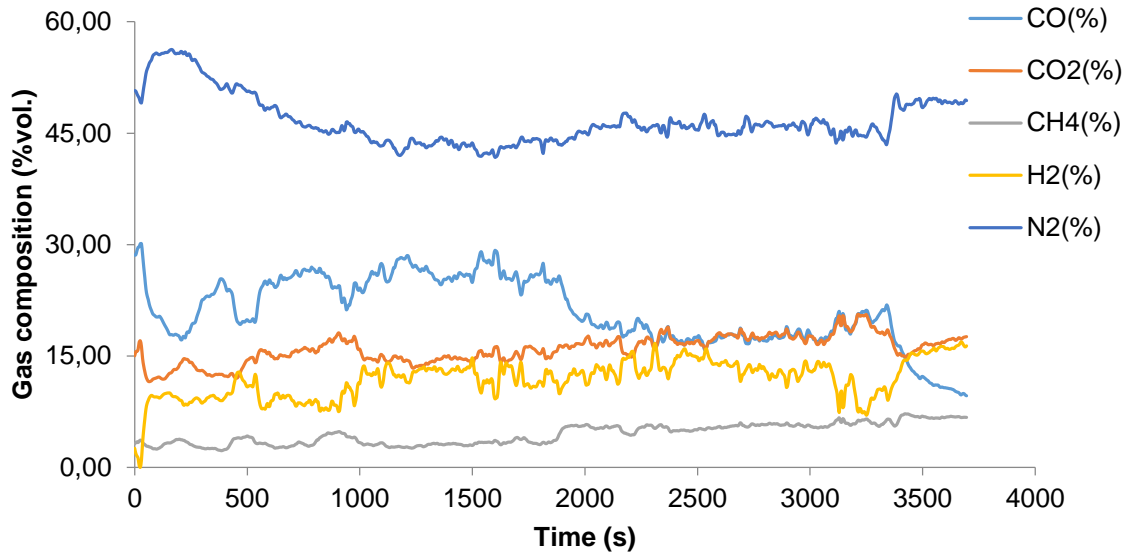


Figure 6-5. Variation of the volumetric syngas composition with the operation time

As can be observed in the above figure, nitrogen (N₂) has the highest volumetric composition in the produced syngas (about of 46.65%). This is because of the gasification experience was performed using air, which dilutes the main syngas combustible components (i.e. H₂, CO₂, CH₄). This trend is common when this gasifying agent is used [193]. The second highest volumetric composition is related to the carbon monoxide (CO), which from the 35th minute begins to decrease until reach a composition near to 15%. This behavior could be explained as an effect of the solids flow into the gasifier, which does not, allows the complete reaction between the solid char in the bottom of the gasifier and the produced gases in the pyrolysis and oxidation zones. In third place, it is possible to find the carbon dioxide (CO₂) as major component into the gas mixture. Its composition varies from 13% to 17%. Finally, hydrogen (H₂) and methane (CH₄) are those gases that have the lowest volumetric composition into the syngas. The hydrogen composition varies from 7.5% to 12%, while the methane composition varies from 2.5% to 6.5%. However, as

can be seen in the figure in the beginning and end of the gasification process, the compositions trend to increase and decrease without an easy behavior to explain. The above is attributed to the unsteady state in the start-up and shut-down of the equipment as well as the solids flow into the gasifier. In addition, a steady behavior can be identified from 200th second to the 2500th second. To conclude, the mean composition of the produced syngas of CO, CO₂, CH₄, H₂ and N₂ in dry basis is 21.01%, 15.91%, 4.46%, 11.87% and 46.65%, respectively. Other trace components such light hydrocarbons are not reported due to its share it too low.

The hydrogen to carbon monoxide ratio can be considered as a critical parameter to determine the applications range of the produced syngas due to some chemical reactions need different amounts of reactants to obtain products such as gasoline, methanol and methane. In this way, the H₂/CO ratio of the produced syngas is 0.565 in volume basis, which is appropriate to obtain gasoline as well as heat and power. Therefore, the produced gas into the gasification experience can be used directly in the above mentioned applications. However, other products such as methanol need to increase the obtained ratio through the water – gas shift reaction until reach a H₂/CO ratio of 2.0. According to Basu [45], the necessary H₂/CO ratio to subject the produced syngas into a Fischer-Tropsch synthesis should be higher than 0.6 and lower than 2.0. On the other hand, if the syngas produced in the gasification process will be used to produce methanol, other requirement must be accomplished. This one is the hydrogen to carbon dioxide and carbon monoxide ratio expressed as H₂/[2CO + 3CO₂]. In this case this ratio is 0.161 in volume basis, which is ten times less than the required ratio. Thus, a reforming stage must be designed to obtain this product.

Once the syngas composition profile in the time has been showed, the temperatures profile during the gasification experience will be analyzed. The temperatures during the run were recorded and plotted in **Figure 6-6**. The recorded temperatures into the gasifier show more clearly the start-up, steady state and shut-down of the equipment. The temperatures at the restriction of the reduction zone (**T_{tred}**) and the temperature at the bottom of the reduction zone (**T_{bred}**) are quite similar due to these are very close between them. Its temperature range was about 650°C – 825°C. However, these temperatures are very close because of they are used as control inputs to verify the correct functioning of the system. The GEK-TOTTI equipment detects any problem into

the gasifier operation measuring four variables. The first two have already been mentioned (i.e. T_{tred} and T_{bred}) and the other two ones are the P_{comb} and P_{reac} , which measures the pressure at the combustion zone and the pressure at the bottom of the gasifier. The method employed to perceive any problem is called the **Masonic Method**. However, this one is not explained in this work. The behavior obtained for T_{tred} and T_{bred} are very similar with the reported profiles by the All Power Labs industry for other raw material as softwood chips, walnut shells and wood pellets. Nevertheless, the range of temperatures reached when these raw materials are used is very different.

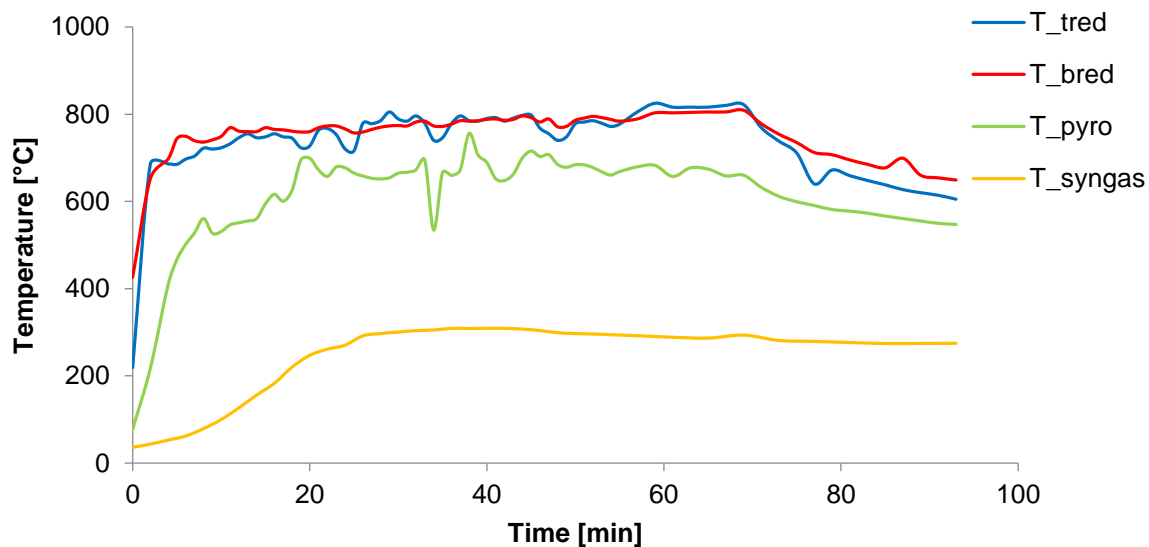


Figure 6-6. Temperature profile in the gasifier vs time.

On the other hand, the T_{pyro} thermocouple measured a temperature range between 550°C to 750°C. However, its mean value was about of 616°C. Its trend during the gasification experience was quite similar with the above mentioned temperatures. In addition, the temperature recorded at the bottom of the gasifier, T_{syngas} , has a lower temperature, which is about 242°C. The temperatures profile during the gasification experience shows that the process was stable in more than of 70% of the operation time. Additionally, it is possible to observe a decrease of the temperatures at the final of the process, which can be explained as fuel reduction inside the gasifier. Finally, it is important to mention that the combustion temperature was not recorded during the oil palm rachis gasification. However, according to the reported temperature profiles for other

raw materials, the oxidation zone temperature is greater in between 100°C to 200°C than the reduction temperature. Therefore, it is possible to give a guess of the oxidation temperature, which could be 950°C.

The syngas obtained in the gasification experience was extracted to measure its volumetric composition. The temperature of this gas was about 105°C

The data showed in **Figure 6-5** can be used to calculate the syngas heating value from equations 5.1 and 5.2. The mean HHV of the produced syngas was 5.46 MJ/Nm³. On the other hand the mean value of the LHV of this gas was 5.46 MJ/Nm³. These values are in agreement with the reported data by Atnaw et al [117]. In addition, these values also are in agreement with the reported data by air-downdraft gasification in general terms [181]. This heating value makes suitable the produced syngas to be used as fuel in steam generator and boiler to produce heat and power.

Once the syngas composition and temperature profiles have been analyzed, it is possible to match the temperature recorded in the reduction zone and the compositional change of each gas. This behavior can be observed in **Figure 6-7**. As can be seen, the CO, H₂ and CH₄ molar composition increase with the reduction temperature meanwhile the CO₂ composition decreases. In general terms, the CO composition varies from 10.06% to 28.57% in a temperature range from 600°C to 850°C. The CO₂ composition decreases in the same above mentioned temperature range. However, its composition varies from 18.17% to 12.33%. On the other hand, H₂ and CH₄ vary from 8.5% to 15% and 2.5% to 6.5%, respectively.

The above mentioned behavior can be explained from the thermodynamic point of view.

The reduction reactions that take place into the gasifier are:

R1	Boudouard	$C + CO_2 \leftrightarrow 2CO$	$\Delta H = 172 \text{ kJ/mol}$
R2	Water – Gas	$C + H_2O \leftrightarrow CO + H_2$	$\Delta H = 131 \text{ kJ/mol}$
R3	Hydrogasification	$C + 2H_2 \leftrightarrow CH_4$	$\Delta H = -74.8 \text{ kJ/mol}$
R4	Steam Reforming	$CH_4 + H_2O \leftrightarrow CO + 3H_2$	$\Delta H = 206 \text{ kJ/mol}$
R5	Water – Gas shift	$CO + H_2O \leftrightarrow CO_2 + H_2$	$\Delta H = -41.2 \text{ kJ/mol}$

The reactions R1, R2 and R4 are highly endothermic and the reactions R3 and R5 are slightly exothermic [194]. Therefore, the neat heat requirements of the reduction zone are 206 kJ/mol. In accordance with the above data, high temperatures are necessary to increase the products formation as is the case of the CO, H₂ and CH₄.

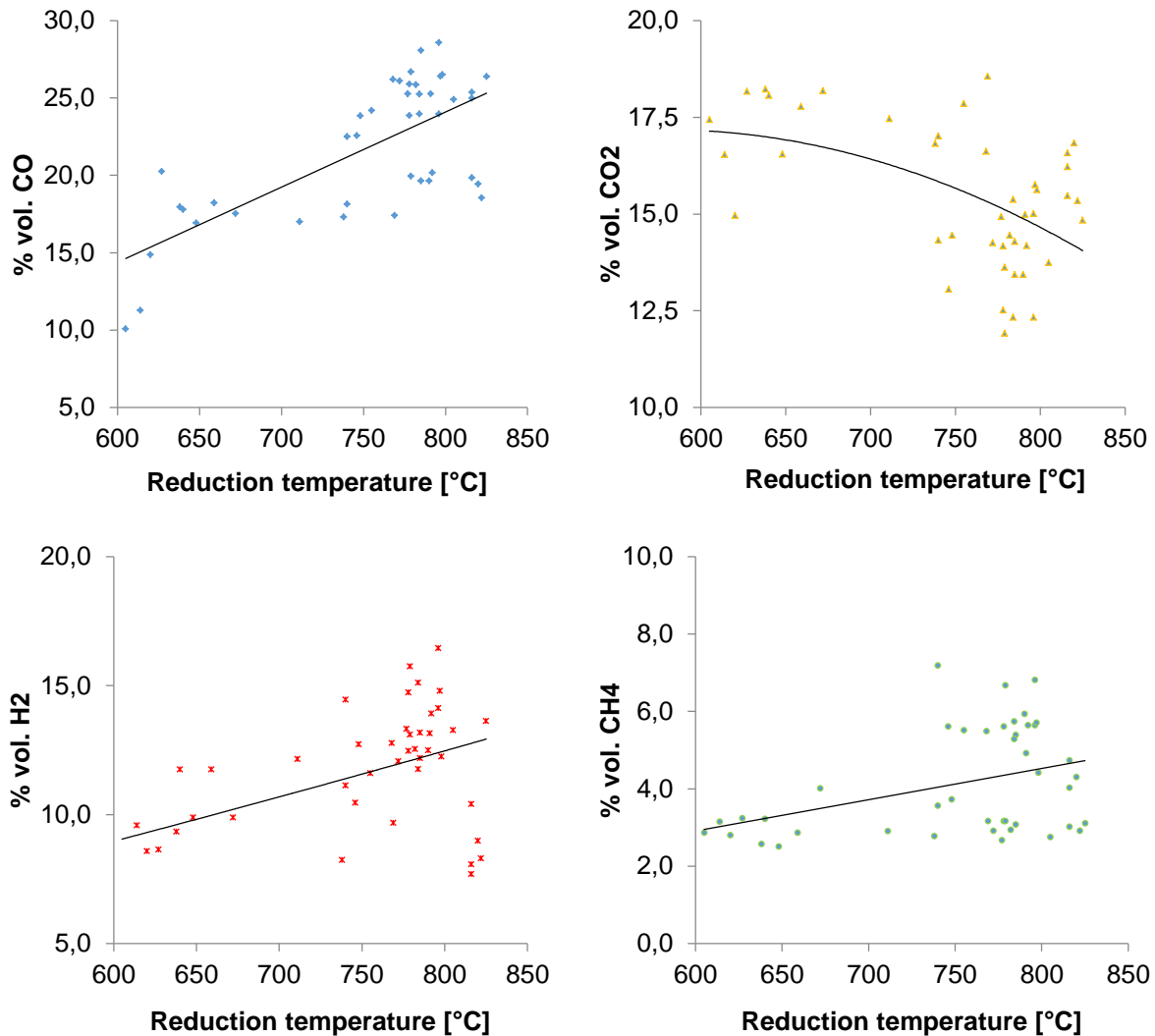


Figure 6-7. Syngas components change with the reduction temperature.

In the CO₂ case, it is present in R1 and R5 reactions. These ones can be differentiated because of the CO₂ acts as reactant and product, respectively. The R1 reaction has an activation energy higher than the R5 reaction, which favors the CO₂ disappearance. In general terms, high temperatures increase the equilibrium constant value favoring the products formation. Thus, the decrease in the relative concentration of CO₂ could be

explained in terms of the increase in the production of other permanent gases mainly CO and H₂ with the temperature.

The scattering plot in **Figure 6-7** shows a large dispersion of the data obtained during gasification of the oil palm rachis. This is because of not only the temperature reached in the reduction zone affect the syngas composition. Also, this one is affected by the heat and mass transfer between the gaseous species produced in the oxidation and pyrolysis zones with the solid char produced in the last one. Thus, parameters such as the surface area, char reactivity, char porosity, char H/O ratio, pressure and residence time are crucial variables that must be taking into account. The same trend was reported by Atnaw et al [128]. However, this author explains this behavior analyzing the gas composition with the oxidation temperature. In addition, differences in the volumetric concentration of the gases can be perceived due to the different temperatures reached in the gasification process and the raw material.

On the other hand, the temperature profile along the gasifier was plotted with the aim to observe the behavior of each one of the equipment stages. This profile is showed **Figure 6-8** as a scatter diagram due to it is more important to observe the tendency of the obtained data.

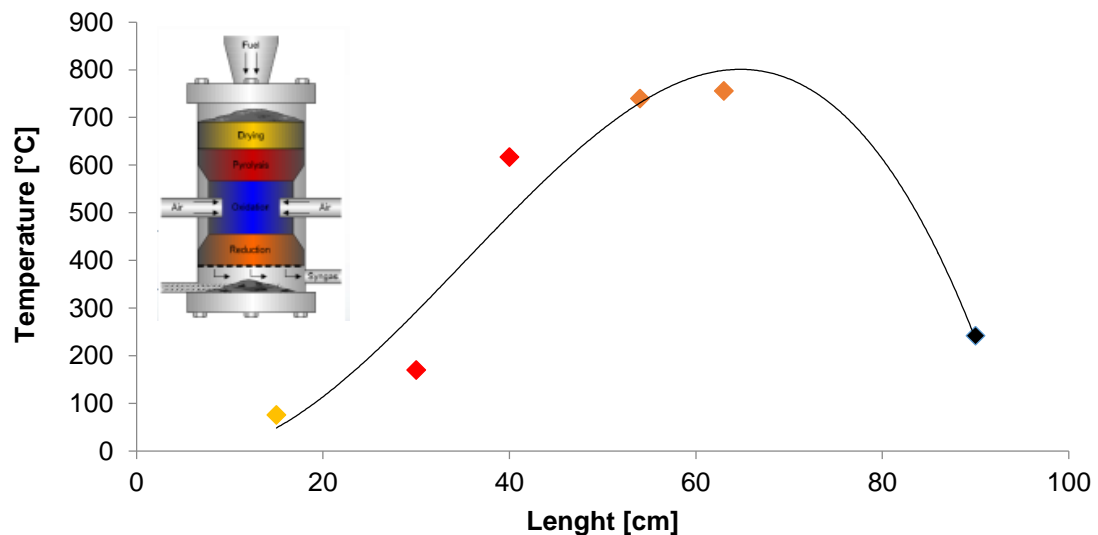


Figure 6-8. Temperature profile along the gasifier

As can be seen in the above figure, the highest temperature into the gasifier are reached in the oxidation zone (points were not recorded). Therefore, according to the trend line the oxidation temperature must be near to 800°C (or even more), which is a good approximation. Then, it is possible to observe the orange points, which are related with the reduction zone of the gasifier showed in the miniature figure. Afterward, the red points correspond to the pyrolysis section because their values are lower than 600°C. Finally, the yellow points and the blue point refer to the drying step and the syngas exit from the gasifier. A maximum is observed in the combustion zone. However, if raw materials with very low bulk density are employed some problems related with the solids flow into the gasifier can occur. The bulk density of the oil palm rachis is about 180 kg/m³, which is comparable with the bulk density of wood chips and bark [178].

As was mentioned at the begging of this section, the inlet air flow rate was about of 110 lpm (6.6 Nm³/h) at 15°C and 101.325 kPa. With this information and the equation reported by the nitrogen method to find the syngas air flow rate it is possible to find a mean syngas flow rate during the experience. Thus, the mean syngas flow that was calculated is 11.52 Nm³/h. The overall mas balance, operation parameters a results of the oil palm rachis gasification are showed in the net figure ant table.

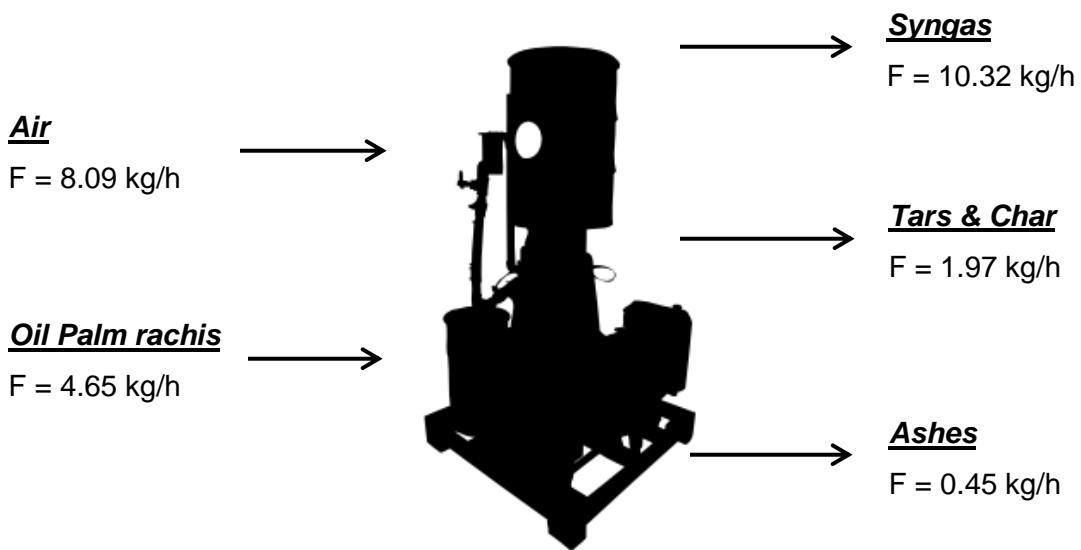


Figure 6-9. GEK TOTTI system mass balance for the oil palm rachis gasification experience.

Table 6-10. Operation parameters and results of the oil palm rachis gasification.

Type of feedstock	Oil palm rachis	Oil palm fronds
Total operation time (min)	93	118
Moisture content (% wet basis)	9.68	22.00
Initial weight of feed (kg)	11.20	12.00
Average initial air flow rate (lpm)	110	180
Air fuel ratio (kg air/kg fuel)	1.74	2.07
Equivalence ratio (ER)	0.35	0.44
Average pyrolysis zone temperature (°C)	620	456
Average reduction zone temperature (°C)	755	510
Average fuel gas output (lpm)	191.9	281.2
Average HHV of fuel gas (MJ/Nm ³)	5.46	4.95
Amount of char obtained (g)	1200	620
Amount of ash obtained (g)	700	N.R
Syngas yield (kg syngas/kg raw material)	2.22	N.R
Carbon conversion efficiency (%)	94.98	93.94
Cold gas efficiency (%)	72.94	70.54

The data showed in the above table is similar with the results reported by Atnaw et al [195]. It can be seen that higher carbon conversion efficiency and cold gas efficiency were obtained in the gasification experience, which can be attributed to the low equivalence ratio employed in it. In accordance with the mass balance expressed in **Figure 6-9**, the char and ash flow is about 1.97 kg/h from which 0.77 kg/h are char (see **Table 6-10** data). Therefore, 1.27 kg/h could be attributed to the tar flow. However, this value is excessive when this flow is compared with the literature. An explanation of this flow is supposed that not only tars are counted here. In fact, inside the gasifier a great amount of ashes is retained, which could explain this high mass flow.

On the other hand, the obtained char from the gasification experience gas characterized in terms of its volatile matter and fixed carbon content to find its heating value. The amount of volatile matter was 15.93%, ash 16.95% and 67.11% fixed carbon. These results suggest that the char produced from the oil palm rachis gasification has a lower heating value than other types of chars obtained from wood gasification. In this way, the

HHV of the produced char using the equation proposed by Nhuchnen et al [188] was 17.25 MJ/kg [196].

After the oil palm rachis gasification process, the obtained ashes were characterized in terms of mineralogical composition using atomic absorption with the aim to calculate the alkali index of the raw material and determine the possible clinker formation during the gasification process. **Table 6-11** shows the oxides composition of these ashes.

Table 6-11. Oxides composition of the gasified oil palm rachis.

Item	% w/w, db.
SiO ₂	80.78
MgO	3.78
Mn ₂ O ₃	0.05
Fe ₂ O ₃	1.22
Al ₂ O ₃	0.24
CaO	7.82
Na ₂ O	0.21
K ₂ O	5.91
Total SiO₂ + Fe₂O₃ + Al₂O₃	82.24

As can be seen in the above table, ashes from oil palm rachis gasification have a high amount of silica oxides, which can be used to produce other value-added products such as additives for concrete or high purity silica [197]. The share of SiO₂, Fe₂O₃ and Al₂O₃ shows that these ashes can be used to produce additives for the cement industry. However, aspects related with their crystallinity index must be evaluated to ensure this option. On the other hand, it can be appreciated that the content of K₂O and Na₂O is 6.12%. The above value is low in comparison with other raw materials that have been employed in gasification processes such as switchgrass and rice straw, which have a K₂O and Na₂O content of 12.18% and 13.26%, respectively. Thus, the alkali index of the oil palm rachis calculated using the 3.14 equation is 0.059 kg/MJ. This result suggest that clinker formation and slagging formation is improbable due to these problems only appears with alkali index higher than 0.17 kg/MJ due to high amounts of ash as well as K₂O and Na₂O decrease the fusion temperatures of other mineral oxides.

6.3.4 Economic value of syngas and biochar.

The main products obtained in the oil palm rachis gasification process are the syngas and biochar. In addition, the ashes produced from this process also can be considered as sub-products according to the above mentioned applications in the construction sector. Nevertheless, these ones at industrial level are not considered as such. Therefore, the economic assessment of the gasification process will not consider them. In literature is difficult to find metrics associated with the economic evaluation of the syngas and biochar due to the quality of the products as well as their amount is an important factor that must be considered. In this way, the economic evaluation proposed by Yao et al [198] will be applied.

The total economic value (V) of the gasification products is expressed as the following:

$$V = P_c \times R_c + P_g \times R_g \quad (6.6)$$

Where P_c is the unit price of biochar, \$/kg; R_c is the production rate of biochar kg/kg feedstock; P_g is the unit price of syngas, \$/Nm³, R_g is the production rate of syngas Nm³/kg feedstock. The unit prices of produced biochar and syngas were obtained from literatures, which are expressed as the following:

$$P_c = f_c \times HHV_c \quad (6.7)$$

$$P_g = f_g \times HHV_g \quad (6.8)$$

Where f_c is the price of biochar per mega Joule (2.528×10^{-3} \$/MJ). HHV_c is the higher heating value of biochar (MJ/kg) On the other hand, f_g is the price of syngas per mega Joule (6.78×10^{-3} \$/MJ). HHV_g is the higher heating value of syngas (MJ/Nm³) [199], [200]

Applying the above equations and the information given in **Table 6-10**, it was possible to calculate the total outcomes of the oil palm rachis gasification process. The calculated unit price of biochar and syngas were 0.043608 USD/kg OPR and 0.0925 USD/kg OPR, respectively. From this information, it is possible to calculate the overall economic benefits of the oil palm rachis gasification process, which were **0.1361 USD/kg OPR**. Therefore,

the net incomes of the process by period (i.e., 1 period = 1 year = 8000 h) were **5064.97 USD/period**. These results are in agreement with the reported data by Yao et al [198], who reported that the biochar prices varies from 0.017 USD/kg to 0.009USD/kg, whereas the syngas price varies from 0.057 USD/kg to 0.077 USD/kg reaching a maximum point at ER 0.25 of 0,091 USD/kg. Nevertheless, a cash flow should be performed aiming to consider the raw materials costs, operating and maintenance costs, utilities costs, general and administrative costs and the depreciation costs. Even so, the above economic approach can give a good estimation of the profitability of the oil palm rachis gasification.

The gasification technology, as was mentioned in the previous chapters, can be used to supply energy in a decentralized way. Nevertheless, the energy production cost of this technology still is a problem that must be solved. In Colombia, the use of non-conventional energy sources to improve the quality of life of thousands of persons can be used due to about 52% of the national territory is not included into the national energy system. This situation divides Colombia in two zones. The first one is the so-called non-interconnected zone, which is characterized to be composed by rural areas. The second one is the integrated zone, which is characterized to be composed by urban areas.

The oil palm crop covers about 70% of the non-interconnected zones in Colombia. Therefore, the oil palm waste (e.g., the oil palm rachis) can be used to produce energy in these zones. Currently, only 6455 kW are produced by solar and wind energy (i.e., 3%) and the other energy needs are supplied by non-sustainable systems based in diesel use (i.e., 92%). In this way, the energy production using the thermochemical pathway can be considered as a solution. However, the electricity price is higher than the electricity price produced by the diesel technology. In fact, the cost of the electricity generated by diesel systems is about **600 COP/kWh** whereas; the cost of the electricity generation using a downdraft gasification system is about **800 COP/kWh**.

In accordance with the above comparison between the electricity costs, the gasification technology needs to be improved in economic terms to be a reliable alternative to be implemented in the non-interconnected zones of the country. These improvements can be related with the implementation of a more efficient gasification system. For instance, the fluidized gasification systems can be used instead of fixed bed systems with the aim to decrease the operating and maintenance costs. Furthermore, the raw material cost and

the conditioning costs can be reduced if part of these costs is assumed by the oil palm mills. Therefore, the oil palm waste use in gasification systems for electricity production can be considered as an idea that could be implemented in a near future as part of the government policies.

6.3.5 Environmental aspects of the oil palm rachis gasification process.

The environmental assessment of the gasification process was carried out using some of the environmental indicators reported by Ruiz-Mercado et al [201], [202]. These environmental indicators have as objective shows the possible impact from the biofuels production. These environmental indicators were normalized using a sustainability percentage aiming to compare it with other indicators reported by other authors [203]. The calculated indicators are listed below:

- ✓ Number of hazardous material input
- ✓ Mass of hazardous material input
- ✓ Specific hazardous raw material input
- ✓ Health hazard irritation factor
- ✓ Total mass of persistent, bioaccumulative and toxic (PBT) chemicals used.
- ✓ Global warming potential.
- ✓ Aquatic acidification potential.
- ✓ Aquatic oxygen demand potential
- ✓ Specific liquid waste production
- ✓ Specific solid waste production.

The above indicators were calculated following the definitions and descriptions reported by Ruiz-Mercado [202], the potency factors listed by IChemE report [204], the hazardous material list [205] and the PBT list published by the EPA [206]. After calculating each indicator, the process sustainability was calculated using the sustainability scale reported in the GREENSCOPE methodology [201]. This sustainability scale was calculated as follows:

$$\text{Sustainability percentage} = \left(\frac{\text{Actual case} - \text{Worst case}}{\text{Best case} - \text{Worst case}} \right) * 100 \quad (6.9)$$

The best case was defined as the case where no releases were produced. On the other side, the worst case was defined as the case where all releases were considered waste. The actual case considered that ashes produced in the gasification process are solid waste and the tars generated are liquid waste.

The results of the environmental analysis of the gasification process were compared with the biodiesel production using palm oil as raw material. **Figure 6-10** shows the indicators calculated for both biodiesel production and gasification.

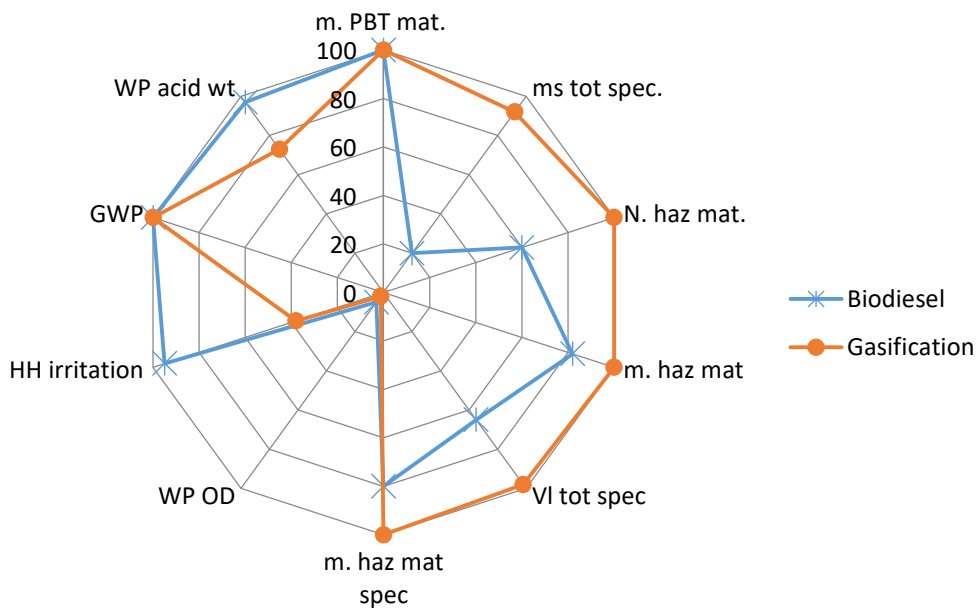


Figure 6-10. Environmental indicators of the biodiesel production process and gasification process using palm oil raw materials.

The results showed in the above figure indicate that the gasification process has high environmental indicators than the biodiesel production when these processes are compared from the hazardous materials management point of view. This can be explained due to the gasification process does not require any chemical compound to carry out the transformation process. Nevertheless, the environmental indicators for the biodiesel production are high in comparison with petrochemical process. This is because the raw materials employed are not dangerous for the persons and the chemicals compounds that are used have well defined their security protocols (i.e. NaOH, H₃PO₄) –

see **Figure 2-9** -. On the other hand, environmental indicators related with the liquid releases (e.g., aquatic oxygen demand and aquatic acidification potential) are lower for the gasification process because of the tars generated in this process are very difficult to treat in a wastewater treatment plant. This can be explained due to the presence of light and heavy hydrocarbons. Furthermore, this mixture (i.e., tars) have considered as carcinogenic residue [207]. In contrast, the biodiesel production process generates large amounts of liquid waste that can be treated easily. Finally, the global warming potential of the gasification process is the lowest possible due to the total flow of syngas is used in other.

In conclusion, the gasification process for energy production is an environmental friendly process due to this process avoid the use of any other chemical compound, also this process has lower solid and gaseous releases. Nevertheless, the tars production is an environmental problem that must be solved aiming to increase the environmental sustainability of the process. In addition, one important aspect of the above analysis is that the system analyzed only comprises the syngas generation process. However, if a gas engine, gas turbine or any other chemical transformation of the syngas is carried out the environmental sustainability of the process will decrease. Even so, indicators such as global warming potential will be lower than the produced by the emissions caused by the use of fossil fuels such as diesel in thermal facilities for energy production.

6.3.6 Energy balance of the pilot-scale downdraft gasification process.

Once the material balance of the gasification process has been completed, a global energy analysis of the input and outputs of the gasification system can be performed. For this, the energy content of the raw material and the gasification products must be taken into account. A graphical method to show the energy balance of the gasification process is the Sankey diagram, which shows the global energy analysis of a process.

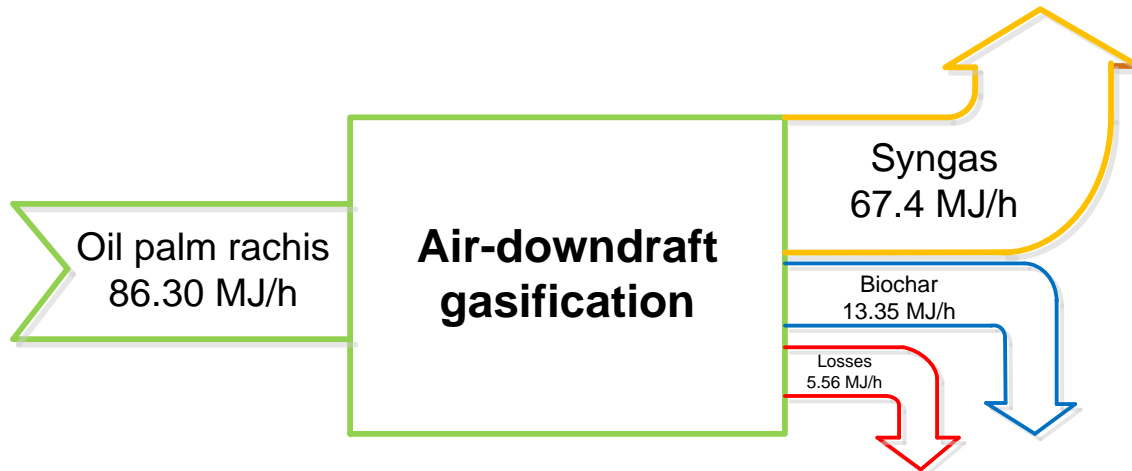


Figure 6-11. Sankey diagram of the oil palm rachis gasification process.

In accordance with **Figure 6-11**, syngas can be classified as the main product of the gasification process. However, the produced biochar also has a potential to generate a relevant amount of energy. Both, syngas and biochar can produce an energy flow of 80.75 MJ/h, which in comparison with the energy content of the oil palm rachis accounts and energy efficiency of 93.56%.

The gasification process can be seen as conversion pathway to add value to the oil palm rachis because of the syngas can be used as versatile energy vector or chemical platform. Moreover, the produced biochar can be used as soil enhancer or heat source in boilers for steam generation. The losses associated with the gasification process are about of 5.56 MJ/h, which can be attributed to the heat losses in the equipment and the irreversibilities produced in the chemical reactions given into the gasifier. The efficiency of the gasification process only considering the amount generated syngas is about 78.09%, which is similar with the energy efficiency reported by García [208] using *Pinus Patula* as raw material (i.e., 79.9%).

The Sankey diagram showed in **Figure 6-11** does not take into account the energy flow that can be obtained from the tars production Nevertheless, this fact can be explained due to the amount of produced tars in the gasification process is low and this compound does not have a well-established used at industrial or agricultural level in contrast with the syngas and biochar. On the other hand, Antonopoulos et al [209] analyzed the energy balance of a downdraft gasifier using olive wood as raw material. The energy efficiency

only considering the syngas as energy vector reported by these authors was 82.31%, which is a similar value to the obtained in this work. Therefore, it can be concluded that the energy efficiency of the downdraft gasification process for softwood and hardwood raw material varies from 75% to 85%, which indicates high energy conservation in the gasification process.

Finally, as was observed in **Figure 5-3**, the GEK TOTTI system has coupled a 4-stroke gas engine, which is able to produce electricity from the syngas combustion. This process consumed the produced syngas in an internal combustion engine to obtain power. Nevertheless, the energy analysis of this process (i.e., syngas combustion and energy production) has different irreversibilities, which can be perceived in heat losses and the mechanical efficiency of the engine. Therefore, an inclusion of an engine into the gasifier decreases the overall energy efficiency of the gasification process. In general terms, an internal combustion engine has a mechanical efficiency of 38%. In this way, the global energy balance of the oil palm rachis gasification process is showed in the Sankey diagram of the **Figure 6-12**.

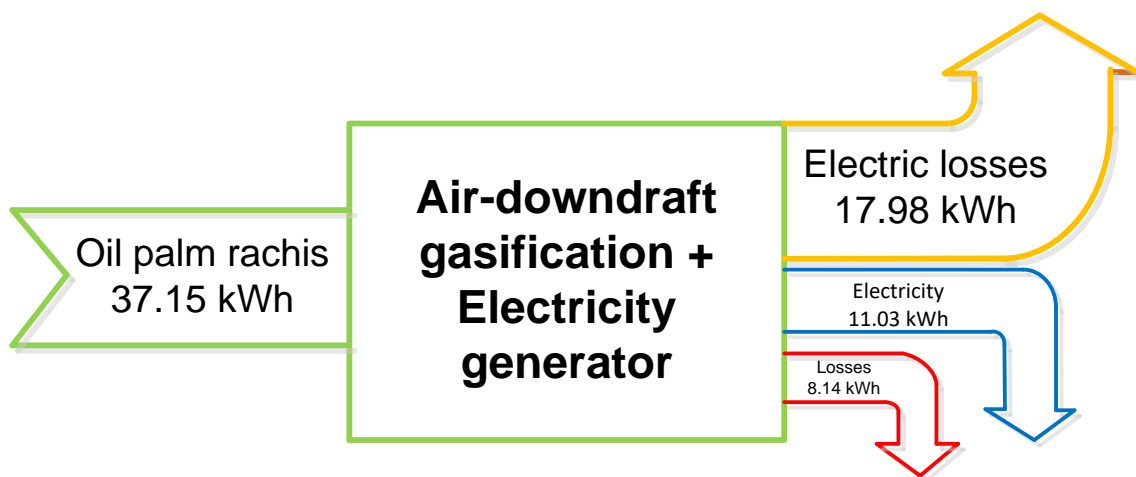


Figure 6-12. Sankey diagram of the oil palm rachis gasification process coupled with an gas engine.

The energy efficiency of the electricity generation process using the syngas produced from the oil palm rachis is 29.9%, which is lower than the obtained efficiency in the above paragraphs. This efficiency could be increased if a gas turbine is placed instead of a gas

engine. The above recommendation is suggested based on the high thermal efficiencies that these systems can reach for heat and power production.

6.4 Final remarks.

The oil palm rachis is lignocellulosic feedstock that can be used to produce different high value-added product using different conversion routes. The above statement can be supported from the compositional point of view. In this way, the applicability of the oil palm rachis as feedstock for thermochemical processes (i.e., gasification) has been validated through proximate, ultimate and atomic absorption analyses. In addition, the pyrolysis kinetic behavior of this raw material was studied using thermogravimetric analysis. The obtained information from this type of analysis can help to develop a more detailed model to simulate the gasification process.

Finally, the experimental gasification of the oil palm rachis was executed. The results indicate that the syngas obtained from this raw material is able to produce heat and power. Moreover, the syngas and biochar prices from this process are competitive with other prices obtained for other type of raw materials. However, a cash flow analysis of the process must be carried out to increase the reliability of the obtained results. On the other hand, the environmental and energy assessment of the process shows that the gasification process has a lower environmental impact that the bioethanol production using this raw material. However, according to the results of the environmental analysis, tars must be classified as hazardous raw material. The sustainability assessment shows that the gasification process is near to environmental sustainability. Finally, the energy assessment verified that the syngas production is an energy efficient process. Nevertheless, the inclusion of a gas engine has a lower mechanical efficiency. Therefore, the use of gas turbines is more recommended because of their high thermal efficiencies.

7. Modeling and simulation of oil palm rachis gasification.

The oil palm rachis gasification process was simulated in using two different software. The first one was MatLab and the second one was Aspen Plus v9.0 MatLab was used to calculate the molar compositions of gases in each step of the gasification process (i.e. pyrolysis, combustion and gasification). These calculations were performed using the empirical formula of the oil palm rachis as well as its chemical characterization. Aspen Plus v9.0 was used to simulate the entire gasification process using as input data the results obtained from MatLab.

7.1 Consecutive blocks simulation.

The gasification of the oil palm rachis was modeled as a consecutive blocks (see **Figure 7-1**). However, this approach only can be used in downdraft gasifier due to the different zones into the equipment are well differentiated. Therefore, the following equations are not suitable to model a fluidized bed gasifier.

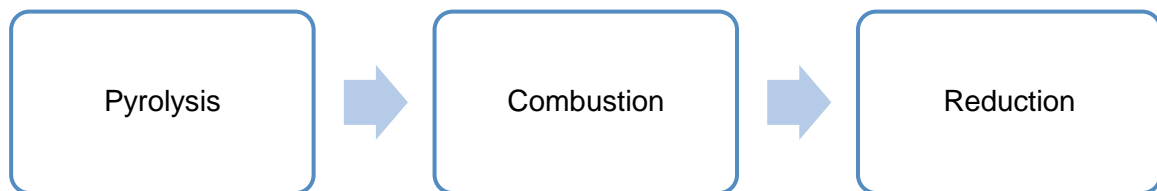
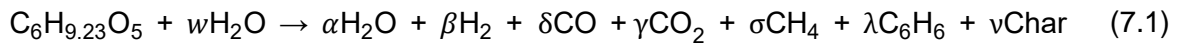


Figure 7-1. Block simulated to perform the oil palm rachis gasification simulation

The kinetic models employed to model the biomass gasification are presented below:

- **Pyrolysis model.**

In the pyrolysis zone, the oil palm fronds samples are decomposed in two main fractions, which are: volatile compounds and char. The volatile compounds are a mixture of gases that are produced due to the thermal and anoxic degradation of the samples. In this sense, water (H₂O) hydrogen (H₂), carbon monoxide (CO), carbon dioxide (CO₂), light hydrocarbons and heavy hydrocarbons (i.e., tars) are produced. The yields of each gas and the obtained char were calculated using the following stoichiometric equation:



The rate of volatilization can be calculated as follows:

$$\frac{dM_{\text{vol}}}{dt} = -A \exp\left(-\frac{E_a}{RT}\right) M_{\text{DB}} Y_{\text{vol}} \quad (7.2)$$

As can be seen in equation (7.1), the moisture content of the raw material has been taken into account in the pyrolysis reaction to calculate its effect in the final volatile fraction composition. In addition, light hydrocarbons and tars were modeled using C₆H₆ and CH₄ chemical formulas, respectively. This assumption is according to the chemical formula employed by Thunman et al. [210]. On the other hand, the strategy proposed by Sharma et al. [189] was applied to find the stoichiometric coefficients of the pyrolysis reaction. In fact, the char content of the oil palm fronds was calculated using the fractional char yields of biomass constituents (i.e., cellulose, hemicellulose and lignin) and the chemical characterization of the samples reported by Cardona et al. [211]. Moreover, the coefficients of the volatile gases were calculated using the following additional equations, which describe the mass ratios of the produced gases as a function of the temperature.

$$Y_{\text{char, ash free}} = Y_{\text{cellulose}} f_{\text{char}} + Y_{\text{hemicellulose}} f_{\text{char}} + Y_{\text{lignin}} f_{\text{char}} \quad (7.3)$$

$$Y_{\text{vol}} = 1 - Y_{\text{char, ash free}} \quad (7.4)$$

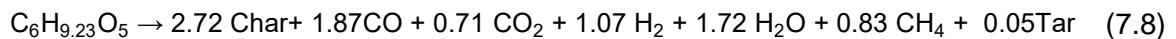
$$Y_{\text{CO}/\text{CO}_2} = e^{-1.8447896 + \frac{7730.317}{T} + \frac{7730.317}{T^2}} \quad (7.5)$$

$$Y_{\text{H}_2\text{O}/\text{CO}_2} = 1 \quad (7.6)$$

$$Y_{\text{ME}/\text{CO}_2} = 5 \times 10^{-16} T^{5.06} \quad (7.7)$$

These equations only can be used in the temperature range of 400 K to 1200 K [189]. The temperature of the pyrolysis process was varied from 450 K to 950 K aiming to analyze the behavior of the volatile fraction. The above temperature range was selected to avoid zero values of the tars fraction [189]. Nevertheless, the average pyrolysis temperature reported by At Naw et al [195] for Malaysian oil palm fronds gasification (i.e., 730 K) was used for subsequent calculations. Then, a system of six equations was obtained (i.e., C balance, H balance, O balance, equations 2, 3 and 4), which was solved using the Engineering Equation Solver (EES) academic version software, giving the necessary restrictions to obtain reliable values (e.g., all coefficients values must be greater than zero).

The results obtained for equation 7.1 are presented in equation 7.8 at the pyrolysis temperature reported in **Table 6-10**.



The above coefficients given in equation 6.8 are function of the temperature. Therefore, these ones are calculated at 893.15 K. The relation between the coefficients for the slow pyrolysis of biomass is linear in the temperature from 400K to 500K. On the other hand, these coefficients depend on the ultimate analysis of the raw material.

Using the above equations and taking into account that the GEK TOTTI system pressure range of working pressure, the gases profile were calculated and they are shown in the following figures:

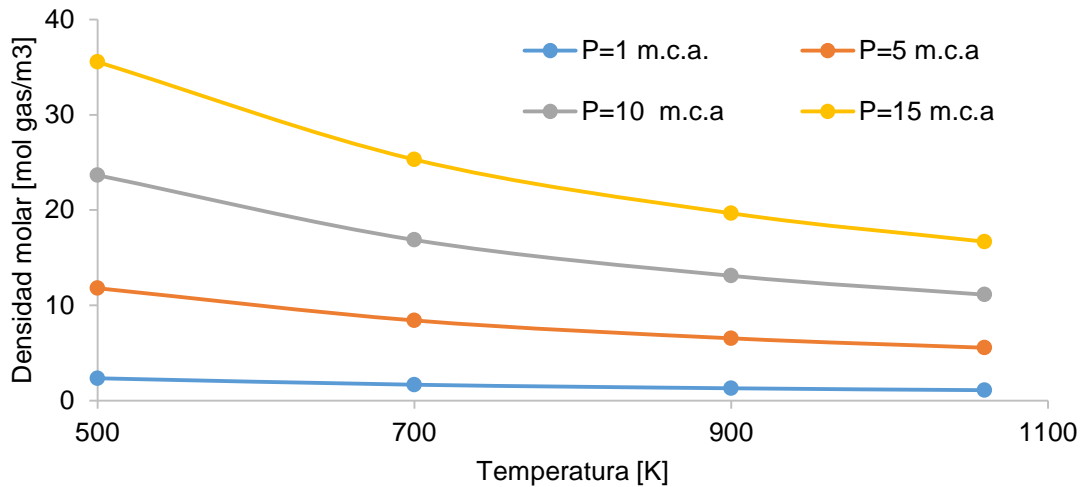


Figure 7-2. Molar density of pyrolysis gases as a function of the temperature and pressure.

From these figures it is possible to observe that the molar composition varies in significant amounts. This implies that the system pressure is an important fact that can affect the gasification process. In fact, pressurized gasification of biomass has been researched by different authors [133], [134]. However, the pressures that are supposed are not higher. These pressures were obtained from the equipment taking into account the suction pressure of the gasifier.

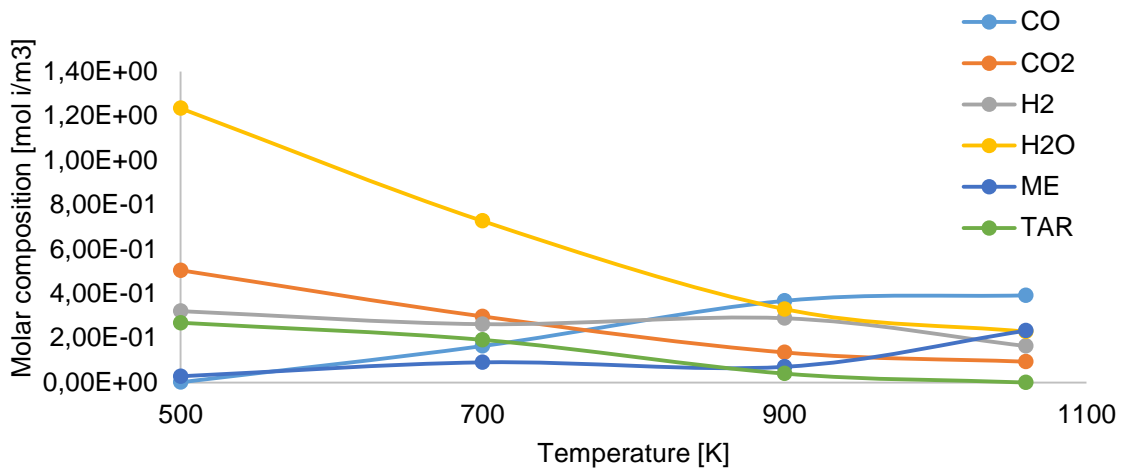


Figure 7-3. Molar composition change of the pyrolysis gas at different temperatures at 1.m.c.a of pressure.

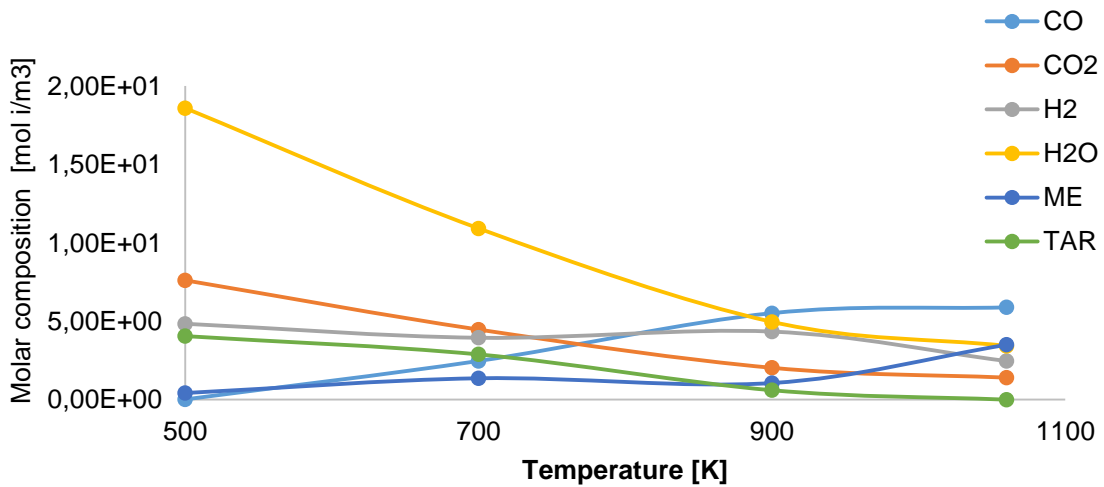


Figure 7-4. Molar composition change of the pyrolysis gas at different temperatures at 15.m.c.a of pressure.

A common tendency can be observed in to oil palm rachis pyrolysis process. The hydrogen content is higher than carbon monoxide, methane and tar content in the gas mixture from 500 K to 800 K. This is an important point due to the temperatures reached in the GEK TOTTI system in the pyrolysis zone can overcome this temperature range. Therefore, the H₂/CO ratio into the gasifier is lower than 1.

As can be seen in **Figure 7-5**, the activation energy of the wood is higher than the oil palm rachis. This fact implies that the wood burn at higher temperatures than the oil palm rachis. Therefore, the oxidation temperatures reached into the gasifier are higher for wood residues.

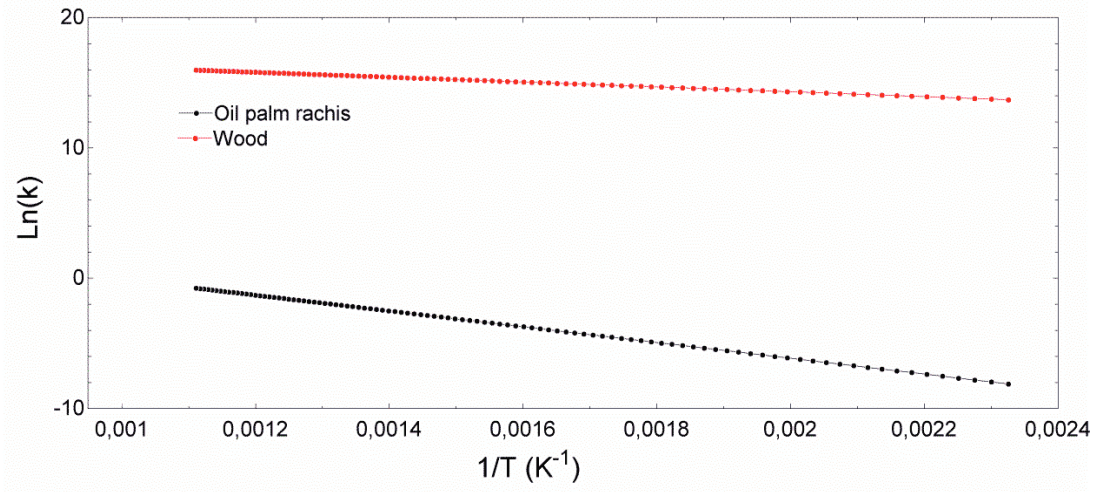


Figure 7-5. Comparison of the pyrolysis constant calculated for the oil palm rachis and wood with the temperature.

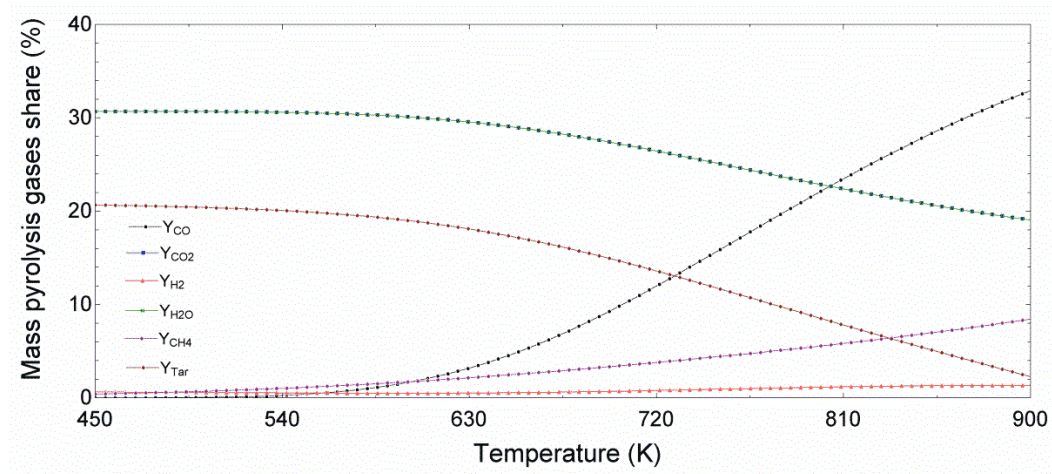


Figure 7-6. Mass composition of the pyrolysis gases.

The same behavior reported with the molar composition of the gases is presented in the above figure. It is necessary to specify that the tars produced in the pyrolysis gases was modeled as a C_6H_6 (i.e. benzene) and light hydrocarbons as CH_4 [189].

➤ **Combustion.**

There are different approaches to calculate the combustion zone of a downdraft gasifier. In this zone the gases that are produced in the pyrolysis zone are burned with air to produce carbon dioxide and water. This reaction is exothermic and provides energy to the other stages into the gasification process (i.e. drying, pyrolysis and reduction). For this reasons, the employed gasifier is called “auto-thermal”. The combustion reactions as well as the kinetic expressions that have been reported in the literature to model the biomass gasification of a downdraft gasifier are presented in **Table 7-1**

Table 7-1. Reactions and kinetic expressions of the combustion zone

Reaction	Reaction rate.	Kinetic parameters	Ref.
$\text{H}_2 + 0.5\text{O}_2 \rightarrow \text{H}_2\text{O}$	$-\text{r}_{\text{H}_2} = k_{\text{RC}_1} [\text{O}_2] [\text{H}_2]^{1.5}$	$k_0 = 1.63 \times 10^9 T^{1.5}$ $E_a/R = 3420$	[212]
$\text{CO} + 0.5\text{O}_2 \rightarrow \text{CO}_2$	$-\text{r}_{\text{CO}} = k_{\text{RC}_2} [\text{O}_2]^{0.5} [\text{H}_2\text{O}]^{0.5} [\text{CO}]$	$k_0 = 1.30 \times 10^8$ $E_a/R = 15106$	[212]
$\text{CH}_4 + 1.5\text{O}_2 \rightarrow \text{CO} + 2\text{H}_2\text{O}$	$-\text{r}_{\text{CH}_4} = k_{\text{RC}_3} [\text{O}_2]^{0.8} [\text{CH}_4]^{0.7}$	$k_0 = 1.58 \times 10^{10}$ $E_a/R = 24157$	[212]
$\text{C}_6\text{H}_6 + 4.5\text{O}_2 \rightarrow 6.0\text{CO} + 3\text{H}_2\text{O}$	$-\text{r}_{\text{C}_6\text{H}_6} = k_{\text{RC}_4} T_g [\text{O}_2] [\text{C}_6\text{H}_6]^{0.5}$	$k_0 = 1.63 \times 10^9$ $E_a/R = 3420$	[213]

As can be seen in **Table 7-1**, only four reactions were considered to model the oxidation zone. These reactions take the pyrolysis gases and are burned with oxygen. However, the last two reactions were simulated taken into account that the component $\text{C}_{1.16}\text{H}_4$ is similar to the methane molecule and the component $\text{C}_6\text{H}_{6.2}\text{O}_{0.2}$ represent all the heavy hydrocarbons present in the pyrolysis vapor. Some authors reports that two types of tar are produced [214]. However, this additional reaction was not considered due to the pyrolysis process was simulated using a low heating rate.

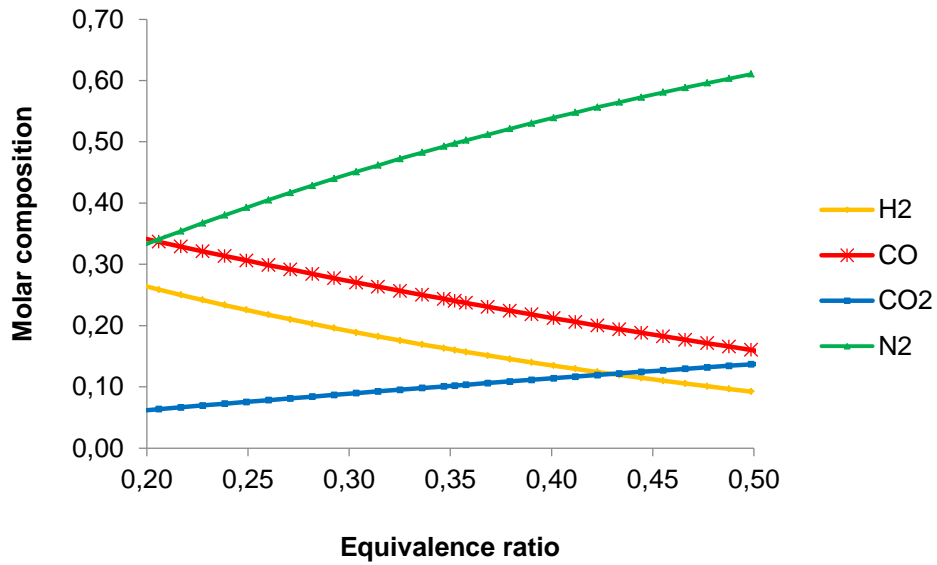


Figure 7-7. Change of the molar composition in the oxidation zone with the equivalence ratio.

The results showed in **Figure 7-7** are in agreement with the behavior expected in a combustion process. High amount of oxidizing agent (i.e. high equivalence ratio) increase the amount of carbon dioxide and nitrogen into the gas in the oxidation zone.

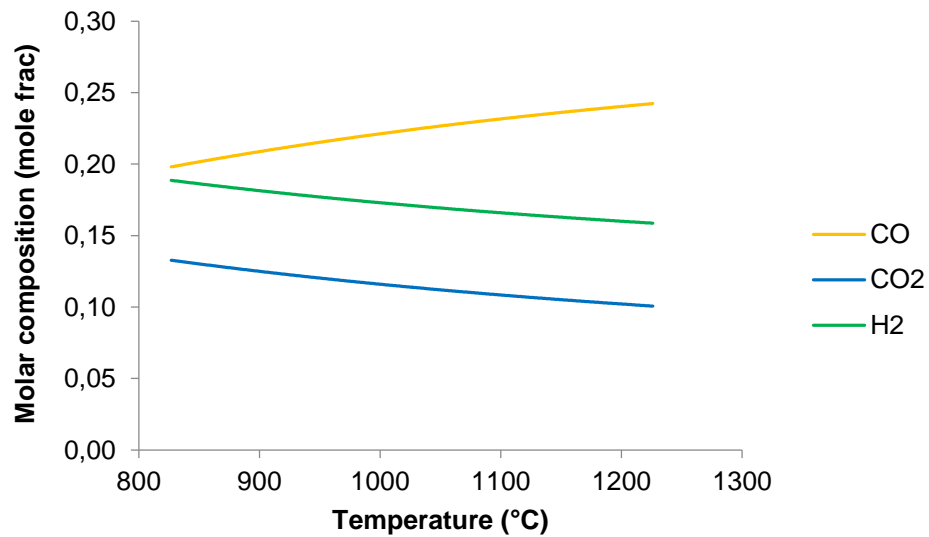


Figure 7-8. CO, CO₂ and H₂ compositional change with oxidation zone temperature.

As can be seen in the above figure at higher temperatures the production of carbon dioxide and hydrogen decrease. This can be explained due to the reactions given in this zone are exothermic, which are not favored at high temperatures.

➤ **Reduction.**

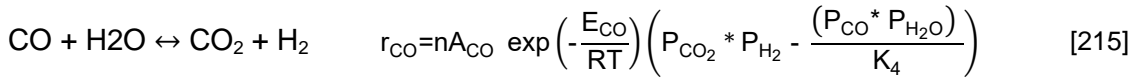
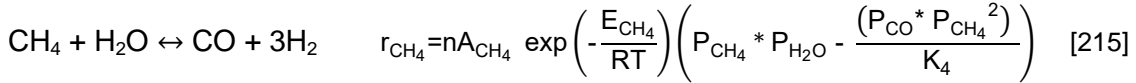
The reduction zone is the most important stage in the gasification since the synthesis gas is generated there[109]. Once all the oxygen that was introduced in the combustion zone has been consumed, the tar cracking from the pyrolysis process has been performed and the high molecular weight compounds are transformed in low molecular compounds, the remaining char from the pyrolysis process undergoes to the reduction zone where the following gas- gas and solid – gas reactions take place.

$C + H_2O \leftrightarrow CO + H_2$	Water – Gas Reaction
$C + CO_2 \leftrightarrow 2CO$	Boudouard Reaction
$C + 2H_2 \leftrightarrow CH_4$	Methanation reaction
$CH_4 + H_2O \leftrightarrow CO + 3H_2$	Steam Reforming reaction
$CO + H_2O \leftrightarrow CO_2 + H_2$	Water gas shift reaction

The kinetic model uses Arrhenius type-equations which are function of the temperature as presented in **Table 7-2**

Table 7-2. Kinetic model employed to simulate the reduction zone of a downdraft gasifier.

Reactions	Rate expressions	Ref.
$C + CO_2 \leftrightarrow 2CO$	$r_{CO_2} = nA_{CO_2} \exp\left(-\frac{E_{CO_2}}{RT}\right) \left(P_{CO_2} - \frac{P_{H_2}^2}{K_1}\right)$	[215]
$C + H_2O \leftrightarrow CO + H_2$	$r_{H_2O} = nA_{H_2O} \exp\left(-\frac{E_{H_2O}}{RT}\right) \left(P_{H_2O} - \frac{(P_{CO} * P_{H_2})}{K_2}\right)$	[215]
$C + 2H_2 \leftrightarrow CH_4$	$r_{H_2} = nA_{H_2} \exp\left(-\frac{E_{H_2}}{RT}\right) \left(P_{H_2} - \frac{P_{CH_4}^2}{K_3}\right)$	[215]



7.2 Aspen plus simulation of the gasification process.

The syngas production using oil palm rachis as raw material is composed by two stages mainly. The first stage is the raw material pretreatment, which is carried out using a chipper machine to decrease the particle size of the feedstock from 15.0 cm to 2.0 cm. This process was simulated in Aspen Plus software using the solids crusher model available in the solids section. The second stage is the oil palm rachis gasification. Nevertheless, Aspen Plus software does not have a gasifier model. For that reason, its simulation was divided in three steps: pyrolysis, combustion and reduction.

The pyrolysis step considers the raw material devolatilization in anoxic conditions. This was simulated using the stoichiometric approach reported by Sharma [21] applied to the lignocellulosic components (i.e. cellulose, hemicellulose and lignin). At last, it was considered that this process occurs at 600°C. The main products considered from the pyrolysis step are char (C), carbon monoxide (CO), carbon dioxide (CO₂), hydrogen (H₂), water (H₂O), light hydrocarbons modeled as methane (CH₄), and heavy hydrocarbons (i.e. tar) modeled with the empirical formula (C₆H₆O_{0.2}) considered by many authors [21], [22].

The combustion step is related with the oxidation of the pyrolysis products. This one was simulated using a kinetic reactor from the Aspen reactors model palette. Finally, the char produced in the pyrolysis and combustion steps passes to the reduction step where char gasification takes place to produce CO₂, CO, H₂ and CH₄ [19]. This step was simulated in Aspen Plus using a RIGBBS reactor to describe the multiphase equilibrium of the system based on the free Gibbs energy minimization method (the equations written above). The remainder char and ashes from the gasification of the oil palm rachis are separated from the syngas using a cyclone. The overall syngas production process described above is presented in **Figure 7-9**

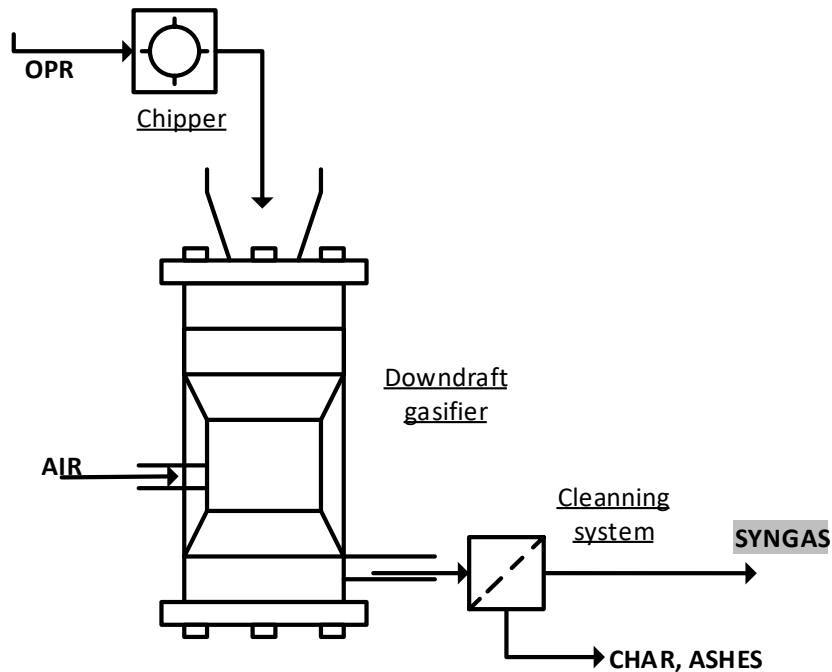


Figure 7-9. Oil palm rachis gasification process flow diagram.

As can be seen in **Figure 7-9**, air was the selected gasifying agent to produce the syngas. The equivalence ratio used was 0.5. This is defined as the relation between the actual air – fuel ratio and the stoichiometric air – fuel ratio.

The experimental results of the oil palm rachis gasification discussed in the above chapter and the results obtained from the simulation are compared with the results reported in the literature. These results are reported in **Table 7-3**. As was mentioned above, the results from the experimental section are similar with those reported by Guangul et al [216] and Atnaw et al [128]. On the other hand, the simulation of the oil palm rachis using the above mentioned kinetic expressions for the pyrolysis, combustion and reduction zones gives a similar composition with the experimental data obtained. In fact, the hydrogen composition obtained via simulation is very similar with the hydrogen content obtained experimentally. However, the carbon monoxide, carbon dioxide and methane as well as the nitrogen content have a small difference. This difference can be attributed to the assumptions that the kinetic model contemplates in terms of gas – gas reactions and solid – gas phase reactions during the gasification process.

Table 7-3. Comparison of experimental data, simulation results and reported data for oil palm rachis gasification.

Gas	Experimental data	Simulation data	Reported data [77]	Reported data [216]
Hydrogen	11.87	12.09	10.70	9.67
Carbon monoxide	21.01	26.93	17.90	22.49
Carbon dioxide	15.91	9.21	12.30	11.24
Methane	4.46	1.10	-----	1.98
Nitrogen	46.65	50.66	58.00	54.62

The relative differences between the simulated data, the experimental data obtained and the reported data in literature show that this process is highly variable and hard to standardize. The above is mentioned due to the difficult to control the entire gasification process. Nevertheless, it is possible to observe that the different efforts performed to model and simulate this process have given good estimates.

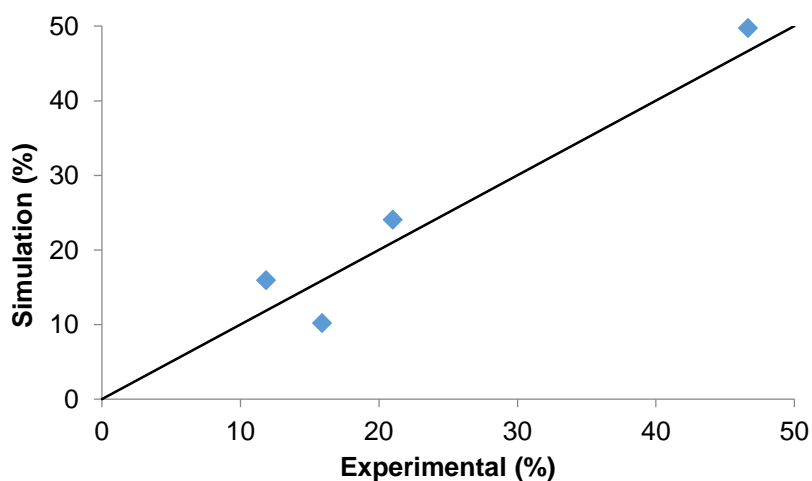


Figure 7-10. Deviation of the simulated data with the experimental data obtained.

After the simulation process, a parametric sensitivity analysis was done to determine the effect of the operating parameters into the oil palm rachis gasification process. The equivalence ratio, moisture content in biomass and relative moisture content in the air were analyzed. The next table shows the evaluated points.

Table 7-4. Points evaluated in the parametric analysis (Box-Behnken based analysis).

Run	Relative humidity (%)	Equivalence ratio (ER)	Feedstock moisture content (%)
1	66.00	0.20	10.00
2	91.00	0.20	10.00
3	66.00	0.50	10.00
4	91.00	0.50	10.00
5	81.00	0.20	5.00
6	81.00	0.50	5.00
7	81.00	0.20	20.00
8	81.00	0.50	20.00
9	66.00	0.35	5.00
10	91.00	0.35	5.00
11	66.00	0.35	20.00
12	91.00	0.35	20.00
13	81.00	0.35	10.00

The variables evaluated changing the above conditions were the composition of the syngas, the LHV of the gas, the H₂/CO ratio and the cold gas efficiency. Surface response curves were obtained and they are presented below:

As can be seen in the next figures, the moisture content of the feedstock increase the hydrogen to carbon monoxide ratio as well as a decrease in the equivalence ratio too. This is because of the amount of water into the gasifier increases, which can result in an increase of the hydrogen concentration. On the other hand, similar behavior was obtained when the H₂/CO ratio was evaluated with the same variables at different relative air humidity.

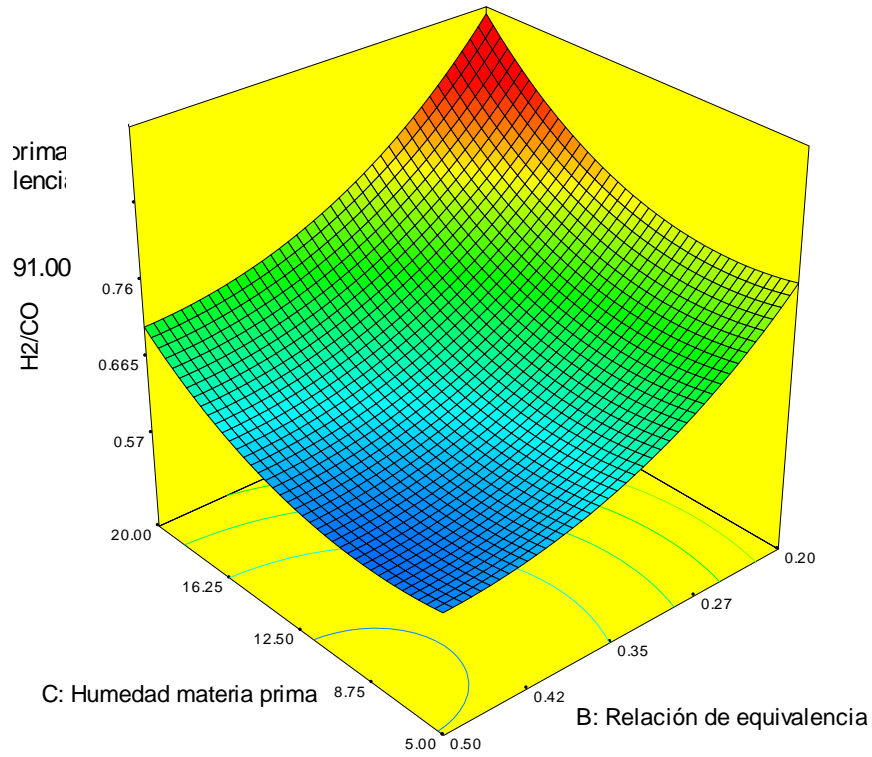


Figure 7-11. Effect of the equivalence ratio and feedstock moisture content in the H₂/CO ratio at a relative air humidity of 91%.

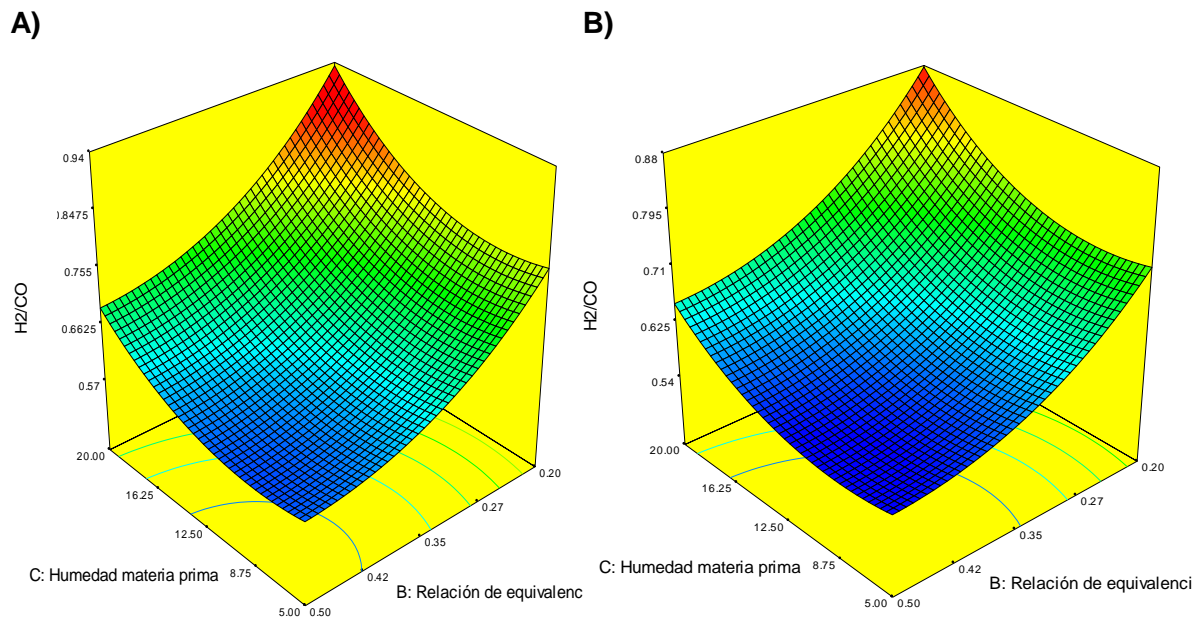


Figure 7-12. Effect of the equivalence ratio and feedstock moisture content in the H₂/CO ratio at a relative air humidity of **A)** 66% and **B)** 81%.

According to the above presented surface areas, it is possible to find a minimum or maximum to obtain the lowest and highest H₂/CO ratio. Moreover, it is possible to find an equation that describes the behavior showed in terms of the evaluated parameters. Thus the conditions that maximized the H₂/CO ratio are:

- **Feedstock moisture content:** 20%
- **Equivalence ratio:** 0.2
- **Relative humidity:** 66%

These values give a H₂/CO ratio maximum of 0.94 and the other parameters such as LHV and cold gas efficiency gives the following values 7.44 MJ/Nm³ and 81.2%, respectively. The high moisture content of the raw material contributes to obtain a high H₂/CO ratio is explained from the mass balance point of view due to the amount of hydrogen atoms into the gasifier is high. However, this high moisture content this moisture content is not recommendable in experimental experience due to the amount of energy required to dry the raw material is a lot. Therefore, high moisture contents can produce low energy efficiencies in the gasification process.

The obtained equation that describes the above surface response is:

$$\log_{10}\left(\frac{H_2}{CO}\right) = 1.31 - 3.05 \times 10^{-2}A - 1.37B - 9.39 \times 10^{-3}C + 8.20 \times 10^{-4}AB - 8.02 \times 10^{-4}BC + 1.94 \times 10^{-4}A^2 + 1.29B^2 + 5.88 \times 10^{-4}C^2 \quad (7.9)$$

Other important parameter that was evaluated is the Low Heating Value. This parameter is important due to denote the quality of the gas for electricity generation. The surface response curves obtained for this variable are presented below:

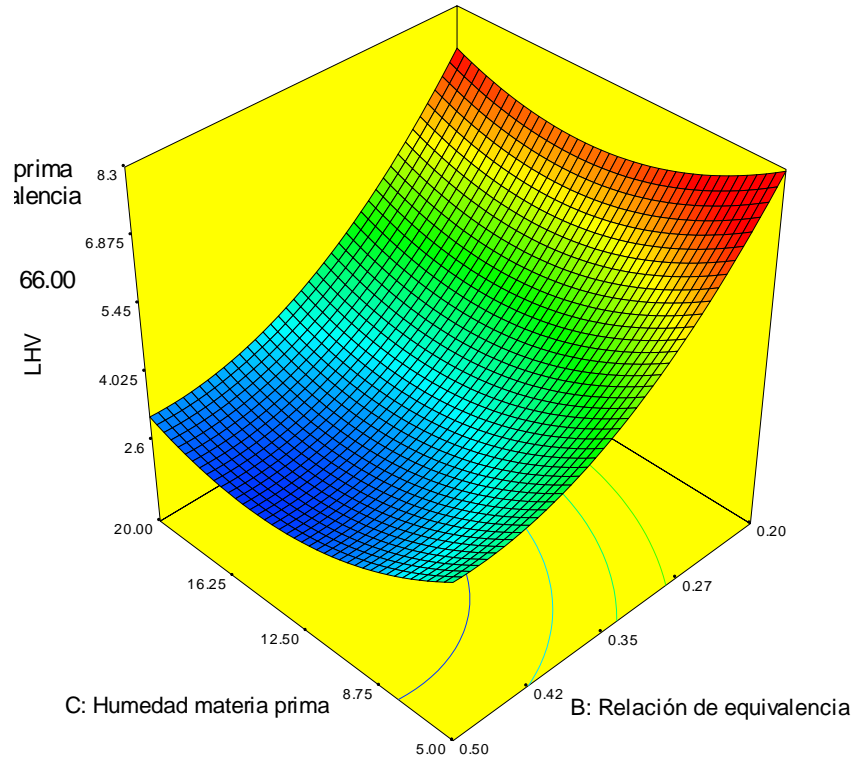


Figure 7-13. Effect of the equivalence ratio and feedstock moisture content in the syngas LHV at a relative humidity of 66%.

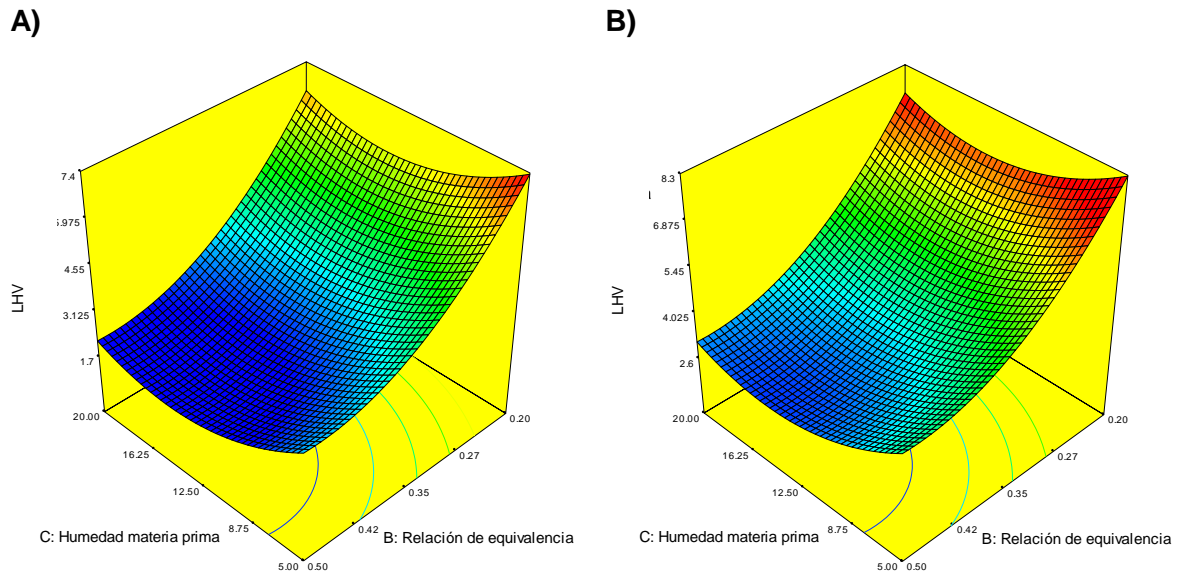


Figure 7-14. Effect of the equivalence ratio and feedstock moisture content in the syngas LHV at a relative air humidity of **A) 81%** and **B) 90%**.

In the same way that in the above presented surface areas, the relative humidity does not have a significant effect on the syngas LHV. Surface responses showed in **Figure 7-13** and **Figure 7-14** shows that the raw material moisture content has a little effect in the syngas LHV. At low moisture content and low equivalence ratio the LHV reaches a maximum. The values of the variables that allow obtaining a maximum of the LHV are written below:

- **Feedstock moisture content:** 5%
- **Equivalence ratio:** 0.2
- **Relative humidity:** 66%

The LHV of the produced syngas after to find the above conditions is 8.26 MJ/Nm³. The other values for the variables H₂/CO and Cold gas efficiency were 0.76 and 86.17%, respectively. The obtained results for this case are more realistic than the results obtained for the H₂/CO ratio. This is because low moisture contents are preferred to perform a gasification process. In addition, the equivalence ratio found is in agreement with the reported data by different authors and books [45], [217], [218].

The obtained equation that describes the above surface response is:

$$\begin{aligned} \log_{10}(\text{LHV}) = & 54.39 - 0.95A - 49.24B - 0.47C + 1.50 \times 10^{-3}AB \\ & - 5.42 \times 10^{-2}BC + 6 \times 10^{-3}A^2 + 51.23B^2 + 1.7 \times 10^{-2}C^2 \end{aligned} \quad (7.10)$$

Finally, the cold gas efficiency of the process also was evaluated. However, the response surface curves are not show in this text because of they have the same tendency that the LHV curves. The equation that describes the response surface curve of the cold gas efficiency of the process is presented below:

$$\begin{aligned} \log_{10}(\text{C. eff}) = & 489.07 - 8.63A - 350.23B - 4.03C + 1.30AB \\ & + 5.55 \times 10^{-2}A^2 + 361.43B^2 + 1.59 \times 10^{-1}C^2 \end{aligned} \quad (7.11)$$

The optimal conditions of the cold gas efficiency were the same presented for the LHV study. This fact can be explained due to the cold gas efficiency is calculated from the syngas LHV.

From the parametric study, it was possible to observe that there are to optimal conditions to operate the gasifiers. Nevertheless, the first optimal conditions indicate that the raw material must have a moisture content of 20%, which will be unbeneficial for the gasification process. This is because the excessive energy that must be used to evaporate the water content of the raw material. Moreover, it can be observed that the relative humidity of the air does not affect the syngas production significantly. In this way, the optimal conditions to produce syngas using the GEK TOTTI system are the above mentioned for the LHV evaluation.

7.3 Final remarks.

The simulation of the oil palm rachis gasification is complex process that involves the different chemical reactions and transformation pathways. Nevertheless, good estimations of the syngas final composition can be obtained using a semi-empirical and equilibrium based approach. Effects related with mass and heat transfer must be taken into account to increase the feasibility of the simulation process. On the other hand, the use of statistical approaches and sensivity analysis are highlighted in this chapter as main tools to find optimal conditions. Thus, it was obtained that the equivalence ratio and the moisture content of the biomass are relevant variables in the gasification process. Therefore, always must be evaluated the equivalence ratio of the process and to add a conditioning step before the gasification.

8. Oil palm rachis and syngas based simulations.

In this chapter simulations using the oil palm rachis and syngas produced from its gasification are performed. This chapter is based mainly in the results of the published paper “Fermentation, thermochemical and catalytic processes in the transformation of biomass through efficient biorefineries”. The above is because the processes that were simulated in this article are related with the use of oil palm rachis as raw material to obtain value-added products in two scenarios applying concepts of heterogeneous catalysis. Other simulation that is presented in this chapter is the production of heat and power from the syngas obtained via gasification and the biomethane obtained via anaerobic digestion.

8.1 Oil palm rachis simulations with and without heterogeneous catalysis.

This simulation uses oil palm rachis as raw material to produce different value added products using the gasification process to produce methanol and other products such as ethanol, lactic acid, ethyl levulinate and pentane. The methodological approach and the results of these simulations are presented below:

8.1.1 Biorefinery without catalysis.

The scheme for processing the OPR into ethanol, xylitol, lactic acid and biogas, in a biorefinery, is depicted in **Figure 8-1**. This biorefinery consists of six stages including the final obtained products. The first stage is the pretreatment of the lignocellulosic material, the second stage is the saccharification to produce fermentable sugars and the other

stages are related with the ethanol, xylitol, lactic acid and biogas production. A description of each stage mentioned above is given next.

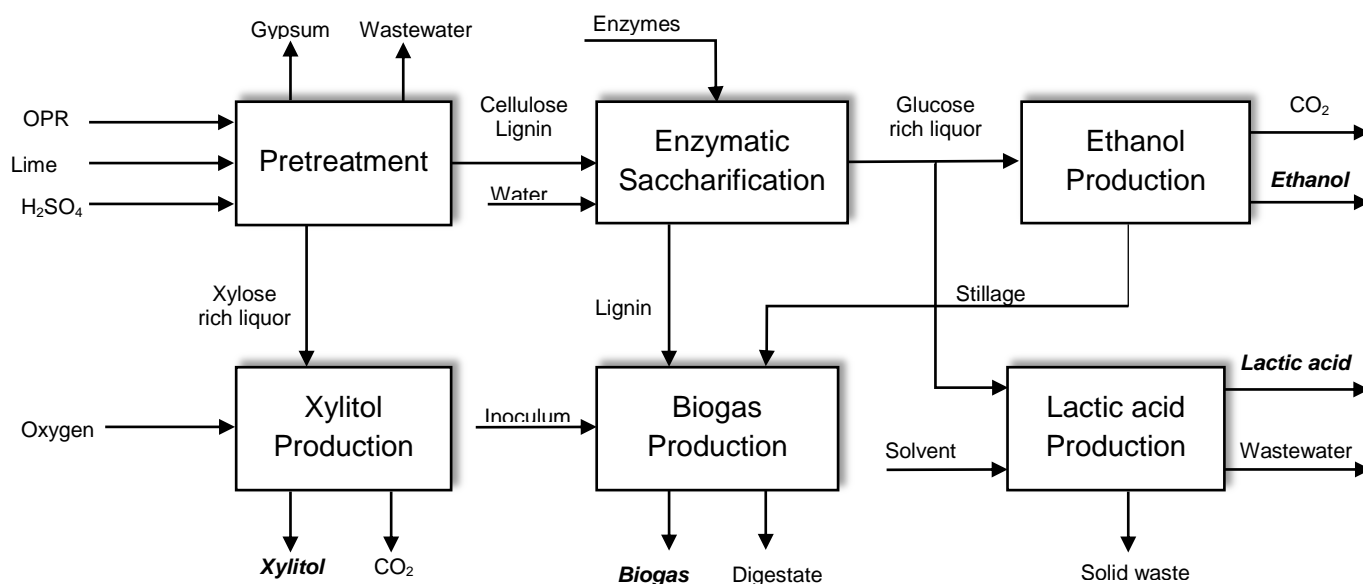


Figure 8-1. Simplified block diagram for the ethanol, lactic acid, xylitol and biogas production using oil palm rachis as feedstock into a biorefinery without heterogeneous catalysis.

The pretreatment stage consists of the particle size reduction and lignocellulosic matrix decomposition. Thus, the OPR is milled until reaching a particle size of 0.5 mm. This sample is treated with a dilute sulfuric acid solution (2%v/v) to remove the hemicellulose content as oligomeric and monomeric sugars (xylose) [219]. Besides, byproducts such as furfural and 5-HMF as well as acetic acid are generated [220]. The xylose liquor produced in the dilute acid hydrolysis is detoxified to reduce the inhibitors presence. The operating conditions of the detoxification process were 333.15 K for 30 minutes using lime as precipitating agent to produce gypsum. Finally, the output stream of this process is neutralized using sulfuric acid [221]. On the other hand, the saccharification stage involves the enzymatic hydrolysis of the produced cellulose in the pretreatment stage. The above is performed using an enzymatic cocktail composed of endo-beta-1,4-glucanase, exo-beta-1,4-glucanase and beta-1,4-glucosidase. This process is carried out at pH 4.8, 323.15 K, 150 rpm with a solids concentration of 20%w/v for 72h. As main product from the saccharification stage, a hexoses rich liquor is obtained[222].

Ethanol production was accomplished using 50% of the hexoses rich stream from the saccharification block. The substrate is consumed by *Saccharomyces cerevisiae* yeast in a chemostat without microorganism recirculation. The fermentation process is carried out at 310.15 K and 1.0 bar. From this, ethanol, glycerol and carbon dioxide as well as biomass and non-converted substrate are present in the outlet stream of bioreactor. Therefore, a hydrocyclone is used to remove the microorganism fraction. Ethanol is purified using two distillation towers and a series of molecular sieves. The first tower concentrates the ethanol until 50%v/v. The second tower separates the ethanol - water mixture until its azeotropic composition. Following this, the rectified ethanol is heated at 391.15 K and 21 psia and dehydrated using molecular sieves to produce anhydrous ethanol [110], [221].

Lactic acid was obtained from 50% of the hexoses rich stream from the enzymatic hydrolysis block. This stream was heated at 353.15 K to sterilize the liquor. The fermentation process is carried out using *Lactobacillus casei* at 315.15 K [223], [52]. The downstream process to purify the lactic acid is composed by the calcium lactate precipitation, lactic acid recovery, lactic acid esterification, methyl lactate hydrolysis and distillation. The precipitation step consists on the lactic acid removal from the broth as calcium lactate at 363.15 K [224]. Lactic acid is recovered using sulfuric acid and concentrated into an evaporator. Then, lactic acid is recovered using sulfuric acid and subjected to an esterification process with methanol to separate it from the impurities. The methyl lactate is distilled and methanol is recovered. After that, methyl lactate is hydrolyzed over D001 acid exchange resin to produce lactic acid again. Finally, it is obtained as an aqueous solution with an 88% w/w concentration.

Xylitol production process was carried out using *Candida Guilliermondii* [225], [226]. The xylose rich stream from the pretreatment block is heated until 353.15 K to sterilize the liquor. After this, the fermentation is performed following the operation conditions reported by Silva et al [225]. In the separation stage, the product stream was concentrated to 0.73 g/m³ of xylitol to avoid the use of ethanol. Then, this stream is crystallized at 268.15 K and filtrated to recover the produced xylitol [227] Finally, biogas is produced using the lignin stream from the enzymatic hydrolysis block and the stillage from the ethanol production

block. The anaerobic digestion was carried out at 310.15 K and the biogas production was calculated using the stoichiometric approach proposed by Buswell [155].

8.1.2 Biorefinery with catalysis

The scheme for processing the OPR into *n*-pentane, methanol, ethyl levulinate, ethanol, and lactic acid in a biorefinery using heterogeneous catalysis is depicted in **Figure 8-2**. This biorefinery consists of ten stages including the final obtained products. The products in this biorefinery are proposed using the platform products mentioned in the introduction section (e.g. fufural, syngas).

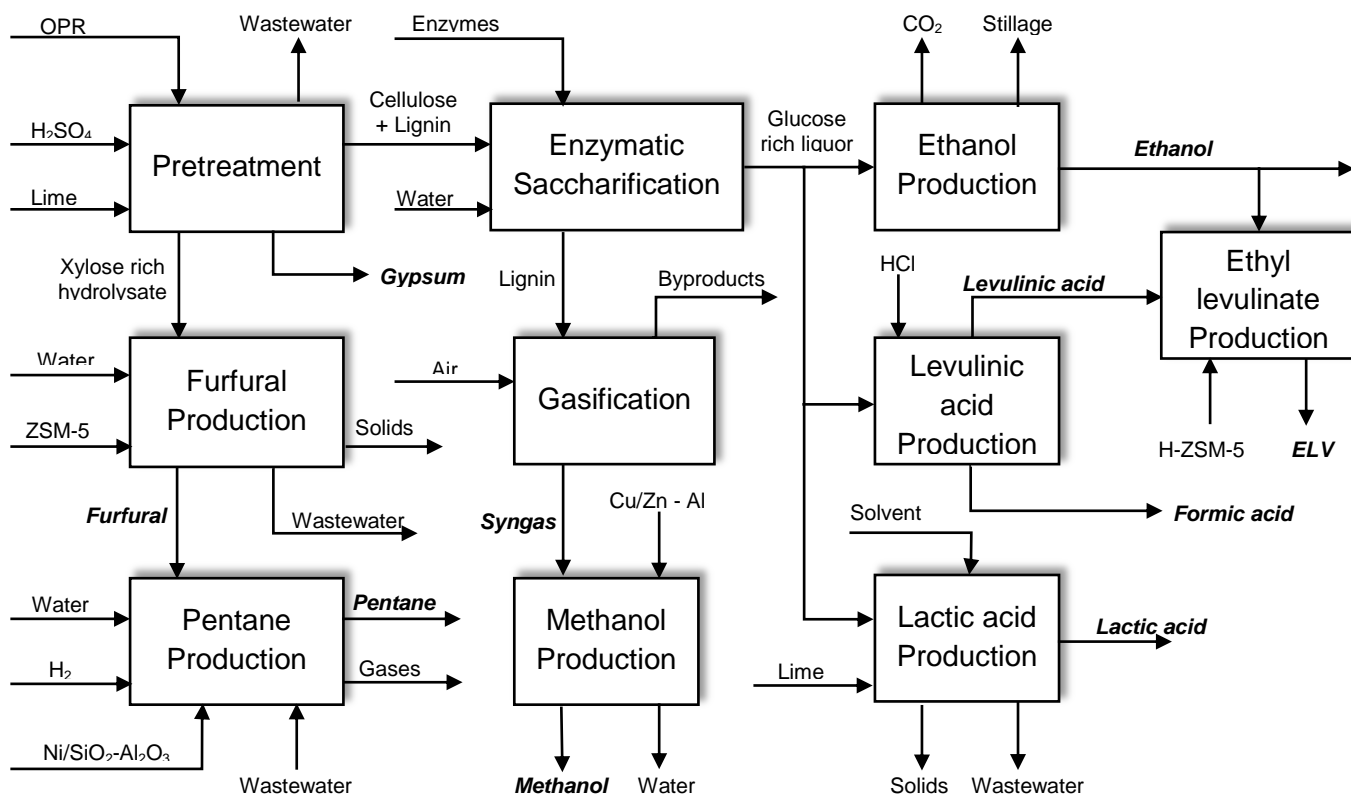


Figure 8-2. Simplified block diagram for the *n*-pentane, methanol, ethyl levulinate, ethanol, and lactic acid using oil palm rachis as feedstock into a biorefinery with heterogeneous catalysis.

The biorefinery shown in the above figure has the same pretreatment, saccharification, ethanol and lactic acid production stages as those in the biorefinery presented in figure 3.

Therefore, these stages are not explained in this section. Also, as can be seen in **Figure 8-2**, the catalyst used to obtain the products is represented as an inlet stream in each stage.

Furfural production block involves the catalytic aqueous-phase xylose dehydration to furfural using ZSM-5 zeolite as heterogeneous catalyst in its H⁺ form. The reaction is carried out at 473 K and 30 bar in an inert atmosphere with an initial xylose concentration of 10%w/w and a catalyst - xylose mass ratio of 0.3 [228]. After the dehydration, a filter is used to remove the solid fraction produced during this step. Then, furfural is separated using a distillation column until reaching the azeotropic composition and carried to the *n*-pentane production process. In this block, the furfural is converted using a nickel based bifunctional catalyst composed by 14%w/w Ni, 25%w/w Al₂O₃ and 61%w/w SiO₂ at 413.15 K and 30 bar [229]. From this, light alkanes (C₁-C₄) and *n*-pentane (C₅) are produced. The former products are separated in gaseous phase while the desired product is obtained in an organic layer after a liquid – liquid separation.

Levulinic acid production is performed using the hexoses rich stream from the saccharification block, which is mixed with a dilute solution of HCl and sent to a CSTR to achieve the sugars degradation. The glucose conversion was carried out at 433.15 K, 5.5 MPa and a residence time less than 100 minutes. Other products such as HMF and formic acid are obtained from this process [82], which are removed using a solid-liquid separator. Finally, the levulinic acid rich stream is carried to a distillation system to obtain the desired product and formic acid as sub-product.

Levulinic acid esterification with ethanol is carried out with H - ZSM5 as solid catalyst. The inlet streams are preheated to 333.15 K for conditioning them. The esterification is performed in liquid phase at 368.15 K and atmospheric pressure. The ethanol to levulinic acid molar ratio employed is 8:1. In addition, the catalyst ratio suggested by Kakasaheb et al [230] were used to carry out the reaction. Then, the product separation is accomplished through two distillation columns. The first tower aims to obtain ethyl levulinate with a mass fraction higher than 95% due to the absence of azeotrope in the system ethanol – water – ethyl levulinate. The second tower recovers the not reacting ethanol at azeotropic composition to be recirculated.

Finally, syngas production is accomplished using lignin as feedstock. A downdraft gasifier with air as oxidizing agent is employed to convert the inlet stream in CH₄, H₂, CO, CO₂, charcoal, tars and ashes. In this process, pyrolysis, combustion and reduction reactions are considered to determine the final syngas composition [109]. After the gasification process, solid, liquid and gaseous fractions are separated [208], [109]. Then, the CO and CO₂ hydrogenation and the reverse water gas shift reactions are performed to give methanol over a Cu based catalyst. The reactions are carried out in a plug-flow reactor (PFR) with a negligible pressure drop according to the process described by De Maria et al [231].

8.1.3 Simulation procedure and economic assessment.

The simulation of each biorefinery, using an OPR mass flow rate of 250 ton/day (dry basis) as feedstock, was accomplished using the Aspen Plus software v8.6 (Aspen Technology Inc. USA) [18]. All simulation process was performed using the Non-Random Two Liquids (NRTL) and Hayden-O'Connell equation of state (HOC EoS) to describe the behavior of the liquid and vapor phases present in each process [232], [233]. The thermodynamic properties reported by the National Research Energy Laboratory (NREL) were used to introduce components such as cellulose, hemicellulose, lignin, enzymes and biomass that are not available in the software database [191].

The reaction steps in each block of the proposed biorefineries were simulated using kinetic models reported in the literature (see table A1). However, yields were used to complete the mass balances of processes where a kinetic model is not available. Instead, separation and purification stages were conceptually designed. The residue curve maps of each mixture in the biorefinery were analyzed applying topologic thermodynamics concepts to identify the distillation regions given by the azeotropes formation [234], [235]. Finally, the distillation columns were calculated using as first estimates the reflux ratio and the theoretical stages obtained from shortcut design methods. The process flow diagram of the pretreatment, saccharification, ethanol, xylitol, gasification, and methanol stages are reported by Quintero et al [221], Dávila et al [236], Garcia et al [109] and Van Dal et al [237]. The other processes were conceived using process engineering tools and the explained procedures reported in the above references. The purposes, methods, Aspen model used, key operating parameters and specifications of the principal equipment of each biorefinery are given for process simulation and they are summarized in **Table 8.1**.

Table 8.1. Summary of purposes, conditions and Aspen models used for the main units in the proposed biorefineries.

Unit	Purpose	Conditions and unit specification	Method	Aspen Model
<i>Pretreatment and Enzymatic blocks</i>				
Crusher	Size reduction to 0.5 mm	1 bar, Gyrotory, Primary	NRTL	Crusher
Dilute acid reactor	Remove hemicellulose as xylose	1 bar, 394 K, 0.75 h, 2% v/v H ₂ SO ₄	NRTL – HOC	RCSTR
Detoxification reactor	Reduce the inhibitors presence	1 bar, 333 K, 0.5 h, 10% w/v lime	NRTL - HOC	RStoic
Drum filter	Solid – liquid separations	1 bar, 298 K, 5 rpm drum speed.	NRTL	Filters
Enzymatic reactor	Fermentable sugars production	1 bar, 323 K, pH = 4.8, 60 FPU.	Yields used	RYield
<i>Ethanol block</i>				
CSTBR	Ethanol production	1 bar, 303 K, D = 0.17 h ⁻¹	Yields used	RYield
Distillation Columns	Ethanol separation	Distillation: 16 trays, 2.75 reflux ratio, total condenser Rectification: 12 trays, 1.4 reflux ratio, total condenser	NRTL – HOC	RadFrac
<i>Biogas block</i>				
Anaerobic digester	Biogas production	1 bar, 310 K, ISR*: 5:1	NRTL – HOC	RStoic

ISR*: Inoculum – substrate ratio.

Table 8.1. Summary of purposes, conditions and Aspen models used for the main units in the proposed biorefineries (continued)

Unit	Purpose	Conditions and unit specification	Method	Aspen Model
<i>Xylitol block</i>				
CSTBR	Xylitol production	1 bar, 303 K, <i>Candida Guilliermondii</i>	Yields reported	RYield
Evaporator	Xylitol concentration	0.15 bar, 303 K.	NRTL – HOC	Flash2
Crystallizer	Xylitol crystallization	1 bar, 268 K, without ethanol.	Yields used	RYield
<i>Lactic acid block</i>				
CSTBR	Lactic acid production	1 bar, 315 K, <i>Lactobacillus casei</i>	Yields used	RYield
Precipitation reactor	Calcium lactate formation	1 bar, 313 K, 20% w/v lime	NRTL	RSotic
Acidification reactor	Lactic acid recovery	1 bar, 363 K, 92% recovery	NRTL	RStoic
Esterification reactor	Methyl lactate formation	1 bar, 333 K, 68% conversion	NRTL - HOC	RCSTR
Hydrolysis reactor	Lactic acid formation	1 bar, 333 K, 84% conversion	NRTL - HOC	RCSTR
Distillation columns	Methanol and lactic acid recovery	Methanol recovery: 16 trays, 1.1 reflux ratio, total condenser Lactic acid purification: 12 trays, 0.1 reflux ratio, total condenser.	NRTL - HOC	RadFrac
<i>Furfural block</i>				
Reactor	Furfural production	30 bar, 493 K, 80% conversion	NRTL - HOC	RCSTR
Distillation column	Furfural purification	12 trays, 0.5 reflux ratio.	NRTL - HOC	RadFrac

Table 8.1. Summary of purposes, conditions and Aspen models used for the main units in the proposed biorefineries (continued)

Unit	Purpose	Conditions and unit specification	Method	Aspen Model
<i>n-pentane block</i>				
Reactor	n-pentane production	30 bar, 413 K, 63% conversion, 85% selectivity <i>n</i> -pentane.	Yields used	RYield
<i>Gasification block</i>				
Gasifier	Syngas production	1 bar, 973 K, 0.25 ER*.	NRTL - RK	RGibbs
<i>Methanol block</i>				
Reactor	Methanol production	110 bar, 523 K	NRTL - RK	RPlug
Distillation column	Methanol purification	12 trays, 1.2 reflux ratio, total condenser	NRTL - RK	RadFrac
<i>Levulinic acid block</i>				
Reactor	Levulinic acid production	55 bar, 453 K, 90% conversion	NRTL – HOC	RCSTR
Distillation column	Levulinic acid recovery	12 trays, 0.12 reflux ratio, total condenser	NRTL – HOC	RadFrac
<i>Ethyl levulinate block</i>				
Reactor	Ethyl levulinate production	4.5 bar, 403 K, 78.5% conversion	NRTL – HOC	RCSTR
Distillation column	Ethyl levulinate recovery	12 trays, 1.8 reflux ratio, condenser	NRTL – HOC	RadFrac

On the other hand, The economic assessment was performed using the commercial software Aspen Process Economic Analyzer v8.4 (Aspen Technology Inc., USA) to calculate the costs associated with the production of the target products. The mass and energy balances from the simulations were used in the sizing of the process equipment. As input data to perform the economic evaluation a 10-years period with an annual interest rate of 17% was considered. In addition, the straight-line method for the capital depreciation calculation and a 25% of tax rate, also were taken into account. The operator and supervisor labor costs were 2.14 USD/h and 4.29 USD/h, respectively, considering the Colombian context [236]. The aforementioned software estimates the total capital investment and the operating costs associated to raw materials, utilities and maintenance [238]. Finally, a period of 8000 h was taken into account to perform the calculations. The main data used in the economic assessment of the two proposed biorefineries is presented in the **Table 8-1**.

Table 8-1. Raw material and utilities costs used in the economic assessment.

Feature	Value	Unit	Reference
Oil palm rachis	19.40	USD/ton	[115]
Enzymes	0.34	USD/gal	[222]
Sulfuric acid virgin 100%	94.00	USD/ton	[239]
Lime hydrated bulk f.o.b*	70.00	USD/ton	[239]
Hydrochloric acid 22° Be	85.43	USD/ton	[239]
Cooling water	0.74	USD/m ³	[152]
Electricity	0.14	USD/kWh	[152]
LP Steam	1.57	USD/ton	[152]
MP steam	8.18	USD/ton	[152]
Fuel	24.58	USD/MW	[152]
ZSM-5	94.55	USD/kg	[240]
Ni/SiO ₂ -Al ₂ O ₃	221.50	USD/kg	This work
Cu/ZnO/Al ₂ O ₃	195.23	USD/kg	This work

f.o.b: free on board

The Ni/SiO₂-Al₂O₃ catalyst cost was calculated considering the preparation method reported by Zhang et al [229]. Similarly, the Cu/ZnO/Al₂O₃ catalyst cost was calculated

according to the mechanical milling and combustion synthesis method reported by Lei et al [241]. In each case, the price of the precursors and its proportions were used as input information to perform this calculation. Additionally, a three catalyst cycles per year was considered to take into account their cost in the economic analysis. Finally, the net present value (NPV), profitability index, the payout period and the internal rate of return (IRR) were used as metrics to evaluate the economic feasibility of the simulated biorefineries. All of these economic metrics are related to cash flows giving an idea of the risk of implementing each process.

8.1.4 Results and discussion.

Mass yields of each biorefinery were calculated using an allocation factor based on the amount of feedstock employed to obtain the proposed products. This considers the cellulose, hemicellulose and lignin content of the feedstock as main platforms. Thus, ethanol, lactic acid and ethyl levulinate production are only attributed to the cellulose content treated in the pretreatment and saccharification blocks. The xylitol and n-pentane production comes from the xylose in the diluted acid hydrolysis step, whereas the biogas and methanol production comes from the lignin fraction. In this sense, the calculated raw material shares employed to obtain the products in both biorefineries are presented in

Figure 8-3.

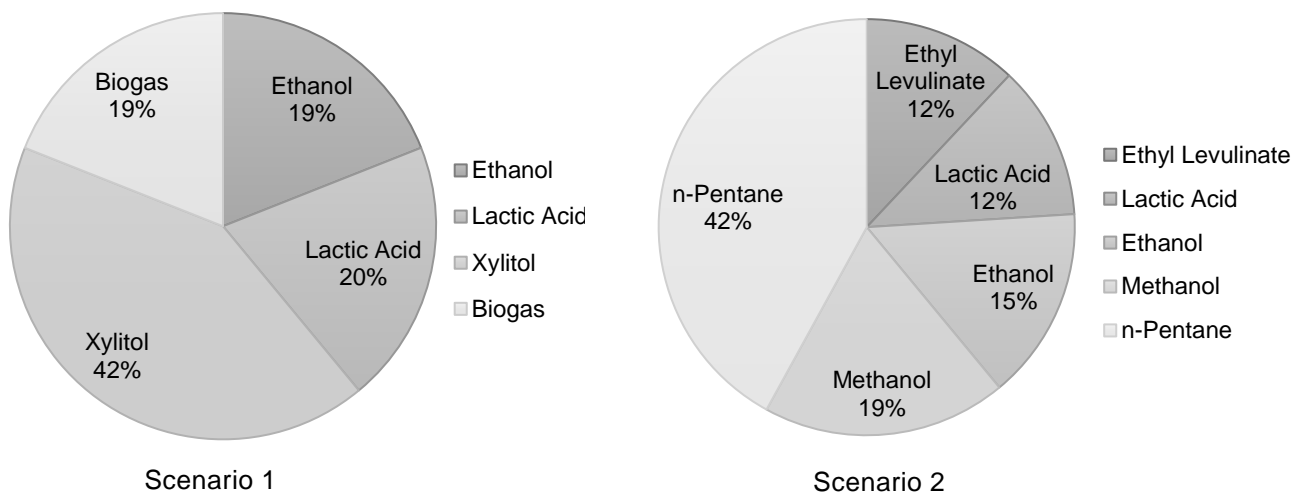


Figure 8-3. Share of the feedstock employed to produce the value-added products proposed in both scenarios.

The pretreatment stage results in both biorefineries were similar. The optimum residence time for the dilute acid process to carry out the hemicellulose conversion minimizing the furfural and 5-HMF formation was 0.74 hours with a conversion of 97.65%. Afterward, the cellulose conversion achieved in the saccharification block was 92.56%. These conversion results are very close with those reported by Quintero et al [221]. Nevertheless, these blocks in the biorefinery with heterogeneous catalysis have lower energy requirements than in the other biorefinery. The above is due to the former's lack of a detoxification stage because the furfural production is not affected by inhibitors. A summary of the calculated mass yields for each product into the simulated biorefineries is presented in **Table 8-2**

Table 8-2. Calculated mass yields for each product obtained from both biorefineries.

Product	Biorefinery without heterogeneous catalysis		Biorefinery with heterogeneous catalysis	
	Flow (kg/h)	Yield (kg/kg ^{**})	Flow (kg/h)	Yield (kg/kg)
Ethanol	735.487	0.372	352.729	0.226
Lactic acid	1407.00	0.675	80.016	0.064
Xylitol	1005.34	0.229	-	-
Biogas*	2066.21	1.044	-	-
Ethyl levulinate	-	-	307.980	0.246
<i>n</i> -Pentane	-	-	347.688	0.079
Methanol	-	-	28.177	0.014
Total	5214.04	0.500	1116.08	0.108

*T=310 K, P=1.0 bar.

**Yields expressed as mass flow of product per allocated mass flow of raw material.

As can be seen in **Table 8-2**, the target products total flow of the biorefinery without heterogeneous catalysis is higher than the total flow of target products obtained in the other biorefinery. This difference can be attributed to the use of the glucose, xylose and lignin streams in more processes. Therefore, the equipment efficiencies and reaction yields from catalytic reactions are a critical point to study in the biorefineries design.

The mass yield obtained in the biorefinery without heterogeneous catalysis for the ethanol production is very close with the reported by Gutierrez et al [242] once the glucose yield from the empty fruit bunch (EFB) is taken into account. However, the yield achieved in the second biorefinery is lower than the first one because part of the anhydrous ethanol was used to produce ethyl levulinate. 40% of the produced ethanol was used to obtain this product considering an ethanol: levulinic acid molar ratio of 8:1. However, this split affects the overall ethanol mass yield as well as the total production cost. Lactic acid and xylitol blocks obtained yields very close to those reported by Gonzales et al [52] and Silva et al [225], respectively. However, the downstream process employed to obtain a commercial solution of lactic acid (i.e. 88% w/w) depends largely on the reaction conditions of the lactic acid esterification and methyl lactate hydrolysis. Therefore, the overall lactic acid yield in the second biorefinery was lower compared with the yield obtained in the first biorefinery. The above is related with the amount of glucose used and the downstream overall efficiency. On the other hand, xylitol yield was similar with that reported by Dávila et al [236].

The ethyl levulinate production process acquired the higher mass yield in the biorefinery with heterogeneous catalysis. The glucose conversion to levulinic acid and formic acid was 90.60% with a levulinic acid selectivity of 50%. After this, a conversion of 60.70% was achieved in the esterification of this organic acid. These results are in accord with the results reported by Weingarten et al [243] and Kakasaheb et al [230], respectively. The higher yield of this product is attributed to the quantity of cellulose destined to its production. In the n-pentane case, the xylose to furfural conversion was 80.30% with a higher selectivity due to the Lyxose decomposition in it.

The mass balances for the n-pentane production were calculated using the conversion and selectivities reported by Xinghua et al [229]. However, the low yield obtained for this product was caused by the high raw material amount destined for its production. Finally, the lowest yield in the second biorefinery was obtained for the methanol production case due to the lower H₂/CO ratio present in the syngas generated. As a result of the low hydrogen mole fraction, a low partial pressure of this component to carry out the reaction was identified as a critical factor. For this reason, the use of steam to produce a syngas with higher amounts of H₂ and low content of N₂ should be considered.

The energy yields of the biorefineries was calculated taken into account the thermal energy supplied by the steam used in each biorefinery and the total mass flow of OPR. Then, the first biorefinery consumed 66.74 ton/h of low pressure steam while the second biorefinery consumed 40.92 ton/h and 1.53 ton/h of low and medium pressure steam, respectively. Therefore, the energy consumption for each biorefinery was 8.93 MJ/kg and 14.63 MJ/kg, respectively. On the other hand, the requirements of cooling water in the first and second biorefineries were 56.52 m³/day and 71.12 m³/day, respectively. The biorefinery without heterogeneous catalysis has a lower energy consumption than the second biorefinery due to that biotechnological processes use moderate temperatures and pressures to maintain the biological activity of the micrograms and enzymes. Instead, lactic acid production in this biorefinery consumed a 35.56% of the total energy needs due to the use of five conceptual reactors. In contrast with the reported shares by Quintero et al [110], the pretreatment and saccharification blocks have a lower energy requirement in comparison with other blocks in the biorefineries.

The biorefinery with heterogeneous catalysis has higher energy requirements owing to the operating conditions employed in the different processes that conform it. Methanol production consumes the highest share of energy because the syngas and methanol production processes working at higher temperature and pressures than the other processes. Finally, approximately 75% of the total energy consumed is attributed to the platform molecules and its derivatives (i.e. n-pentane, methanol and ethyl levulinate) production. The consumed energy distribution by block in both biorefineries is presented in **Figure 8-4**.

The economic evaluation of the proposed biorefineries was performed using the mass and energy balances obtained from the simulation considering an oil palm rachis mass flow rate of 250 ton/day.

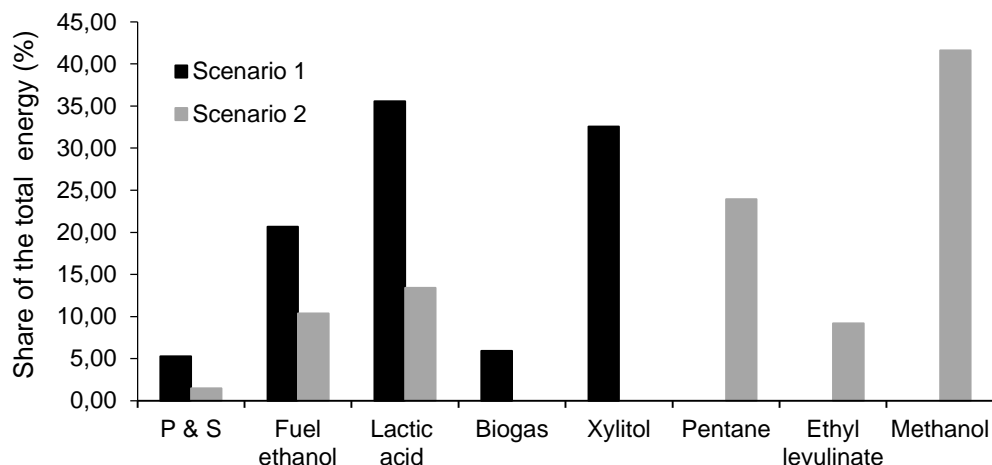


Figure 8-4. Share of energy consumed by the proposed products in each biorefinery. (P&S: Pretreatment and Saccharification).

Table 8-3. Annualized costs and economic metrics for each biorefinery scenario

Feature	Biorefinery without		Biorefinery with	
	heterogeneous catalysis		heterogeneous catalysis	
	Thousands USD/year	(%)	Thousands USD/year	(%)
Raw materials	6356.79	27.25	6857.11	25.05
Utilities	9407.54	40.33	11933.20	43.59
Operating labor	222.64	0.95	239.76	0.88
Maintenance	856.12	3.67	889.00	3.25
Operating charges	55.66	0.24	59.94	0.22
Plant overhead	539.32	2.31	564.38	2.06
G and A costs*	1395.04	5.98	1640.00	5.99
Depreciation	4490.00	19.25	5190.00	18.96
Total cost	23323.18	100.00	27373.39	100.00
Sales (M. USD/year)**	68.14	-	74.76	-
Internal Rate Return (%)	49.47	-	46.29	-
Profitability index	1.50	-	1.43	-
Payout Period (years)	4.07	-	4.55	-
NPV (M USD/year)	15.82	-	8.03	-

*General and Administrative costs. (Thousand USD) **M. USD/year = Million USD/year.

The effect of the catalytic processes implementation into the biorefinery design is mainly reflected on the total raw material and utilities costs. The OPEX of the first biorefinery was 17.43 M.USD/year while the OPEX of the second biorefinery was 20.54 M.USD/year. The OPEX was calculated as the sum of the direct variable costs (e.g. raw material, operating labor) and the costs of the indirect manufacturing materials (e.g. utilities). The difference of 3.11 M.USD/year can be attributed to the new raw materials as well as the utilities employed to perform the chemical conversion of the platform molecules. Therefore, the raw materials and utilities costs are higher in the second biorefinery due to the use of new elements to obtain the target products as well as the high energy needs.

The total capital investment was calculated taking into account the equipment (e.g. reactors, distillation columns) used to obtain each one of the final products of both biorefineries. As can be seen in **Table 8-4** the total capital investment for the first biorefinery is lower than the second one due to the amount of new equipment that the latter needs to carry out all the OPR processing. Also, it is possible to observe that the investment cost for ethanol and lactic acid production is higher in the first biorefinery. The above is related with the equipment size.

Table 8-4. Capital investments of both biorefineries to obtain the desired products.

Product	Capital investment (M.USD)	
	First biorefinery	Second Biorefinery
Ethanol	7.10	6.54
Lactic acid	13.80	9.34
Xylitol	1.59	-
Biogas*	2.31	-
Ethyl levulinate	-	8.43
<i>n</i> -Pentane	-	8.92
Methanol	-	3.41
Total	24.81	36.64

The capital cost of the first and second biorefinery were 56.13 M.USD and 64.93 M.USD, respectively. These values were calculated using the above information and the obtained data from the economic evaluation using the software Aspen Process Economic Analyzer

v8.4. However, these results could have an uncertainty between of 30% - 50% associated with the capital investment calculations due to the complexity level of the analysis [238], [244].

The results showed in **Table 8-3** for the first scenario are different to those reported by Moncada et al [23], who simulated a similar biorefinery. This situation is attributed to the plant capacity. The total operating costs reported by this author were 73.23 M USD/year. However, the feedstock mass flow rate specified by this author to the biorefinery was 200 ton/h. Therefore, it is reasonable to assume that the total operating cost obtained in this work is reliable. Nevertheless, a sensitivity analysis of the plant capacity of both biorefineries was performed to understand the variability of the total operating cost. For this, the following mass flow rates of dry OPR were considered: 125 ton/day, 250 ton/day and 1250 ton/day. The obtained results are illustrated in **Figure 8-5**

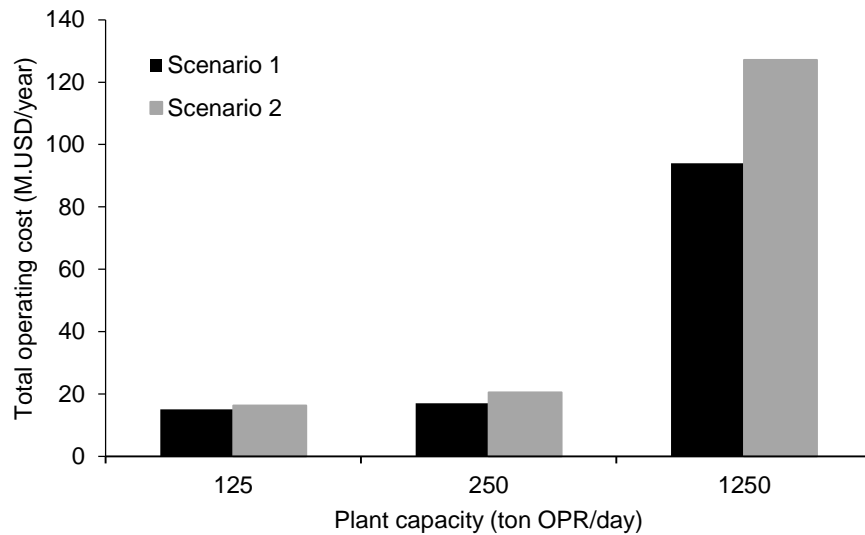


Figure 8-5. Plant capacity of scenarios 1 and 2 vs total operating cost.

As can be seen in the above figure, the total operating costs of both biorefineries increase with plant capacity. The relation between both biorefineries must be similar at different scales because the operating costs (e.g. raw materials) are directly associated with plant capacity. However, the raw materials and utilities costs will have the highest shares of the items presented in table 4 at high feedstock flow rates. Therefore, the maximum plant

capacity must be found performing a sensitivity analysis of the fixed costs of each project vs the operating costs at different plant capacities

The metrics employed to evaluate the feasibility of both biorefineries were calculated taking into account the cash flows obtained from the economic assessment and the expected products sales in the Colombian context. Table 4 shows that both scenarios are feasible because the profit margins obtained for xylitol and ethyl levulinate in each case exceeds the 50%, compensating the negative profit margins obtained for ethanol and lactic acid products. Furthermore, it is possible to observe that both biorefineries have economic indicators that suggest that they are feasible. Thus, the profitability indexes are higher than unity and the initial investment will be recover in the fifth year of the lifetime of both biorefineries [23]. The net present value of the biorefineries is presented in **Figure 8-6**

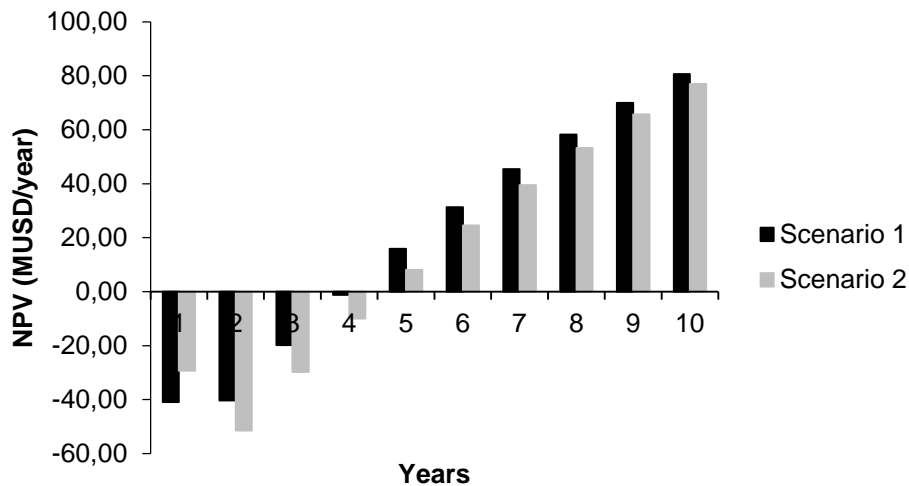


Figure 8-6. Net Present Value of oil palm rachis biorefinery without (scenario 1) and with (scenario 2) heterogeneous catalysis.

As can be seen in **Figure 8-6**, the net present value (NPV) for the biorefinery without heterogeneous catalysis is higher than the biorefinery with catalysis. However, both biorefineries reach a positive net present value (NPV) in the fifth year. A NPV of 15.82 M.USD/year was obtained for the first biorefinery and a NPV of 8.03 M.USD/year was obtained for the second one. These results suggest that the first biorefinery is better than the second one. Nevertheless, factors such as the scale, mass integration and energy

integration are important aspects that must be taken into account when a multi-product biorefinery is proposed. In this sense, the production of value-added products as fine and specialty chemicals takes a great importance when catalytic processes are included. Finally, in accordance with the above results, the implementation of catalytic processes to convert biotechnological products in a great variety of value-added products is possible from a techno-economic point of view. However, the obtained results suggest that the use of catalytic processes in biorefineries is feasible but not economically favorable at its current stage. This last result can explain by the incipient development of biorefineries at the commercial level (most of the so called biorefineries are really biofuels plants). Then, it is imperative for scientists to increase the efforts to make possible in the future years the wide use of catalysis into biorefineries design, implementation and industry commercialization.

8.2 Heat and power generation.

The production of heat and power using syngas is an alternative that has been evaluated in the last years. However, other energy vectors such as biogas and biomethane (similar to natural gas) can be used to produce heat and power in a cogeneration system. Therefore, the aim of this section is to compare the heat and power generation using the syngas and biomethane as fuels in a cogeneration system.

8.2.1 Simulation procedure.

The simulation procedure to gasify the oil palm rachis was described in the chapter 6 (scenario 1). On the other hand, the biogas and biomethane production processes will be explained using as raw material the oil palm rachis. The anaerobic digestion of lignocellulosic biomass can be improved using a pretreatment stage. In this simulation, two scenarios were proposed. The first scenario (scenario 2) consists in three stages: particle size reduction, anaerobic digestion and upgrading, while for the second scenario (scenario 3) implies a liquid hot water (LHW) pretreatment stage previously to the anaerobic digestion such as is showed in **Figure 8-7**. The selection of this technology was based in the pretreatment effect on oil palm fronds and the anaerobic digestion of materials with similar composition [245]–[249]. Moreover, the key factors mentioned by Alvira et al. 2010 also were considered [36].

In the particle size reduction step was considered the milling with the help of shredders to obtain a maximum particle size of 2.0 mm and comminution to enable a particle size distribution between 0.1-1.0 mm [247]. After the mechanical operation, the ground OPR was submitted to the LHW pretreatment with conditions of 175 °C, 10 bar and liquid solid ratio of 8.0 (v/w) due to improve the OPF digestibility [247]. The compositional changes in that work were assimilated during simulation as a conversion of each lignocellulosic component into lignocellulosic soluble and monosaccharides compounds. In the anaerobic digestion (AD) of both scenarios were used the conditions (i.e., thermophilic conditions and substrate inoculum ratio of 46.92 %wt. volatile solids) and biodegradability results of Kaparaju et al. [250]. The above due to the similarity of OPR with wheat straw in its lignocellulosic composition, volatile solids content and fibril appearance. The AD and pretreatment stages were simulated with RSTOIC blocks considering the empirical and primary stoichiometric equations of each lignocellulosic component proposed by Buswell (i.e. for the methane and carbon dioxide generation) and Demirbas et al. 2005 (i.e. for the cellulose and hemicellulose hydrolysis during pretreatment) [251], [252]. Finally, in the biogas upgrading to biomethane was used the technology of water scrubbing where water absorbs CO₂ content of biogas [58]. In this section compressors, exchangers, absorption tower, flash and stripper column are specified in the simulation as describe Cozma et al. [70].

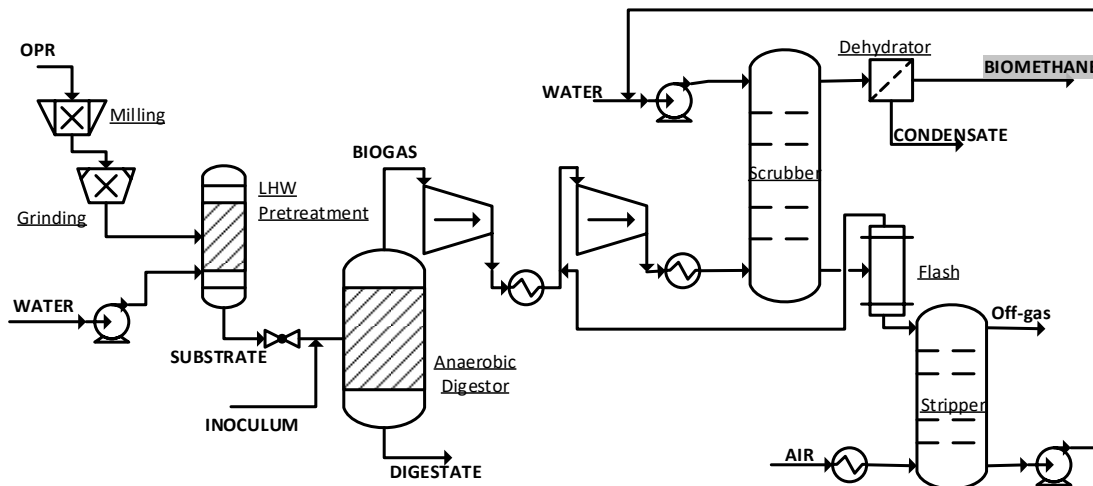


Figure 8-7. Biomethane production process with a liquid hot water pretreatment stage.

The cogeneration or CHP plant simulated is composed by a gas turbine, heat recovery steam generator (HRSG) and steam turbine. Each one of these elements is described as follows. The gas turbine uses the fuels generated by gasification to produce power and exhaust gases. It is composed by a series of two compressors, one burner and two turbines in an intercooling, reheating and regenerative cycle (ICRHR). This type of turbine was selected to be used in the simulation due to the high thermal efficiencies obtained in comparison with the simple cycle gas turbines. The above is achieved due to this cycle decrease the heat input requirements of the system. The ICRHR gas turbine was simulated in Aspen Plus using atmospheric air (288 K, 1 bar). With the aim to minimize the compressors work input, the pressure ratio in both was the same. Similarly, the turbines work output was maximized using the same pressure ratio [253]. The syngas combustion was performed in an air rich mixture to ensure complete combustion products formation. The boiler was simulated using a RSTOIC block. The main characteristics of the simulated gas turbine are presented in **Table 8-5**

Table 8-5. Main characteristics of the simulated gas turbine.

Item	Value	Item	Value
Compressors pressure ratio	10.0	Turbine pressure ratio	5.0
Compressor isentropic efficiency	85.0%	Turbines isentropic efficiency	90%
Intercooler pressure drop	1.0%	Re-heater pressure drop	2.0%
Boiler pressure drop	5.0%	Turbine entrance temperature	1600.0 K
Air – fuel ratio	6.4	Equivalence ratio	4.0

The out gases from the gas turbine are mixed and combusted with more fuel (i.e. syngas) to rise up its temperature. This secondary combustion is performed in a firing system that was modeled as a RSTOIC block in Aspen Plus. The hot gases from this system were carried out to three steam generators that produce steam at different pressures and temperatures. All the steam generators are composed by an economizer to rise the water temperature until its saturation point, an evaporator that supplies the necessary heat to transform the saturated liquid in a saturated steam and a super heater that rises the steam temperature over its saturation point. Furthermore, only in the HP-steam generator

was considered an attemporator with the end to prevent damages in the HP-turbine [254]. The above described process is denominated as a heat recovery steam generator (HRSG) and it is showed in **Figure 8-8**.

The HRSG system was modeled in Aspen Plus using the HeatX and Flash2 blocks. The HRSG system was simulated to give a HP-Steam at 60 bars, IP-Steam at 30 bars and LP-Steam at 3 bars. Also, it was simulated taken into account a flue gases temperature of 50°C in all cases. However, the water used in this system varies between syngas. Finally, the steam produced in the HRSG unit was sent to a high and middle pressure steam turbine with the end to produce more power.

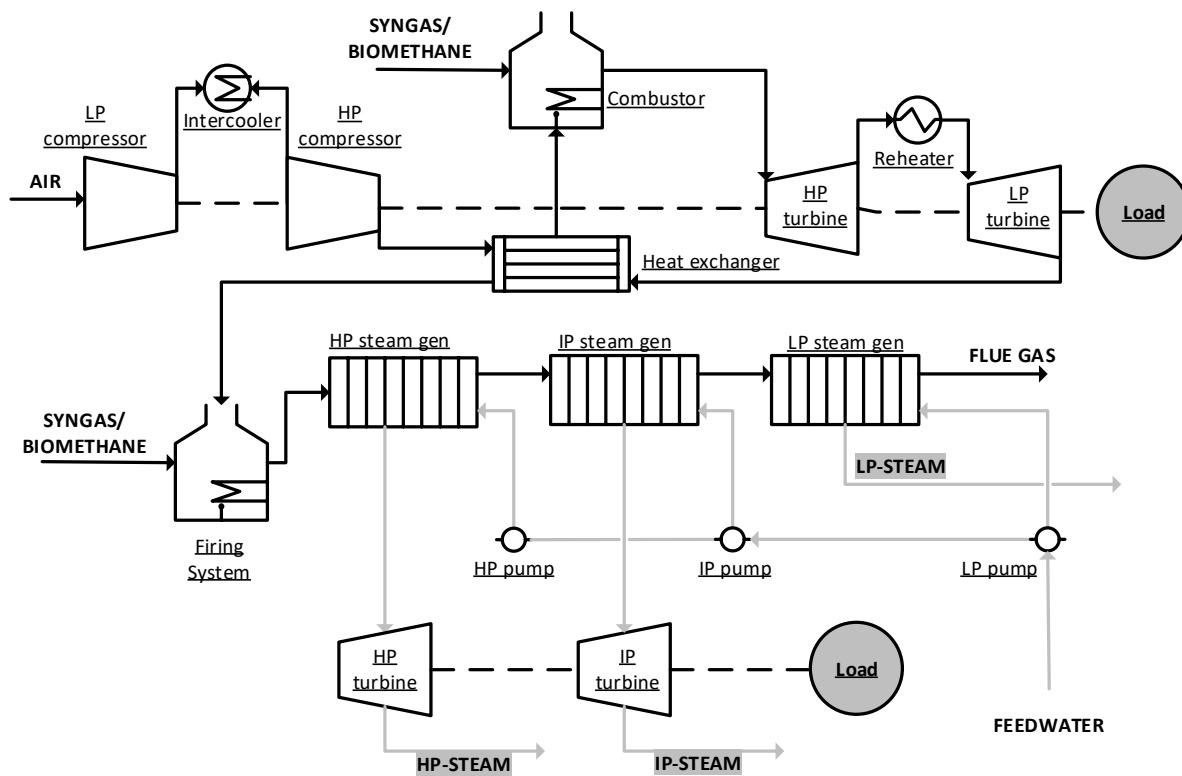


Figure 8-8. Cogeneration system plant.

8.2.2 Simulation results.

The mass balance of the oil palm rachis gasification process and the heat and power generation are showed in **Table 8-6**.

Table 8-6. Mass balances of the cogeneration plant

Item	Inlet mass flow (kg/h)	Outlet mass flow (kg/h)
Water	18999,0	0,0
Oil palm rachis (wet)	8333,3	0,0
High pressure steam	0,0	5624,5
Middle pressure steam	0,0	874,5
Low pressure steam	0,0	12500,0
Power	0,0	2638,25 kW
Moisture	0,0	3666,5
Air	51250,0	0,0
Char	0,0	88,4
Ashes	0,0	83,0
Exhaust gases	0,0	54374,3
Tars	0,0	1371,1
Total	78582,3	78582,3

As can be seen in the above table, 0.31 kW/kg of oil palm rachis are generated in the process. On the other hand, the char and ash yields are similar with the obtained in the gasification process. However, the tars yield is higher than the obtained in the gasification process.

Table 8-7. Syngas process mass balances.

Item	Value	Unit
Oil palm rachis (db.)	4666,8	kg/h
Char yield	1,9	%
Ash yield	1,8	%
Syngas mass flow	11047,5	kg/h
Syngas volumetric flow	9769,3	m ³ /h
Syngas density	1,13	kg/Nm ³
Air flow	7500	kg/h
Gasification temperature	973	K
Equivalence Ratio	0,25	

The yields obtained from the simulations of scenarios 1, 2 and 3 were calculated and compared to each other. The syngas composition obtained from the simulation was 13.5%, 15.5%, 9.0% and 60.0% of CO, CO₂, H₂ and N₂, respectively. This results are in agreement with the syngas composition reported for OPF by Atnaw et al [77]. Also, it was obtained that the syngas production has the highest mass yield in terms of fuel and steam production. However, this situation is given by the high air flow that was needed to carry out a complete combustion of the syngas in the combustion chamber inside of the gas turbine to maintain an equivalence ratio of 4.0. In contrast, the biomethane composition obtained in both scenarios after the upgrading step was 94.4%. Nevertheless, the scenario 3 achieved a higher fuel and steam yields than the scenario 2. The summary of the mass yields obtained in each scenario is presented in **Table 8-8**.

Table 8-8. Mass yields obtained from the simulation procedure

Scenario	Fuel yield [kg fuel/kg OPR]	Total steam yield [kg steam/kg OPR]
1	3.60	3.50
2	0.21	2.75
3	0.26	2.37

The above results do not necessary implies that the syngas production process is the best option to produce heat and power in the proposed cogeneration plant. The above is performed to give a series of characteristics from different points of view to identify the advantages and disadvantages that each technology can offer. In this sense, the energy analysis can provide more information related with the considered scenarios. The energy analysis was carried out calculating the low heating value of the syngas and biomethane generated, the thermal efficiency of the gas turbine, the net energy value and the global efficiency of the process. These results are presented in **Table 8-9**.

Table 8-9. Energy parameters of the scenarios.

Scenario	LHV [kJ/kg]	n_{th} [%]	Generated Power [MW]	NEV [kJ/kg OPR]
1	6.98	41.8	23.7	28574
2	26.1	39.5	20.2	26603
3	47.4	52.2	43.5	23432

The CAPEX and OPEX obtained from the economic evaluation are presented in **¡Error! No se encuentra el origen de la referencia..** These results shows that the scenarios 1 and 2 have a similar capital and operational expenditures. Thus, these results suggest that the implementation of a gasification or AD without pretreatment for heat and power generation does not have a great difference under the gas turbine and HRSG stipulated conditions. Nevertheless, the amount of heat in steam form and generated power as well as the gas turbine thermal efficiency is higher than the AD process. Also, it is important to note the fact that the economic indicators are similar does not mean that the technology cost are the same. At last, these costs are related mainly with the gas turbine and HRSG capacity to allow the gas turbine stipulated conditions and the flue gases outlet temperature of 60°C. The above can be seen in the generated power in scenario 1 and the steam yield presented in **¡Error! No se encuentra el origen de la referencia..**

Moreover, the scenario 3 has the highest CAPEX and OPEX compared with the other two scenarios. These results are attributed mainly to the gas turbine capacity due the amount of air that it is necessary to accomplish an equivalence ratio of 4.0. Therefore, the CAPEX and OPEX increase of the scenario 3 does not be related directly with the implementation of LHW pretreatment. The obtained results are in agreement with the costs of a commercial gas turbines prices which vary according to their capacity. For instance, scenarios 1 and 2 a can use a SGT-400 gas turbine to produce 15 MW and the scenario 3 can use a SGT A-45 TR gas turbine to produce 40 MW.

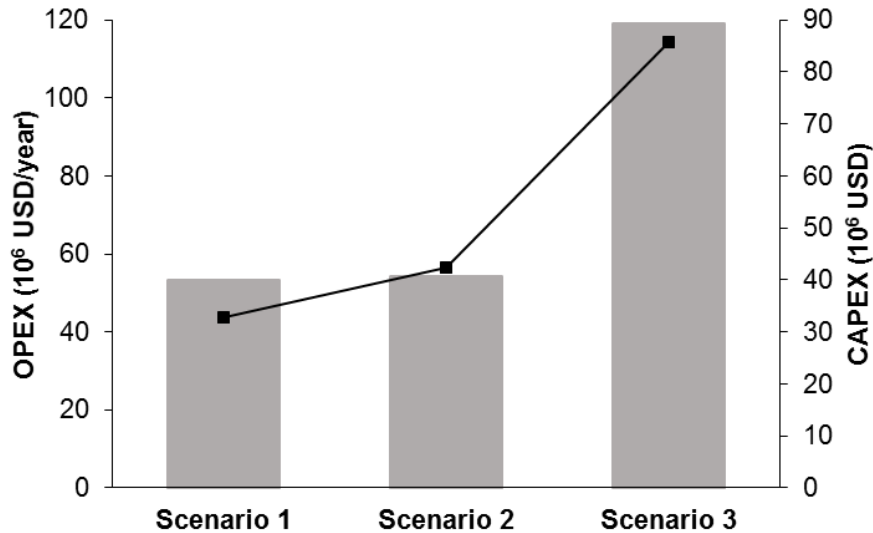


Figure 8-9. Economic analysis of each scenario according to the OPEX (gray bars) and CAPEX (black line).

The global warming potential results for the evaluated scenarios implies that the amount of CO₂ generated in the outputs of scenario 3 is bigger than the CO₂ emissions in scenario 2 corresponding to 1346.93, 1294.79 kg CO₂/ ton OPR, respectively. This result is directly related with the flue gas composition leaving the CHP plant since during combustion of syngas can be produced more amount of CO₂. While the emissions of biochemical pathway are derived mainly for the biogas upgrading process which intensifies when the yield of biomethane is achieved having the scenario 3 a value of 1294.79 kg CO₂/ ton OPR.

The result of this simulation leads to conclude the potential of the OPR as raw material to produce fuel gases through thermochemical and biochemical pathways. On the other hand the syngas and biomethane use to produce heat and power are possible from the techno-economic, energy and environmental point of view. Nevertheless, the syngas is a more suitable option because this one obtained the highest steam yields and low costs. The above is concluded without regarding that the AD process is an essential part of the future biorefineries and a technology that can be improved through the raw materials pretreatment.

8.3 Final remarks.

Simulations based on the use of oil palm rachis as feedstock shows that the implementation of thermochemical, biotechnological and catalytic pathways are suitable to obtain different value-added products. In addition, the use of the Aspen Economic Analyzer as tool to estimate the production costs and the fixed capital cost of a project is a good approach to understand the complexity of a biorefinery based on lignocellulosic materials. On the other hand, oil palm rachis is a suitable raw material for both biogas and syngas generation. Nevertheless, according to the results, the syngas from oil palm rachis gasification can be used to provide heat and power at industrial level. Meanwhile, biomethane is a suitable for energy generation due to this energy vector has more calorific value than the air-downdraft produced syngas.

Conclusions.

- The palm oil rachis is a promising raw material to be included in the palm oil production chain for the production of value-added products such as heat and electricity or other products that have commercial application in the chemical industry.
- Biomass gasification is a technology that can be applied in the Colombian context or even in the Latin-American context to produce electricity in non-interconnected zones. However, downdraft gasifiers must be changed for fluidized bed gasifier due to its great applicability at commercial scale.
- Syngas for air-downdraft gasification can be used as chemical platform to produce a great variety of products using heterogeneous catalysis. However, the technical and economic feasibility of this process must be analyzed in the next years.
- The biorefinery concept can be applied to increase the economic and environmental feasibility of thermochemical processes to produce value-added products derived from petrochemical industry. However, the energy vectors production is an option that must be considered with the aim to overcome all challenges that are present in recent years.

APENDIX I.

Table A1. Kinetic models employed in each block of the simulated biorefineries and their operating conditions.

Block	Process	Catalyst	Kinetic expression	Operating Conditions	Ref.
Pretreatment	Hemicellulose decomposition	Sulfuric acid	$r_{Xylan} = -k_1 C_{Xylan}$	T = 394 K	[220]
			$r_{Xylose} = k_1 C_{Xylan} - k_2 C_{Xylose}$	P = 2 bar	
			$r_{Inhibitors} = -k_2 C_{Xylose}$	$\tau = 45 \text{ min}$	
Ethanol	Fermentation	N.P	$\mu_v = \mu_{max} \frac{C_S}{K_1 + C_S} \left(1 - \frac{C_P}{C_{Pc}} \frac{C_S}{K_2 + C_S} \right)$	T = 310 K	[255]
			$\mu_v = \mu'_{max} \frac{C_S}{K_1 + C_S} \left(1 - \frac{C_P}{C_{Pc}} \frac{C_S}{K_2 + C_S} \right) - \mu_v$	P = 1 bar.	
			$\mu_d = -\mu_v$	D = 0.17 h ⁻¹	
Lactic acid	Fermentation	N.P.	$\mu = \mu_{max} \frac{C_S}{K_S + C_S} \left(1 - \frac{P}{P_{max}} \right)^n$	T = 315 K P = 1 bar D=0.11 h ⁻¹	[52]

Methyl lactate hydrolysis	D001 acid resin.		$r = (k_0 + k_w) \exp\left(-\frac{E_a}{RT}\right) \left(C_{ML} C_{H_2O} - \frac{C_{HL} C_{MeOH}}{K_{eq}}\right)$	T = 373 K P = 1 bar $\tau = 4.0$ h	[256], [257]
Levulinic acid	Glucose dehydration	HCl	$r_{Glucose} = -(k_1 + k_2)C_{Glucose}$ $r_{HMF} = k_1 C_{Glucose} - (k_3 + k_4)C_{HMF}$ $r_{Levulinic\ acid} = k_3 C_{HMF}$	T = 453 K P = 5.5 MPa $\tau = 3.33$ h	[243]
Ethyl levulinate	Esterification	H-ZSM-5	$-r_{Levulinic\ acid} = k(C_{Levulinic\ acid})^n$	T = 413 K P = 4-5 bar	[230]
Furfural	Xylose dehydration	ZSM-5	$r_{Xylose} = -k_1 C_{Xylose} - k_3 C_{Xylose} + k_2 C_{Lyxose}$ $r_{Furfural} = k_3 C_{Xylose} + k_8 C_{Solids} + k_4 C_{Lyxose} - k_6 C_{Furfural} - k_5 C_{Furfural}$ $r_{Lyxose} = k_1 C_{Xylose} - k_2 C_{Xylose} - k_4 C_{Lyxose}$ $r_{Acids} = k_5 C_{Furfural} - k_7 C_{Acids}$ $r_{Solids} = k_7 C_{Acids} + k_6 C_{Furfural} - k_8 C_{Solids}$	T = 493 K P = 30 bar $\tau = 2.0$ h	[228]

	Water Gas Shift reaction		$r_{\text{WGS}} = \frac{K_5 P_{\text{CO}_2} - K_7 P_{\text{H}_2\text{O}} P_{\text{CO}} P_{\text{H}_2}^{-1}}{1 + K_2 P_{\text{H}_2\text{O}} P_{\text{H}_2}^{-1} + K_3 P_{\text{H}_2}^{1/2} + K_4 P_{\text{H}_2\text{O}}}$			
Methanol		Cu/ZnO/Al ₂ O ₃			T = 493 K	[232],
	Methanol production reaction		$r_{\text{Methanol}} = \frac{K_1 P_{\text{CO}_2} P_{\text{H}_2} - K_6 P_{\text{H}_2\text{O}} P_{\text{CH}_3\text{OH}} P_{\text{H}_2}^{-2}}{(1 + K_2 P_{\text{H}_2\text{O}} P_{\text{H}_2}^{-1} + K_3 P_{\text{H}_2}^{1/2} + K_4 P_{\text{H}_2\text{O}})^3}$		P = 60 bar	[233], [237]
Xylitol	Fermentation	N.P	Yields were used.		T = 493 K	[225]
					P = 60 bar	
n-Pentane	Reaction	Ni/SiO ₂ -Al ₂ O ₃	Yields were used.		T = 303 K	[229]
					P = 1 bar	

References.

- [1] Anco S. Blazev, *Energy Security for The 21st Century*. CRC Press, 2015.
- [2] REN21, "Renewables 2016 Global Status Report," Paris.
- [3] International Energy Agency (IEA), "World Energy Outlook 2016," 2016.
- [4] R. C. Saxena, D. K. Adhikari, and H. B. Goyal, "Biomass-based energy fuel through biochemical routes: A review," *Renew. Sustain. Energy Rev.*, vol. 13, no. 1, pp. 167–178, 2009.
- [5] J. Popp, Z. Lakner, M. Harangi-R?kos, and M. F??ri, "The effect of bioenergy expansion: Food, energy, and environment," *Renew. Sustain. Energy Rev.*, vol. 32, pp. 559–578, 2014.
- [6] BP, "BP Statistical Review of World Energy," London, UK, 2016.
- [7] R. Singh, B. B. Krishna, G. Mishra, J. Kumar, and T. Bhaskar, "Strategies for selection of thermo-chemical processes for the valorisation of biomass," *Renew. Energy*, pp. 1–12, 2016.
- [8] J. Moncada, V. Aristizábal, and C. A. Cardona, "Design strategies for sustainable biorefineries," *Biochem. Eng. J.*, vol. 116, pp. 122–134, 2016.
- [9] Y.-C. Lin and G. W. Huber, "The critical role of heterogeneous catalysis in lignocellulosic biomass conversion," *Energy Environ. Sci.*, vol. 2, no. 1, p. 68, 2009.
- [10] C.-H. Zhou, X. Xia, C.-X. Lin, D.-S. Tong, and J. Beltramini, "Catalytic conversion of lignocellulosic biomass to fine chemicals and fuels.," *Chem. Soc. Rev.*, vol. 40, no. 11, pp. 5588–617, 2011.
- [11] Enerdata, "Global Energy Statistical Yearbook 2016," 2016. [Online]. Available: <https://yearbook.enerdata.net/#crude-oil-production.html>. [Accessed: 07-Jan-2017].
- [12] S. H. Mohr, J. Wang, G. Ellem, J. Ward, and D. Giurco, "Projection of world fossil fuels by country," *Fuel*, vol. 141, pp. 120–135, 2015.
- [13] B. W. Ang, W. L. Choong, and T. S. Ng, "Energy security: Definitions, dimensions and indexes," *Renew. Sustain. Energy Rev.*, vol. 42, pp. 1077–1093, 2015.

- [14] IEA, "Energy Technology Perspectives 2014 Harnessing Electricity ' s Potential. International Energy Agency," 2014.
- [15] EIO, "World energy demand and economic outlook EIA's handling of non-U.S. policies in the International Energy Outlook," in *International Energy Outlook*, 2016, pp. 7–17.
- [16] A. Hussain, S. M. Arif, and M. Aslam, "Emerging renewable and sustainable energy technologies: State of the art," *Renew. Sustain. Energy Rev.*, vol. 71, no. June 2015, pp. 12–28, 2017.
- [17] G. . Tiwari and R. . Mishra, *Advanced Renewable Energy Sources*. Royal Society of Chemistry, 2012.
- [18] A. A. Ahmad, N. A. Zawawi, F. H. Kasim, A. Inayat, and A. Khasri, "Assessing the gasification performance of biomass: A review on biomass gasification process conditions, optimization and economic evaluation," *Renew. Sustain. Energy Rev.*, vol. 53, pp. 1333–1347, 2016.
- [19] C. L. Williams, A. Dahiya, and P. Porter, "Introduction to bioenergy," in *Bioenergy: Biomass to Biofuels*, First Ed., A. Dahiya, Ed. Elsevier Inc., 2015, p. 670.
- [20] S. Lee and Y. . Shah, "Introduction to biofuels and bioenergy," in *Biofuels and Bioenergy: Processes and Technologies*, CRC Press, 2012, p. 341.
- [21] C. L. Williams, A. Dahiya, and P. Porter, "Chapter 1 - Introduction to Bioenergy," in *Bioenergy*, Anju Dahiya, 2015, pp. 5–36.
- [22] V. K. Gupta, R. Potumarthi, A. O'Donovan, C. P. Kubicek, G. D. Sharma, and M. G. Tuohy, "Bioenergy Research: An Overview on Technological Developments and Bioresources," in *Bioenergy Research: Advances and Applications*, First Ed., V. G. Gupta, M. Tuohy, C. P. Kubicek, J. Saddler, and F. Xu, Eds. Elsevier B.V., 2014, pp. 23–47.
- [23] J. Moncada, J. A. Tamayo, and C. A. Cardona, "Integrating first, second, and third generation biorefineries: Incorporating microalgae into the sugarcane biorefinery," *Chem. Eng. Sci.*, vol. 118, pp. 126–140, 2014.
- [24] B. Kamm and M. Kamm, "Principles of biorefineries," *Appl. Microbiol. Biotechnol.*, vol. 64, no. 2, pp. 137–145, 2004.
- [25] Ó. J. Sánchez and C. A. Cardona, "Trends in biotechnological production of fuel ethanol from different feedstocks," *Bioresour. Technol.*, vol. 99, no. 13, pp. 5270–5295, 2008.
- [26] T. Koizumi, "Biofuels and food security," *Renew. Sustain. Energy Rev.*, vol. 52, pp.

- 829–841, 2015.
- [27] D. Pimentel *et al.*, “Food versus biofuels: Environmental and economic costs,” *Hum. Ecol.*, vol. 37, no. 1, pp. 1–12, 2009.
- [28] International Renewable Energy Agency, “Renewable energy technologies: cost analysis series,” *Int. Renew. Energy Agency Copyr. IRENA 2012*, vol. 1, no. June, p. 274, 2012.
- [29] A. Demirbas, *Biorefineries for biomass upgrading facilities*. Springer, 2010.
- [30] W. a. Sirignano, “Combustion fundamentals,” *Combust. Flame*, vol. 63, no. 1–2, p. 309, 1986.
- [31] A. Molino, S. Chianese, and D. Musmarra, “Biomass gasification technology: The state of the art overview,” *J. Energy Chem.*, vol. 25, no. 1, pp. 10–25, 2016.
- [32] J. Zheng, Y. Tashiro, T. Yoshida, M. Gao, Q. Wang, and K. Sonomoto, “Continuous butanol fermentation from xylose with high cell density by cell recycling system,” *Bioresour. Technol.*, vol. 129, pp. 360–365, 2013.
- [33] A. Demirbas, “Biofuels securing the planet’s future energy needs,” *Energy Convers. Manag.*, vol. 50, no. 9, pp. 2239–2249, 2009.
- [34] M. Fatih Demirbas, “Biorefineries for biofuel upgrading: A critical review,” *Appl. Energy*, vol. 86, no. SUPPL. 1, pp. S151–S161, 2009.
- [35] M. Junginger, C. S. Goh, and A. Faaij, *International Bioenergy Trade: History status & outlook on securing sustainable bioenergy supply, demand and markets*. 2014.
- [36] P. Alvira, E. Tomás-Pejó, M. Ballesteros, and M. J. Negro, “Pretreatment technologies for an efficient bioethanol production process based on enzymatic hydrolysis: A review,” *Bioresour. Technol.*, vol. 101, no. 13, pp. 4851–4861, 2010.
- [37] D. M. Alonso, J. Q. Bond, and J. A. Dumesic, “Catalytic conversion of biomass to biofuels,” *Green Chem.*, vol. 12, pp. 1493–1513, 2010.
- [38] L. G. Wade, *Química Orgánica*, 5th editio. Pearson, 2004.
- [39] H. Fukuda, A. Kondo, and H. Noda, “Biodiesel fuel production by transesterification of oils,” *J. Biosci. Bioeng.*, vol. 92, no. 5, pp. 405–416, 2001.
- [40] K. Pal, “Investigations of transesterification of canola oil with methanol and ethanol for a new efficient method of biodiesel production,” no. December, pp. 1–195, 2011.
- [41] L. C. Meher, D. Vidya Sagar, and S. N. Naik, “Technical aspects of biodiesel production by transesterification - A review,” *Renew. Sustain. Energy Rev.*, vol. 10, no. 3, pp. 248–268, 2006.

- [42] C. A. Cardona, J. C. Solarte, J. A. Tamayo, A. Castro, and B. A. García, "Palm Oil for Food or Biodiesel, a Disjunction in Tropical Countries," in *Advances in Chemistry Research. Volume 32*, 2017, pp. 1–36.
- [43] R. P. Overend, "Direct Combustion of Biomass," in *Renewable Energy Sources Charged with Energy from the Sun and Originated from Earth-Moon Interaction*, Volume I., E. E. Shpilrain, Ed. Encyclopedia of Life Support Systems, pp. 74–101.
- [44] D. Chakraborty, N. K. Mondal, and J. K. Datta, "Indoor pollution from solid biomass fuel and rural health damage: A micro-environmental study in rural area of Burdwan, West Bengal," *Int. J. Sustain. Built Environ.*, vol. 3, no. 2, pp. 262–271, 2014.
- [45] P. Basu, *Biomass Gasification and Pyrolysis: Practical Design*. Elsevier Inc., 2010.
- [46] R. C. Brown, *Thermochemical Processing of Biomass: Conversion into Fuels, Chemicals and Power*. 2011.
- [47] M. Puig-Arnavat, J. C. Bruno, and A. Coronas, "Review and analysis of biomass gasification models," *Renew. Sustain. Energy Rev.*, vol. 14, no. 9, pp. 2841–2851, 2010.
- [48] V. Kirubakaran, V. Sivaramakrishnan, R. Nalini, T. Sekar, M. Premalatha, and P. Subramanian, "A review on gasification of biomass," *Renew. Sustain. Energy Rev.*, vol. 13, no. 1, pp. 179–186, 2009.
- [49] N. Couto, A. Rouboa, V. Silva, E. Monteiro, and K. Bouziane, "Influence of the biomass gasification processes on the final composition of syngas," *Energy Procedia*, vol. 36, pp. 596–606, 2013.
- [50] L. G. Pereira, M. O. S. Dias, A. P. Mariano, R. Maciel Filho, and A. Bonomi, "Economic and environmental assessment of n-butanol production in an integrated first and second generation sugarcane biorefinery: Fermentative versus catalytic routes," *Appl. Energy*, vol. 160, pp. 120–131, 2015.
- [51] K. Olofsson, M. Bertilsson, and G. Lidén, "A short review on SSF - an interesting process option for ethanol production from lignocellulosic feedstocks.," *Biotechnol. Biofuels*, vol. 1, no. 1, p. 7, 2008.
- [52] K. Gonzalez *et al.*, "Modeling the continuous lactic acid production process from wheat flour," *Appl. Microbiol. Biotechnol.*, vol. 100, no. 1, pp. 147–159, 2016.
- [53] L. D. Santos, M. D. B. Sousa, C. Z. Guidini, M. M. De Resende, V. L. Cardoso, and E. J. Ribeiro, "Continuous ethanol fermentation in tower reactors with cell recycling using flocculent *Saccharomyces cerevisiae*," *Process Biochem.*, vol. 50, no. 11, pp.

1725–1729, 2015.

- [54] M. Devarapalli and H. K. Atiyeh, “A review of conversion processes for bioethanol production with a focus on syngas fermentation,” *Biofuel Res. J.*, vol. 7, pp. 268–280, 2015.
- [55] D. Deublein and A. Steinhauser, *Biogas from Waste and Renewable Resources: An Introduction*. Wiley, 2010.
- [56] J. Solarte, J. Mariscal, and B. Aristizábal, “Evaluación de la digestión y co-digestión anaerobia de residuos de comida y de poda en bioreactores a escala laboratorio,” *Rev. Ión*, vol. 30, no. 1, pp. 105–116, 2017.
- [57] C. A. Lemos Chernicharo, *Anaerobic Reactors*. IWA publications, 2007.
- [58] M. Beil and W. Beyrich, “Biogas upgrading to biomethane,” in *The Biogas Handbook*, 2013, pp. 342–377.
- [59] C. Da costa gomez, “Biogas as an energy option: an overview,” in *The Biogas Handbook: Science, Production and Applications.*, A. Wellinger, J. Patrick Murphy, and D. Baxter, Eds. Woodhead, 2013, pp. 1–16.
- [60] I. Angelidaki *et al.*, “Defining the biomethane potential (BMP) of solid organic wastes and energy crops: A proposed protocol for batch assays,” *Water Sci. Technol.*, vol. 59, no. 5, pp. 927–934, 2009.
- [61] F. Cotana, G. Cavalaglio, A. Petrozzi, and V. Coccia, “Lignocellulosic biomass feeding in biogas pathway: State of the art and plant layouts,” *Energy Procedia*, vol. 81, pp. 1231–1237, 2015.
- [62] N. Dussadee, R. Ramaraj, and T. Cheunbarn, “Biotechnological application of sustainable biogas production through dry anaerobic digestion of Napier grass,” *3 Biotech*, vol. 7, no. 1, 2017.
- [63] I. Ullah *et al.*, “Biogas as a renewable energy fuel – A review of biogas upgrading , utilisation and storage,” *Energy Convers. Manag.*, vol. 150, pp. 277–294, 2017.
- [64] R. Mohsin, Z. A. Majid, A. H. Shihnan, N. S. Nasri, and Z. Sharer, “Effect of biodiesel blends on engine performance and exhaust emission for diesel dual fuel engine,” *Energy Convers. Manag.*, vol. 88, no. x, pp. 821–828, 2014.
- [65] I. Renewable and E. Agency, “Renewable Energy and Jobs (2013),” no. December, pp. 1–20, 2013.
- [66] P. Bajpai, *Advances in Bioethanol*. .
- [67] O. J. Sanchez and C. A. Cardona, “Biotechnological production of fuel alcohol I: production from different feedstocks,” *Interciancia*, vol. 30, no. 11, pp. 671–678,

2005.

- [68] S. Haghghi Mood *et al.*, “Lignocellulosic biomass to bioethanol, a comprehensive review with a focus on pretreatment,” *Renew. Sustain. Energy Rev.*, vol. 27, pp. 77–93, 2013.
- [69] Q. Sun, H. Li, J. Yan, L. Liu, Z. Yu, and X. Yu, “Selection of appropriate biogas upgrading technology-a review of biogas cleaning , upgrading and utilisation,” *Renew. Sustain. Energy Rev.*, vol. 51, pp. 521–532, 2015.
- [70] P. Cozma, W. Wukovits, I. Mămăligă, A. Friedl, and M. Gavrilescu, “Modeling and simulation of high pressure water scrubbing technology applied for biogas upgrading,” *Clean Technol. Environ. Policy*, vol. 17, no. 2, pp. 373–391, Feb. 2015.
- [71] F. Ma and M. a Hanna, “Biodiesel production: a review,” *Bioresour. Technol.*, vol. 70, pp. 1–15, 1999.
- [72] C. A. Cardona, C. E. Orrego, and L. F. Guitiérrez, *Biodiesel*, 1st ed. Manizales: Universidad Nacional de Colombia - Sede Manizales, Gobernación de Caldas, 2009.
- [73] C. Carraretto, A. Macor, A. Mirandola, A. Stoppato, and S. Tonon, “Biodiesel as alternative fuel: Experimental analysis and energetic evaluations,” *Energy*, vol. 29, no. 12–15 SPEC. ISS., pp. 2195–2211, 2004.
- [74] S. Döring, *Power from Pellets: Technology and Applications*. Springer, 2013.
- [75] H. Thomson and C. Liddell, “The suitability of wood pellet heating for domestic households: A review of literature,” *Renew. Sustain. Energy Rev.*, vol. 42, pp. 1362–1369, 2015.
- [76] D. J. Wilhelm, D. R. Simbeck, A. D. Karp, and R. L. Dickenson, “Syngas production for gas-to-liquids applications: Technologies, issues and outlook,” *Fuel Process. Technol.*, vol. 71, no. 1–3, pp. 139–148, 2001.
- [77] S. Atnaw, S. Sulaiman, and S. Yusup, “Syngas production from downdraft gasification of oil palm fronds,” *Energy*, vol. 61, pp. 491–501, 2013.
- [78] R. UN Food and Agriculture Organisation, “FAOSTAT Statistics Data Base,” *FAOSTAT*, 2016. .
- [79] S. M. Rincòn and D. M. Martínez, “Análisis de las propiedades del aceite de palma en el desarrollo de su industria An Analysis of the Properties of Oil Palm in the Development of the its Industry Introducción,” *Palmas*, vol. 30, no. 2, pp. 11–24, 2009.
- [80] S. Mekhilef, S. Siga, and R. Saidur, “A review on palm oil biodiesel as a source of

- renewable fuel,” *Renew. Sustain. Energy Rev.*, vol. 15, no. 4, pp. 1937–1949, 2011.
- [81] J. Sayer, J. Ghazoul, P. Nelson, and A. Klintuni Boedhihartono, “Oil palm expansion transforms tropical landscapes and livelihoods,” *Glob. Food Sec.*, vol. 1, no. 2, pp. 114–119, 2012.
- [82] I. E. Henson, “A Brief History of the Oil Palm,” in *Palm Oil: Production, Processing Characterization and Uses*, O.-M. Lai, C.-P. Tan, and C. C. Akoh, Eds. 1: Elsevier Inc., 2012, pp. 1–29.
- [83] D. Sheil *et al.*, *The impacts and opportunities of oil palm in Southeast Asia*. 2009.
- [84] C. A. Cardona, V. Aristizábal, and J. C. Solarte, “Improvement of Palm Oil Production for Food Industry through Biorefinery Concept,” in *Advances in Chemistry Research*, 2016, pp. 1–36.
- [85] M. F. Awalludin, O. Sulaiman, R. Hashim, and W. N. A. W. Nadhari, “An overview of the oil palm industry in Malaysia and its waste utilization through thermochemical conversion, specifically via liquefaction,” *Renew. Sustain. Energy Rev.*, vol. 50, pp. 1469–1484, 2015.
- [86] Sime Darby Plantation, “Palm oil facts and figures.” .
- [87] S. Rocha and J. N. Vesga, “Análisis termodinámico del proceso real de extracción de aceite de palma africana Thermodynamic analysis to a real palm oil extraction process,” vol. 10, no. 1, pp. 61–70, 2012.
- [88] P. B. Tinker, *The Oil Palm*. .
- [89] A. Kamal-Eldin and R. Andersson, “A multivariate study of the correlation between tocopherol content and fatty acid composition in vegetable oils,” *J. Am. Oil Chem. Soc.*, vol. 74, no. 4, pp. 375–380, 1997.
- [90] Federación Nacional de Cultivadores de Palma de Aceite, “Balance económico del sector palmero colombiano en el primer trimestre de 2015,” pp. 1–4, 2015.
- [91] H. Escalante, J. Orduz, H. Zapata, M. Cardona, and M. Duarte, *Atlas del potencial energético de la biomasa residual en Colombia 2010*. Unidad de Planeación Minero Energética de la República de Colombia (UPME), 2010.
- [92] B. Herrera, J. Leyva, V. Ortiz, J. F. Cárdenas, and E. Garzón, “Biocombustibles en Colombia,” Bogotá, 2009.
- [93] L. F. Gutiérrez and C. A. Cardona, *Diseño de procesos: Reacción - Separación Aplicados a la Agroindustria y la Minería*, 1st ed. Universidad Nacional de Colombia - Sede Manizales, Gobernación de Caldas, 2008.

- [94] B. Likozar and J. Levec, "Transesterification of canola, palm, peanut, soybean and sunflower oil with methanol, ethanol, isopropanol, butanol and tert-butanol to biodiesel: Modelling of chemical equilibrium, reaction kinetics and mass transfer based on fatty acid composition," *Appl. Energy*, vol. 123, pp. 108–120, 2014.
- [95] A. K. Endalew, Y. Kiros, and R. Zanzi, "Heterogeneous catalysis for biodiesel production from *Jatropha curcas* oil (JCO)," *Energy*, vol. 36, no. 5, pp. 2693–2700, 2011.
- [96] Y. Jiang, J. Lu, K. Sun, L. Ma, and J. Ding, "Esterification of oleic acid with ethanol catalyzed by sulfonated cation exchange resin: Experimental and kinetic studies," *Energy Convers. Manag.*, vol. 76, pp. 980–985, 2013.
- [97] C. A. Cardona, C. E. Orrego, and L. F. Gutiérrez, *Biodiesel*, Primera Ed. Manizales: Universidad Nacional de Colombia - Sede Manizales, 2009.
- [98] L. A. Follegatti-Romero, M. B. Oliveira, F. R. M. Batista, E. A. C. Batista, J. A. P. Coutinho, and A. J. A. Meirelles, "Liquid-liquid equilibria for ternary systems containing ethyl esters, ethanol and glycerol at 323.15 and 353.15 K," *Fuel*, vol. 94, pp. 386–394, 2012.
- [99] L. A. Follegatti-Romero, M. B. Oliveira, E. A. C. Batista, J. A. P. Coutinho, and A. J. A. Meirelles, "Liquid-liquid equilibria for ethyl esters + ethanol + water systems: Experimental measurements and CPA EoS modeling," *Fuel*, vol. 96, pp. 327–334, 2012.
- [100] A. B. MacHado, Y. C. Ardila, L. H. De Oliveira, M. Aznar, and M. R. Wolf Maclel, "Liquid-liquid equilibria in ternary and quaternary systems present in biodiesel production from soybean oil at (298.2 and 333.2) K," *J. Chem. Eng. Data*, vol. 57, no. 5, pp. 1417–1422, 2012.
- [101] USDA Foreign Agricultural Services, "Colombia Biofuels Annual Report," no. May, 2016.
- [102] O. I. Mba, M.-J. Dumont, and M. Ngadi, "Palm Oil: Processing, Characterization and Utilization in the Food Industry – A Review," *Food Biosci.*, vol. 10, pp. 26–41, 2015.
- [103] D. Piarpuzán, J. A. Quintero, and C. A. Cardona, "Empty fruit bunches from oil palm as a potential raw material for fuel ethanol production," *Biomass and Bioenergy*, vol. 35, no. 3, pp. 1130–1137, 2011.
- [104] C. B. S. Teh, "Availability, use, and removal of oil palm biomass in Indonesia," *Rep. Prep. Int. Counc. Clean Transp.*, pp. 1–39, 2016.

- [105] T. Ogi, M. Nakanishi, Y. Fukuda, and K. Matsumoto, "Gasification of oil palm residues (empty fruit bunch) in an entrained-flow gasifier," *Fuel*, vol. 104, pp. 28–35, 2013.
- [106] N. Abdullah, F. Sulaiman, and H. Gerhauser, "Characterisation of oil palm empty fruit bunches for fuel application," *J. Phys. Sci.*, vol. 22, no. 1, pp. 1–24, 2011.
- [107] C. A. Cardona Alzate, J. C. Solarte Toro, and Á. Gómez Peña, "Fermentation, thermochemical and catalytic processes in the transformation of biomass through efficient biorefineries," *Catal. Today*, 2017.
- [108] A. Demirbas, *Biodiesel: A Realistic Fuel Alternative for Diesel Engines*. 2008.
- [109] C. A. García, R. Betancourt, and C. A. Cardona, "Stand-alone and biorefinery pathways to produce hydrogen through gasification and dark fermentation using *Pinus Patula*," *J. Environ. Manage.*, vol. 1, no. 203, pp. 695–703, 2017.
- [110] J. A. Quintero, J. Moncada, and C. A. Cardona, "Techno-economic analysis of bioethanol production from lignocellulosic residues in Colombia: A process simulation approach," *Bioresour. Technol.*, vol. 139, pp. 300–307, 2013.
- [111] J. K. Raman and E. Gnansounou, "Furfural production from empty fruit bunch - A biorefinery approach," *Ind. Crops Prod.*, vol. 69, pp. 371–377, 2015.
- [112] K. T. Lee and C. Ofori-Boateng, "Oil Palm Biomass as Feedstock for Biofuel Production," in *Sustainability of Biofuel Production from Oil Palm Biomass*, First edit., Malaysia: Springer, 2013, pp. 77–106.
- [113] N. M. Han and C. Y. May, "Determination of antioxidants in oil palm leaves (*Elaeis guineensis*)," *Am. J. Appl. Sci.*, vol. 7, no. 9, pp. 1243–1247, 2010.
- [114] N. G. S. Yin, S. Abdullah, and C. K. Phin, "Phytochemical Constituents From Leaves of *Elaeis Guineensis* and Their Antioxidants and Antimicrobial Activities Article," *Int. J. Pharm. Pharm. Sci.*, vol. 5, no. May 2014, 2013.
- [115] J. P. Tan, J. M. Jahim, S. Harun, T. Y. Wu, and T. Mumtaz, "Utilization of oil palm fronds as a sustainable carbon source in biorefineries," *Int. J. Hydrogen Energy*, vol. 41, no. 8, pp. 4896–4906, 2016.
- [116] R. . Konda, S. . Sulaiman, and B. Ariwahjoedi, "Syngas Production from Gasification of Oil Palm Fronds wit an Updraft Gasifier," *J. Appl. Sci.*, vol. 12, no. 24, pp. 2555–2561, 2012.
- [117] S. M. Atnaw, S. A. Sulaiman, and S. Yusup, "Syngas production from downdraft gasification of oil palm fronds," *Energy*, vol. 61, pp. 491–501, 2013.
- [118] P. Basu, *Biomass Gasification and Pyrolysis: Practical Design*, First Editi.

Kidlington, Oxford: Elsevier, 2010.

- [119] Q.-V. Bach and K.-Q. Tran, "Dry and Wet Torrefaction of Woody Biomass – A Comparative Study on Combustion Kinetics," *Energy Procedia*, vol. 75, pp. 150–155, Aug. 2015.
- [120] B. B. Uzun, A. E. Pütün, and E. Pütün, "Fast pyrolysis of soybean cake: Product yields and compositions," *Bioresour. Technol.*, vol. 97, no. 4, pp. 569–576, 2006.
- [121] J. Rezaian and N. Cheremisinoff, *Gasification Technologies: A Primer for Engineers and Scientists*. CRC Press, Taylor and Francis, 2005.
- [122] L. Matsakas, Q. Gao, S. Jansson, U. Rova, and P. Christakopoulos, "Green conversion of municipal solid wastes into fuels and chemicals," *Electron. J. Biotechnol.*, vol. 26, pp. 69–83, 2017.
- [123] G. and S. T. Council, "The gasification industry." [Online]. Available: <http://www.gasification-syngas.org/resources/the-gasification-industry/>. [Accessed: 01-Aug-2017].
- [124] T. Y. Ahmed, M. M. Ahmad, S. Yusup, A. Inayat, and Z. Khan, "Mathematical and computational approaches for design of biomass gasification for hydrogen production: A review," *Renew. Sustain. Energy Rev.*, vol. 16, no. 4, pp. 2304–2315, 2012.
- [125] D. H. Jang *et al.*, "Gasification of hazelnut shells in a downdraft gasifier," *Energy*, vol. 27, no. 5, pp. 415–427, 2002.
- [126] T. K. Patra and P. N. Sheth, "Biomass gasification models for downdraft gasifier: A state-of-the-art review," *Renew. Sustain. Energy Rev.*, vol. 50, pp. 583–593, 2015.
- [127] R. Bain and K. Broer, "Gasification," in *Thermochemical Processing of Biomass: Conversion into Fuels, Chemicals and Power*, R. C. Brown, Ed. Wiley, 2011, pp. 47–77.
- [128] S. M. A. and A. O. M. S.A. Sulaiman^{1*}, S. Balamohan², M.N.Z. Moni¹, "Feasibility study of gasification of oil palm fronds," *J. Chem. Inf. Model.*, vol. 53, no. 9, pp. 1689–1699, 2015.
- [129] C. A. Alzate, F. Chejne, C. F. Valdés, A. Berrio, J. D. La Cruz, and C. A. Londoño, "CO-gasification of pelletized wood residues," *Fuel*, vol. 88, no. 3, pp. 437–445, 2009.
- [130] A. N. Rollinson and O. Williams, *Experiments on torrefied wood pellet: study by gasification and characterization for waste biomass to energy applications*, vol. 3, no. 5. 2016.

- [131] D. Mallick, P. Mahanta, and V. S. Moholkar, "Co-gasification of coal and biomass blends: Chemistry and engineering," *Fuel*, vol. 204, pp. 106–128, 2017.
- [132] N. Soponpongpipat, D. Sittikul, and P. Comsawang, "Prediction model of higher heating value of torrefied biomass based on the kinetics of biomass decomposition," *J. Energy Inst.*, vol. 89, no. 3, pp. 425–435, 2016.
- [133] H. Kitzler, C. Pfeifer, and H. Hofbauer, "Pressurized gasification of woody biomass—Variation of parameter," *Fuel Process. Technol.*, vol. 92, no. 5, pp. 908–914, May 2011.
- [134] C. Berrueco, J. Recari, B. M. Güell, and G. del Alamo, "Pressurized gasification of torrefied woody biomass in a lab scale fluidized bed," *Energy*, vol. 70, pp. 68–78, Jun. 2014.
- [135] F. N. Cayan, M. Zhi, S. R. Pakalapati, I. Celik, N. Wu, and R. Gemmen, "Effects of coal syngas impurities on anodes of solid oxide fuel cells," *J. Power Sources*, vol. 185, no. 2, pp. 595–602, 2008.
- [136] S. H. Lee, S. J. Yoon, H. W. Ra, Y. Il Son, J. C. Hong, and J. G. Lee, "Gasification characteristics of coke and mixture with coal in an entrained-flow gasifier," *Energy*, vol. 35, no. 8, pp. 3239–3244, 2010.
- [137] B. N. Murthy, A. N. Sawarkar, N. A. Deshmukh, T. Mathew, and J. B. Joshi, "Petroleum coke gasification: A review," *Can. J. Chem. Eng.*, vol. 92, no. 3, pp. 441–468, 2014.
- [138] M. Niu, Y. Huang, B. Jin, and X. Wang, "Simulation of Syngas Production from Municipal Solid Waste Gasification in a Bubbling Fluidized Bed Using Aspen Plus," *Ind. Eng. Chem. Res.*, vol. 52, no. 42, pp. 14768–14775, 2013.
- [139] M. Asadullah, "Barriers of commercial power generation using biomass gasification gas: A review," *Renew. Sustain. Energy Rev.*, vol. 29, pp. 201–215, 2014.
- [140] L. A. Pfaltzgraff and J. . Clark, "Green chemistry, biorefineries and second generation strategies for re-use of waste: an overview," in *Advances in Biorefineries: Biomass and Waste Supply Chain Exploitation*, K. . Waldron, Ed. 2014, pp. 3–33.
- [141] E. Jong and G. Jungmeier, "Biorefinery Concepts in Comparison to Petrochemical Refineries," in *Industrial Biorefineries and White Biotechnology*, A. Pandey, R. Hofer, C. Larroche, M. Taherzadeh, and M. K. Nampoothiri, Eds. Elsevier, 2015, pp. 3–33.
- [142] D. . Hines, "Biotechnology today and tomorrow," *Enzyme Microb. Technol.*, vol. 2,

no. 4, pp. 327–329, 1980.

- [143] H. J. Huang, S. Ramaswamy, U. W. Tschirner, and B. V. Ramarao, “A review of separation technologies in current and future biorefineries,” *Sep. Purif. Technol.*, vol. 62, no. 1, pp. 1–21, 2008.
- [144] A. R. Morais and R. Bogel-Lukasik, “Green chemistry and the biorefinery concept,” *Sustain. Chem. Process.*, vol. 1, no. 18, pp. 1–3, 2013.
- [145] J. Moncada, V. Aristizábal, and C. A. Cardona, “Design strategies for sustainable biorefineries,” *Biochem. Eng. J.*, vol. 116, pp. 122–134, 2016.
- [146] G. Jungmeier, M. Hingsamer, and R. Ree, “Biofuel-driven Biorefineries A selection of the most promising biorefinery concepts to produce large volumes of road transportation biofuels by 2025,” 2013.
- [147] Z. Yue, D. Ma, P. Shuchuan, X. Zhao, T. Chen, and J. Wang, “Integrated utilization of algal biomass and corn stover for biofuel production,” *Fuel*, vol. 168, pp. 1–6, 2016.
- [148] J. Trivedi, M. Aila, D. . Bangwal, S. Kaul, and M. . Garg, “Algae based biorefinery—How to make sense?,” *Renew. Sustain. Energy Rev.*, vol. 47, pp. 295–307, 2015.
- [149] N. Shabani, S. Akhtari, and T. Sowlati, “Value chain optimization of forest biomass for bioenergy production: A review,” *Renew. Sustain. Energy Rev.*, vol. 23, pp. 299–311, 2013.
- [150] P. a. M. Claassen *et al.*, “Utilisation of biomass for the supply of energy carriers,” *Appl. Microbiol. Biotechnol.*, vol. 52, no. 6, pp. 741–755, 1999.
- [151] J. D. Martínez, K. Mahkamov, R. V. Andrade, and E. E. Silva Lora, “Syngas production in downdraft biomass gasifiers and its application using internal combustion engines,” *Renew. Energy*, vol. 38, no. 1, pp. 1–9, 2012.
- [152] C. A. Cardona, V. Aristizábal, and J. C. Solarte Toro, “Improvement of Palm Oil Production for Food Industry through Biorefinery Concept,” in *Advances in Chemistry Research. Volume 32*, J. C. Taylor, Ed. Nova Science Publishers, 2016.
- [153] J. Moncada, M. M. El-Halwagi, and C. A. Cardona, “Techno-economic analysis for a sugarcane biorefinery: Colombian case,” *Bioresour. Technol.*, vol. 135, pp. 533–543, 2013.
- [154] A. Sluiter, R. Ruiz, C. Scarlata, J. Sluiter, and D. Templeton, “Determination of Extractives in Biomass,” 2008.
- [155] L. V. Daza Serna, J. C. Solarte Toro, S. Serna Loaiza, Y. Chacón Perez, and C. A. Cardona Alzate, “Agricultural Waste Management Through Energy Producing

- Biorefineries: The Colombian Case,” *Waste and Biomass Valorization*, pp. 1–10, 2016.
- [156] J. S. Han and J. S. Rowell, “Chemical composition of fibers,” in *Paper and Composites from Agro-based Resources*, 1997, pp. 83–134.
- [157] A. Pandey, S. Negi, P. Binod, and C. Larroche, *Pretreatment of Biomass: Processes and Technologies*. Elsevier B.V, 2015.
- [158] a Sluiter, B. Hames, R. Ruiz, C. Scarlata, J. Sluiter, and D. Templeton, “Determination of Sugars , Byproducts , and Degradation Products in Liquid Fraction Process Samples Laboratory Analytical Procedure (LAP) Issue Date : 12 / 08 / 2006 Determination of Sugars , Byproducts , and Degradation Products in Liquid Fraction Proce,” *Lab. Anal. Proced. NREL/TP-510-42623*, no. January, pp. 1–14, 2008.
- [159] J. C. Carvajal, Á. Gómez, and C. A. Cardona, “Comparison of lignin extraction processes: Economic and environmental assessment,” *Bioresour. Technol.*, vol. 214, pp. 468–476, 2016.
- [160] J. C. Martínez-Patiño, I. Romero, E. Ruiz, C. Cara, J. M. Romero-García, and E. Castro, “Design and optimization of sulfuric acid pretreatment of extracted olive tree biomass using response surface methodology,” *BioResources*, vol. 12, no. 1, pp. 1779–1797, 2017.
- [161] A. Sluiter, B. Hames, R. Ruiz, C. Scarlata, J. Sluiter, and D. Templeton, “Determination of Ash in Biomass,” Colorado, 2008.
- [162] ASTM E1756-01, “Standard Test Method for Determination of Total Solids in Biomass,” *West Conshohocken, PA*, 2001.
- [163] a Sluiter *et al.*, “Determination of total solids in biomass and total dissolved solids in liquid process samples,” *Natl. Renew. Energy Lab.*, no. March, p. 9, 2008.
- [164] ASTM E1690-08, “Standard Test Method for Determination of Ethanol Extractives in Biomass,” *ASTM Int. West Conshohocken, PA*, 2016.
- [165] H. Rabemanolontsoa and S. Saka, “Holocellulose determination in biomass,” in *Zero-Carbon Energy Kyoto 2011*, Special Ed., 2012, pp. 135–140.
- [166] ASTM E1755-01, “Standard Test Method for Ash in Biomass,” *ASTM Int. West Conshohocken, PA*, 2015.
- [167] ASTM E870-82, “Standard Test Methods for Analysis of Wood Fuels,” *West Conshohocken, PA*, 2013.
- [168] M. Graboski and R. Baln, “Properties of Biomass Relevant to Gasification,” in A

- survey of biomass gasification*, Volume II., Springfield, 1979, pp. 21–67.
- [169] ASTM E872-82, “Standard Test Method for Volatile Matter in the Analysis of Particulate Wood Fuels,” *West Conshohocken, PA*, 2013.
- [170] ASTM E871-82, “Standard Test Method for Moisture Analysis of Particulate Wood Fuels,” *West Conshohocken, PA*, 2013.
- [171] ASTM E8777-17, “Standard Test Method for Carbon and Hydrogen in the Analysis Sample of Refuse-Derived Fuel,” *West Conshohocken, PA*.
- [172] ASTM E878, “Standard Test Methods for Nitrogen in Refuse-Derived Fuel Analysis Samples,” *West Conshohocken, PA*, 2015.
- [173] ASTM E775, “Standard Test Methods for Total Sulfur in the Analysis Sample of Refuse-Derived Fuel,” *West Conshohocken, PA*, 2015.
- [174] J. . Dunn, “Thermogravimetric Analysis,” in *Characterization of Materials*, 2002.
- [175] S. Munir, S. S. Daood, W. Nimmo, A. M. Cunliffe, and B. M. Gibbs, “Thermal analysis and devolatilization kinetics of cotton stalk, sugar cane bagasse and shea meal under nitrogen and air atmospheres.,” *Bioresour. Technol.*, vol. 100, no. 3, pp. 1413–8, Feb. 2009.
- [176] D. D. Miller and M. Rutzke, “Atomic Absorption Spectroscopy, Atomic Emission Spectroscopy, and Inductively Coupled Plasma-Mass Spectrometry,” in *Food Analysis*, Fourth edi., Springer, 2009, pp. 421–442.
- [177] T. B. Reed and A. Das, “Handbook of biomass downdraft gasifier engine systems,” no. March, 1988.
- [178] FAO, *Wood Fuels Handbook*, vol. 53, no. 9. 2013.
- [179] F. M. Guangul, S. A. Sulaiman, and A. Ramli, “Study of the effects of operating factors on the resulting producer gas of oil palm fronds gasification with a single throat downdraft gasifier,” *Renew. Energy*, vol. 72, pp. 271–283, 2014.
- [180] J. Shen, S. Zhu, X. Liu, H. Zhang, and J. Tan, “The prediction of elemental composition of biomass based on proximate analysis,” *Energy Convers. Manag.*, vol. 51, no. 5, pp. 983–987, May 2010.
- [181] T. Waldheim, L. Nilsson, “Heating value of gases from biomass gasification,” 2001.
- [182] C. S. Goh, K. T. Lee, and S. Bhatia, “Hot compressed water pretreatment of oil palm fronds to enhance glucose recovery for production of second generation bio-ethanol,” *Bioresour. Technol.*, vol. 101, no. 19, pp. 7362–7367, 2010.
- [183] E. Triwahyuni, S. Hariyanti, D. Dahnum, M. Nurdin, and H. Abimanyu, “Optimization of Saccharification and Fermentation Process in Bioethanol

- Production from Oil Palm Fronds,” *Procedia Chem.*, vol. 16, pp. 141–148, 2015.
- [184] T. Srimachai and V. Thonglimp, “Ethanol and Methane Production from Oil Palm Frond by Two Stage SSF,” *Energy Procedia*, vol. 52, pp. 352–361, Jan. 2014.
- [185] S. Kumneadklang, S. Larpiattaworn, and C. Niyasom, “Bioethanol Production from Oil Palm Frond by Simultaneous Saccharification and Fermentation,” *Energy Procedia*, vol. 79, pp. 784–790, Nov. 2015.
- [186] K. S. Lin, H. P. Wang, C.-J. Lin, and C.-I. Juch, “A process development for gasification of rice husk,” *Fuel Process. Technol.*, vol. 55, no. 3, pp. 185–192, 1998.
- [187] C. A. García, J. Moncada, V. Aristizábal M., and C. A. Cardona, “Techno-economic and energetic assessment of hydrogen production through gasification in the Colombian context: Coffee Cut-Stems case,” *Int. J. Hydrogen Energy*, vol. 42, no. 9, pp. 5849–5864, 2017.
- [188] D. R. Nhuchhen and P. Abdul Salam, “Estimation of higher heating value of biomass from proximate analysis: A new approach,” *Fuel*, vol. 99, pp. 55–63, Sep. 2012.
- [189] A. K. Sharma, M. R. Ravi, and S. Kohli, “Modelling product composition in slow pyrolysis of wood,” *Sol. Energy Soc. India*, vol. 16, no. 1, pp. 1–11, 2006.
- [190] H. Yang, R. Yan, T. Chin, D. T. Liang, H. Chen, and C. Zheng, “Thermogravimetric Analysis–Fourier Transform Infrared Analysis of Palm Oil Waste Pyrolysis,” *Energy & Fuels*, vol. 18, no. 6, pp. 1814–1821, 2004.
- [191] R. J. Wooley and V. Putsche, “Development of an Aspen Plus property database for biofuels components,” National Renewable Energy Laboratory, 1996.
- [192] V. S. Y. Soon, B. L. F. Chin, and A. C. R. Lim, “Kinetic Study on Pyrolysis of Oil Palm Frond,” *IOP Conf. Ser. Mater. Sci. Eng.*, vol. 121, p. 12004, 2016.
- [193] M. Simone, F. Barontini, C. Nicolella, and L. Tognotti, “Gasification of pelletized biomass in a pilot scale downdraft gasifier,” *Bioresour. Technol.*, vol. 116, pp. 403–412, 2012.
- [194] N. V. Khartchenko and V. M. Kharchenko, *Advanced energy systems*, 2nd editio. CRC Press, Taylor and Francis, 2010.
- [195] S. M. Atnaw, S. A. Sulaiman, and S. Yusup, “Influence of fuel moisture content and reactor temperature on the calorific value of Syngas resulted from gasification of oil palm fronds,” *Sci. World J.*, vol. Article ID, p. 9 pages, 2014.
- [196] M. G. E. D. Z. S. J. R. B. Miodrag Belosevic, “Degradation of Alizarin Yellow R

- using UV / H₂O₂ Advanced Oxidation Process,” *Environ. Sci. Technol.*, vol. 33, no. 2, pp. 482–489, 2014.
- [197] I. J. Fernandes *et al.*, “Characterization of rice husk ash produced using different biomass combustion techniques for energy,” *Fuel*, vol. 165, pp. 351–359, 2016.
- [198] Z. Yao, S. You, T. Ge, and C. H. Wang, “Biomass gasification for syngas and biochar co-production: Energy application and economic evaluation,” *Appl. Energy*, vol. 209, no. July 2017, pp. 43–55, 2018.
- [199] J. Wang, T. Mao, J. Sui, and H. Jin, “Modeling and performance analysis of CCHP (combined cooling, heating and power) system based on co-firing of natural gas and biomass gasification gas,” *Energy*, vol. 93, pp. 801–815, 2015.
- [200] J. Yoder, S. Galinato, D. Granatstein, and M. Garcia-Pérez, “Economic tradeoff between biochar and bio-oil production via pyrolysis,” *Biomass and Bioenergy*, vol. 35, no. 5, pp. 1851–1862, 2011.
- [201] G. J. Ruiz-Mercado, R. L. Smith, and M. A. Gonzalez, “Sustainability indicators for chemical processes: I. Taxonomy,” *Ind. Eng. Chem. Res.*, vol. 51, no. 5, pp. 2309–2328, 2012.
- [202] G. J. Ruiz-Mercado, R. L. Smith, and M. A. Gonzalez, “Sustainability Indicators for Chemical Processes: II. Data Needs,” *Ind. Eng. Chem. Res.*, vol. 51, no. 5, pp. 2329–2353, 2012.
- [203] G. J. Ruiz-Mercado, M. A. Gonzalez, and R. L. Smith, “Sustainability indicators for chemical processes: III. biodiesel case study,” *Ind. Eng. Chem. Res.*, vol. 52, no. 20, pp. 6747–6760, 2013.
- [204] IChemE, “The Sustainability Metrics: Sustainable development progress metrics recommended for use in process industries,” 2002.
- [205] U. S. Dept. of Transportation, “Hazardous Materials List.” [Online]. Available: <https://environmentalchemistry.com/yogi/hazmat/table/>. [Accessed: 15-Jan-2017].
- [206] U. S. E. P. Agency., “Toxic Releases Inventory (TRI) Program. PBT list.” [Online]. Available: www.epa.gov/toxics-release-inventory-tri-program/persistent-bioaccumulative-toxic-pbt-chemicals-covered-tri. [Accessed: 15-Jan-2017].
- [207] G. Chidikofan *et al.*, “Assessment of Environmental Impacts of Tar Releases from a Biomass Gasifier Power Plant for Decentralized Electricity Generation,” *Energy Procedia*, vol. 118, pp. 158–163, 2017.
- [208] C. A. García Velásquez, “Hydrogen production through gasification and dark fermentation,” p. 181, 2016.

- [209] I. S. Antonopoulos, A. Karagiannidis, A. Gkouletsos, and G. Perkoulidis, "Modelling of a downdraft gasifier fed by agricultural residues," *Waste Manag.*, vol. 32, no. 4, pp. 710–718, 2012.
- [210] H. Thunman, F. Niklasson, F. Johnsson, and B. Leckner, "Composition of volatile gases and thermochemical properties of wood for modeling of fixed or fluidized beds," *Energy and Fuels*, vol. 15, no. 6, pp. 1488–1497, 2001.
- [211] C. A. Cardona Alzate, J. C. Solarte-Toro, and Á. G. Peña, "Fermentation, thermochemical and catalytic processes in the transformation of biomass through efficient biorefineries," *Catal. Today*, vol. 302, pp. 61–72, 2018.
- [212] E. Desroches-ducarme, J. C. Dolignier, E. Marty, G. Martin, and L. Delfosse, "Modelling of gaseous pollutants emissions in circulating fluidized bed combustion of municipal refuse," *Fuel*, vol. 77, no. 13, pp. 1399–1410, 1998.
- [213] A. K. Sharma, "Modeling and simulation of a downdraft biomass gasifier 1. Model development and validation," *Energy Convers. Manag.*, vol. 52, no. 2, pp. 1386–1396, 2011.
- [214] T. K. Patra, K. R. Nimisha, and P. N. Sheth, "A comprehensive dynamic model for downdraft gasifier using heat and mass transport coupled with reaction kinetics," *Energy*, vol. 116, pp. 1230–1242, 2016.
- [215] N. Gao and A. Li, "Modeling and simulation of combined pyrolysis and reduction zone for a downdraft biomass gasifier," *Energy Convers. Manag.*, vol. 49, no. 12, pp. 3483–3490, Dec. 2008.
- [216] F. M. Guangul, S. A. Sulaiman, and A. Ramli, "Study of the effects of operating factors on the resulting producer gas of oil palm fronds gasification with a single throat downdraft gasifier," *Renew. Energy*, vol. 72, pp. 271–283, 2014.
- [217] F. Guo, Y. Dong, L. Dong, and C. Guo, "Effect of design and operating parameters on the gasification process of biomass in a downdraft fixed bed: An experimental study," *Int. J. Hydrogen Energy*, vol. 39, no. 11, pp. 5625–5633, 2014.
- [218] A. K. Sharma, "Equilibrium modeling of global reduction reactions for a downdraft (biomass) gasifier," *Energy Convers. Manag.*, vol. 49, no. 4, pp. 832–842, 2008.
- [219] A. Esteghlalian, A. G. Hashimoto, J. J. Fenske, and M. H. Penner, "Modeling and optimization of the dilute-sulfuric-acid pretreatment of corn stover, poplar and switchgrass," *Bioresour. Technol.*, vol. 59, no. 2–3, pp. 129–136, 1997.
- [220] J. Jensen, J. Morinelly, A. Aglan, A. Mix, and D. Shonnard, "Kinetic characterization of biomass dilute sulfuric acid hydrolysis: Mixtures of hardwoods,

- softwood and switchgrass,” *Environ. energy Eng.*, vol. 54, no. 6, pp. 1637–1645, 2008.
- [221] J. A. Quintero and C. A. Cardona, “Process simulation of fuel ethanol production from lignocellulosics using aspen plus,” *Ind. Eng. Chem. Res.*, vol. 50, no. 10, pp. 6205–6212, 2011.
- [222] D. Humbird *et al.*, “Process Design and Economics for Biochemical Conversion of Lignocellulosic Biomass to Ethanol,” *Renew. Energy*, vol. 303, no. May, p. 147, 2011.
- [223] S. Lee and Y. Koo, “Model Development for Lactic Acid Fermentation and Parameter Optimization Using Genetic Algorithm,” *Simulation*, vol. 14, pp. 1163–1169, 2004.
- [224] D.-J. Min, K. H. Choi, Y. K. Chang, and J.-H. Kim, “Effect of operating parameters on precipitation for recovery of lactic acid from calcium lactate fermentation broth,” *Korean J. Chem. Eng.*, vol. 28, no. 10, pp. 1969–1974, Oct. 2011.
- [225] C. J. S. M. Silva, S. I. Mussatto, and I. C. Roberto, “Study of xylitol production by *Candida guilliermondii* on a bench bioreactor,” *J. Food Eng.*, vol. 75, no. 1, pp. 115–119, 2006.
- [226] S. I. Mussatto and I. C. Roberto, “Establishment of the optimum initial xylose concentration and nutritional supplementation of brewer’s spent grain hydrolysate for xylitol production by *Candida guilliermondii*,” *Process Biochem.*, vol. 43, no. 5, pp. 540–546, 2008.
- [227] D. De Faveri, M. Lambri, A. Converti, P. Perego, and M. Del Borghi, “Xylitol recovery by crystallization from synthetic solutions and fermented hemicellulose hydrolyzates,” *Chem. Eng. J.*, vol. 90, no. 3, pp. 291–298, 2002.
- [228] R. O’Neil, M. N. Ahmad, L. Vanoye, and F. Aiouache, “Kinetics of aqueous phase dehydration of xylose into furfural catalyzed by ZSM-5 zeolite,” *Ind. Eng. Chem. Res.*, vol. 48, no. 9, pp. 4300–4306, 2009.
- [229] X. Zhang, T. Wang, L. Ma, and C. Wu, “Aqueous-phase catalytic process for production of pentane from furfural over nickel-based catalysts,” *Fuel*, vol. 89, no. 10, pp. 2697–2702, 2010.
- [230] K. Y. Nandiwale, P. S. Niphadkar, S. S. Deshpande, and V. V. Bokade, “Esterification of renewable levulinic acid to ethyl levulinate biodiesel catalyzed by highly active and reusable desilicated H-ZSM-5,” *J. Chem. Technol. Biotechnol.*, vol. 89, no. 10, pp. 1507–1515, 2014.

- [231] R. De María, I. Díaz, M. Rodríguez, and A. Sáiz, "Industrial methanol from syngas: Kinetic study and process simulation," *Int. J. Chem. React. Eng.*, vol. 11, no. 1, pp. 469–477, 2013.
- [232] G. H. Graaf, P. J. J. M. Sijtsema, E. J. Stamhuis, and G. E. H. Joostes, "Chemical Equilibria in Methanol Synthesis," *Chem. Eng. Sci.*, vol. 41, no. 86, pp. 2883–2890, 1986.
- [233] G. H. Graaf, E. J. Stamhuis, and A. A. C. M. Beenackers, "Kinetics of low-pressure methanol synthesis," *Chem. Eng. Sci.*, vol. 43, no. 12, pp. 3185–3195, 1988.
- [234] J. A. López, V. M. Trejos, and C. A. Cardona, "Parameters estimation and VLE calculation in asymmetric binary mixtures containing carbon dioxide + n-alkanols," *Fluid Phase Equilib.*, vol. 275, no. 1, pp. 1–7, 2009.
- [235] I. C. Paz Astudillo and C. A. Cardona Alzate, "Importance of stability study of continuous systems for ethanol production," *J. Biotechnol.*, vol. 151, no. 1, pp. 43–55, 2011.
- [236] J. A. Dávila, M. Rosenberg, and C. A. Cardona, "A biorefinery approach for the production of xylitol, ethanol and polyhydroxybutyrate from brewer's spent grain," *AIMS Agric. Food*, vol. 1, no. 1, pp. 52–66, 2016.
- [237] É. S. Van-Dal and C. Bouallou, "Design and simulation of a methanol production plant from CO₂ hydrogenation," *J. Clean. Prod.*, vol. 57, pp. 38–45, 2013.
- [238] M. Ghanta, D. R. Fahey, D. H. Busch, B. Subramaniam, and Ullmans - Propylene Oxide, "Comparative Economic and Environmental Assessments of H₂O₂-based and Tertiary Butyl Hydroperoxide-based Propylene Oxide Technologies," *Rep. Carcinog.*, vol. 12, no. 30, pp. 268–277, 2013.
- [239] "Indicative Chemical Prices A-Z." [Online]. Available: <http://www.icis.com/chemicals/channel-info-chemicals-a-z/>. [Accessed: 20-Nov-2016].
- [240] "No Title." [Online]. Available: <https://www.fishersci.com/shop/products/zeolite-type-zsm-5-acros-organics-3/p-3777048>. [Accessed: 20-Nov-2016].
- [241] H. Lei, R. Nie, J. Fei, and Z. Hou, "Preparation of Cu/ZnO/Al₂O₃ catalysts in a solvent-free routine for CO hydrogenation," *J. Zhejiang Univ. Sci. A*, vol. 13, no. 5, pp. 395–406, 2012.
- [242] L. F. Gutiérrez, Ó. J. Sánchez, and C. A. Cardona, "Process integration possibilities for biodiesel production from palm oil using ethanol obtained from lignocellulosic residues of oil palm industry," *Bioresour. Technol.*, vol. 100, no. 3,

- pp. 1227–1237, 2009.
- [243] R. Weingarten, J. Cho, R. Xing, W. C. Conner, and G. W. Huber, “Kinetics and reaction engineering of levulinic acid production from aqueous glucose solutions,” *ChemSusChem*, vol. 5, no. 7, pp. 1280–1290, 2012.
- [244] M. Ghanta, T. Ruddy, D. Fahey, D. Busch, and B. Subramaniam, “Is the Liquid-Phase H₂O₂-Based Ethylene Oxide Process More Economical and Greener Than the Gas-Phase O₂-Based Silver-Catalyzed Process?,” *Ind. Eng. Chem. Res.*, vol. 52, pp. 18–29, 2013.
- [245] Y. Zheng, J. Zhao, F. Xu, and Y. Li, “Pretreatment of lignocellulosic biomass for enhanced biogas production,” *Prog. Energy Combust. Sci.*, vol. 42, pp. 35–53, 2014.
- [246] M. R. Zakaria, S. Fujimoto, S. Hirata, and M. A. Hassan, “Ball Milling Pretreatment of Oil Palm Biomass for Enhancing Enzymatic Hydrolysis,” *Appl. Biochem. Biotechnol.*, vol. 173, no. 7, pp. 1778–1789, Aug. 2014.
- [247] C. S. Goh, H. T. Tan, and K. T. Lee, “Pretreatment of oil palm frond using hot compressed water: An evaluation of compositional changes and pulp digestibility using severity factors,” *Bioresour. Technol.*, vol. 110, pp. 662–669, 2012.
- [248] A. Kristiani, H. Abimanyu, A. H. Setiawan, Sudiarmanto, and F. Aulia, “Effect of Pretreatment Process by Using Diluted Acid to Characteristic of oil Palm’s Frond,” *Energy Procedia*, vol. 32, pp. 183–189, 2013.
- [249] L.-W. Lai and A. Idris, “Disruption of Oil Palm Trunks and Fronds by Microwave-Alkali Pretreatment,” *BioResources*, vol. 8, no. 2, pp. 2792–2804, Apr. 2013.
- [250] P. Kaparaju, M. Serrano, A. B. Thomsen, P. Kongjan, and I. Angelidaki, “Bioethanol, biohydrogen and biogas production from wheat straw in a biorefinery concept,” *Bioresour. Technol.*, vol. 100, no. 9, pp. 2562–2568, May 2009.
- [251] A. Demirbas, “Bioethanol from Cellulosic Materials: A Renewable Motor Fuel from Biomass,” *Energy Sources*, vol. 27, no. 4, pp. 327–337, 2005.
- [252] Y. Li, R. Zhang, G. Liu, C. Chen, Y. He, and X. Liu, “Comparison of methane production potential, biodegradability, and kinetics of different organic substrates,” 2013.
- [253] A. M. Y. Razak, *Industrial Gas Turbines: Performance and Operability*. 2007.
- [254] L. Zheng and E. Furimsky, “ASPEN simulation of cogeneration plants,” *Energy Convers. Manag.*, vol. 44, no. 11, pp. 1845–1851, 2003.
- [255] I. C. Paz Astudillo, “Diseño Integral de Biorreactores Continuos de Tanque Agitado

Aplicados a Procesos de Fermentación,” Universidad Nacional de Colombia - Sede Manizales, 2010.

- [256] S. tong Jiang, M. Liu, and L. jun Pan, “Kinetic study for hydrolysis of methyl lactate catalyzed by cation-exchange resin,” *J. Taiwan Inst. Chem. Eng.*, vol. 41, no. 2, pp. 190–194, 2010.
- [257] L. Mo, J. Shao-Tong, P. Li-Jun, Z. Zhi, and L. Shui-Zhong, “Design and control of reactive distillation for hydrolysis of methyl lactate,” *Chem. Eng. Res. Des.*, vol. 89, no. 11, pp. 2199–2206, 2011.